

REACTION NETWORK AND KINETICS OF VAPOR-PHASE
CATALYTIC HYDRODENITROGENATION OF QUINOLINE

by

JOSEPH FRANCIS COCCHETTO

B.S., Cornell University (1973)

S.M., Massachusetts Institute of Technology (1974)

Submitted in Partial Fulfillment
of the Requirements for the
Degree of Doctor of Philosophy

at the

Massachusetts Institute of Technology

November, 1979

(i.e. February 1980)

© Massachusetts Institute of Technology, 1979

Signature of Author _____
Department of Chemical Engineering
November 15, 1979

Certified by _____
Charles N. Satterfield, Thesis Supervisor

Michael Modell, Thesis Supervisor

Accepted by _____
Glenn C. Williams, Chairman
Departmental Committee on Graduate Theses

ARCHIVES
MASSACHUSETTS INSTITUTE
OF TECHNOLOGY

JUN 13 1980

LIBRARIES

Reaction Network and Kinetics of Vapor-Phase
Catalytic Hydrodenitrogenation of Quinoline

by

Joseph Francis Cocchetto

Submitted to the Department of Chemical Engineering
on November 15, 1979 in partial fulfillment of the
requirements for the Degree of Doctor of Philosophy

Abstract

The reaction network and kinetics of quinoline hydrodenitrogenation (HDN) were studied in a flow microreactor packed with presulfided NiMo/Al₂O₃ catalyst. Reactor temperatures were 330 to 420°C, and total pressure was either 3.55 or 7.0 MPa (500 or 1000 psig). Partial pressure of the reactant compound (quinoline or one of its hydrogenated derivatives) was 13.3 or 26.7 kPa, and reactant feed rates varied from 41.7 to 667 hr g catalyst/g-mol.

The results indicated that the initial ring saturation reactions of quinoline are all reversible over a wide range of HDN conditions; also, saturation of the aromatic ring is thermodynamically (but not necessarily kinetically) more favorable than saturation of the heteroring. Nitrogen removal from quinoline occurred primarily through the decahydroquinoline intermediate, and propylcyclohexane was the major hydrocarbon product. The NiMo/Al₂O₃ catalyst exhibited little selectivity for the reaction pathway of minimum hydrogen consumption, due to insufficient hydrogenolysis activity.

Adsorptivities of the nitrogen compounds in the quinoline HDN network varied significantly. A Langmuir-Hinshelwood kinetic model, allowing for these different adsorptivities, was developed for the hydrogenolysis and nitrogen removal reactions. On active catalyst sites, the Py-tetrahydroquinoline and decahydroquinoline reaction intermediates appeared to adsorb about six times as strongly as the less basic aromatic amines (quinoline, Bz-tetrahydroquinoline, and o-propylaniline), which in turn showed an adsorption strength approximately four times greater than that of ammonia.

Thesis Supervisors: Charles N. Satterfield
Professor of Chemical Engineering

Michael Modell
Associate Professor of Chemical
Engineering

Department of Chemical Engineering
Massachusetts Institute of Technology
Cambridge, Massachusetts 02139

November, 1979

Professor George C. Newton, Jr.
Secretary of the Faculty
Massachusetts Institute of Technology
Cambridge, Massachusetts 02139

Dear Professor Newton:

In accordance with the regulations of the Faculty, I herewith submit a thesis, entitled "Reaction Network and Kinetics of Vapor-Phase Catalytic Hydrodenitrogenation of Quinoline", in partial fulfillment of the requirements for the degree of Doctor of Philosophy in Chemical Engineering at the Massachusetts Institute of Technology.

Respectfully submitted,

Joseph F. Cocchetto

This Thesis is Dedicated to my Family

Acknowledgements

First, I want to thank my thesis advisors, Professors Charles N. Satterfield and Michael Modell, for their support, guidance, and especially for the freedom given to me during the course of this investigation. Special thanks are extended to both of them for their assistance in non-thesis pursuits as well. I wish to thank Professor Glenn C. Williams, for his friendship, and also for his efforts in arranging financial support during some hard times. The friendship and support of Professor Robert C. Reid, throughout my M.I.T. career, are gratefully acknowledged.

I thank Mr. Thomas Irwin for his assistance in the synthesis work, Mr. Stanley Mitchell for drawing the many figures in this thesis, and Dr. Richard Schlosberg for coordinating sample analyses at Exxon. I also want to thank Ms. Catherine Stacy for her perseverance and patience in typing this thesis.

Life at M.I.T. has been tolerable through the friendships of Dr. Albert Sacco, Jr., Ms. Alice Marie Sprouse, Dr. Terry M. Copeland, Mr. Anthony DiLeo, Mr. Kevin O. Meyers, Mr. George A. Huff, Jr., Mr. Richard J. Arena, and Dr. Peter R. Greene.

Finally, I thank my family for their love,
encouragement, patience, and understanding through all the
difficult times, and for making this long educational
process possible.

Joseph F. Cocchetto
Cambridge, Massachusetts
November, 1979

Table of Contents

I. Summary	18
I. A. Introduction	18
I. B. Objectives	19
I. C. Literature Review	20
I. C. 1. Hydrotreating Catalysts	20
I. C. 2. Hydrodenitrogenation Studies	21
I. D. Quinoline Hydrodenitrogenation Reaction Network and Thermodynamics	24
I. E. Experimental Apparatus and Procedure	25
I. F. Results	28
I. F. 1. Catalyst Activity	30
I. F. 2. Hydrodenitrogenation of Quinoline and Py-Tetrahydroquinoline	31
I. F. 3. Hydrodenitrogenation of o-Propylaniline	32
I. F. 4. Hydrodenitrogenation of Bz-Tetrahydro- quinoline and Decahydroquinoline	33
I. F. 5. Hydrocarbon Products	34
I. F. 6. Homogeneous Reaction	35
I. F. 7. Initial Ring Saturation Equilibria	36
I. G. Discussion of Results	38
I. G. 1. Quinoline Hydrodenitrogenation Reaction Network and Thermodynamics	38
I. G. 2. Catalyst Activity	40
I. G. 3. Quinoline Hydrodenitrogenation Kinetics	41
I. G. 4. Behavior of the Quinoline/Py-Tetrahydro- quinoline Product Ratio	44
I. G. 5. Kinetic Modelling	45
I. H. Conclusions	51
I. H. 1. Catalyst Activity	51
I. H. 2. Hydrodenitrogenation of o-Propylaniline	51
I. H. 3. Hydrodenitrogenation of Quinoline	52

II. Introduction	77
II. A. Background	77
II. B. Literature Review	83
II. B. 1. Hydrotreating Catalysts	83
II. B. 2. Hydrodenitrogenation Studies	85
II. B. 3. Quinoline Hydrodenitrogenation Studies	88
II. B. 4. Adsorption Phenomena in Catalytic Hydrodenitrogenation	91
II. C. Quinoline Hydrodenitrogenation Reaction Network and Thermodynamics	94
II. D. Thesis Objectives	102
III. Apparatus and Procedure	103
III. A. Experimental Apparatus	103
III. A. 1. Reactant Feed Section	105
III. A. 2. Reactor Section	107
III. A. 3. Sampling and Analysis Section	110
III. A. 4. Gas Chromatographic Analyses	111
III. A. 5. Miscellaneous Details	117
III. B. Catalyst	118
III. C. Experimental Procedure	122
III. D. Data Reduction	124
III. E. Experimental Problems	125
IV. Results	128
IV. A. Catalyst Activity	130
IV. B. Hydrodenitrogenation of Quinoline and Py-Tetrahydroquinoline	138
IV. B. 1. Nitrogen Removal	138
IV. B. 2. Product Distributions: Nitrogen-bearing Intermediates	143
IV. B. 3. Product Distributions: Hydrocarbon Products	157
IV. C. Hydrodenitrogenation of o-Propylaniline	160
IV. C. 1. Nitrogen Removal	160
IV. C. 2. Product Distributions	162

IV. D.	Hydrodenitrogenation of Bz-Tetrahydroquinoline and Decahydroquinoline	164
IV. D. 1.	Nitrogen Removal	165
IV. D. 2.	Product Distributions	165
IV. E.	Hydrogenation of Propylbenzene	171
IV. F.	Homogeneous Reactions	173
IV. G.	Initial Ring Saturation Equilibria	176
V.	Discussion of Results	185
V. A.	Quinoline Hydrodenitrogenation Reaction Network and Thermodynamics	185
V. A. 1.	Formation of Hydrocarbon Products	187
V. A. 2.	Initial Ring Saturation Reactions	189
V. B.	Catalyst Activity	192
V. C.	Quinoline Hydrodenitrogenation Kinetics	198
V. C. 1.	Relevant Plug-Flow Reactor Equations	198
V. C. 2.	Qualitative Discussion	203
V. D.	Behavior of the Quinoline/Py-Tetrahydroquinoline Product Ratio	208
V. E.	Kinetic Modelling	216
V. E. 1.	Kinetics of o-Propylaniline HDN	219
V. E. 2.	Kinetics of the Hydrogenolysis Reactions in Quinoline HDN	225
VI.	Conclusions	236
VI. A.	Catalyst Activity	236
VI. B.	Hydrodenitrogenation of o-Propylaniline	236
VI. C.	Hydrodenitrogenation of Quinoline	237
VII.	Appendix	239
VII. A.	Physical Properties of Some Relevant Compounds	240
VII. B.	Specifications for Chemicals Used	241
VII. C.	Estimated Standard Free Energies of Formation	242

VII. D. Metering Pump Calibration Curves	244
VII. E. Gas Chromatographic Detector Response Factors	247
VII. F. Data Reduction Sample Calculations	249
VII. G. Summary of Data and Calculated Values	253
VII. H. Location of Original Data	284
Bibliography	285

List of Figures

1-1	Quinoline HDN Reaction Network	54
1-2	Quinoline/Py-Tetrahydroquinoline Equilibrium	55
1-3	Schematic of Experimental Apparatus	56
1-4	Catalyst Deactivation During Quinoline HDN - Severe Standard Conditions	57
1-5	Quinoline Denitrogenation at 420°C	58
1-6	Quinoline and Py-Tetrahydroquinoline Denitrogenation at 375°C	59
1-7	Product Distributions for Quinoline HDN at 420°C, 3.55 MPa, 13.3 kPa Q (Run 20)	60
1-8	Product Distributions for Quinoline HDN at 420°C, 3.55 MPa, 26.7 kPa Q (Run 19)	61
1-9	Product Distributions for Quinoline HDN at 420°C, 7.0 MPa, 26.7 kPa Q (Run 21)	62
1-10	Product Distributions for Quinoline HDN at 375°C, 7.0 MPa, 13.3 kPa Q (Run 23)	63
1-11	Product Distributions for Py-Tetrahydro- quinoline HDN at 375°C, 7.0 MPa, 13.3 kPa PyTHQ (Run 33)	64
1-12	o-Propylaniline Denitrogenation at 7.0 MPa	65
1-13	Denitrogenation of Individual Nitrogen Compounds at 375°C, 7.0 MPa, 13.3 kPa Feed Partial Pressure	66
1-14	Product Distributions for Bz-Tetrahydro- quinoline HDN at 375°C, 7.0 MPa, 13.3 kPa BzTHQ (Run 35)	67
1-15	Product Distributions for Decahydro- quinoline HDN at 375°C, 7.0 MPa, 13.3 kPa DHQ (Run 38)	68

1-16	Estimated Equilibria Among Quinoline, Tetrahydroquinolines, and Decahydroquinoline at 3.53 MPa Hydrogen Partial Pressure	69
1-17	Estimated Equilibria Among Quinoline, Tetrahydroquinolines, and Decahydroquinoline at 6.98 MPa Hydrogen Partial Pressure	70
1-18	Hydrogen Consumption in Quinoline HDN During Catalyst Deactivation - Severe Standard Conditions	71
1-19	Behavior of Q/PyTHQ Product Ratio in Quinoline HDN (13.3 kPa Q)	72
1-20	Comparison of Langmuir-Hinshelwood Kinetic Models for o-Propylaniline Denitrogenation at 375°C and 7.0 MPa	73
1-21	Arrhenius Plot of the Pseudo Rate Constant for o-Propylaniline Denitrogenation	74
1-22	Arrhenius Plot of the Pseudo Rate Constant for Hydrogenolysis of Py-Tetrahydroquinoline to o-Propylaniline	75
1-23	Arrhenius Plot of the Pseudo Rate Constant for Hydrogenolysis of Decahydroquinoline to Hydrocarbons and Ammonia	76
2-1	Quinoline HDN Reaction Network	95
2-2	Equilibrium Constants for Initial Ring Saturation Reactions in Quinoline HDN	96
2-3	Equilibrium Constants for Hydrogenolysis Reactions in Quinoline HDN	97
2-4	Equilibrium Constants for Miscellaneous Reactions in Quinoline HDN	98
2-5	Quinoline/Py-Tetrahydroquinoline Equilibrium	101
3-1	Schematic of Experimental Apparatus	104
3-2	Chromatogram Illustrating Separation of Products from Quinoline HDN	116

4-1	Catalyst Deactivation During Quinoline HDN - Mild Standard Conditions	132
4-2	Catalyst Deactivation During Quinoline HDN - Severe Standard Conditions	133
4-3	Catalyst Deactivation During Quinoline HDN	134
4-4	Changes in Quinoline HDN Product Distribution During Catalyst Deactivation - Mild Standard Conditions	136
4-5	Changes in Quinoline HDN Product Distribution During Catalyst Deactivation - Severe Standard Conditions	137
4-6	Quinoline Denitrogenation at 420°C	139
4-7	Quinoline and Py-Tetrahydroquinoline Denitrogenation at 375°C	141
4-8	Quinoline and Py-Tetrahydroquinoline Denitrogenation at 330°C	142
4-9	Product Distributions for Quinoline HDN at 420°C, 3.55 MPa, 13.3 kPa Q (Run 20)	144
4-10	Product Distributions for Quinoline HDN at 420°C, 3.55 MPa, 26.7 kPa Q (Run 19)	145
4-11	Product Distributions for Quinoline HDN at 420°C, 7.0 MPa, 13.3 kPa Q (Run 22)	146
4-12	Product Distributions for Quinoline HDN at 420°C, 7.0 MPa, 26.7 kPa Q (Run 21)	147
4-13	Product Distributions for Quinoline HDN at 375°C, 3.55 MPa, 13.3 kPa Q (Run 18)	149
4-14	Product Distributions for Quinoline HDN at 375°C, 7.0 MPa, 13.3 kPa Q (Run 23)	150
4-15	Product Distributions for Quinoline HDN at 375°C, 7.0 MPa, 26.7 kPa Q (Run 24)	151
4-16	Product Distributions for Py-Tetra- hydroquinoline HDN at 375°C, 7.0 MPa, 13.3 kPa PyTHQ (Run 33)	153

4-17	Product Distributions for Quinoline HDN at 330°C, 3.55 MPa, 13.3 kPa Q (Run 25)	154
4-18	Product Distributions for Quinoline HDN at 330°C, 7.0 MPa, 13.3 kPa Q (Run 26)	155
4-19	Product Distributions for Py-Tetrahydroquinoline HDN at 330°C, 3.55 MPa, 13.3 kPa PyTHQ (Run 34)	156
4-20	Propylbenzene/Propylcyclohexane Equilibrium	159
4-21	o-Propylaniline Denitrogenation at 7.0 MPa	161
4-22	o-Propylaniline Denitrogenation at 375°C	163
4-23	Denitrogenation of Individual Nitrogen Compounds at 375°C, 7.0 MPa, 13.3 kPa Feed Partial Pressure	166
4-24	Product Distributions for Bz-Tetrahydroquinoline HDN at 375°C, 7.0 MPa, 13.3 kPa BzTHQ (Run 35)	167
4-25	Product Distributions for Bz-Tetrahydroquinoline HDN at 330°C, 3.55 MPa, 13.3 kPa BzTHQ (Run 36)	169
4-26	Product Distributions for Decahydroquinoline HDN at 375°C, 7.0 MPa, 13.3 kPa DHQ (Run 38)	170
4-27	Propylbenzene Hydrogenation at 375°C, 7.0 MPa, 13.3 kPa PB (Run 16)	172
4-28	Estimation of Equilibrium Q/BzTHQ and PyTHQ/DHQ Ratios at 375°C and 7.0 MPa from Experimental Data	177
4-29	Comparison of Experimental and Theoretical Estimates of Equilibrium Constants for Hydrogenation of Quinoline to Tetrahydroquinolines	179

4-30	Comparison of Experimental and Theoretical Estimates of Equilibrium Constants for Hydrogenation of Tetrahydroquinolines to Decahydroquinoline	180
4-31	Estimated Equilibria Among Quinoline, Tetrahydroquinolines, and Decahydroquinoline at 3.53 MPa Hydrogen Partial Pressure	182
4-32	Estimated Equilibria Among Quinoline, Tetrahydroquinolines, and Decahydroquinoline at 6.98 MPa Hydrogen Partial Pressure	183
5-1	Quinoline HDN Reaction Network	186
5-2	Hydrogen Consumption in Quinoline HDN During Catalyst Deactivation - Mild Standard Conditions	194
5-3	Hydrogen Consumption in Quinoline HDN During Catalyst Deactivation - Severe Standard Conditions	195
5-4	Behavior of Q/PyTHQ Product Ratio in Quinoline HDN (13.3 kPa Q)	209
5-5	Comparison of Langmuir-Hinshelwood Kinetic Models for o-Propylaniline Denitrogenation at 375°C and 7.0 MPa	222
5-6	Arrhenius Plot of the Pseudo Rate Constant for o-Propylaniline Denitrogenation	224
5-7	Arrhenius Plot of the Pseudo Rate Constant for Hydrogenolysis of Py-Tetrahydroquinoline to o-Propylaniline	230
5-8	Arrhenius Plot of the Pseudo Rate Constant for Hydrogenolysis of Decahydroquinoline to Hydrocarbons and Ammonia	231
7-1	Metering Pump Calibration for 2 cc/hr Range	245

7-2	Metering Pump Calibration for 8 cc/hr Range	246
7-3	Detector Response Factors for Gas Chromatographic Analysis of Quinoline HDN Products	248

List of Tables

2-1	Typical Sulfur and Nitrogen Contents of Petroleum and Synthetic Liquids	78
2-2	Representative Heterocyclic Nitrogen Compounds in Petroleum and Synthetic Liquids	80
2-3	Reaction Conditions for Hydro- desulfurization of Petroleum Fractions	82
3-1	Typical Properties of American Cyanamid AERO HDS-3A Catalyst	119
3-2	Catalyst Sulfiding Procedures	121
4-1	Quinoline HDN Without NiMo/Al ₂ O ₃ Catalyst ("Blank" Experiment-Run 39)	174

I. Summary

I. A. Introduction

As energy demand increases and the availability of petroleum decreases, it will become necessary to process residual petroleum fractions and liquids derived from coal, oil shale, and tar sand, which contain much higher concentrations of organic nitrogen compounds than most petroleum processed today. Organic nitrogen compounds poison the acidic catalysts used in processes such as cracking and reforming, impart undesirable properties to refined products, and, unless in low concentration in fuels, can lead to unacceptably high levels of NO_x in combustion gases. The nitrogen compounds in petroleum and synthetic liquids are primarily unsaturated heterocyclic structures, which distribute by boiling point in the various distillate fractions.

In petroleum refining, hydrotreating processes are used extensively to remove heteroatoms (sulfur, nitrogen, oxygen, and metals) from their organic combinations, but hydrodesulfurization has been by far the most important application. Nitrogen removal by hydrodenitrogenation (HDN) occurs to some extent during hydrodesulfurization, but this has been of secondary importance due to the low nitrogen content of petroleum processed to date. However,

nitrogen removal is generally more difficult than sulfur removal, so hydrodenitrogenation could well become one of the limiting problems in processing high-nitrogen synthetic liquids.

I. B. Objectives

The present study focused on HDN of quinoline, a heterocyclic nitrogen compound representative of those found in middle distillate fractions of petroleum and synthetic liquids. Quinoline is a particularly good model compound for HDN studies as it contains an aromatic ring as well as the heterocyclic ring, thus providing the opportunity to examine catalyst selectivity. It was desired to determine in detail the kinetics of quinoline HDN under industrially relevant reaction conditions, to obtain a better fundamental understanding of the reaction network and the nature of the catalytic action. The basic approach was to determine the effects of reaction variables on product distribution not only from quinoline HDN but also from HDN of each of the nitrogen-bearing intermediates in the reaction network.

I. C. Literature Review

I. C. 1. Hydrotreating Catalysts

Most hydrotreating catalysts consist of a major metal component such as molybdenum or tungsten and a promoter, usually cobalt or nickel, supported on alumina. The metals are generally present as oxides in the fresh catalyst, but are converted to sulfides either in a pretreatment step or in actual operation where organic sulfur compounds and H_2S are present. Also, a properly sulfided catalyst is more active for HDN than the oxidic or reduced form of the catalyst. The most widely used desulfurization catalyst is $CoMo/Al_2O_3$, but $NiMo/Al_2O_3$ is more active for denitrogenation.

Hydrotreating catalysts are bifunctional in that they possess both hydrogenation and hydrogenolysis activity. The hydrogenation activity of the catalyst is believed to be associated with the metal sulfides, while the hydrogenolysis activity could be due to acidic support sites or to interaction between the support and metal sulfides (Weisser and Landa, 1973). The surface acidity of sulfide catalysts is known to affect catalyst activity and selectivity, and this acidity can be associated with the metal sulfides as well as with the alumina support.

I. C. 2. Hydrodenitrogenation Studies

Model compound studies have shown that hydrodenitrogenation of heterocyclic nitrogen compounds proceeds via saturation (hydrogenation) of the heterocyclic ring, followed by hydrogenolysis of C-N bonds to first open the heteroring and then convert the resulting aliphatic or aromatic amine intermediates to hydrocarbons and ammonia. Under HDN reaction conditions, hydrogenolysis of C-N bonds is essentially irreversible, but saturation of heterocyclic rings is potentially reversible or thermodynamically limited (Cocchetto, 1974; Cocchetto and Satterfield, 1976). Thermodynamic limitation on heterocyclic ring saturation can adversely affect the overall HDN rate if the kinetics of the various reaction steps are such that heterocyclic ring opening is substantially rate-limiting (Satterfield and Cocchetto, 1975). In general, both hydrogenation and hydrogenolysis rates may be important in determining the overall HDN rate, though their relative importance is undoubtedly a function of reaction conditions, catalyst employed, and nature of the nitrogen compound.

Relatively few quinoline HDN studies have been reported. Doelman and Vlugter (1963) used a prereduced CoMo/Al₂O₃ catalyst and concluded that nitrogen removal from quinoline proceeded primarily through Py-tetrahydroquinoline (PyTHQ) and various aniline intermediates, with breakdown of the

anilines as the rate-determining step. With the same catalyst, Madkour et al. (1969) observed a significant increase in the quinoline HDN rate when large excesses of hydrogen chloride were present, due to acceleration of the hydrogenolysis reactions. Aboul-Gheit and Abdou (1973) concluded that hydrogenolysis of PyTHQ was the rate-determining step in quinoline HDN with oxidic $\text{CoMo}/\text{Al}_2\text{O}_3$, and postulated that the basicity of nitrogen compounds plays a role in their HDN mechanisms. More recently, Satterfield and co-workers at M.I.T. studied quinoline HDN in a vapor-phase reactor with presulfided $\text{NiMo}/\text{Al}_2\text{O}_3$ catalyst, and observed rapid equilibration between quinoline and PyTHQ at all reaction conditions (Declerck, 1976; Satterfield et al., 1978). At lower temperatures this equilibrium favored PyTHQ, which was then converted to either o-propylaniline (OPA) or decahydroquinoline (DHQ), but at higher temperatures the conversion rate of quinoline to Bz-tetrahydroquinoline (BzTHQ) and subsequently to DHQ became significant. Shih et al. (1977) investigated the kinetics of quinoline HDN in a batch liquid-phase (slurry) reactor employing sulfided $\text{NiMo}/\text{Al}_2\text{O}_3$ catalyst and a paraffinic white oil carrier liquid. They, too, observed rapid equilibration between quinoline and PyTHQ, but the other hydrogenation reactions as well as the hydrogenolysis reactions were reported to be kinetically controlled. These reaction rates were each

modelled by first order kinetics, and the corresponding rate constants were determined by a computer fitting technique. It was concluded from the kinetic analysis that nitrogen removal occurred primarily through the BzTHQ and DHQ intermediates.

The rates of HDN reactions have often been adequately described by first order kinetics, in which the first order rate constant decreases with increased initial nitrogen concentration, or by pseudo first order kinetics (Flinn et al., 1963; Sonnemans et al., 1973; Shih et al., 1977). This behavior is the result of inhibition of the reaction rates by the strongly adsorbed nitrogen compounds, and can be interpreted through a Langmuir-Hinshelwood kinetic model assuming equal adsorptivities of the nitrogen compounds. However, some HDN reaction studies as well as adsorption studies indicate that the strength of adsorption of nitrogen compounds may vary significantly. In a study of shale oil HDN, for example, Koros et al. (1967) found that indole-type compounds were less reactive than the quinolines, but the opposite reactivities have been reported for indole and quinoline when studied separately (Flinn et al., 1963; Aboul-Gheit and Abdou, 1973). This apparent discrepancy was attributed to competitive adsorption effects in mixtures, in which the more basic quinoline-type compounds were preferentially adsorbed and converted. Reaction and adsorption studies also suggest that hydrogen and the nitrogen compounds adsorb on different, perhaps

neighboring, catalyst sites, while the adsorption of hydrocarbons is relatively weak and can usually be neglected (Sonnemans et al., 1973).

I. D. Quinoline Hydrodenitrogenation Reaction Network and Thermodynamics

The reaction network for quinoline HDN is shown in Figure 1-1. This network is consistent with the results of the present investigation, and, except for consideration of the reversibility of all the initial ring saturation reactions, is basically in agreement with the less detailed reaction networks proposed in earlier studies (Shih et al., 1977; Satterfield et al., 1978). Note that in addition to the reactions of the heterocyclic ring, the aromatic ring can also be saturated, either as the initial reaction step or during the nitrogen removal process. Standard free energies of formation for the organic nitrogen compounds were estimated by group contribution techniques, and equilibrium constants for each reaction in the quinoline HDN network were then estimated. The initial ring saturation reactions are all reversible over a wide range of HDN conditions. Lower temperature and increased hydrogen partial pressure shift each of these equilibria toward the saturated species. This is exemplified in Figure 1-2 for the quinoline/PyTHQ equilibrium, the behavior of which has been well established from previous experimental

studies (Declerck, 1976; Satterfield et al., 1978; Shih et al., 1977). In contrast, the hydrogenolysis reactions are essentially irreversible under HDN conditions, since their equilibrium constants are very large. Saturation of OPA and the reactions involving propylcyclohexene (PCHE) can also be considered irreversible reactions, at least under the reaction conditions of the present study.

I. E. Experimental Apparatus and Procedure

The HDN studies were carried out in a continuous flow, fixed-bed catalytic reactor system employing a presulfided commercial NiMo/Al₂O₃ hydrotreating catalyst (American Cyanamid AERO HDS-3A, containing about 3 wt. % NiO and 15 wt. % MoO₃). A schematic of the experimental apparatus is shown in Figure 1-3; the heavy lines indicate the primary flows during steady-state operation. Liquid reactant (quinoline or one of its hydrogenated derivatives) was metered into the system with a high-pressure pump, and was flash-vaporized into a stream of heated hydrogen. The resulting vapor-phase mixture was preheated to reaction temperature, and fed downward through the vertically mounted reactor. The final preheating coil and the reactor were both immersed in a fluidized sand bed heater for controlled isothermal operation. The reactor was a 3.86 mm ID

stainless steel tube, packed with 1.5 grams of 20/24 mesh catalyst particles (0.774 mm average diameter). A single charge of catalyst was used for all experiments reported here. Reactor pressure was maintained at the desired level by the reactant hydrogen cylinder regulator, and total flow rate through the system was controlled with a very fine metering valve downstream from the reactor. Flow through this valve was accompanied by a pressure drop from reactor pressure (3.55 or 7.0 MPa) to nearly atmospheric pressure. Soap-film flowmeters were used to measure exhaust gas flow rates, which varied from about 100 to 4000 standard cc/min.

The tar trap in the reactor exit line was maintained at approximately 240°C - a temperature too high to condense any of the reactants or major reaction products, but sufficiently low to condense very high-boiling "tar" compounds that would otherwise have condensed in cooler downstream portions of the apparatus, particularly in the analytical system.

Vapor-phase samples of the reactor effluent were injected into an on-line gas chromatograph by means of a heated gas sampling valve. The gas chromatograph was equipped with a thermal conductivity detector, dual columns, and temperature programming capability. A 10-ft X 2 mm ID glass column packed with 10% SP-2300 on Chromosorb T (a Teflon support) was used for separation of reaction products. The relatively inert Teflon support virtually eliminated the "tailing" of basic amines,

particularly ammonia, observed with more conventional diatomite supports. Absolute detector response factors were determined by injecting known quantities of the relevant compounds into the gas chromatograph and measuring the corresponding peak areas, at the same conditions used for analysis of reactor effluent samples.

An experimental run consisted of the determination of steady-state product distributions for the reactant compound under study, at typically five different feed rates, for a constant reactor temperature, pressure, and feed composition. A run was started by heating the reactor to the desired temperature (330, 375, or 420°C) under an argon purge, and then pressurizing with hydrogen to 3.55 MPa or 7.0 MPa. Hydrogen flow was established, and liquid feed was commenced only after system temperatures had been adjusted to prevent condensation. The system was started up at the highest feed rates to be studied during the run, to minimize the time required to reach steady state. A set of 3 to 5 steady-state samples was taken over a period of 1.5 to 2.5 hours, and analyzed. The hydrogen and liquid feed rates were then reduced in the same proportion, and after a one hour re-equilibration period, another set of steady-state samples was taken. This procedure was repeated for each of the remaining feed rates to be studied.

After the last set of samples had been taken, the feeds were stopped, the system was depressurized, and the reactor temperature was adjusted to 350°C in preparation for catalyst resulfiding. Since sulfur compounds were not present (intentionally) in the reactor feed, the catalyst was resulfided with a 10% H₂S in H₂ mixture after each run, to maintain reproducible activity. The duration of an experimental run was typically 16 to 18 hours.

The averaged component peak areas from each set of steady state samples were converted to the equivalent number of moles of each component. The product distribution was then calculated for each set of reaction conditions.

I. F. Results

The effects of reaction variables on nitrogen removal and on product distribution from HDN of quinoline and each individual nitrogen-bearing intermediate (PyTHQ, BzTHQ, DHQ, and OPA) in the reaction network will be presented. The reaction variables investigated are summarized below.

Temperature: 330°C, 375°C, 420°C

Total pressure: 3.55 MPa (500 psig or 35 atm)

7.0 MPa (1000 psig or 69 atm)

Reactant partial pressure: 13.3 kPa (0.13 atm)

26.7 kPa (0.26 atm)

W/F_{i_o}: 41.7 to 667 hr g catalyst/g-mol i

In this study, hydrogen partial pressure and total pressure were essentially the same. The reactor time variable most appropriate for presentation of results and for quantitative kinetic analysis is W/F_{i_0} , where W was the mass of virgin catalyst (before sulfiding) in the reactor and F_{i_0} was the molar feed rate of the reactant nitrogen compound to the reactor. At constant reactor temperature, total pressure, and W/F_{i_0} , different initial partial pressures of reactant corresponded to different hydrogen feed rates.

Nitrogen removal, or denitrogenation, is defined here as the mole percentage of the reactant nitrogen compound converted to pure hydrocarbons. The product distributions are calculated on the basis of organic products only (i.e. on an ammonia-free basis), so the mole percentage of each organic product (including, of course, unconverted reactant) is equivalent to the mole percentage of the reactant converted into that product, if minor side reactions such as coking are neglected. Due to limitations on the quantity of data that can be presented clearly in a single graph, however, only the organic nitrogen compounds are shown in the graphical product distributions.

I. F. 1. Catalyst Activity

The activity of the presulfided NiMo/Al₂O₃ catalyst was checked periodically by reacting quinoline at carefully selected standard conditions. The degree of nitrogen removal was used as a simple measure of overall catalyst activity. Significant deactivation of the catalyst was observed (see Figure 1-4). At 375°C, 7.0 MPa, 13.3 kPa Q, and 667 hr g catalyst/g-mol Q, complete denitrogenation was achieved with 116 hour-old catalyst, but only 65% nitrogen removal was attained after 340 hours of catalyst use. The catalyst finally reached a stable level of activity (corresponding to about 45% denitrogenation) after approximately 400 hours on stream, at which time the quinoline HDN product distribution at standard conditions also stabilized.

In each of two experimental runs at different reaction conditions, data taken at the beginning of the run were reproduced at the end of the same run. This is evidence that no significant catalyst deactivation (as by sulfur loss) took place during individual experimental runs, at least not after the catalyst had been used for 340 hours. Thus catalyst activity can safely be eliminated as a variable in the HDN kinetic experiments, essentially all of which were conducted after 400 hours of catalyst use.

I. F. 2. Hydrodenitrogenation of Quinoline and
Py-Tetrahydroquinoline

Figures 1-5 and 1-6 summarize the effects of reaction variables on nitrogen removal from quinoline. The percent denitrogenation was quite insensitive to initial quinoline partial pressure at constant temperature, hydrogen pressure, and W/F_{Q_0} . For each quinoline feed rate, doubling the hydrogen pressure increased nitrogen removal by a factor of about four at 420°C, but the effect was less dramatic at lower temperatures. Quinoline denitrogenation was very sensitive to temperature; at 7.0 MPa and 667 hr g catalyst/g-mol Q, nitrogen removal increased from only 6% at 330°C (not shown here) to 42% at 375°C, and was 100% at 420°C. Note that the same percent denitrogenation was achieved for either quinoline or PyTHQ feed, at the same reaction conditions.

Some of the HDN product distributions corresponding to the denitrogenation results just presented are shown in Figures 1-7 through 1-11. In general, quinoline HDN product distributions were relatively unaffected by changes in initial quinoline partial pressure (compare, for example, Figures 1-7 and 1-8). As W/F_{Q_0} increased, the concentrations of PyTHQ, BzTHQ, and DHQ intermediates each passed through a maximum, as did the OPA concentration at the most extreme reaction conditions where complete denitrogenation was observed. The Q/PyTHQ product ratio

during each of the 420°C runs was nearly constant, at essentially the equilibrium ratio. This equilibrium was much more favorable toward PyTHQ at the higher hydrogen pressure, which also favored DHQ relative to the tetrahydroquinolines (compare Figures 1-8 and 1-9). One would expect lower temperatures to favor the hydrogenated species in each of the initial ring saturation equilibria, and the product distributions from quinoline HDN at 375°C and 420°C are consistent with this expectation (compare Figures 1-9 and 1-10). At 375°C, quinoline was rapidly hydrogenated to an equilibrium amount of PyTHQ, but as W/F_{Q_0} increased, the amount of unreacted quinoline levelled off while the amount of PyTHQ in the products decreased quite rapidly (see Figure 1-10). In other words, quinoline and PyTHQ were in equilibrium at the shortest reaction times (lowest W/F_{Q_0}), but did not remain in equilibrium at longer reaction times. Product distributions for either quinoline or PyTHQ HDN at 375°C and 7.0 MPa were essentially the same (compare Figures 1-10 and 1-11); thus the peculiar behavior of the Q/PyTHQ product ratio was observed with PyTHQ feed as well.

I. F. 3. Hydrodenitrogenation of o-Propylaniline

Figure 1-12 illustrates the effects of reaction variables on nitrogen removal from OPA at 7.0 MPa total pressure. Doubling the partial pressure of OPA from 13.3

kPa to 26.7 kPa in the reactor feed, at constant W/F_{OPA_0} , had no effect on percent nitrogen removal at 375°C. The rate of denitrogenation of OPA increased significantly with temperature, and also with hydrogen pressure (not shown here). No heterocyclic nitrogen compounds were detected in the products from OPA HDN, as expected.

I. F. 4. Hydrodenitrogenation of Bz-Tetrahydroquinoline and Decahydroquinoline

The percent denitrogenation of BzTHQ or DHQ at 375°C and 7.0 MPa is shown as a function of W/F_{i_0} in Figure 1-13. Similar results previously presented for quinoline, PyTHQ, or OPA feed at the same reaction conditions are also shown for comparison. It is apparent that nitrogen removal from DHQ was significantly easier than from BzTHQ, while the compounds most resistant to denitrogenation were quinoline and PyTHQ. The most striking result was the relative ease with which OPA denitrogenated compared to the heterocyclic nitrogen compounds.

The distribution of nitrogen-bearing products from BzTHQ HDN at 375°C and 7.0 MPa is shown in Figure 1-14. BzTHQ hydrogenated quite rapidly to DHQ, from which hydrocarbon products were formed. The concentration of DHQ went through a maximum as W/F_{BzTHQ_0} increased, reflecting its role as a reaction intermediate. Some

dehydrogenation of BzTHQ or DHQ occurred, as evidenced by the formation of quinoline and PyTHQ. Figure 1-15 illustrates the product distribution from DHQ HDN at 375°C and 7.0 MPa. The DHQ was simultaneously converted to hydrocarbon products and dehydrogenated to BzTHQ. Some dehydrogenation of DHQ to PyTHQ occurred to a lesser extent, but no OPA and only traces of quinoline were detected in the reaction products. A distinct maximum in BzTHQ formation was observed as W/F_{DHQ_0} increased. This most likely reflects an approach to hydrogenation/dehydrogenation equilibrium between BzTHQ and DHQ, since BzTHQ was not converted to any other products.

I. F. 5. Hydrocarbon Products

The same hydrocarbons were formed from denitrogenation of OPA or each individual heterocyclic nitrogen compound, and the same qualitative behavior was observed. The dominant hydrocarbon product was always propylcyclohexane (PCH). Smaller amounts of propylbenzene (PB) and propylcyclohexene (PCHE) were also formed, while ethylcyclohexane (ECH) and ethylbenzene (EB) were detected only at the higher temperatures. As W/F_{i_0} increased, PCHE formation usually went through a maximum, in contrast to the behavior of the other hydrocarbon products. The PCHE/PB and PCHE/PCH product ratios exceeded the corresponding equilibrium ratios, particularly at lower W/F_{i_0} . In

addition, PCH and PB were not formed in equilibrium amounts; at some reaction conditions the PCH/PB product ratio was less than the equilibrium ratio, but at other conditions the corresponding equilibrium ratio was exceeded. At the same reaction conditions, denitrogenation of BzTHQ or DHQ yielded a somewhat higher PCH/PB product ratio than did denitrogenation of quinoline, PyTHQ, or especially OPA.

I. F. 6. Homogeneous Reaction

A key experiment was conducted in which quinoline was exposed to a variety of HDN reaction conditions in the absence of the NiMo/Al₂O₃ catalyst. Even at the most severe reaction conditions (420°C, 7.0 MPa, and a quinoline feed rate corresponding to 667 hr g catalyst/g-mol Q), only the hydrogenation of quinoline to PyTHQ took place "homogeneously" at an appreciable rate, but equilibrium was not attained. It is not clear whether this reaction was truly homogeneous (occurring in the gas phase) or was catalyzed by the stainless steel surfaces of the preheater and reactor walls. For a quinoline feed rate corresponding to 667 hr g catalyst/g-mol Q, "homogeneous" reaction at 7.0 MPa resulted in a 41%, 63%, and 79% approach to Q/PyTHQ equilibrium at 330°C, 375°C, and 420°C, respectively. This was in sharp contrast to

the rapid equilibration of quinoline and PyTHQ at all reaction conditions, in the presence of the NiMo/Al₂O₃ catalyst.

I. F. 7. Initial Ring Saturation Equilibria

Each of the heterocyclic nitrogen compounds was studied separately at 375°C and 7.0 MPa, so each of the initial ring saturation equilibria was approached from both sides at these reaction conditions. For example, with PyTHQ feed the PyTHQ/DHQ equilibrium was approached via hydrogenation of PyTHQ to DHQ; with DHQ feed, the same equilibrium was approached via dehydrogenation of DHQ to PyTHQ. Though the initial ring saturation equilibria were not approached from both sides at all reaction conditions, careful examination of the ratios of saturated to unsaturated species in the HDN products as a function of feed nitrogen compound, W/F_{i_0} , temperature, and hydrogen pressure provided estimates of the positions of these equilibria at other reaction conditions. A self-consistent set of equilibrium constants for the ring saturation reactions were then derived from these data, with the guidance of the relatively accurate standard heats of reaction provided by theoretical estimates of the equilibrium constants (calculated from estimated standard free energies of formation). The equilibrium constants estimated from the experimental data are much more reliable than the

theoretical estimates, as the latter could be in error by one to two orders of magnitude.

The experimental estimates of the ring saturation reaction equilibrium constants were used to estimate the equilibrium composition of the heterocyclics (Q, PyTHQ, BzTHQ, and DHQ) as a function of temperature, at each of the two hydrogen partial pressures employed in this study. Ideal gas behavior was assumed in the calculations, and the results are shown in Figures 1-16 and 1-17. The thermodynamics favor DHQ at lower temperature and higher hydrogen pressure, while quinoline is favored at higher temperature and lower hydrogen pressure. The equilibrium behavior of the tetrahydroquinolines is more complex, since they are partially saturated species subject to either hydrogenation or dehydrogenation. Thus at constant hydrogen partial pressure, the equilibrium concentration of PyTHQ or BzTHQ proceeds through a maximum as temperature increases. Also, the equilibrium concentration of PyTHQ or BzTHQ may either increase or decrease with hydrogen pressure, depending on the temperature. It is noteworthy that under HDN conditions, BzTHQ is thermodynamically more stable than PyTHQ.

I. G. Discussion of Results

I. G. 1. Quinoline Hydrodenitrogenation Reaction Network and Thermodynamics

The quinoline HDN reaction network proposed in Figure 1-1 is well supported by the experimental results. Propylcyclohexylamine (PCHA) was not detected in the HDN products, but is a plausible reaction intermediate which presumably denitrogenated very rapidly. Similar compounds, such as cyclohexylamine and ethylcyclohexylamine, have been shown to denitrogenate readily under HDN conditions (Stengler et al., 1964; Stern, 1979). The behavior of the hydrocarbon products indicates that PCHE was formed by elimination of ammonia from PCHA, a reaction known to occur with aliphatic amines. In addition, PCHE was a reaction intermediate, converted to either PB or PCH. Formation of PB from DHQ HDN must be attributed to dehydrogenation of PCHE, since no OPA was formed (see Figure 1-15). It is unlikely that PB and PCH were reactive in the presence of the strongly adsorbed nitrogen compounds. Instead, PB and PCH were formed by parallel reactions, and their ratio was controlled primarily by kinetics rather than by thermodynamics.

Reaction of each individual heterocyclic nitrogen compound resulted in the formation of all the other heterocyclics, confirming the predicted reversibility of

the initial ring saturation reactions. Only small quantities of quinoline were found in the products from BzTHQ or DHQ HDN at 375°C and 7.0 MPa, since quinoline formation was thermodynamically unfavorable (see Figure 1-17). The heterocyclics can equilibrate under HDN conditions only if the hydrogenation/dehydrogenation reactions are fast relative to the PyTHQ and DHQ hydrogenolysis reactions. In this study, partial equilibration of the heterocyclics was observed at some reaction conditions, but in general the initial ring saturation reactions were subject to complex interactions between kinetics and thermodynamics.

In commercial hydrotreating processes aimed at nitrogen removal, it is desirable to minimize hydrogen consumption for economic reasons. The equilibrium behavior of the heterocyclics has significant implications in this regard. For quinoline HDN, particularly at the higher hydrogen pressures required to achieve satisfactory HDN rates, the thermodynamics favor oversaturation to DHQ (see Figure 1-17). In addition, saturation of the aromatic ring is thermodynamically more favorable than saturation of the heteroring. These results can most likely be extended, at least qualitatively, to other multiring heterocyclic nitrogen compounds such as acridine and carbazole. Thus the burden of selectively hydrogenating only the heterorings is placed solely on the HDN catalyst.

I. G. 2. Catalyst Activity

Significant deactivation of the presulfided NiMo/Al₂O₃ catalyst was observed during its first 400 hours of use for quinoline HDN (see Figure 1-4), but the relative changes in hydrogenation and hydrogenolysis activities of the catalyst are not readily apparent from the changes in product distribution that occurred. However, from the quinoline HDN product distribution and a knowledge of the reaction network, one can calculate the separate amounts of hydrogen consumed in saturation and in hydrogenolysis reactions, as measures of the hydrogenation and hydrogenolysis activities of the catalyst. During catalyst deactivation, hydrogenolysis activity decreased by nearly 60% while there was only a 20% loss in hydrogenation activity (see Figure 1-18). This markedly different behavior of the hydrogenation and hydrogenolysis activities is experimental evidence, albeit indirect, that these functionalities are associated with different catalyst sites.

The deactivation of the catalyst was most likely due to the accumulation of carbonaceous deposits (coke) on the surface. A theory advanced by Beuther and Larson (1965) to explain the deactivation of hydrocracking catalysts seems to be applicable to the NiMo/Al₂O₃ catalyst as well. It is postulated that during deactivation, coking eventually occurs on all hydrogenolysis sites not in the

vicinity of a "protective" hydrogenation site, which through its catalytic activity is much less susceptible to coking.

I. G. 3. Quinoline Hydrodenitrogenation Kinetics

In quinoline HDN, hydrocarbons and ammonia were formed from the DHQ and OPA reaction intermediates (PCHA presumably reacted as rapidly as it was formed). As a result, the percent denitrogenation versus W/F_{i_0} curves for quinoline, PyTHQ, or BzTHQ feed are S-shaped; the denitrogenation rates (slopes of the curves) were zero initially, increased with W/F_{i_0} as the concentrations of DHQ and OPA increased, and eventually decreased at high W/F_{i_0} as the concentrations of intermediates, particularly DHQ, decreased and the ammonia concentrations became significant (see Figures 1-13, 1-10, 1-11 and 1-14). For HDN of DHQ or OPA, the percent denitrogenation versus W/F_{i_0} curve is concave downward; the denitrogenation rate was highest initially, and decreased with W/F_{i_0} as the concentration of DHQ or OPA decreased (see Figures 1-13 and 1-15).

As can be seen from Figure 1-13, nitrogen removal from DHQ was substantially easier than from the other heterocyclics, since DHQ is already completely saturated and its hydrogenolysis rate was relatively high. For PyTHQ HDN at 375°C and 7.0 MPa, the primary reaction pathway for nitrogen removal was through the DHQ (rather than the OPA)

intermediate, since hydrogenation of PyTHQ to DHQ was much faster than hydrogenolysis of PyTHQ to OPA (see Figure 1-11). Comparison of Figures 1-11 and 1-14 reveals that the rate of hydrogenation of BzTHQ to DHQ was higher than the PyTHQ to DHQ hydrogenation rate. These factors account for the higher rates of nitrogen removal from BzTHQ than from PyTHQ (see Figure 1-13). For either quinoline or PyTHQ feed at the same reaction conditions, the same product distribution and percent denitrogenation were observed, as the Q/PyTHQ equilibrium was established very rapidly (compare Figures 1-10 and 1-11). This does not necessarily imply, however, that the equilibrium between quinoline and PyTHQ was maintained at longer reaction times (higher W/F_{i_0}).

At 375°C and 7.0 MPa, nitrogen removal from OPA was much easier than from any of the heterocyclics, when each compound was studied individually (see Figure 1-13). The dominant hydrocarbon product from OPA HDN was always PCH, indicating that hydrogenation of OPA (to PCHA) was much faster than its direct hydrogenolysis to PB. Resonance stabilization of the C-N bond in OPA is undoubtedly responsible for the relative difficulty of direct hydrogenolysis. Only low concentrations of OPA were observed in the products from reaction of each heterocyclic, as a result of the relatively slow hydrogenolysis of PyTHQ to OPA. However, in light of the high reactivity of OPA in the absence of the heterocyclics, the survival of even low

concentrations of OPA at long reaction times is somewhat surprising. Apparently, in the presence of sufficient concentrations of the heterocyclics, the active catalyst sites were not as accessible to OPA due to competitive adsorption effects.

Denitrogenation of quinoline occurred primarily through the DHQ intermediate, and PCH was always the major hydrocarbon product. Thus the presulfided NiMo/Al₂O₃ catalyst, a widely used commercial hydrotreating catalyst, exhibited little selectivity for the reaction pathway of minimum hydrogen consumption. At lower temperatures the heteroring in quinoline was selectively hydrogenated, at least initially (forming primarily PyTHQ instead of BzTHQ; see Figure 1-10), but the catalyst did not possess sufficient hydrogenolysis activity to readily convert the PyTHQ to OPA and then to PB and ammonia, so significant saturation of the aromatic ring also occurred. At 420°C, the hydrogenation rates of quinoline to PyTHQ and to BzTHQ were comparable, and DHQ was formed to a significant extent from BzTHQ as well as from PyTHQ (see Figures 1-7 through 1-9). The relatively low concentrations of DHQ in the products from quinoline HDN at 420°C are due to thermodynamic, rather than kinetic, limitations (see Figures 1-16 and 1-17).

I. G. 4. Behavior of the Quinoline/Py-Tetrahydroquinoline Product Ratio

In Figure 1-19, the relative amounts of quinoline and PyTHQ in the products from quinoline HDN are shown as a function of reaction conditions, and are compared with the corresponding equilibrium ratios (see Figure 1-2). The peculiar departure of the Q/PyTHQ product ratio from equilibrium at longer reaction times can be explained by competitive adsorption effects, if quinoline were more weakly adsorbed than PyTHQ and at least some of its reaction products (such as DHQ or ammonia). The active catalyst sites, for hydrogenation as well as hydrogenolysis, are most likely acidic in nature. Adsorption of nitrogen compounds is believed to occur through interaction of the basic nitrogen group with acidic sites on the catalyst, so the more basic nitrogen compounds are likely to be more strongly adsorbed. In quinoline HDN, the PyTHQ and DHQ reaction intermediates are the most basic species. Thus, after initial equilibration with PyTHQ, quinoline was prevented from adsorbing and reacting on the catalyst until the concentrations of PyTHQ and DHQ decreased significantly.

The more dramatic departure from Q/PyTHQ equilibrium at lower temperatures agrees well with the observed "homogeneous" hydrogenation of quinoline to PyTHQ in the absence of the NiMo/Al₂O₃ catalyst. Only at 420°C was the "homogeneous" reaction rate high enough to maintain Q/PyTHQ

equilibrium at longer reaction times.

I. G. 5. Kinetic Modelling

Consideration of the adsorption phenomena in quinoline HDN suggests that the catalytic reaction rates might best be described by Langmuir-Hinshelwood kinetic expressions, allowing for strong competitive adsorption of the nitrogen compounds. It is assumed that hydrogen and the nitrogen compounds adsorb on different catalyst sites, as suggested by adsorption measurements and other reaction studies (Sonnemans et al., 1973).

For OPA feed, the appropriate Langmuir-Hinshelwood rate expression is:

$$-r_{\text{OPA}} = r_{\text{HC}} = r_{\text{NH}_3} = \frac{k_1' K_{\text{OPA}} P_{\text{OPA}}}{1 + K_{\text{OPA}} P_{\text{OPA}} + K_{\text{NH}_3} P_{\text{NH}_3}}$$

where r_j is the net rate of formation of j , K_j and P_j are the adsorption equilibrium constant and partial pressure of j , and k_1' , which varies with both temperature and hydrogen pressure, is termed the pseudo rate constant for OPA denitrogenation. The "1" in the denominator of the above expression is assumed to be negligible, and a material balance over a differential element in the reactor gives:

$$-r_{\text{OPA}} = \frac{-1}{P_{\text{OPA}_0}} \frac{dP_{\text{OPA}}}{d(W/F_{\text{OPA}_0})} = \frac{k_1' P_{\text{OPA}}}{P_{\text{OPA}} + (K_{\text{NH}_3}/K_{\text{OPA}}) (P_{\text{OPA}_0} - P_{\text{OPA}})}$$

Note that if $K_{\text{NH}_3}/K_{\text{OPA}} = 1$ (equal adsorptivities of OPA and ammonia), a pseudo first order rate expression results, while zero order kinetics corresponds to $K_{\text{NH}_3}/K_{\text{OPA}} = 0$ (negligible adsorption of ammonia). Integration of this equation yields:

$$k_1' \left(\frac{W}{F_{\text{OPA}_0}} \right) = \left[1 - \left(\frac{K_{\text{NH}_3}}{K_{\text{OPA}}} \right) \right] X_{\text{OPA}} - \left(\frac{K_{\text{NH}_3}}{K_{\text{OPA}}} \right) \ln (1 - X_{\text{OPA}})$$

where X_{OPA} is the fractional conversion (disappearance) of OPA, equivalent to the fractional denitrogenation. This equation can be tested against the experimental data by plotting the right hand side as a function of W/F_{OPA_0} , at constant temperature and hydrogen pressure. The "best" value of $K_{\text{NH}_3}/K_{\text{OPA}}$ should result in a linear correlation, which passes through the origin; the pseudo rate constant is determined from the slope of this line. For OPA conversions greater than about 80%, pseudo first order kinetics predicts lower conversions than were actually observed (see Figure 1-20), suggesting that the ammonia product inhibited the denitrogenation rate less than the OPA reactant did ($K_{\text{NH}_3}/K_{\text{OPA}} < 1$). The "best" $K_{\text{NH}_3}/K_{\text{OPA}}$ value for correlating all of the OPA HDN data is 0.25, implying that OPA adsorbed about four times as strongly as ammonia on the active sites. Note that this kinetic model correctly predicts that percent denitrogenation is independent of initial OPA partial pressure, at constant temperature,

hydrogen pressure, and W/F_{OPA_0} (see Figures 1-12 and 1-20). The Arrhenius plot of the pseudo rate constants at 7.0 MPa is linear (see Figure 1-21), and the activation energy for denitrogenation of OPA is 79 kJ/g-mol (19 kcal/g-mol).

Knowledge of the OPA denitrogenation kinetics permits relatively easy determination of the kinetics of both PyTHQ hydrogenolysis (to OPA) and DHQ hydrogenolysis (to hydrocarbons and ammonia) from HDN data for any of the heterocyclics. The previous rate expression for OPA denitrogenation must, of course, be modified to allow for competitive adsorption of the heterocyclics as well as OPA and ammonia. The secondary amines PyTHQ and DHQ are assumed to adsorb equally strongly, with an adsorption equilibrium constant K_{SA} . Equal adsorptivities of the aromatic amines (Q, BzTHQ, and OPA) are likewise assumed, characterized by the adsorption constant K_{AA} . In the presence of heterocyclics, OPA is formed by hydrogenolysis of PyTHQ but is also converted to hydrocarbons and ammonia, so the net rate of formation of OPA is given by:

$$r_{\text{OPA}} = \frac{k_2' K_{\text{SA}}^{\text{P}} \text{PyTHQ} - k_1' K_{\text{AA}}^{\text{P}} \text{OPA}}{K_{\text{AA}}^{\text{P}} + K_{\text{SA}}^{\text{P}} + K_{\text{NH}_3}^{\text{P}}}$$

where k_2' is the pseudo rate constant for hydrogenolysis of PyTHQ to OPA, and the "1" in the denominator has again been neglected. This equation is more conveniently expressed in terms of dimensionless partial pressures, Y_j ($= P_j/P_{i_0}$):

$$r_{\text{OPA}} = \frac{dY_{\text{OPA}}}{d(W/F_{i_0})} = \frac{k_2'(K_{\text{SA}}/K_{\text{AA}})Y_{\text{PyTHQ}} - k_1'Y_{\text{OPA}}}{Y_{\text{AA}} + (K_{\text{SA}}/K_{\text{AA}})Y_{\text{SA}} + (K_{\text{NH}_3}/K_{\text{AA}})Y_{\text{NH}_3}}$$

For $K_{\text{NH}_3}/K_{\text{AA}} = 0.25$ and an assumed $K_{\text{SA}}/K_{\text{AA}}$ value, k_2' is derived by numerical integration of the above equation at constant temperature and hydrogen pressure, using Y_j versus W/F_{i_0} data provided by the HDN product distributions. Quality of fit can be assessed from the degree of linearity of the Arrhenius plot, and by checking calculated k_2' values for constancy as the integrations are carried out to higher W/F_{i_0} . The pseudo rate constant for DHQ hydrogenolysis is derived in a similar fashion, recognizing that hydrocarbons and ammonia are formed from both OPA and DHQ. Pseudo first order kinetics

($K_{\text{NH}_3}/K_{\text{AA}} = 1$, $K_{\text{SA}}/K_{\text{AA}} = 1$) results in very poor correlation of the experimental data, which is not surprising in view of the strong evidence for preferential adsorption of PyTHQ and DHQ. A $K_{\text{SA}}/K_{\text{AA}}$ value of about 6 (with $K_{\text{NH}_3}/K_{\text{OPA}} = 0.25$) gives the "best" correlation

of the data; thus, the kinetic modelling results are consistent with the qualitative expectations discussed earlier.

Arrhenius plots of the pseudo rate constants for hydrogenolysis of PyTHQ and DHQ are shown in Figures 1-22 and 1-23. Note that the same pseudo rate constants are derived from the HDN data, independent of the starting heterocyclic nitrogen compound (see Figure 1-23), further demonstrating the adequacy of the kinetic model. The activation energies of the hydrogenolysis reactions are comparable - an average of 155 kJ/g-mol (37 kcal/g-mol) for hydrogenolysis of PyTHQ, and about 138 kJ/g-mol (33 kcal/g-mol) for DHQ hydrogenolysis. These activation energies vary somewhat with hydrogen pressure, so the temperature and hydrogen pressure dependencies of the pseudo rate constants for the hydrogenolysis reactions are to some extent interrelated. This is not surprising, since adsorbed hydrogen was presumably involved in the catalytic reactions, and the fraction of available sites actually occupied by hydrogen depends on temperature as well as hydrogen pressure. The pseudo rate constants for DHQ hydrogenolysis are about an order of magnitude larger than those for hydrogenolysis of PyTHQ (compare Figures 1-22 and 1-23), while those for OPA denitrogenation are the largest of all. Note, however, that the kinetic model correctly predicts a substantially lower OPA denitrogenation rate when significant concentrations of heterocyclics,

particularly PyTHQ and DHQ, are present. The activation energies for the hydrogenolysis reactions are much higher than the OPA denitrogenation activation energy, which is comparable to those reported for the hydrogenation reactions in quinoline HDN (Shih et al., 1977). This is consistent with the conclusion here, that the rate of nitrogen removal from OPA was determined primarily by the rate of hydrogenation of OPA (to PCHA). Finally, the Langmuir-Hinshelwood reaction rate expressions used for kinetic modelling are dependent on the relative concentrations of nitrogen compounds (Y_j), but not on the absolute concentrations (P_j or P_{i_0}). This results from the assumption that the "1" in the denominator of the rate expressions is negligible, which is equivalent to postulating that the catalyst surface was always saturated with nitrogen compounds, even at the lower reactant partial pressure. The fact that HDN product distributions were virtually independent of initial reactant partial pressure, at constant W/F_{i_0} , temperature, and hydrogen pressure, indicates that this assumption is justified.

I. H. Conclusions

I. H. 1. Catalyst Activity

The HDN activity of virgin (but sulfided) NiMo/Al₂O₃ catalyst is substantially higher than the "steady-state" level of activity attained after several hundred hours of catalyst use. This deactivation is due primarily to carbon deposition (coking). During deactivation, there is a much greater loss in hydrogenolysis activity than in hydrogenation activity, suggesting that these functionalities are associated with different catalyst sites.

I. H. 2. Hydrodenitrogenation of o-Propylaniline

Direct hydrogenolysis of OPA to PB and ammonia is slow relative to hydrogenation of the aromatic ring and denitrogenation of the resulting aliphatic amine (PCHA). The rate of conversion of OPA to hydrocarbons and ammonia can be described by a Langmuir-Hinshelwood kinetic model, with an OPA adsorption strength about four times that of ammonia. Denitrogenation of OPA is much easier than denitrogenation of any of the heterocyclics, when the compounds are studied individually. The presence of significant concentrations of the heterocyclics, particularly PyTHQ and DHQ, greatly inhibits the OPA denitrogenation rate, due to competitive adsorption effects.

I. H. 3. Hydrodenitrogenation of Quinoline

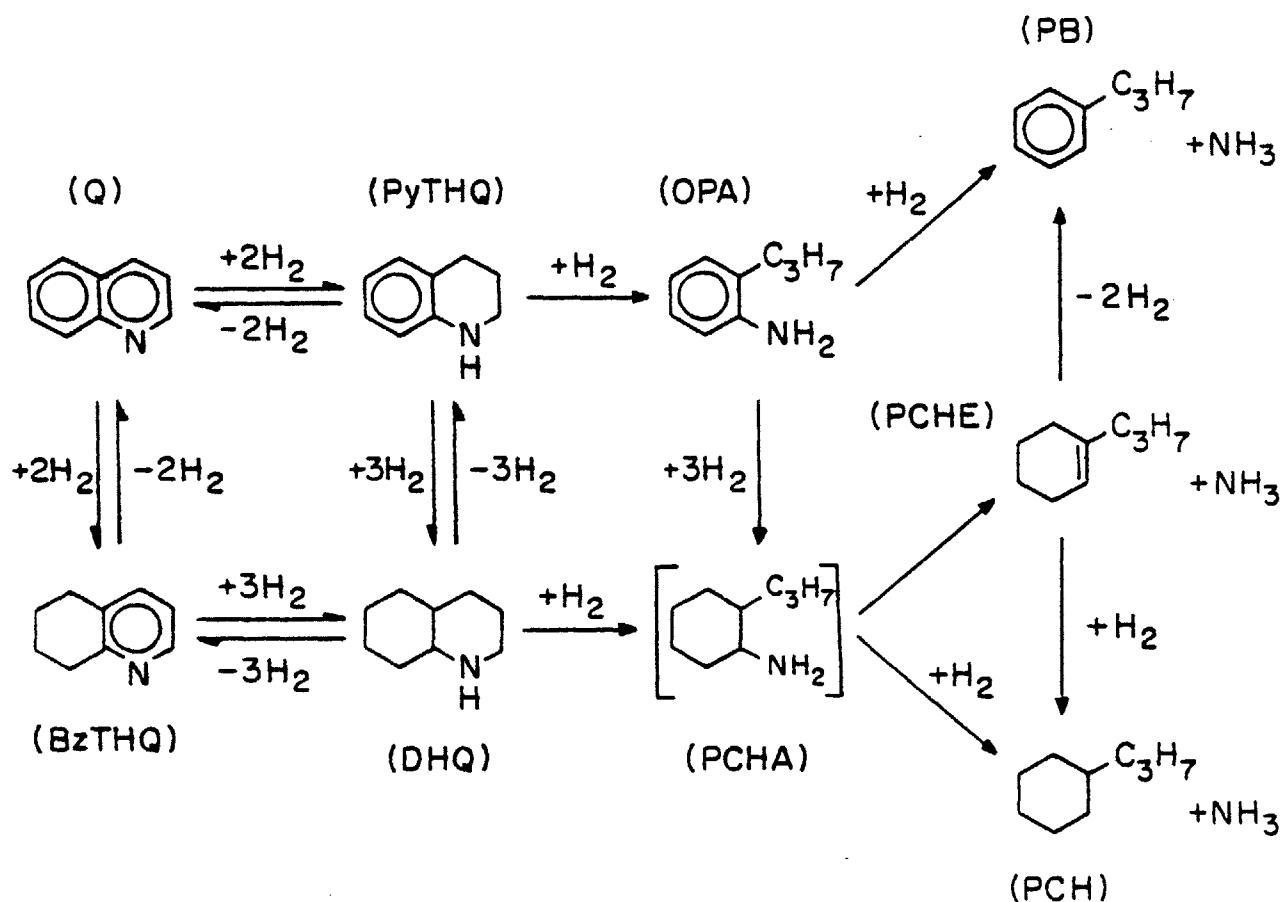
The initial ring saturation reactions of quinoline are all reversible over a wide range of HDN conditions. Saturation of the aromatic ring is thermodynamically (but not necessarily kinetically) more favorable than saturation of the heteroring. In general, these reactions are subject to complex interactions between kinetics and thermodynamics.

Denitrogenation of quinoline occurs primarily through the DHQ intermediate, and PCH is the major hydrocarbon product. The commercial NiMo/Al₂O₃ hydrotreating catalyst (in sulfide form) exhibits little selectivity for the HDN reaction pathway of minimum hydrogen consumption. At lower temperatures the heteroring in quinoline is selectively hydrogenated, initially, but the catalyst does not possess sufficient hydrogenolysis activity to remove the nitrogen without extensive saturation of the aromatic ring.

Quinoline HDN is influenced by strong competitive adsorption of the nitrogen compounds, which vary significantly in adsorptivity. A Langmuir-Hinshelwood kinetic model has been developed for the hydrogenolysis and nitrogen removal reactions, and the HDN data are well-correlated only if the different adsorptivities of the nitrogen compounds are considered. On both the hydrogenation and the hydrogenolysis catalyst sites, the secondary amines PyTHQ and DHQ appear to adsorb about six

times as strongly as the aromatic amines (quinoline, BzTHQ, and OPA), which in turn show an adsorption strength approximately four times greater than that of ammonia.

FIGURE 1-1
QUINOLINE HDN REACTION NETWORK



Q	quinoline
PyTHQ	Py (or 1,2,3,4) - tetrahydroquinoline
BzTHQ	Bz (or 5,6,7,8) - tetrahydroquinoline
DHQ	decahydroquinoline (cis and trans isomers)
OPA	o-propylaniline
PCHA	propylcyclohexylamine
PB	propylbenzene
PCHE	propylcyclohexene
PCH	propylcyclohexane

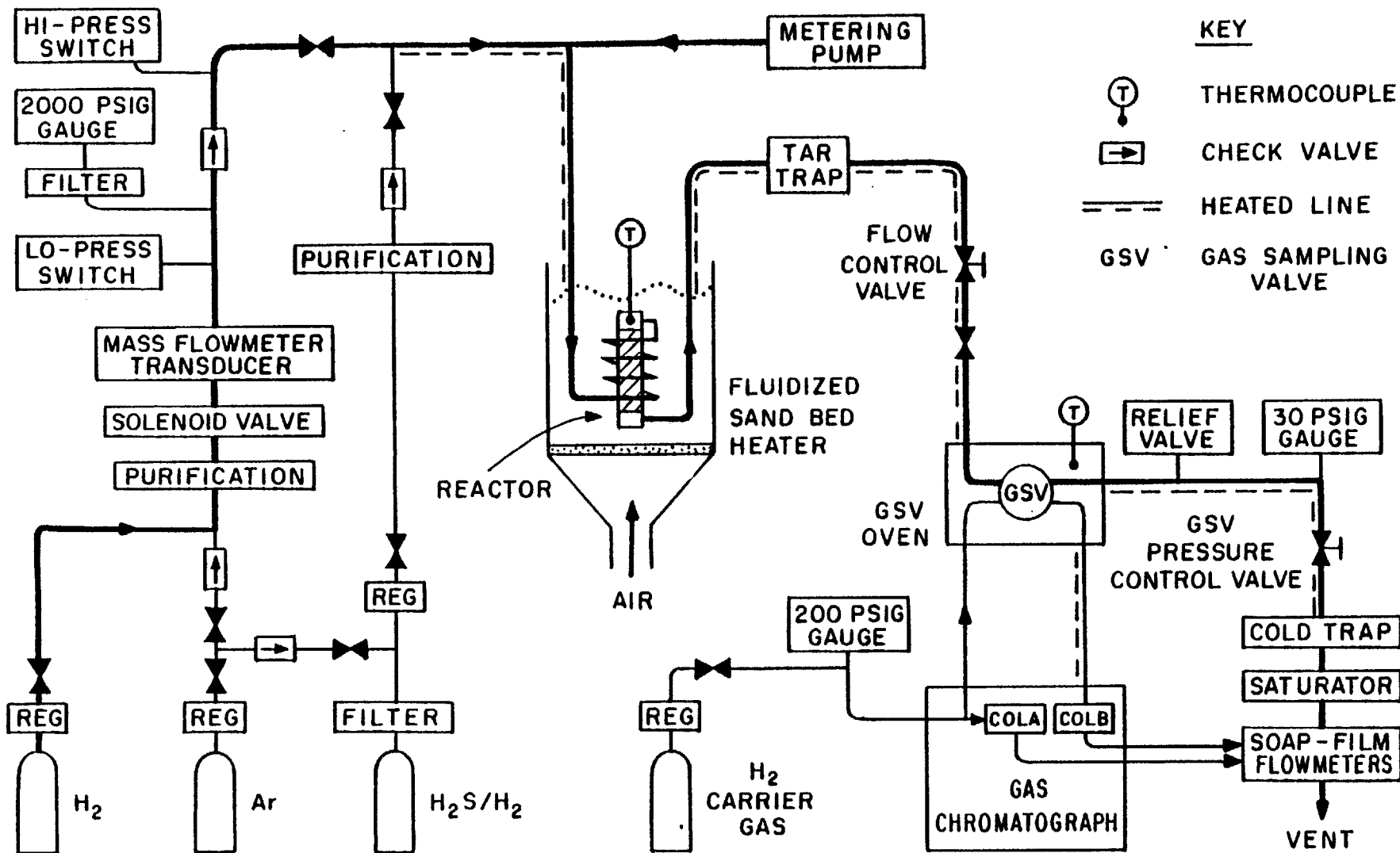


FIGURE I -3: SCHEMATIC OF EXPERIMENTAL APPARATUS

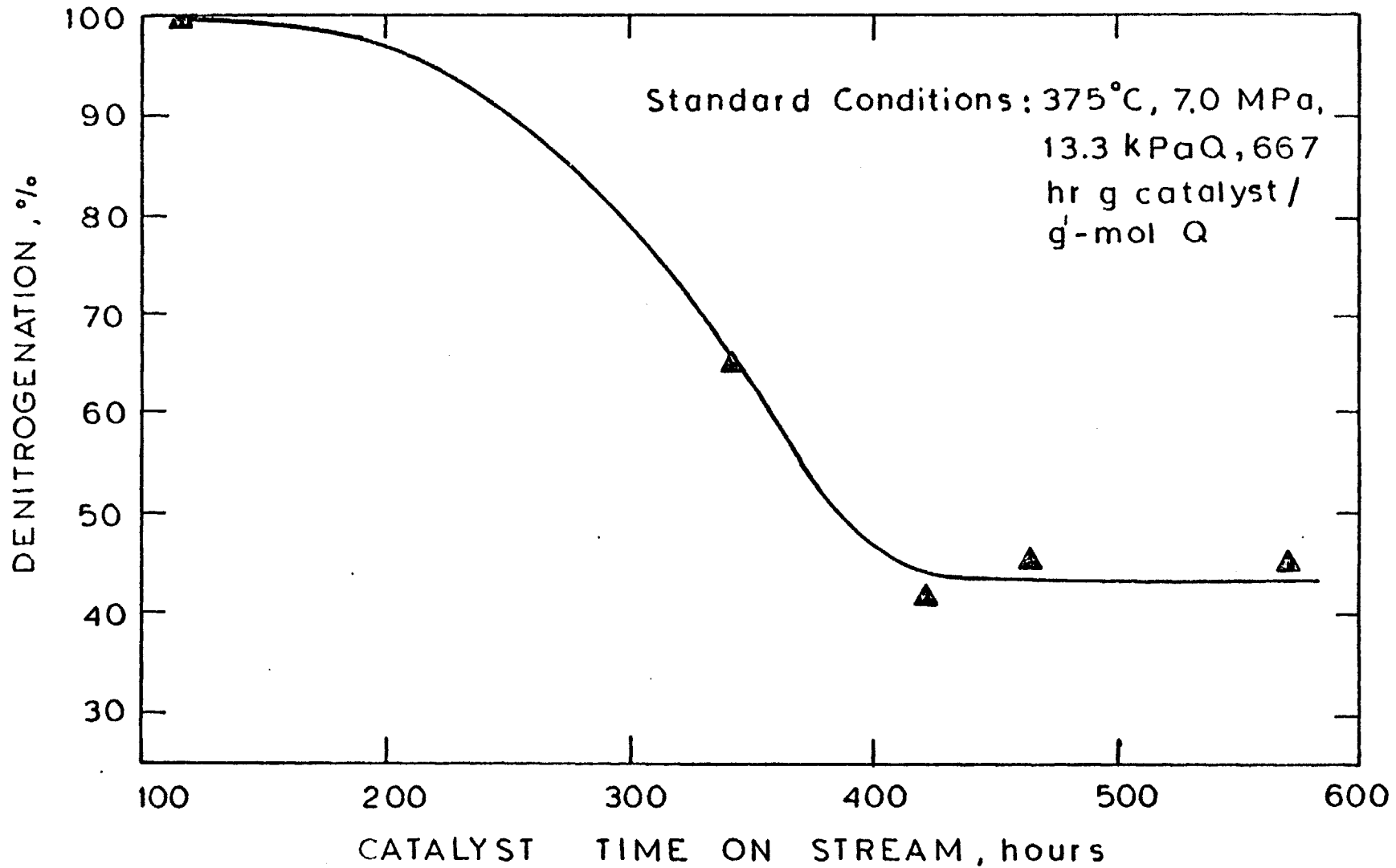


Figure 1-4: Catalyst Deactivation During Quinoline HDN -
Severe Standard Conditions

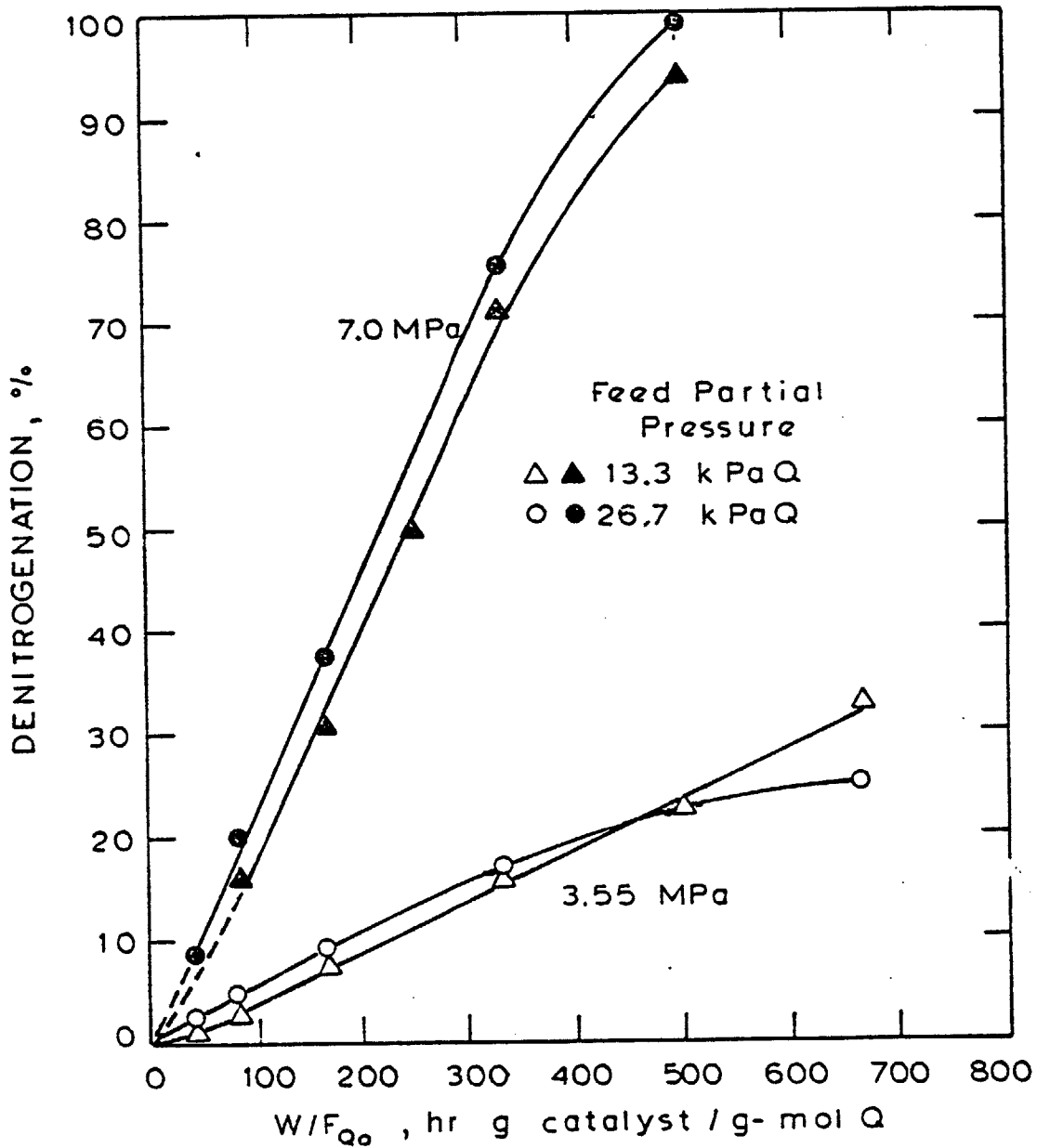


Figure 1-5: Quinoline Denitrogenation at 420°C

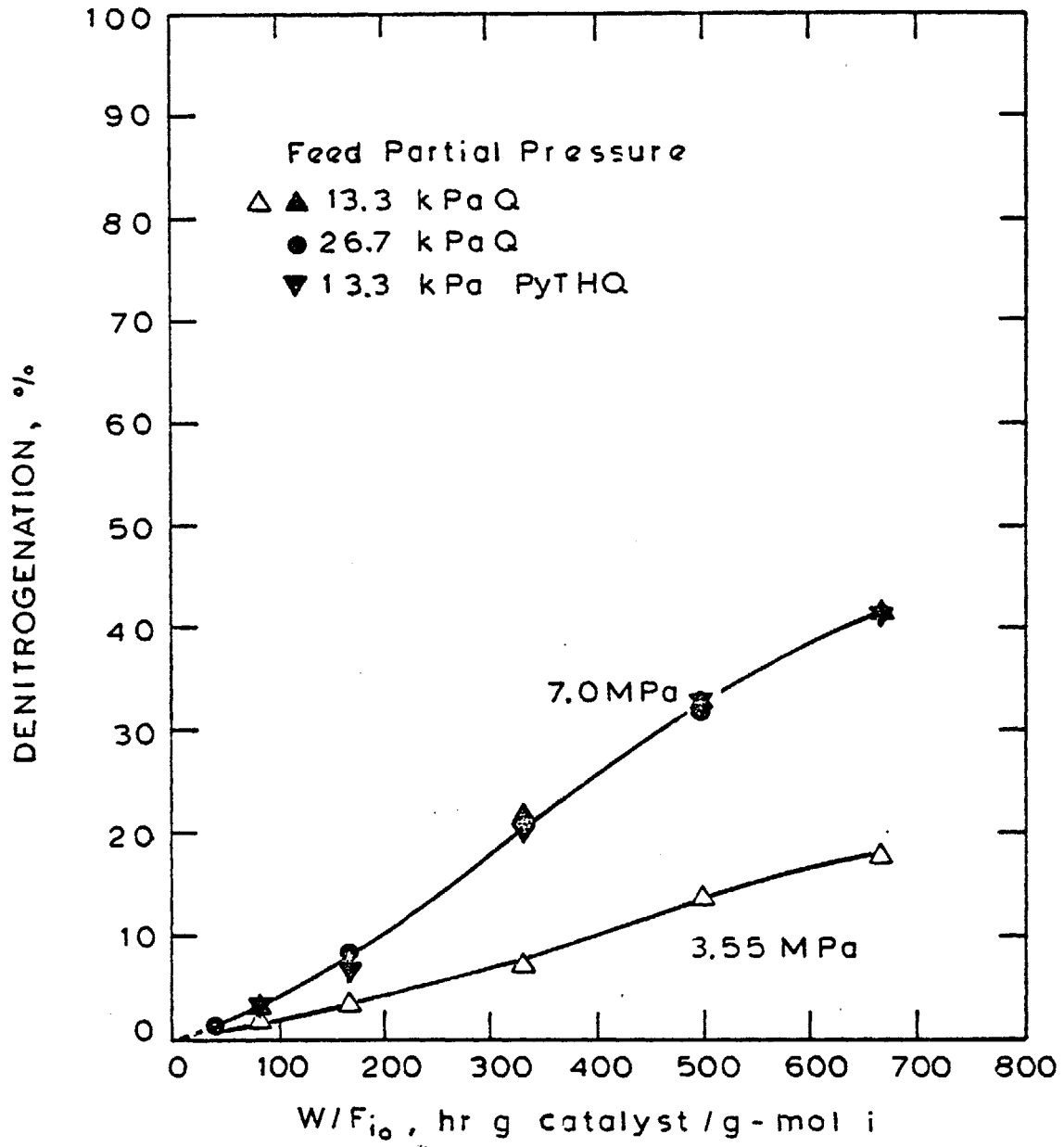


Figure 1-6: Quinoline and Py-Tetrahydroquinoline Denitrogenation at 375 °C

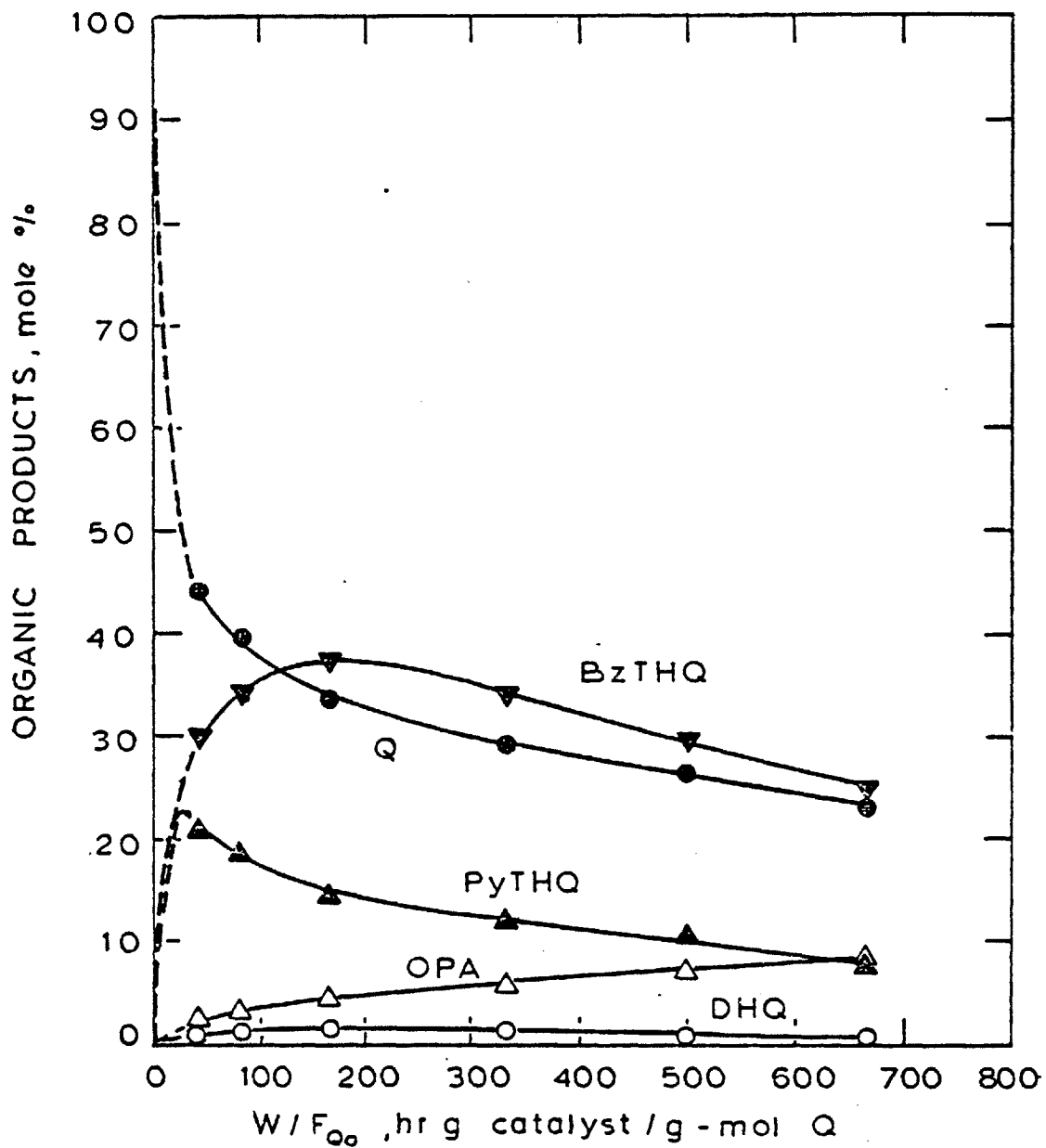


Figure 1-7: Product Distributions for Quinoline HDN
at 420°C, 3.55 MPa, 13.3 kPa Q (Run 20)

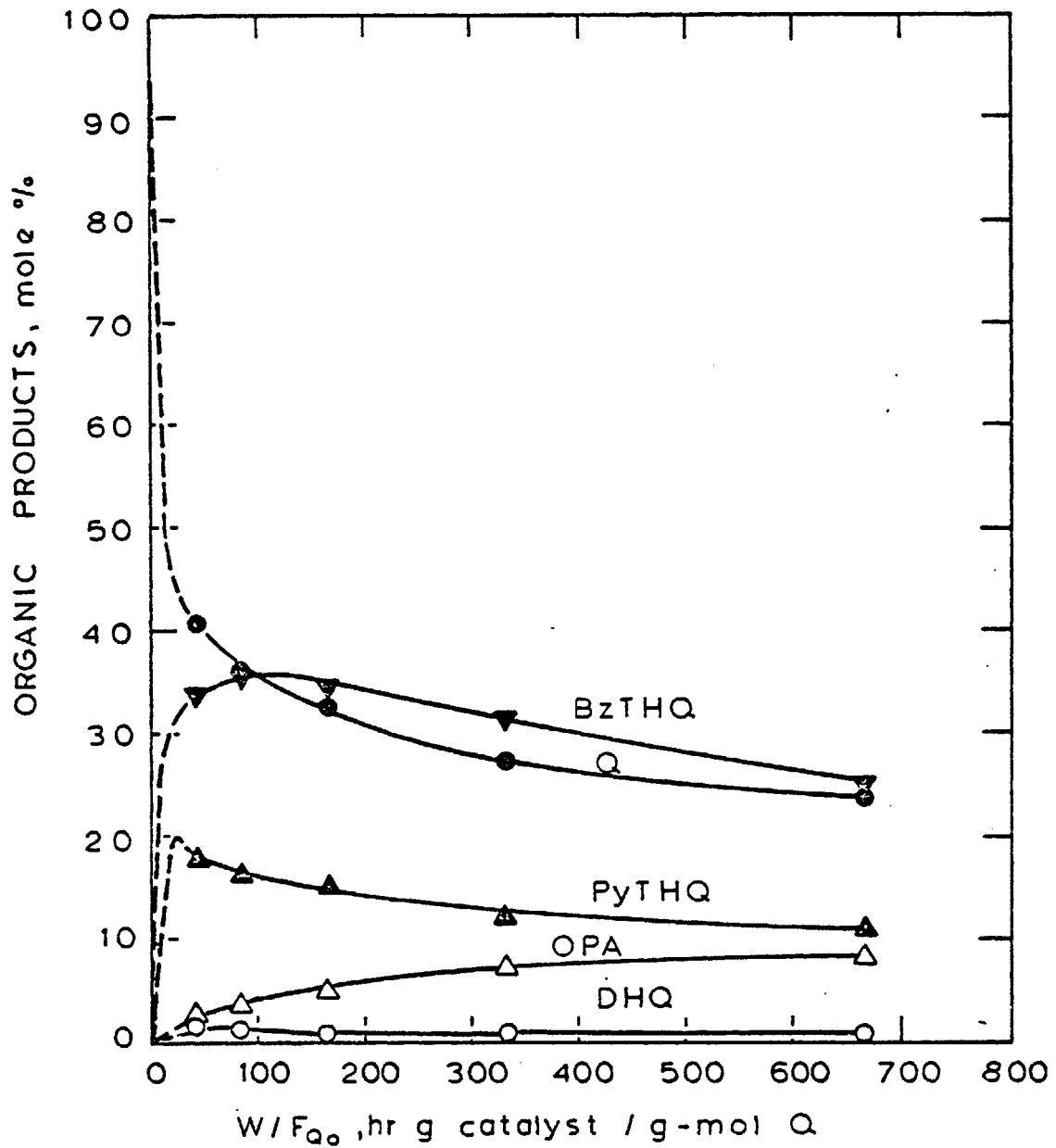


Figure 1-8: Product Distributions for Quinoline HDN at 420°C, 3.55 MPa, 26.7 kPa Q (Run 19)

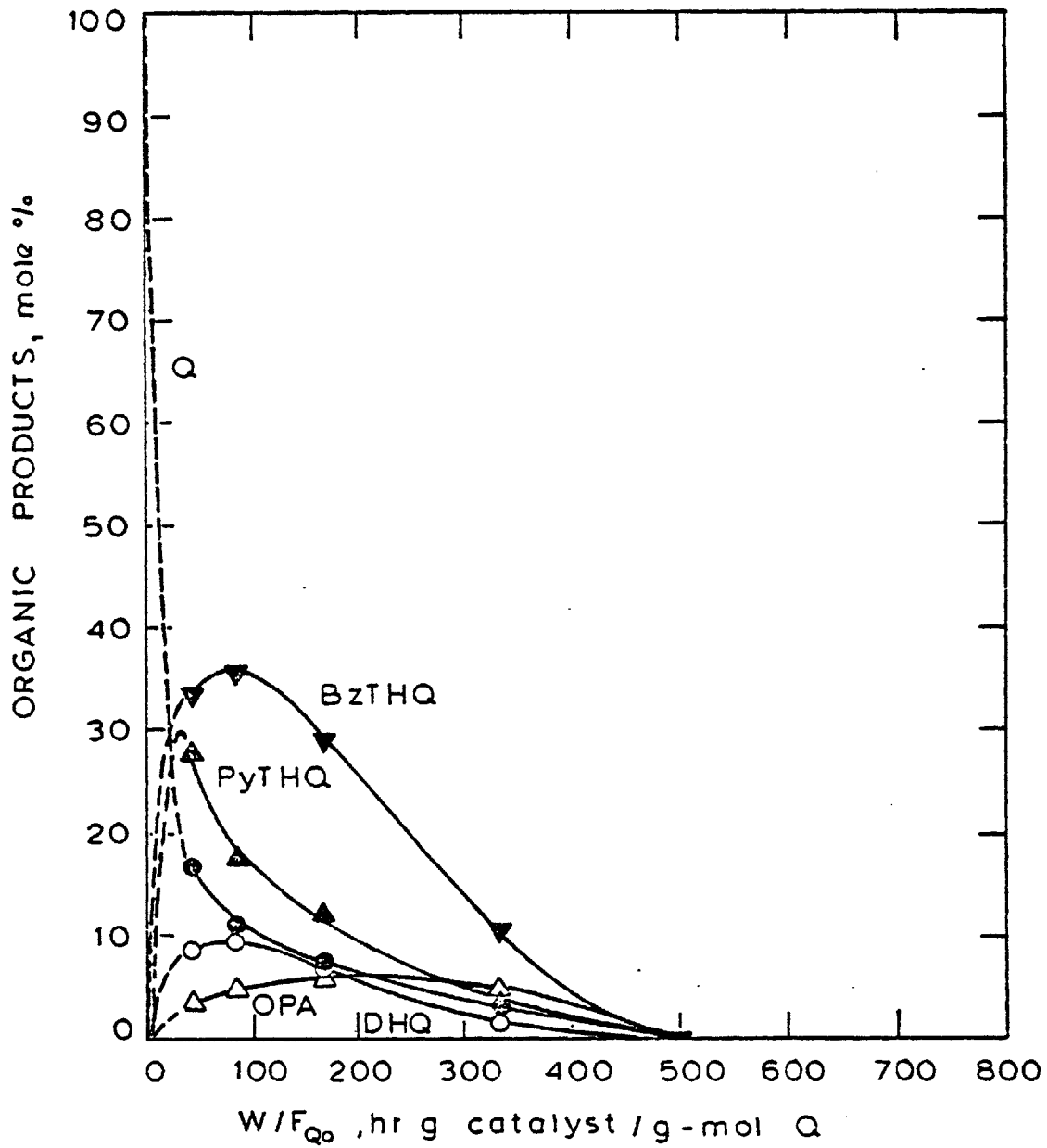


Figure 1-9: Product Distributions for Quinoline HDN at 420°C, 7.0 MPa, 26.7 kPa Q (Run 21)

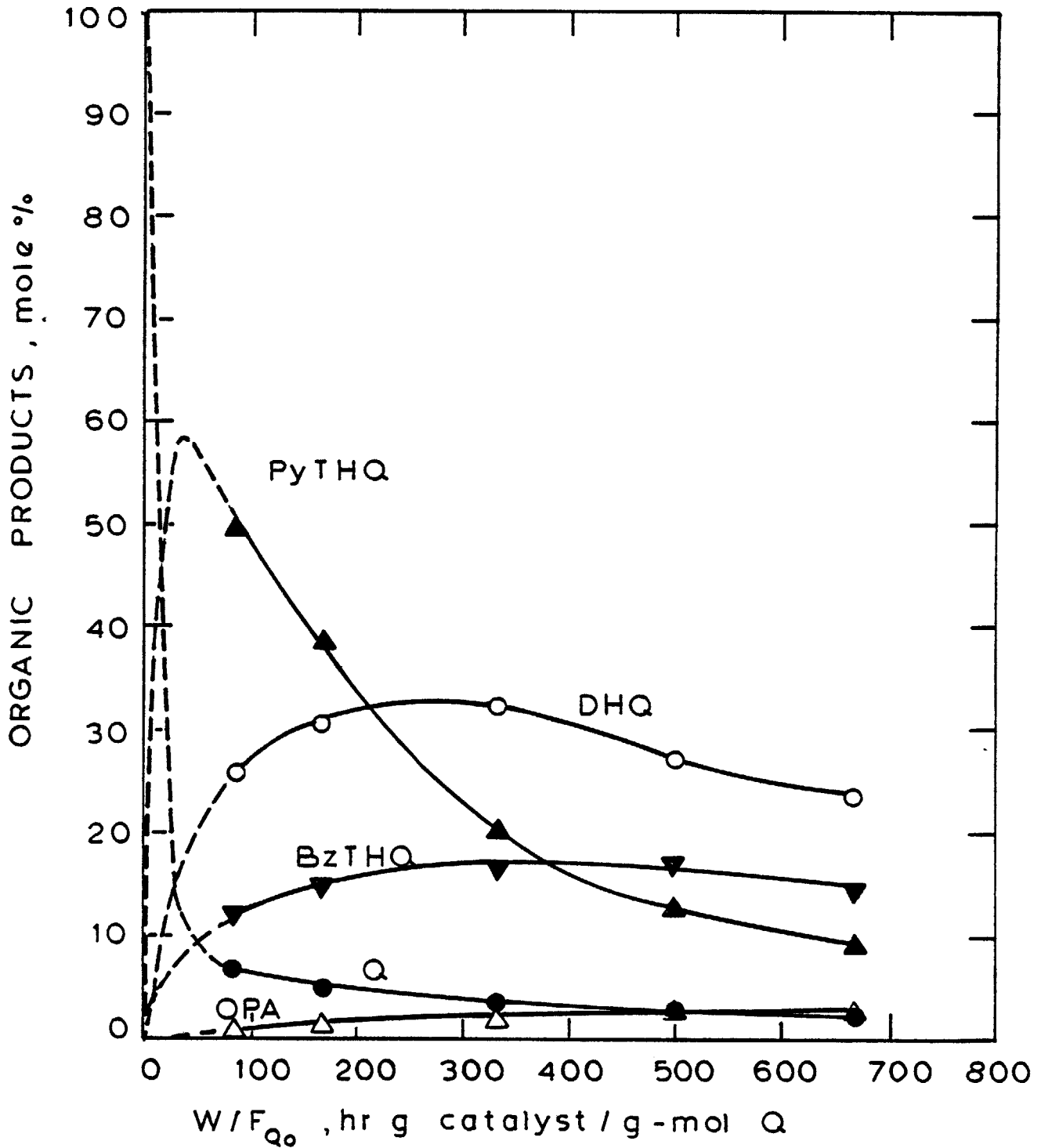


Figure 1-10: Product Distributions for Quinoline HDN at 375 °C, 7.0 MPa, 13.3 kPa Q (Run 23)

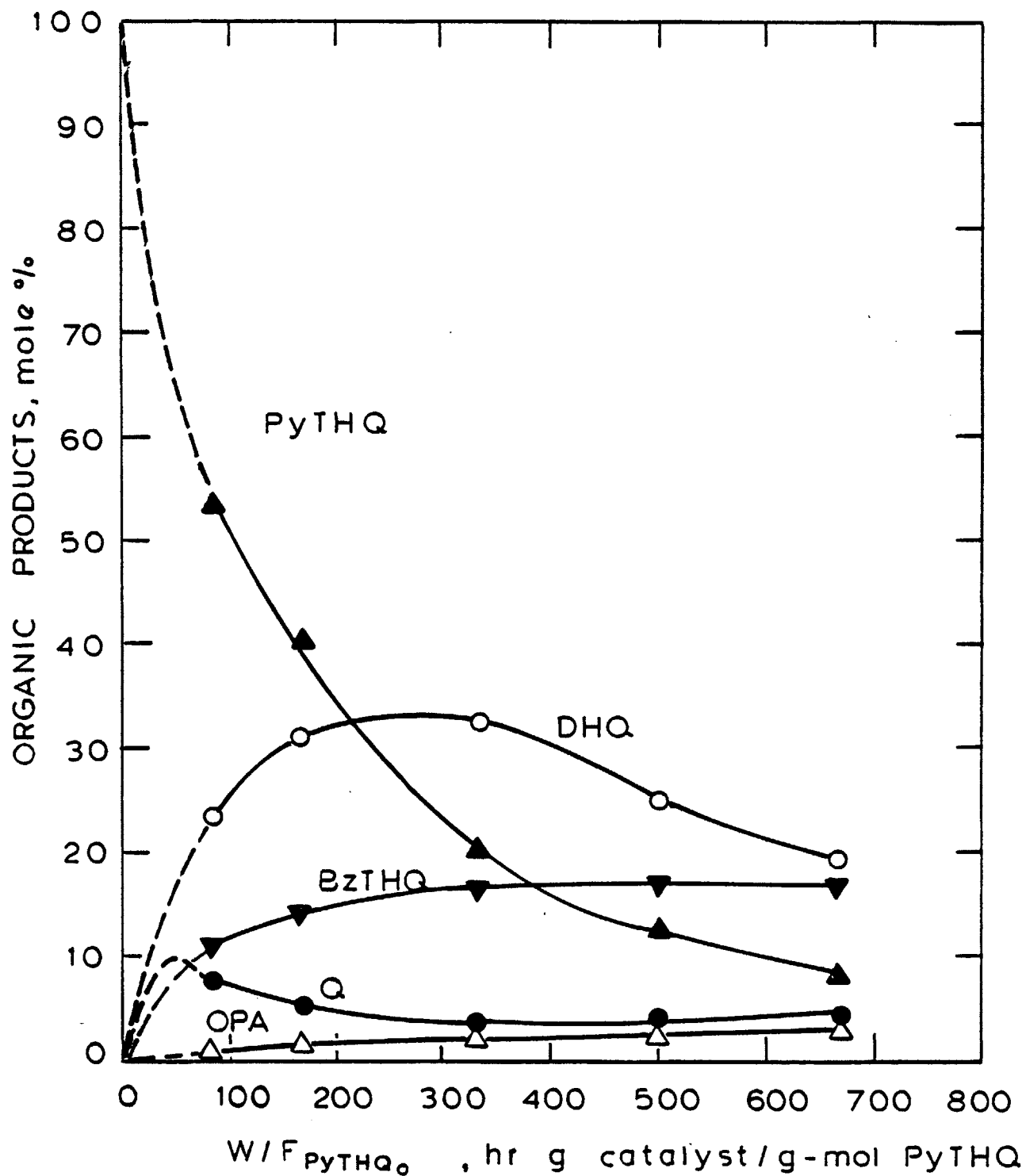


Figure 1-11 : Product Distributions for Py-Tetrahydroquinoline HDN at 375 °C, 7.0 MPa, 13.3 kPa PyTHQ (Run 33)

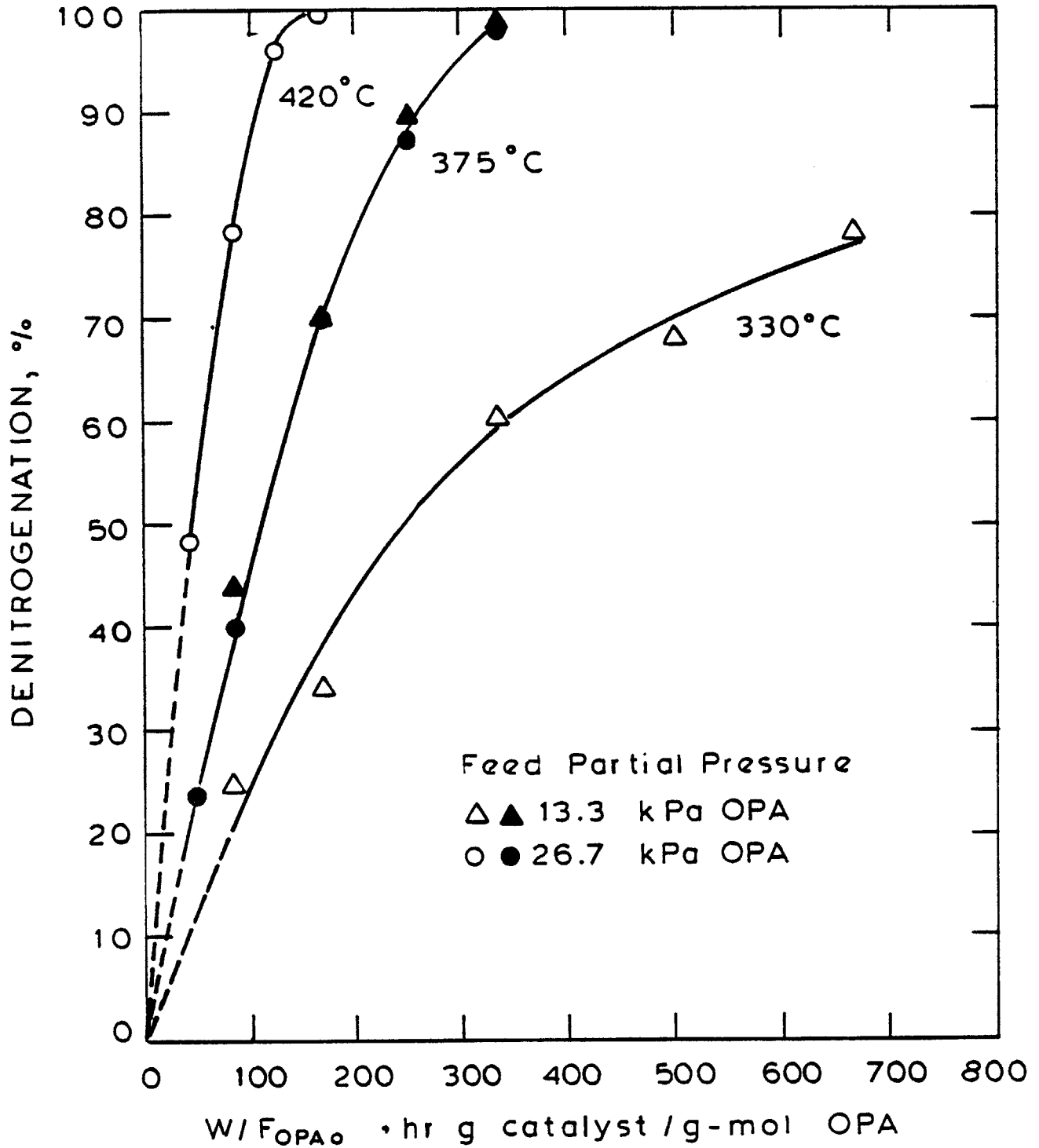


Figure 1-12: o - Propylaniline Denitrogenation at 7.0 MPa

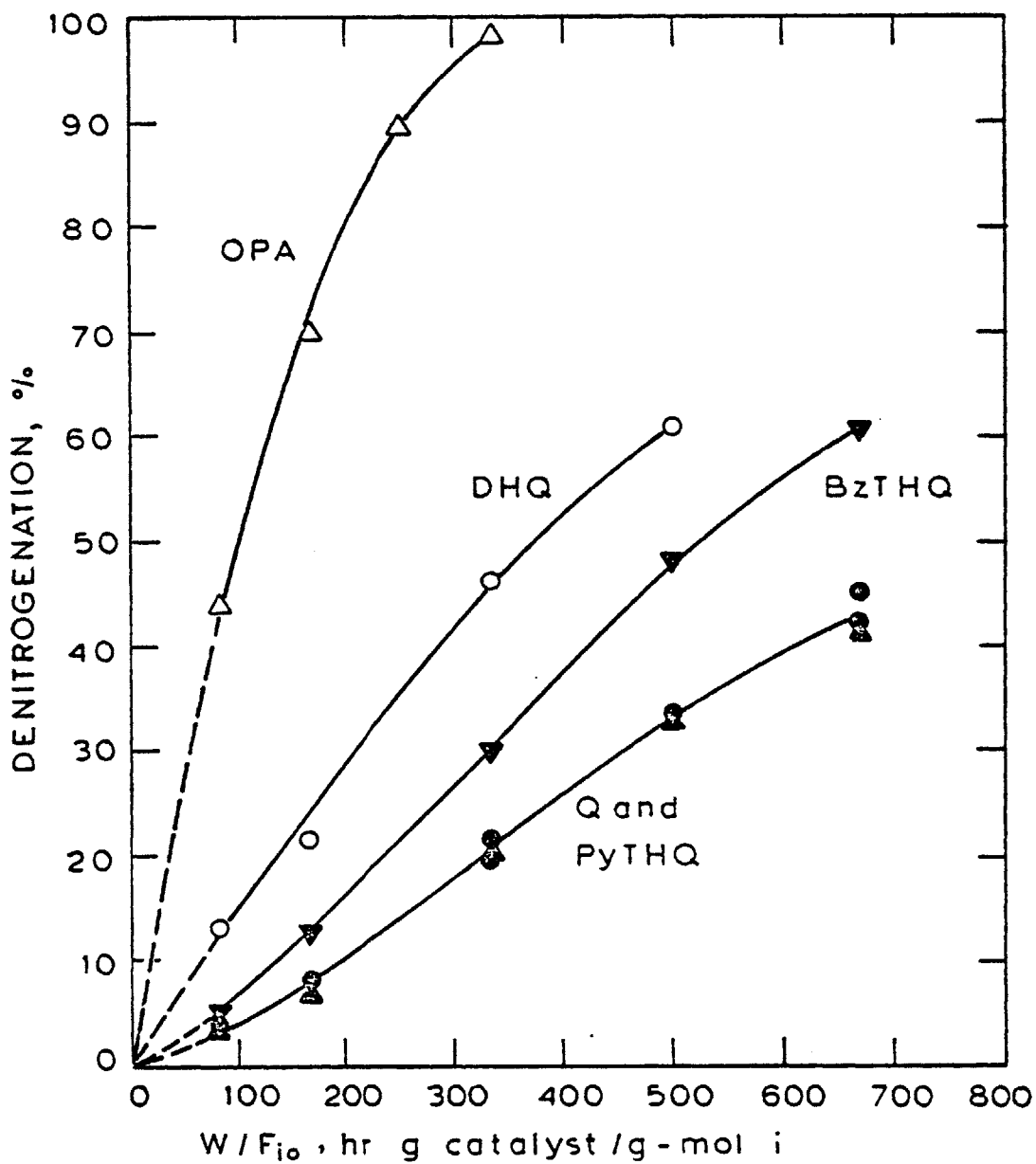


Figure 1-13: Denitrogenation of Individual Nitrogen Compounds at 375 °C, 7.0 MPa, 13.3 kPa Feed Partial Pressure

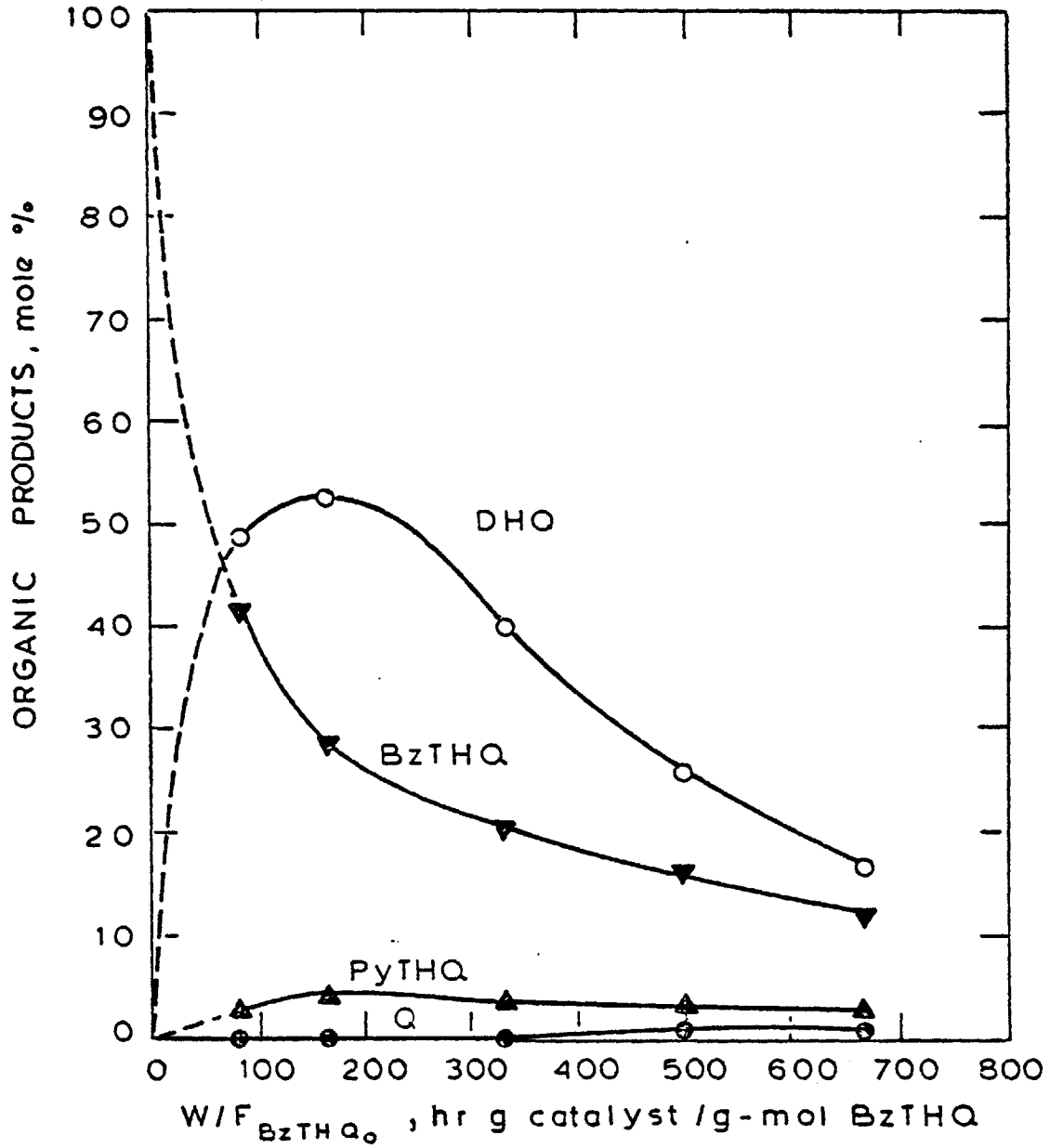


Figure 1-14: Product Distributions for Bz-Tetrahydroquinoline HDN at 375 °C, 7.0 MPa, 13.3 kPa BzTHQ (Run 35)

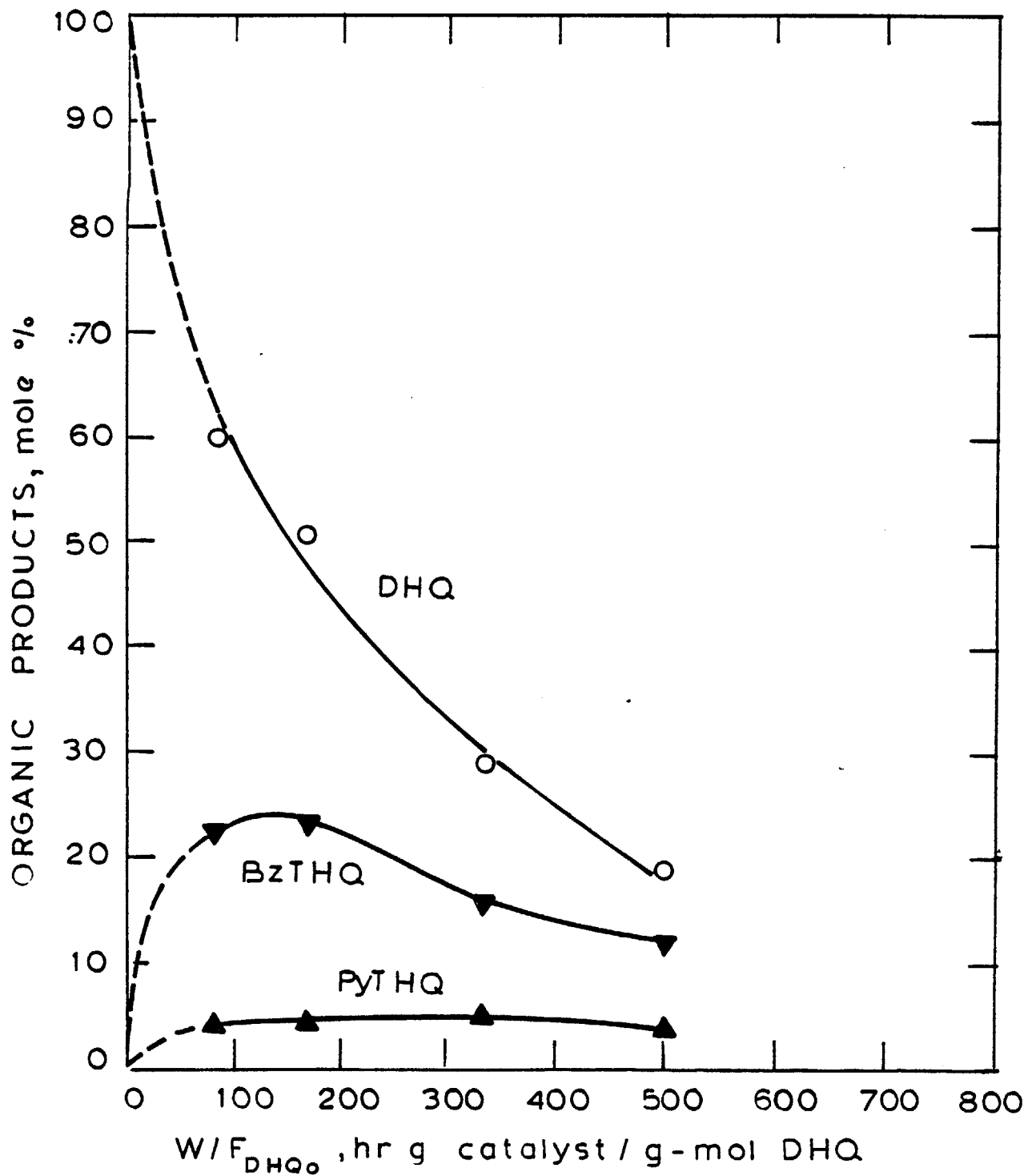


Figure 1-15: Product Distributions for Decahydroquinoline HDN at 375 °C, 7.0 MPa, 13.3 kPa DHQ (Run 38)

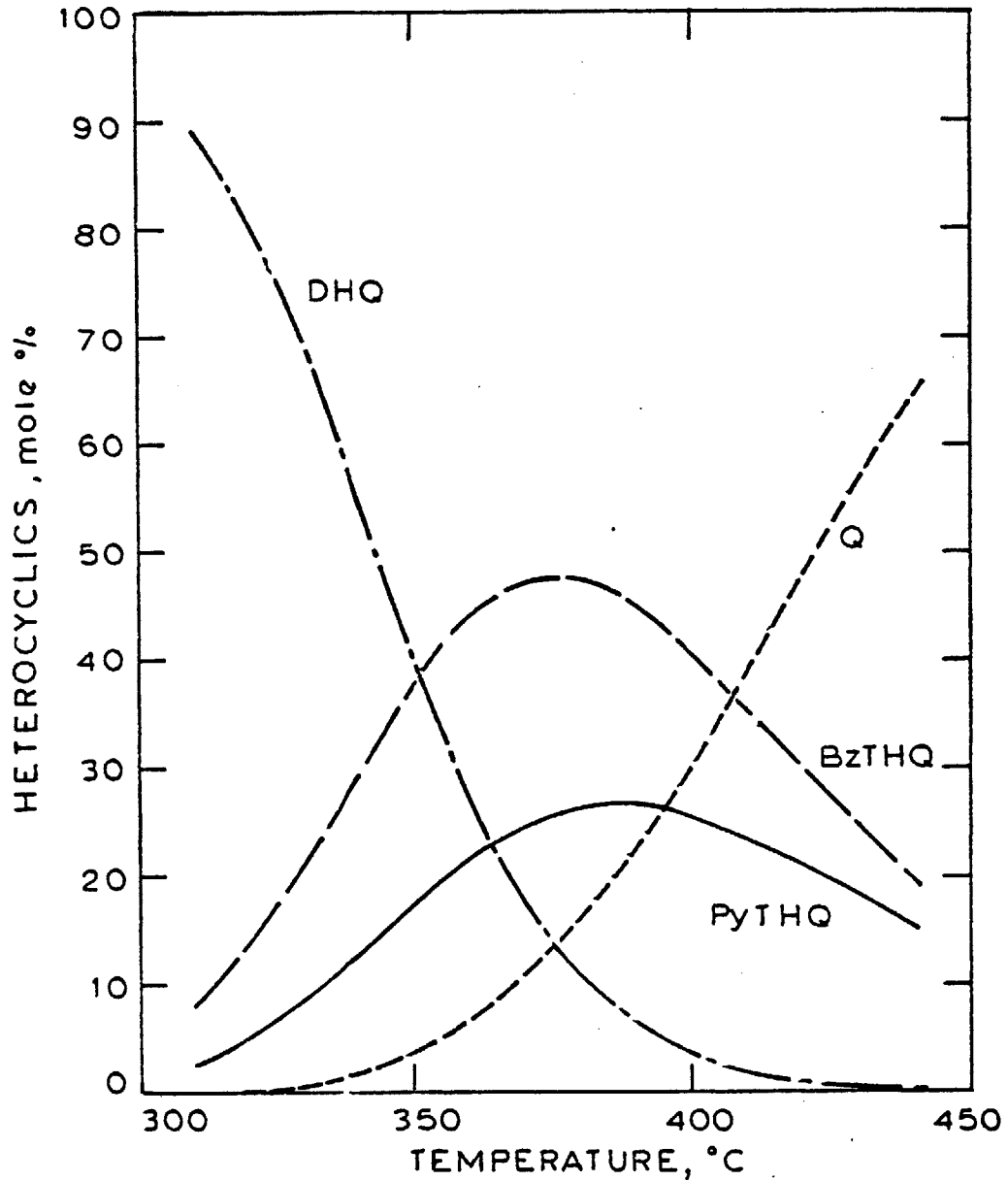


Figure 1-16: Estimated Equilibria Among Quinoline, Tetrahydroquinolines, and Decahydroquinoline at 3.53 MPa Hydrogen Partial Pressure

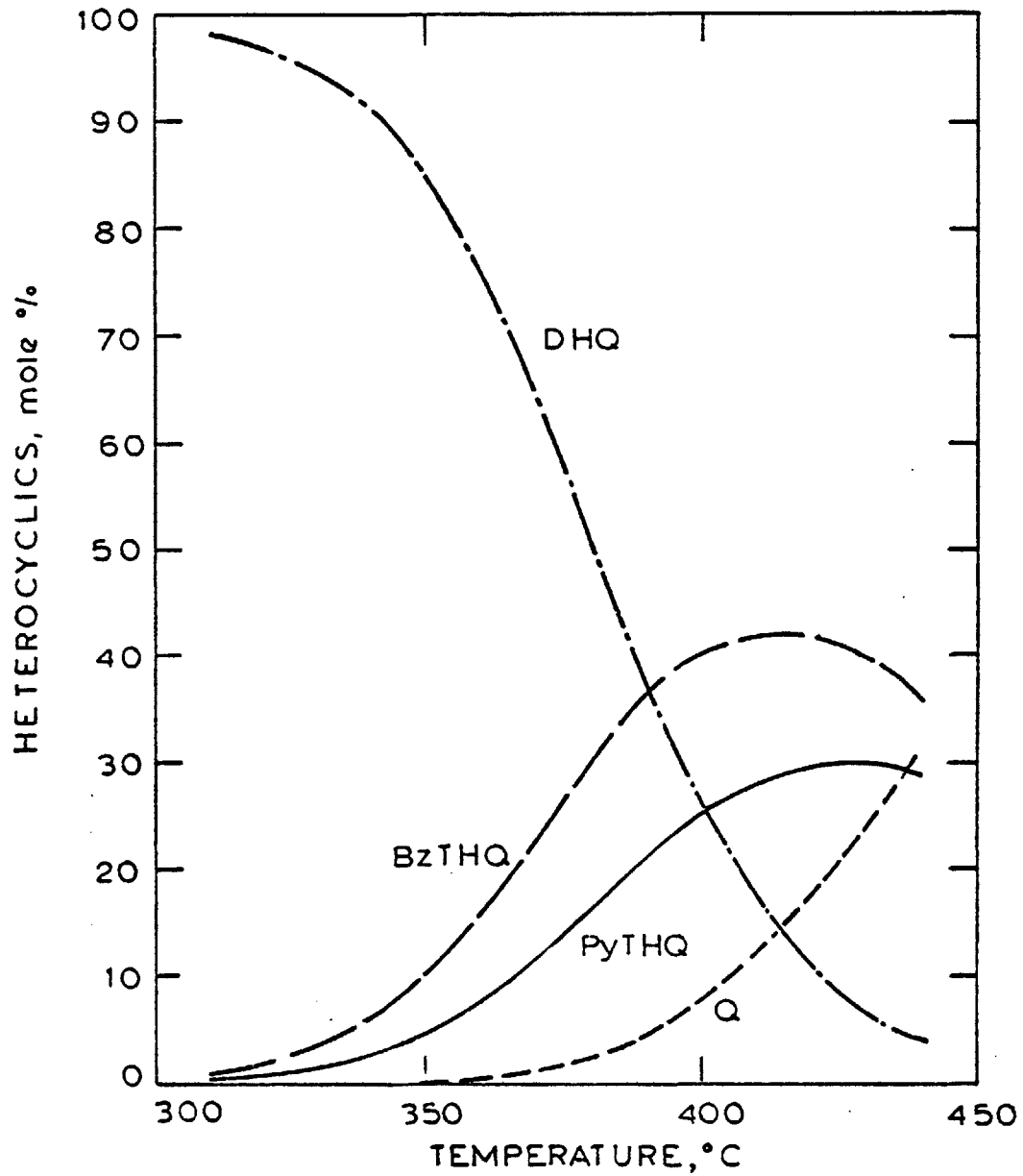


Figure 1-17: Estimated Equilibria Among Quinoline, Tetrahydroquinolines, and Decahydroquinoline at 6.98 MPa Hydrogen Partial Pressure

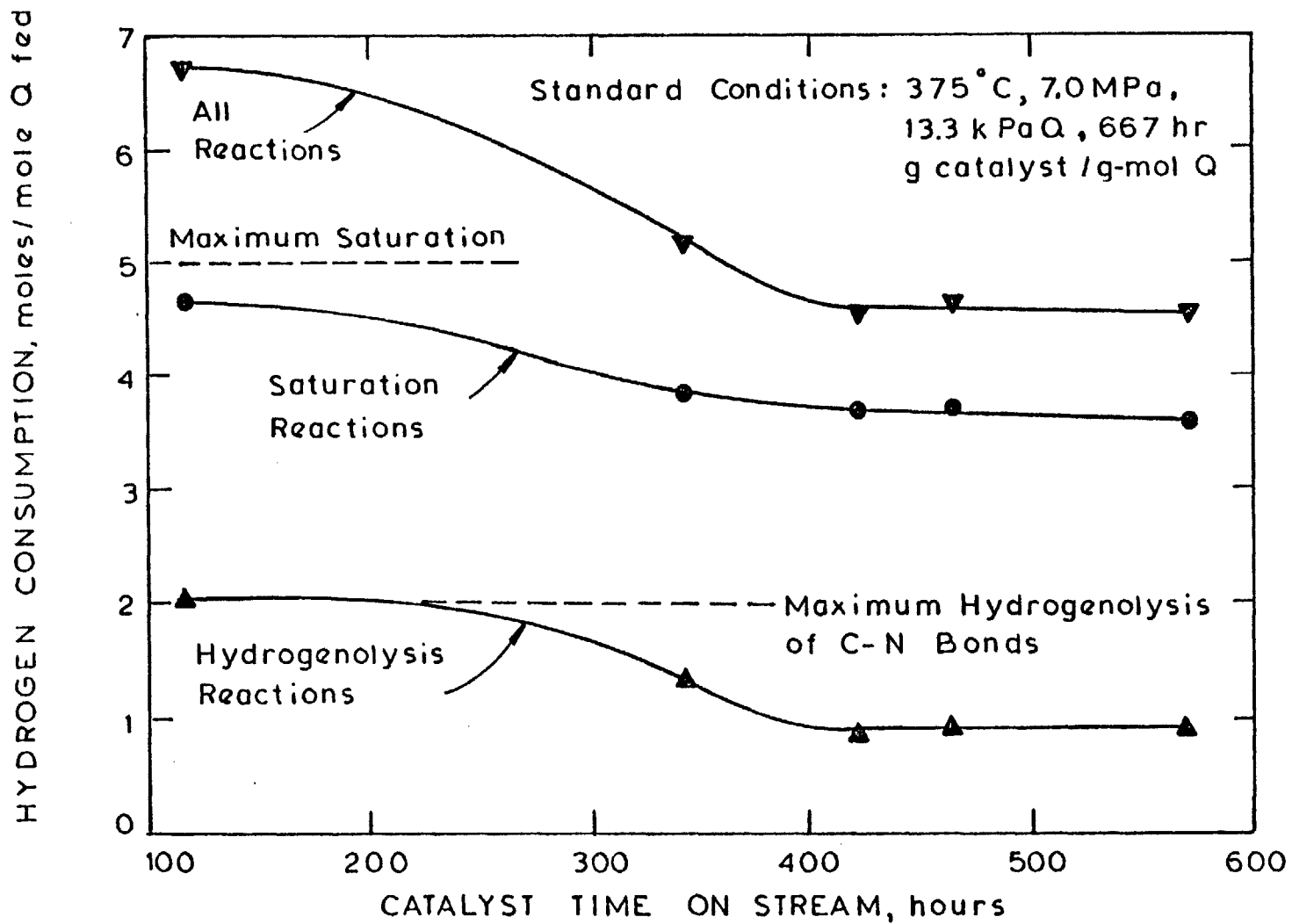


Figure 1-18: Hydrogen Consumption in Quinoline HDN During Catalyst Deactivation - Severe Standard Conditions

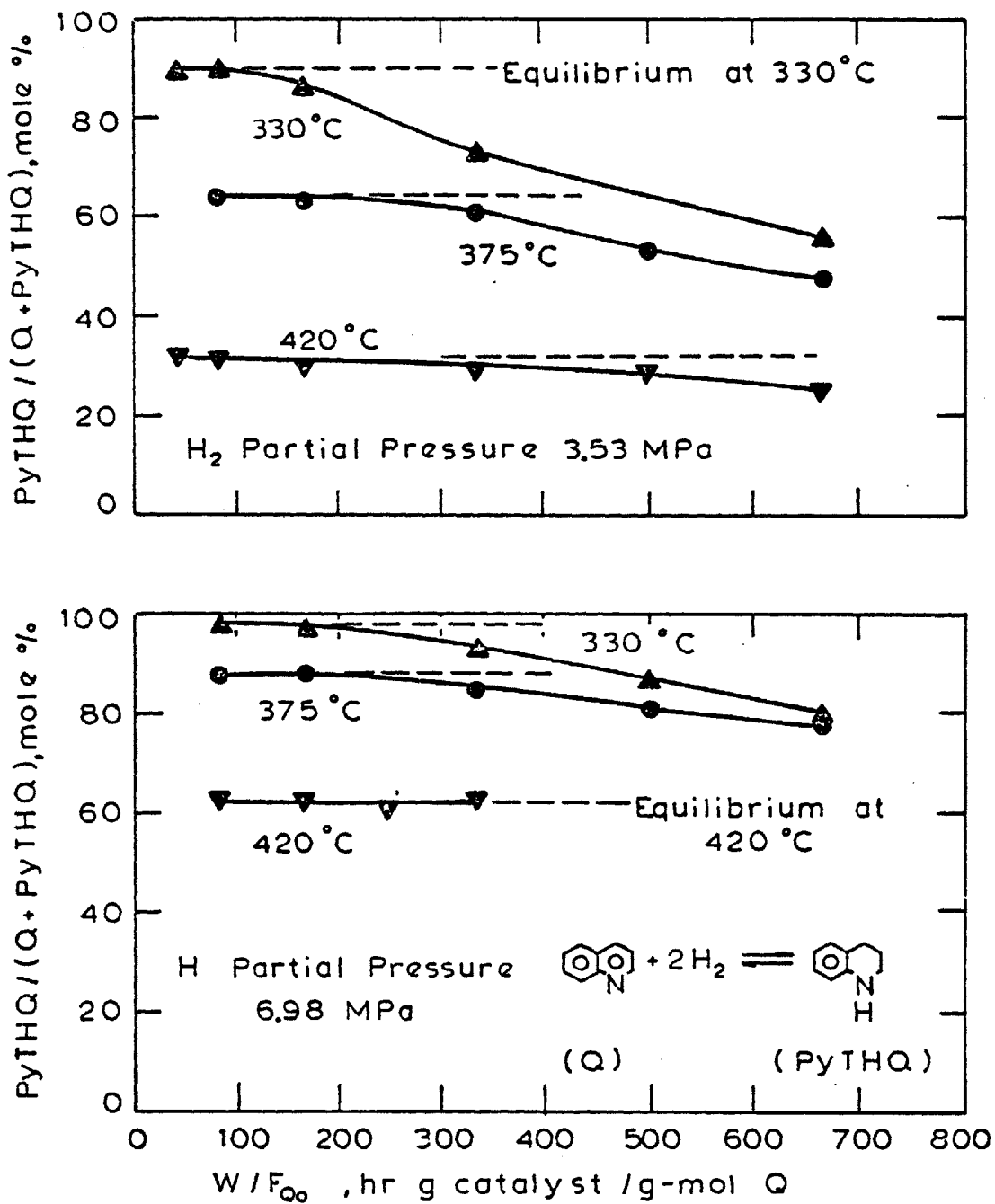


Figure 1-19: Behavior of Q / PyTHQ Product Ratio in Quinoline HDN (13.3 kPa Q)

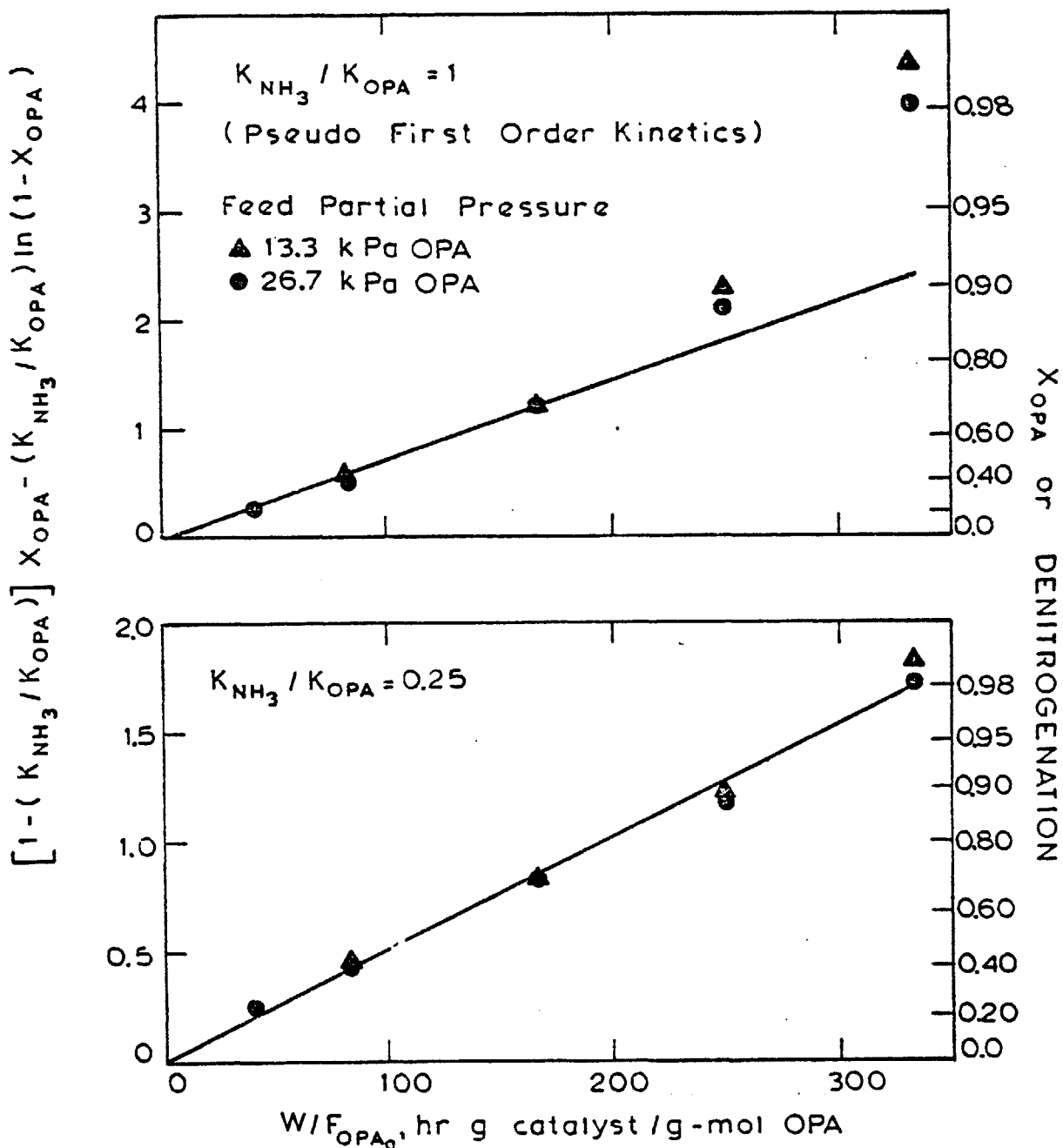


Figure 1-20: Comparison of Langmuir-Hinshelwood Kinetic Models for o-Propylaniline Denitrogenation at 375°C and 7.0 MPa

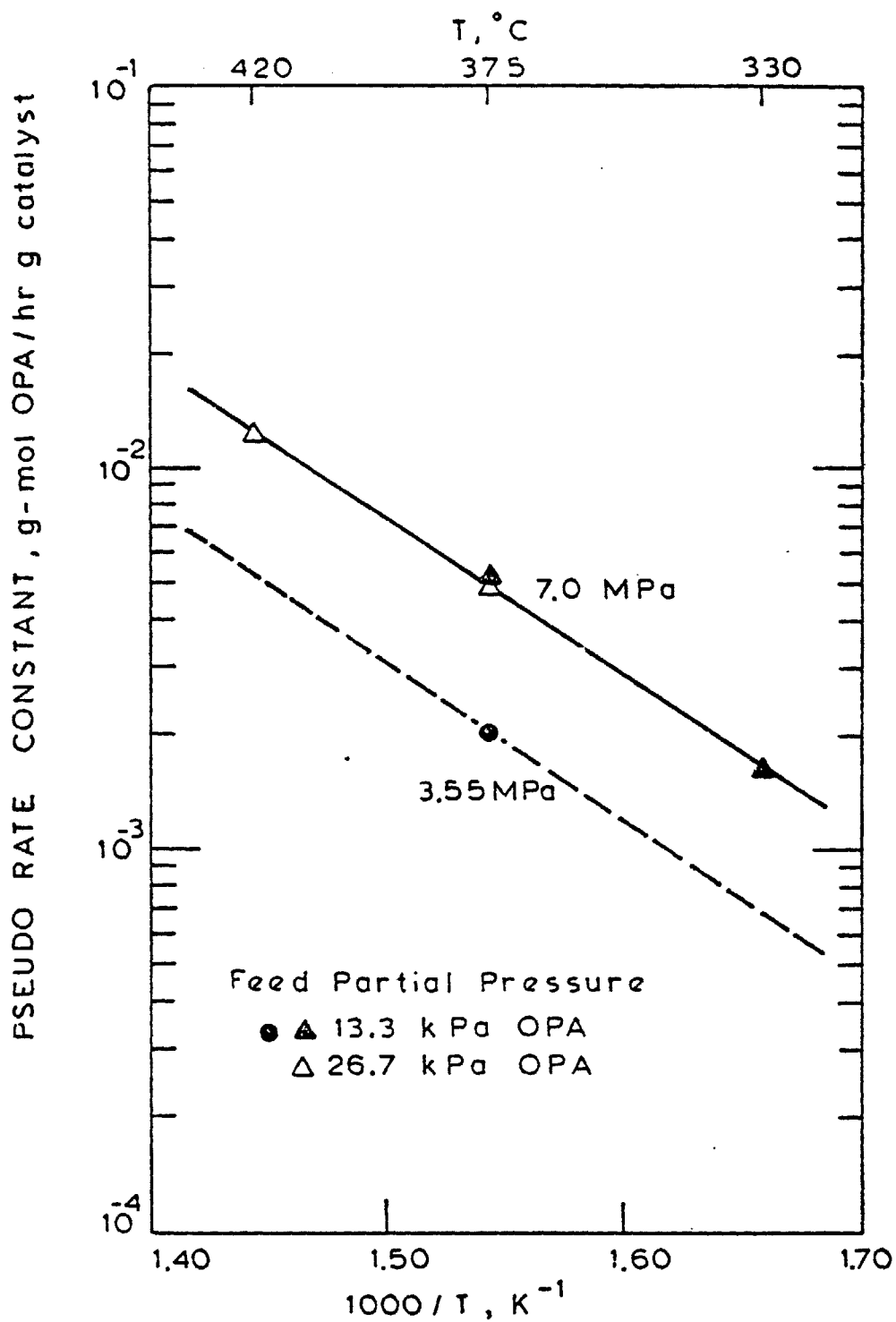


Figure 1-21: Arrhenius Plot of the Pseudo Rate Constant for o-Propylaniline Denitrogenation

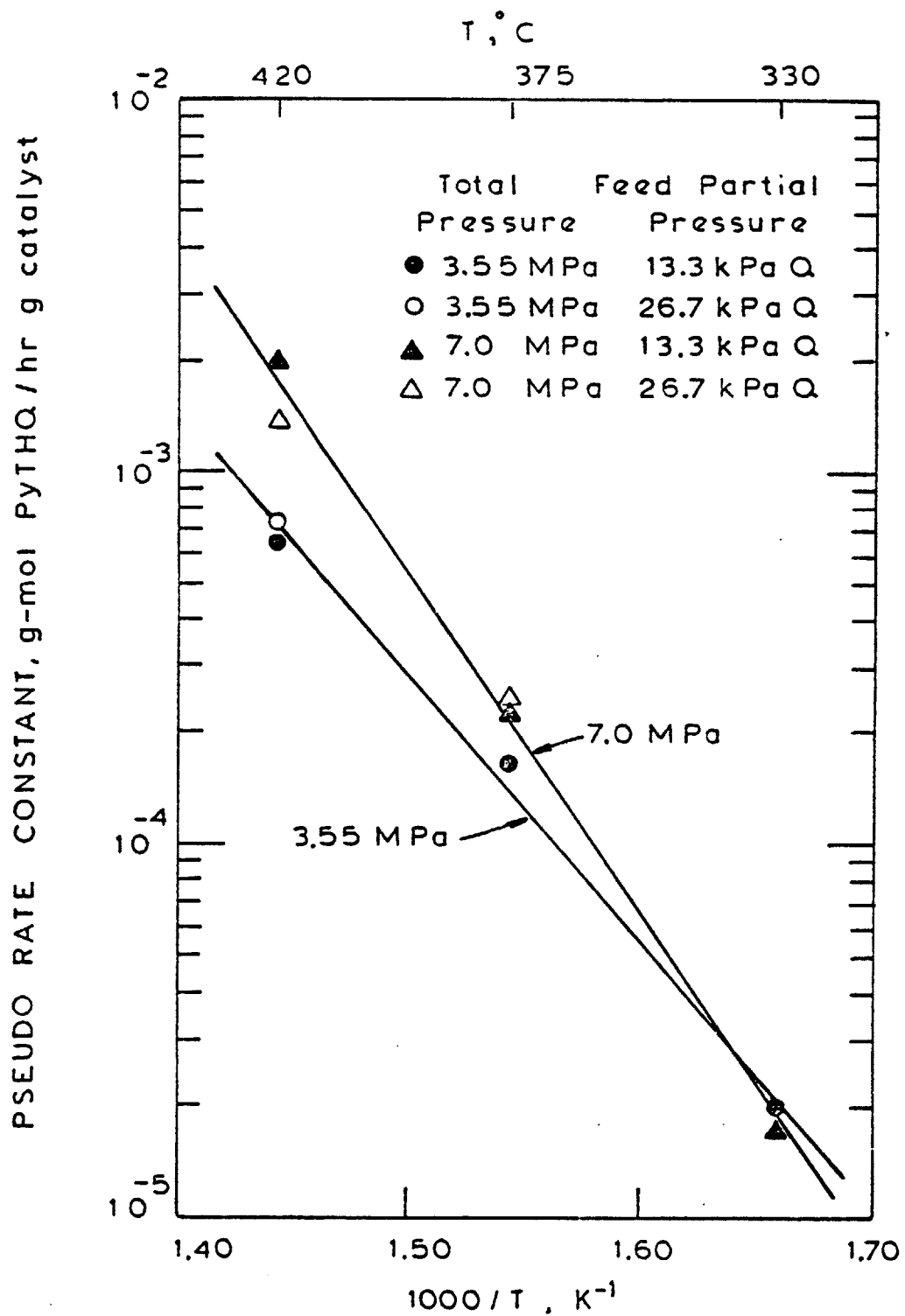


Figure 1-22: Arrhenius Plot of the Pseudo Rate Constant for Hydrogenolysis of Py-Tetrahydroquinoline to o-Propylaniline

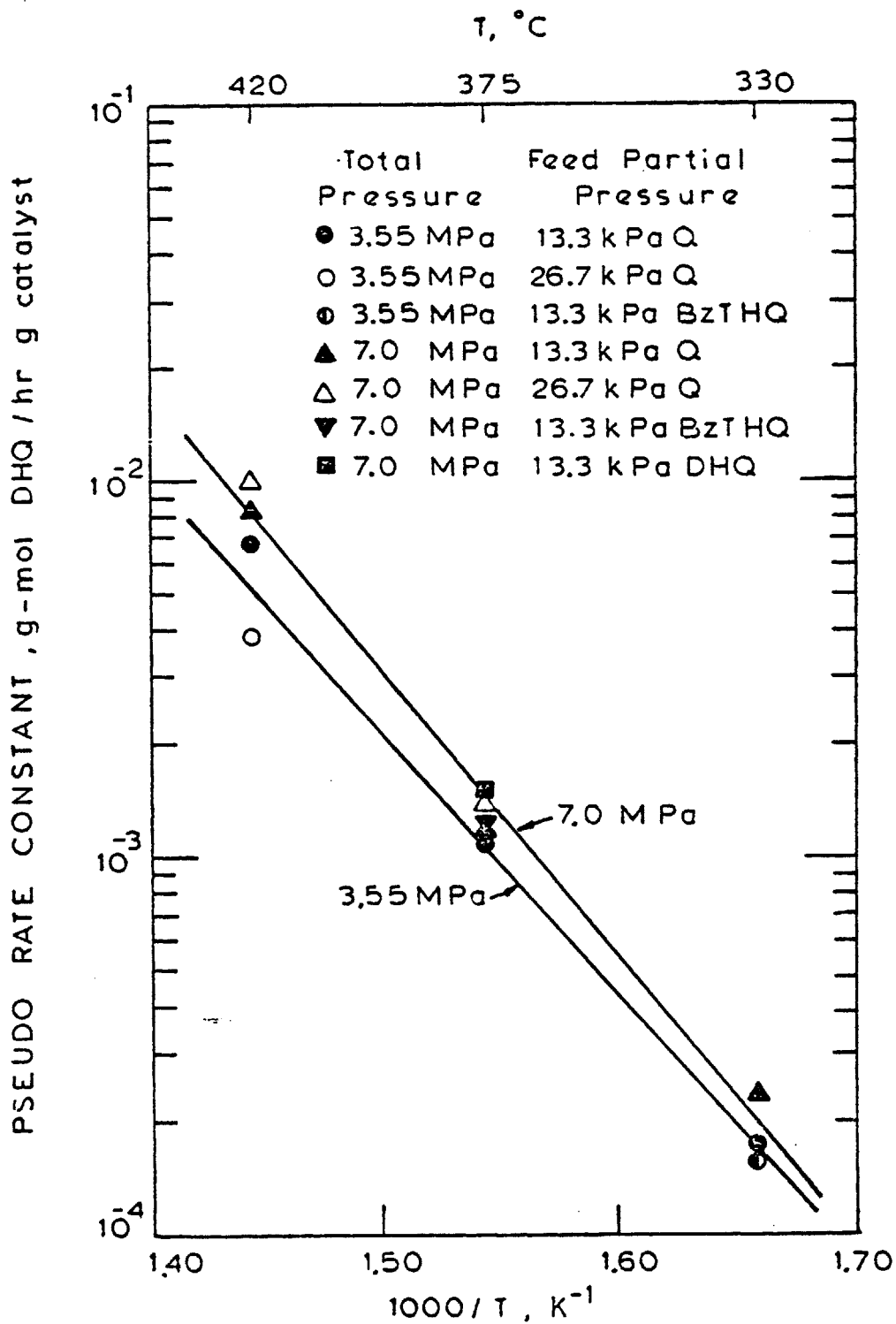


Figure 1-23: Arrhenius Plot of the Pseudo Rate Constant for Hydrogenolysis of Decahydroquinoline to Hydrocarbons and Ammonia

II. Introduction

II. A. Background

Liquid fuels derived from coal, oil shale, tar sand, and residual petroleum fractions are expected to increase in importance as energy demand increases and the availability of petroleum decreases. The synthetic liquids, however, contain a much higher concentration of organic nitrogen compounds than is encountered in most petroleum processed today (see Table 2-1). Crude petroleum contains 0.01 to 0.3% (w/w) nitrogen, while the nitrogen content of synthetic liquids is typically about 1% (w/w).

The United States Environmental Protection Agency (EPA) has established standards for emission of nitrogen oxides from stationary sources as well as from vehicles. Fixation of atmospheric nitrogen during the combustion process is the primary source of this emission with conventional low-nitrogen fuels. Combustion of high-nitrogen fuels in stationary furnaces converts about one-third of the fuel nitrogen to nitrogen oxides, depending on the form of the nitrogen and the firing process. This contribution is in addition to that from the fixation mechanism. Thus the nitrogen content of most synthetic liquids must be significantly reduced if they are to be environmentally acceptable fuels for stationary power plants. For example, the EPA target for coal-derived fuel oil is a maximum nitrogen

Table 2-1
Typical Sulfur and Nitrogen Contents of
Petroleum and Synthetic Liquids

	<u>Wt. % Sulfur</u>	<u>Wt. % Nitrogen</u>
Petroleum		
Deep River, Mich.	0.58	0.12
Yates, Texas	2.79	0.16
Coal Liquids		
Syncrude (COED process*)	0.1	0.3
Fuel oils (SRC process)	0.2-0.5	>1
Syncrude (H-Coal process)	0.19	0.68
Shale Oil (Colorado)	0.75	2
Tar Sand Oil (Utah)	0.75	1.00

*Product quality dependent on severity of hydrotreating

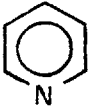
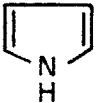
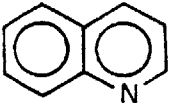
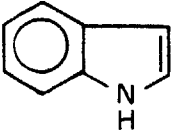
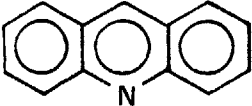
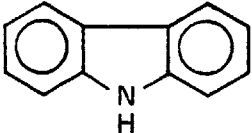
Source: U.S. Environmental Protection Agency

content of 0.3% (w/w).

The use of synthetic liquids as refinery feedstocks also requires significant reduction in nitrogen content, since organic nitrogen compounds (many of which are quite basic) poison the acidic catalysts used in such processes as reforming, cracking, and hydrocracking. Catalytic reformer feedstocks should not contain more than a few ppm (w) nitrogen, while feedstocks containing more than a few hundred ppm (w) are unsatisfactory for catalytic cracking processes. The presence of organic nitrogen compounds in refined products has an adverse effect on color, odor, and storage stability; in addition, some of these compounds may even be carcinogenic.

The nitrogen compounds in petroleum and synthetic liquids are primarily unsaturated heterocyclic structures with the nitrogen incorporated in five- or six-membered rings (see Table 2-2). Pyridine derivatives are generally quite basic, while the pyrrole derivatives are only weakly basic. The nitrogen compounds distribute by boiling point in the various distillate fractions, but the distribution is by no means uniform. Nitrogen content increases sharply with increased average boiling point of petroleum fractions. Thus petroleum naphtha may contain only a few ppm (w) nitrogen, while the corresponding residuum is over 4000 ppm (w) nitrogen. In shale oil fractions the nitrogen is somewhat more evenly distributed, from perhaps 1 weight percent in the naphtha to 2 weight percent in the

Table 2-2
Representative Heterocyclic Nitrogen Compounds
in Petroleum and Synthetic Liquids

	<u>Structure</u>	<u>n.b.p. (°C)</u>
Pyridine		115
Pyrrole		130
Quinoline		238
Indole		254
Acridine		345
Carbazole		355

residuum (Dinneen, 1962).

In petroleum refining today, hydrotreating processes are used extensively to improve the quality of various feedstocks and of petroleum products by selective removal of heteroatoms (sulfur, nitrogen, oxygen, and metals) from their organic combinations, and by hydrogenation of undesirable hydrocarbons such as diolefins. Hydrotreating is accomplished by contacting the feedstock with a suitable catalyst, in the presence of hydrogen at elevated temperatures and pressures. Hydrogenation and hydrogenolysis reactions convert organic sulfur, nitrogen, and oxygen compounds into "clean" hydrocarbons (which remain in the feedstock) and H_2S , NH_3 , and H_2O , respectively. Organometallic compounds are decomposed, and the metals are retained on the hydrotreating catalyst. Hydrotreating processes usually employ fixed bed catalytic reactors, which are operated as trickle-bed reactors for all but the lightest feedstocks (e.g. naphthas, for which vapor-phase operation is possible).

By far the most important application of hydrotreating has been desulfurization of petroleum feedstocks, commonly referred to as hydrodesulfurization (HDS). Representative reaction conditions for hydrodesulfurization of the usual petroleum fractions are summarized in Table 2-3. Sulfided, supported metal catalysts are employed, and are discussed in detail below. Nitrogen removal from feedstocks by hy-

Table 2-3

Reaction Conditions for Hydrodesulfurization of Petroleum Fractions

	<u>Naphtha</u>	<u>Kerosine</u>	<u>Gas Oil</u>	<u>Vacuum Gas Oil</u>	<u>Residua</u>
Temperature, °C	288-399	316-427	343-427	343-454	371-454
Hydrogen partial pressure, psig	100-450	150-500	150-700	450-800	750-2250
Liquid hourly space velocity, V/hr/V	10-2	6-1	6-1	5-1	2-0.2
Hydrogen rate, standard cubic feet per barrel	250-1500	500-1500	1000-2000	1000-4000	1500-10,000
Ultimate catalyst life, barrels per pound	1200-500	600-300	400-200	350-50	50-2

Source: Considine, 1977, p. 3-260

hydrodenitrogenation (HDN) occurs to some extent during hydrodesulfurization, but this has been of secondary importance due to the low nitrogen content of petroleum processed to date. However, nitrogen removal is generally more difficult than sulfur removal, so hydrodenitrogenation could well become one of the limiting problems in processing high-nitrogen synthetic liquids.

II. B. Literature Review

II. B. 1. Hydrotreating Catalysts

Most hydrotreating catalysts consist of a major metal component such as molybdenum or tungsten and a promoter, usually cobalt or nickel, supported on porous high surface area alumina ($\gamma\text{-Al}_2\text{O}_3$). The metals are generally present as oxides in the fresh catalyst, but are converted to sulfides either in a pretreatment step or in actual operation where organic sulfur compounds and H_2S are present. Also, a properly sulfided catalyst is more active for hydrodenitrogenation than the oxidic or reduced catalyst. The most widely used desulfurization catalyst is $\text{CoMo}/\text{Al}_2\text{O}_3$, but $\text{NiMo}/\text{Al}_2\text{O}_3$ is more active for denitrogenation.

The properties and applications of sulfide catalysts are discussed in detail in the book by Weisser and Landa (1973). The brief discussion that follows draws heavily

from this book.

Hydrotreating catalysts are bifunctional in that they possess both hydrogenation and hydrogenolysis activity. It is still questionable as to whether the alumina carrier is inert, or whether it functions like a promoter in contributing significantly to the overall activity of the catalyst. The hydrogenation activity of the catalyst is believed to be associated with the metal sulfides, while the hydrogenolysis activity could be due to acidic support sites or to interaction between the support and metal sulfides. The activity of the metal sulfides is most likely related to crystal lattice defects such as anion vacancies on the crystal edges. The surface acidity of sulfide catalysts is known to affect catalyst activity and selectivity. This acidity can be associated with the metal sulfides as well as with the alumina support. The non-stoichiometric sulfur content of sulfide catalysts also affects activity and selectivity, by influencing primarily the acidic properties of the catalyst. Thus sulfur atoms are a significant component of the active sites in sulfide catalysts. The metal centers undoubtedly play a role as well, but it has been reported that hydrogen adsorbed on sulfur atoms is more active than hydrogen adsorbed on the metals (Samoilov and Rubinshtein, 1960). Hydrogen chemisorbed on sulfur atoms is able to form a large number of hydrosulfide groups (-SH) which contribute greatly to the overall acidity of the catalyst.

An interesting feature of hydrodenitrogenation reactions is the fact that they are also catalyzed by the oxidic (or reduced) form of hydrotreating catalysts. The nature of the active sites must be somewhat different in the oxidic and sulfide forms of the catalyst, so differences in activity and selectivity must also be expected. This may account for some of the seemingly contradictory hydrodenitrogenation results reported in the literature, as a variety of catalysts in both oxidic and sulfide forms have been studied.

II. B. 2. Hydrodenitrogenation Studies

HDN studies have been conducted with actual feedstocks, and with model nitrogen compounds either in pure form or dissolved in simulated or actual feedstocks. Actual feedstock studies are by necessity more empirical, providing perhaps scalable kinetic data and allowing some general observations to be made about the overall HDN process. Little fundamental understanding is gained, however, about HDN reaction networks and the mechanism of catalytic action. Model compound studies can be of great assistance in obtaining a more fundamental understanding of HDN reactions, though the significant engineering task of applying these results toward improvement of industrial operations remains.

Overall nitrogen removal from petroleum feedstocks, shale oils, and coal liquids has generally been found to be first order in nitrogen concentration, at least with respect to reaction time (Flinn et al., 1963; Frost and Jensen, 1973; Qader et al., 1968). Flinn et al. (1963) also reported a decrease in the HDN rate of various petroleum fractions with increased average boiling point of the feedstock. The authors attributed this to steric hindrance effects in higher molecular weight nitrogen compounds, making effective adsorption onto the catalyst more difficult, and to the tendency of higher boiling fractions to contain more of the less reactive aromatic-type heterocyclic nitrogen compounds. More recently, however, Katzer and Sivasubramanian (1979) point out that nitrogen compounds inhibit their own rates of reaction due to competitive adsorption of the reactants and reaction products. As a result, higher boiling feedstocks are more difficult to denitrogenate because of their higher concentration of nitrogen compounds and resultant increased HDN rate inhibition.

Model compound studies have been conducted, most often with pyridine, but also with other representative nitrogen compounds. These studies indicate that HDN reaction networks for heterocyclic nitrogen compounds all involve initial saturation (hydrogenation) of the heterocyclic ring, followed by heterocyclic ring opening through hydrogenolysis of a C-N bond. The resulting aliphatic or

aromatic amine intermediates can then be converted to hydrocarbons and ammonia via hydrogenolysis of another C-N bond. Many side reactions can also occur, particularly for the multiring heterocyclic nitrogen compounds. Aromatic ring saturation, hydrocracking (hydrogenolysis of C-C bonds), alkyl transfer reactions, disproportionation, dehydrocyclization, and condensation (coking) reactions have all been observed.

The thermodynamics of HDN reactions have been reported (Cocchetto, 1974; Cocchetto and Satterfield, 1976). Equilibrium constants for HDN reactions of various heterocyclic nitrogen compounds were estimated, and it was concluded that under HDN reaction conditions hydrogenolysis of C-N bonds is essentially irreversible, while initial saturation of heterocyclic rings is potentially reversible or thermodynamically limited. This potential thermodynamic limitation on heterocyclic ring saturation can adversely affect the overall HDN rate if the kinetics of the various reaction steps are such that the heterocyclic ring opening step is substantially rate-limiting (Satterfield and Cocchetto, 1975).

There is no general agreement on the rate-limiting step(s) in HDN reaction networks. In fact, both hydrogenation and hydrogenolysis rates may be important in determining the overall HDN rate, though their relative importance is undoubtedly a function of reaction conditions, catalyst employed, and nature of the nitrogen

compound.

II. B. 3. Quinoline Hydrodenitrogenation Studies

Doelman and Vlugter (1963) studied quinoline HDN in a continuous fixed-bed reactor system using prereduced CoMo/Al₂O₃ catalyst. They concluded that nitrogen removal proceeded primarily through Py-tetrahydroquinoline (PyTHQ) and various aniline intermediates, and that breakdown of the anilines was the rate-determining step. The effect of chlorides on quinoline HDN was investigated by Madkour et al. (1969), using a batch reactor system and prereduced CoMo/Al₂O₃. Nitrogen removal from quinoline was significantly increased when a large excess of hydrogen chloride, generated in situ from dichloroethane, was present in the reactor. The hydrogen chloride appeared to accelerate hydrogenolysis reactions. Aboul-Gheit and Abdou (1973) also employed a batch reactor system and oxidic CoMo/Al₂O₃ catalyst for hydrodenitrogenation studies of quinoline and other model nitrogen compounds. Nitrogen removal from quinoline was reported to follow pseudo first order kinetics, with an activation energy of 126 kJ/g-mol (30 kcal/g-mol). The authors concluded that hydrogenolysis of the heterocyclic ring in PyTHQ was the rate-determining step in quinoline HDN, and postulated that the basicity of nitrogen compounds plays a role in their HDN mechanisms.

More recently, Satterfield and co-workers at M.I.T. studied the intermediate reactions in quinoline HDN over a presulfided NiMo/Al₂O₃ catalyst, in a continuous vapor-phase reactor (Declerck, 1976; Satterfield et al., 1978). Under all reaction conditions investigated, quinoline was rapidly hydrogenated to essentially an equilibrium concentration of PyTHQ. The dominant initial reaction pathway was reported to vary with temperature. Thus at lower temperatures the concentration of quinoline was much less than that of PyTHQ, and the latter was converted to either o-propylaniline or decahydroquinoline (DHQ). At higher temperatures the equilibrium concentration of quinoline relative to PyTHQ was greatly increased, and the conversion rate of quinoline to Bz-tetrahydroquinoline (BzTHQ) and subsequently to DHQ became significant. Finally, the formation of high molecular weight compounds, some containing nitrogen, was observed under the more extreme reaction conditions.

A significant HDN research effort is currently under way at the University of Delaware. Shih et al. (1977) investigated the kinetics of quinoline HDN in a batch liquid phase (slurry) reactor using sulfided NiMo/Al₂O₃ catalyst and a paraffinic white oil carrier liquid. Quinoline was again rapidly hydrogenated to an equilibrium concentration of PyTHQ, but the other hydrogenation reactions as well as the hydrogenolysis reactions were reported to be kinetically controlled. The rates of each

of these reactions were described by first order kinetics, and the corresponding rate constants were estimated by a computer fitting technique. These rate constants varied with initial quinoline concentration and with hydrogen partial pressure as well as with temperature. They were interpreted through a Langmuir-Hinshelwood kinetic model in which hydrogen and nitrogen compounds compete for active catalyst sites, and all nitrogen compounds have comparable adsorption constants. Activation energies were about 84 kJ/g-mol (20 kcal/g-mol) for the hydrogenation reactions, about 147 kJ/mole (35 kcal/g-mol) for the hydrogenolysis reactions, and 105 kJ/g-mol (25 kcal/g-mol) for total nitrogen removal. The hydrogenation reactions were reported to be second order in hydrogen, but the hydrogenolysis reactions were of lower order in hydrogen. It was concluded from the kinetic analysis that nitrogen removal occurred primarily through the BzTHQ and DHQ intermediates. The effects of different catalysts, presulfiding, and H_2S on quinoline HDN were also investigated (Shih et al., 1978). Presulfided NiMo/ Al_2O_3 was a slightly better catalyst for nitrogen removal than presulfided CoMo/ Al_2O_3 or NiW/ Al_2O_3 . Presulfided NiMo/ Al_2O_3 was also about twice as active as the oxidic form for nitrogen removal. Finally, the presence of H_2S in the reaction environment, even with a presulfided catalyst, increased the rate of nitrogen removal.

Additional quinoline HDN studies in a liquid phase flow microreactor have been reported (Eliezer et al., 1977), but it is questionable whether enough hydrogen could be dissolved in the liquid feed to avoid hydrogen deficiency at high conversions.

II. B. 4. Adsorption Phenomena in Catalytic Hydrodenitrogenation

Nitrogen compounds adsorb strongly and competitively on hydrotreating catalysts (in either the oxidic or sulfide form), as shown by a variety of reaction studies and adsorption measurements. The rates of HDN reactions have often been adequately described by first order kinetics, in which the first order rate constant decreases with increased initial nitrogen concentration, or by pseudo first order kinetics (Flinn et al., 1963; Sonnemans et al., 1973; Shih et al., 1977). This behavior is attributed to inhibition of the reaction rates by the strongly adsorbed nitrogen compounds, and can be interpreted in terms of a Langmuir-Hinshelwood kinetic model assuming equally strong adsorption of the nitrogen compounds. There is evidence, however, that the strength of adsorption of nitrogen compounds may vary significantly. In a study of shale oil HDN, Koros et al. (1967) found that the indole-type compounds were less reactive than the quinolines, but the opposite reactivities have been reported for indole and

quinoline when studied individually (Flinn et al., 1963; Aboul-Gheit and Abdou, 1973). This apparent discrepancy was attributed to competitive adsorption effects in mixtures, in which the more basic quinoline-type compounds were preferentially adsorbed and converted. In a study of pyridine HDN over presulfided NiCoMo/Al₂O₃ catalyst, McIlvried (1971) observed increased inhibition in the rate of hydrogenation of pyridine to piperidine as conversion increased, implying that some reaction product was more strongly adsorbed on the hydrogenation sites than the pyridine reactant. A Langmuir-Hinshelwood kinetic expression, in which ammonia was assumed to be the only compound strongly adsorbed on the hydrogenation sites, fitted the pyridine hydrogenation data. In contrast, the kinetics of piperidine hydrogenolysis suggested equal adsorption strengths for the nitrogen compounds on the hydrogenolysis sites.

Sonnemans et al. (1973) studied the competitive adsorption of pyridine and ammonia, from a mixture, on prereduced (oxidic) Mo/Al₂O₃ catalyst and on the alumina support alone. The competitive adsorption of pyridine and piperidine on the Mo/Al₂O₃ catalyst was similarly investigated. Pyridine adsorbed about four times as strongly as ammonia on both Mo/Al₂O₃ and Al₂O₃, while the adsorption strength of piperidine was

about six times that of pyridine on the Mo/Al₂O₃ catalyst. Adsorption measurements such as these, however, may be misleading in that adsorption may occur in part on sites that are inactive for reaction.

It is often assumed that hydrogen and the nitrogen compounds adsorb on different catalyst sites. This is supported by adsorption measurements (Sonnemans et al., 1973) and by HDN kinetic studies. On sulfide catalysts, hydrogen is believed to adsorb dissociatively on sulfur atoms, forming hydrosulfide groups (Weisser and Landa, 1973, p. 78; Gates et al., 1979, p. 423). The active catalyst sites are most likely associated with defects such as anion (S⁻²) vacancies in the metal sulfides, and possibly with the support. Thus it seems plausible, from a mechanistic view as well, that hydrogen and the nitrogen compounds adsorb on different, perhaps neighboring, sites.

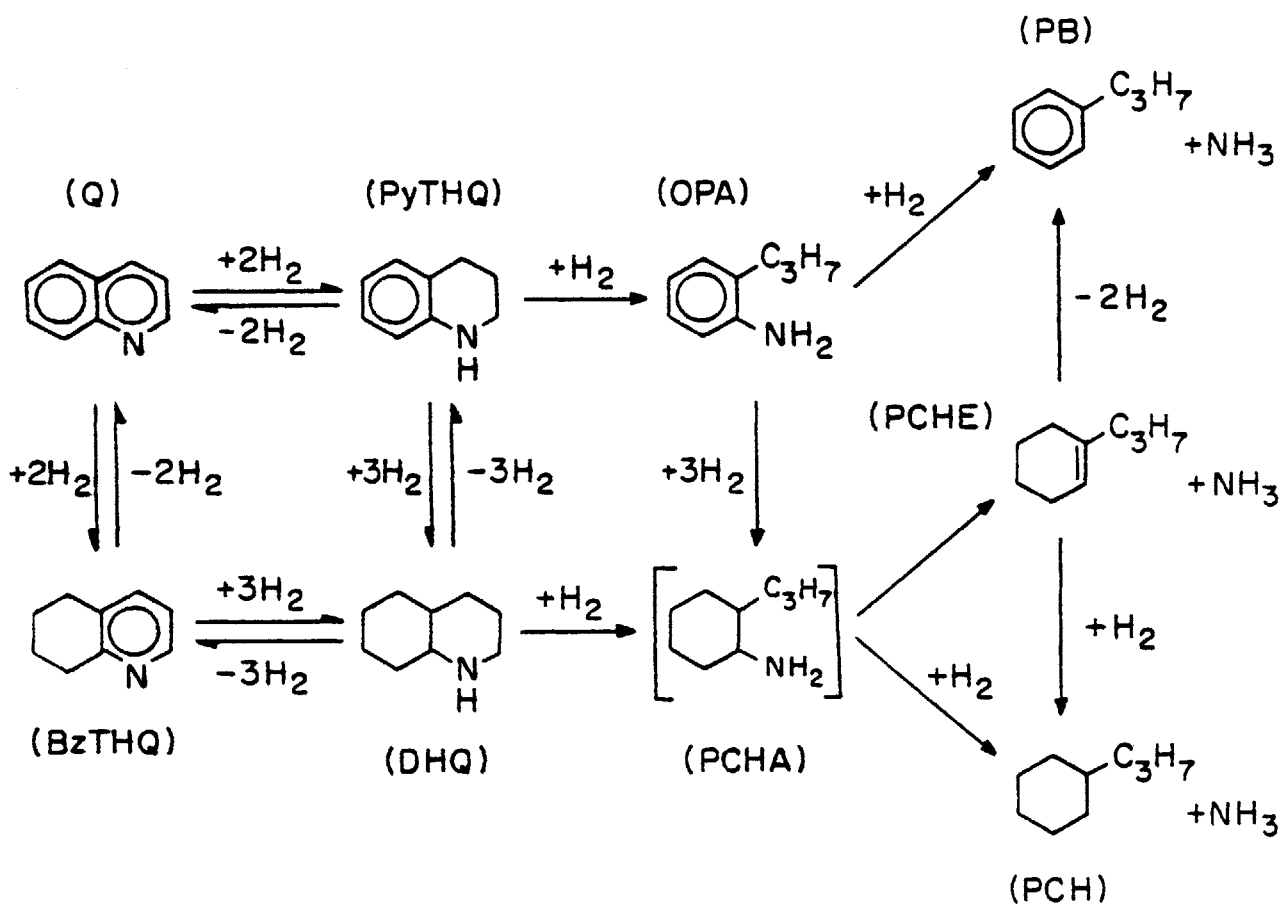
The adsorption of most hydrocarbons is very weak compared with that of the nitrogen compounds. Thus hydrotreating catalysts with significant hydrogenation activity for aromatics or olefins in the absence of nitrogen compounds, have negligible activity for hydrogenation of unsaturated hydrocarbons in the presence of even low concentrations of nitrogen compounds (see for example Goudriaan, 1974, pp. 82-9). In model compound HDN studies, adsorption of hydrocarbon products or solvent is usually safely ignored.

II. C. Quinoline Hydrodenitrogenation Reaction Network and Thermodynamics

The reaction network for quinoline HDN is shown in Figure 2-1. This network is consistent with the results of the present investigation, and, except for consideration of the reversibility of all the initial ring saturation reactions is basically in agreement with the less detailed reaction networks proposed in earlier studies (Shih et al., 1977; Satterfield et al., 1978). Saturation of the heterocyclic ring is required before hydrogenolysis of C-N bonds and nitrogen removal reactions can proceed. The aromatic ring in quinoline can also be saturated, either as the initial reaction step or during the nitrogen removal process.

Equilibrium constants have been estimated for each of the reaction steps proposed in quinoline HDN, and are shown as a function of temperature in Figures 2-2, 2-3, and 2-4. It should be pointed out that both cis and trans isomers of DHQ were considered in estimating the equilibrium constants for reactions involving DHQ. Also, the equilibrium constants for quinoline hydrogenation to PyTHQ, shown in Figure 2-2, and for the PyTHQ and o-propylaniline hydrogenolysis reactions, shown in Figure 2-3, are identical to the equilibrium constants reported previously for these reactions (Cocchetto, 1974; Cocchetto and

FIGURE 2 - I
QUINOLINE HDN REACTION NETWORK



Q	quinoline
PyTHQ	Py (or 1,2,3,4) - tetrahydroquinoline
BzTHQ	Bz (or 5,6,7,8) - tetrahydroquinoline
DHQ	decahydroquinoline (cis and trans isomers)
OPA	o-propylaniline
PCHA	propylcyclohexylamine
PB	propylbenzene
PCHE	propylcyclohexene
PCH	propylcyclohexane

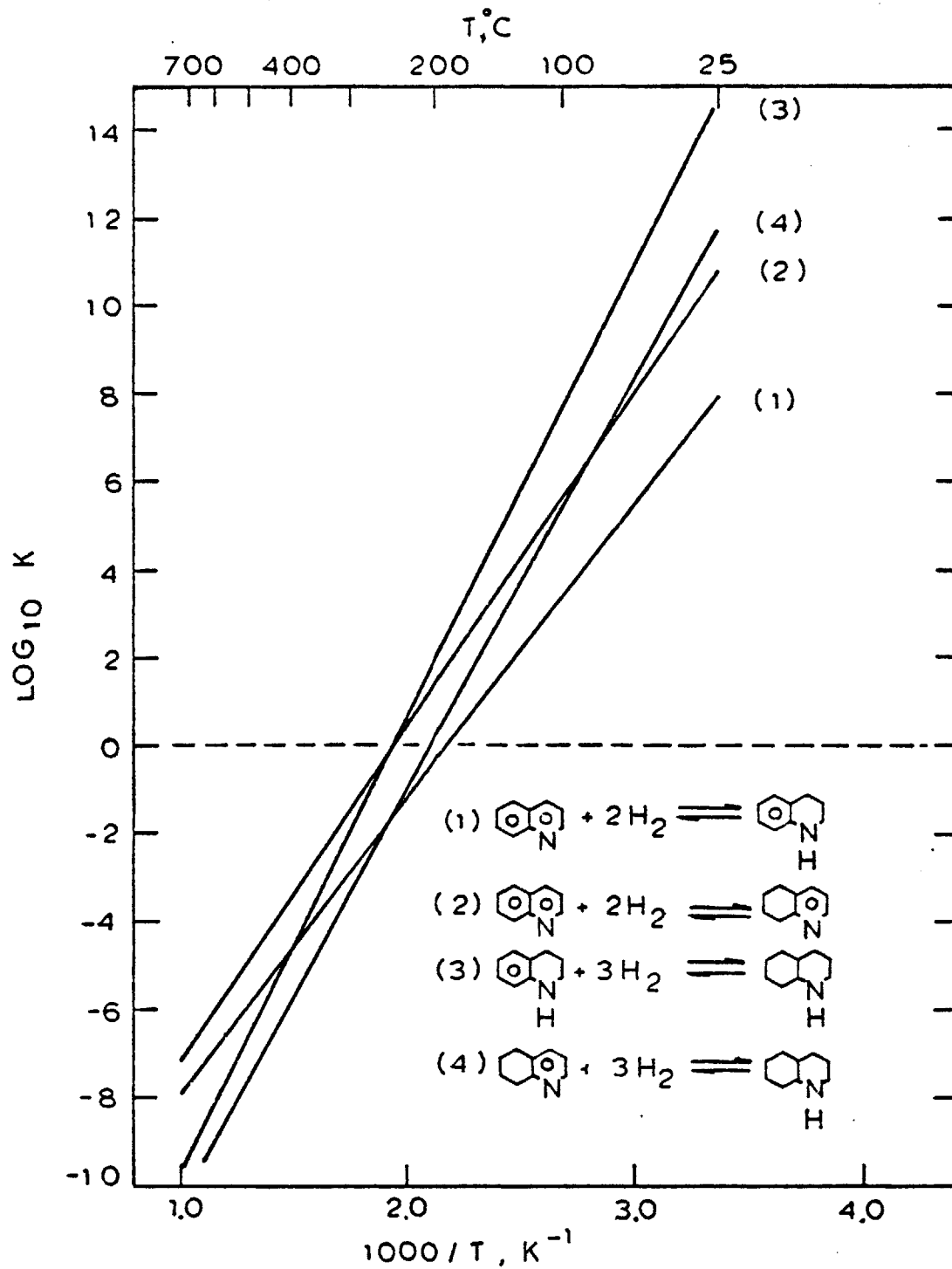


Figure 2-2: Equilibrium Constants for Initial Ring Saturation Reactions in Quinoline HDN

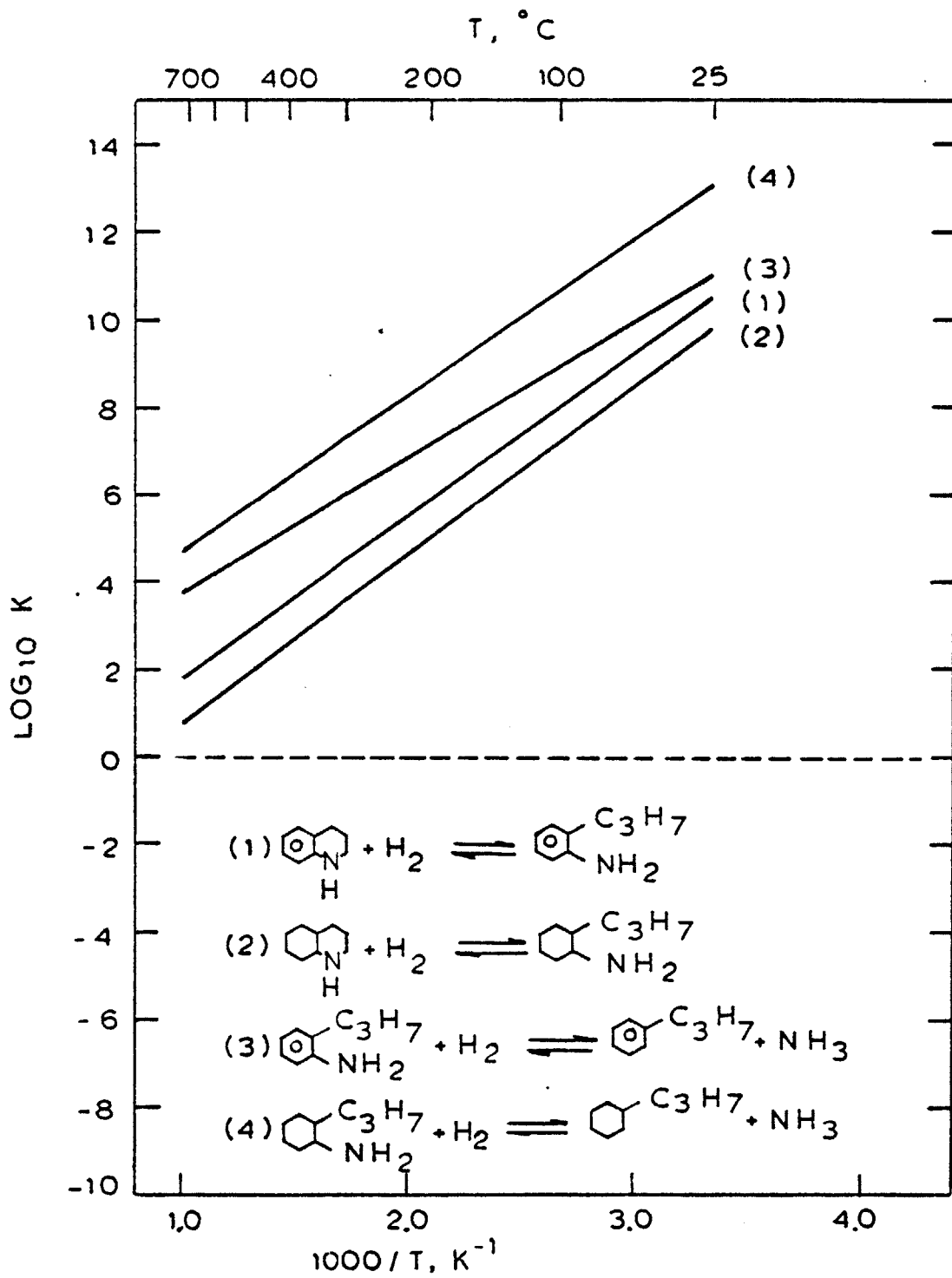


Figure 2-3 : Equilibrium Constants for Hydrogenolysis Reactions in Quinoline HDN

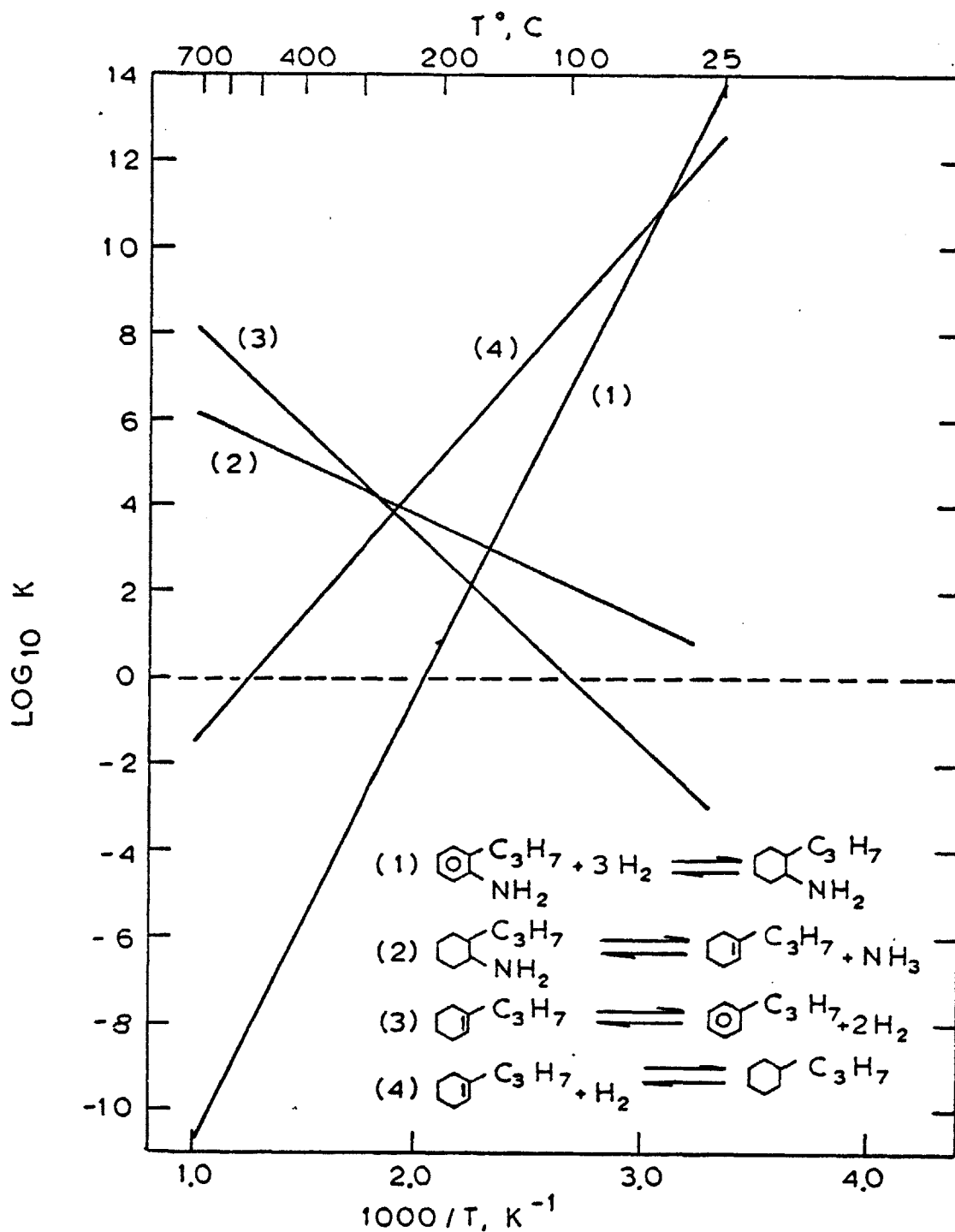


Figure 2-4: Equilibrium Constants for Miscellaneous Reactions in Quinoline HDN

Satterfield, 1976). Standard free energies of formation are available only for ammonia, propylbenzene, and propylcyclohexane (Stull et al., 1969). The standard free energies of formation of o-propylaniline, propylcyclohexylamine, and propylcyclohexene were estimated by Benson's group contribution technique (Benson et al., 1969), while those for the heterocyclic nitrogen compounds (for which Benson's method was inapplicable) were estimated by a less accurate modified van Krevelen group contribution technique (van Krevelen and Chermin, 1951; Cocchetto, 1974). The estimated standard free energies of formation are listed in the Appendix, and details of the estimation techniques are given by Cocchetto (1974). Estimated equilibrium constants for reactions involving heterocyclic nitrogen compounds could be in error by one to two orders of magnitude, while those for the other reactions are more accurate, perhaps within an order of magnitude. In spite of this limitation some important generalizations can be made regarding the thermodynamics of quinoline HDN. The initial saturation reactions are all exothermic, with unfavorable equilibrium constants ($K < 1$, $\log_{10} K < 0$) at the higher temperatures relevant to HDN (see Figure 2-2). Since hydrogen is consumed in each of these saturation reactions, increased hydrogen partial pressure shifts these equilibria toward the saturated species. Thus, under HDN conditions, saturation of the aromatic ring as well as the heterocyclic ring of quinoline is potentially

reversible; that is, significant quantities of the saturated and unsaturated species could be present if each of these reactions approached equilibrium, depending on the temperature and hydrogen partial pressure. The hydrogenolysis reactions are less exothermic than the saturation reactions (less hydrogen is consumed), but the hydrogenolysis reactions are essentially irreversible under HDN conditions since their equilibrium constants are so large (see Figure 2-3). The estimated equilibrium constants for the other reactions proposed in the quinoline HDN network are shown in Figure 2-4. For introductory purposes, suffice it to say that these reactions can also be considered irreversible, at least under the conditions of the presented study.

As mentioned previously, the hydrogenation of quinoline (Q) to PyTHQ has been observed to proceed rapidly to equilibrium under HDN conditions (Declerck, 1976; Shih et al., 1977; Satterfield et al., 1978). The equilibrium constants for this reaction were estimated by each of these investigators from their experimental data, and are in excellent agreement. These experimentally determined equilibrium constants were used to calculate the equilibrium ratio of PyTHQ to quinoline as a function of temperature and hydrogen partial pressure (see Figure 2-5). This information will be useful in the presentation and discussion of the experimental results.

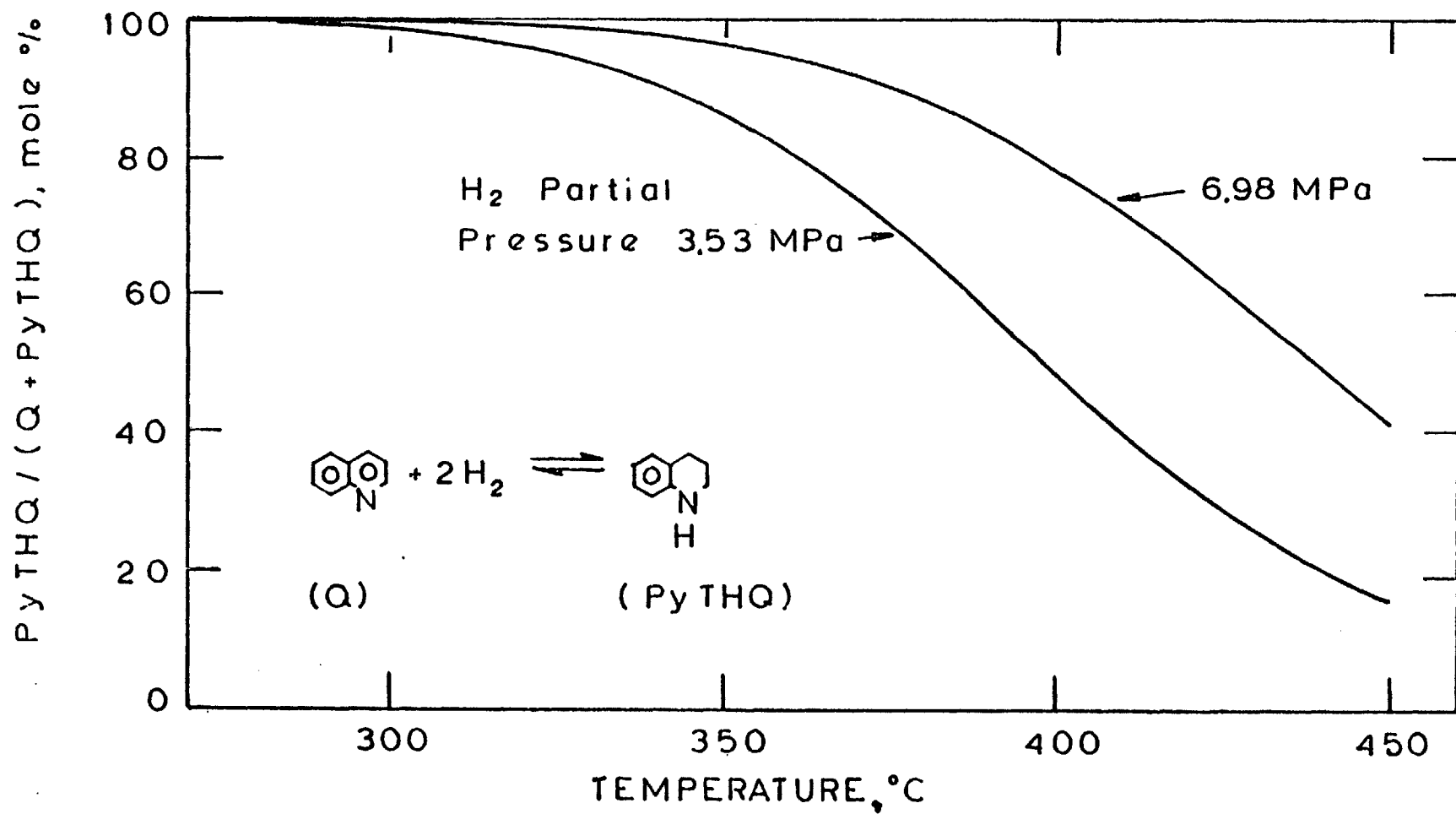


Figure 2-5: Quinoline / Py - Tetrahydroquinoline Equilibrium

II. D. Thesis Objectives

A continuing HDS/HDN research program at M.I.T. has had as its objective the development of a more fundamental understanding of HDS and HDN reactions, with a view toward improved processing schemes for removal of sulfur and especially nitrogen from synthetic liquid fuels. Model compound studies have been employed to meet this objective, and to set the groundwork for more complex future studies.

The present study focused on HDN of quinoline, a heterocyclic nitrogen compound representative of those found in middle distillate fractions of petroleum and synthetic liquids. Quinoline is also a good model compound for HDN studies as it contains an aromatic ring as well as the heterocyclic ring, thus providing the opportunity to examine the extent of aromatic ring saturation during nitrogen removal. It was desired to determine in detail the kinetics of quinoline HDN under industrially relevant reaction conditions, to obtain a better fundamental understanding of the reaction network and the nature of the catalytic action. The basic approach was to determine the effects of reaction variables on product distribution not only from quinoline HDN but also from HDN of each of the nitrogen-bearing intermediates in the reaction network. This permitted experimental investigation of the potential reversibility of the initial ring saturation reactions, and segmented the complex quinoline HDN reaction network thus simplifying kinetic analysis.

III. Apparatus and Procedure

III. A. Experimental Apparatus

The HDN experiments were carried out in a continuous flow, fixed-bed catalytic reactor system employing a pre-sulfided commercial NiMo/Al₂O₃ catalyst. The reactor was operated isothermally, in the integral mode. Reaction temperatures ranged from 330 to 420°C; reactor pressure was either 3.55 MPa (500 psig) or 7.0 MPa (1000 psig).

Liquid reactant (quinoline or one of its hydrogenated derivatives) was metered into the system by a high-pressure pump and flash-vaporized into a stream of heated hydrogen. The resulting vapor-phase mixture was preheated to reaction temperature, and fed to the reactor. Samples of the reactor effluent were injected into an on-line gas chromatograph by means of a heated gas sampling valve. Product distributions and reactant conversions were determined from the gas chromatographic analyses.

A schematic of the experimental apparatus is shown in Figure 3-1; the heavy lines indicate the primary flows during steady-state operation. The main sections of this apparatus are described in detail below.

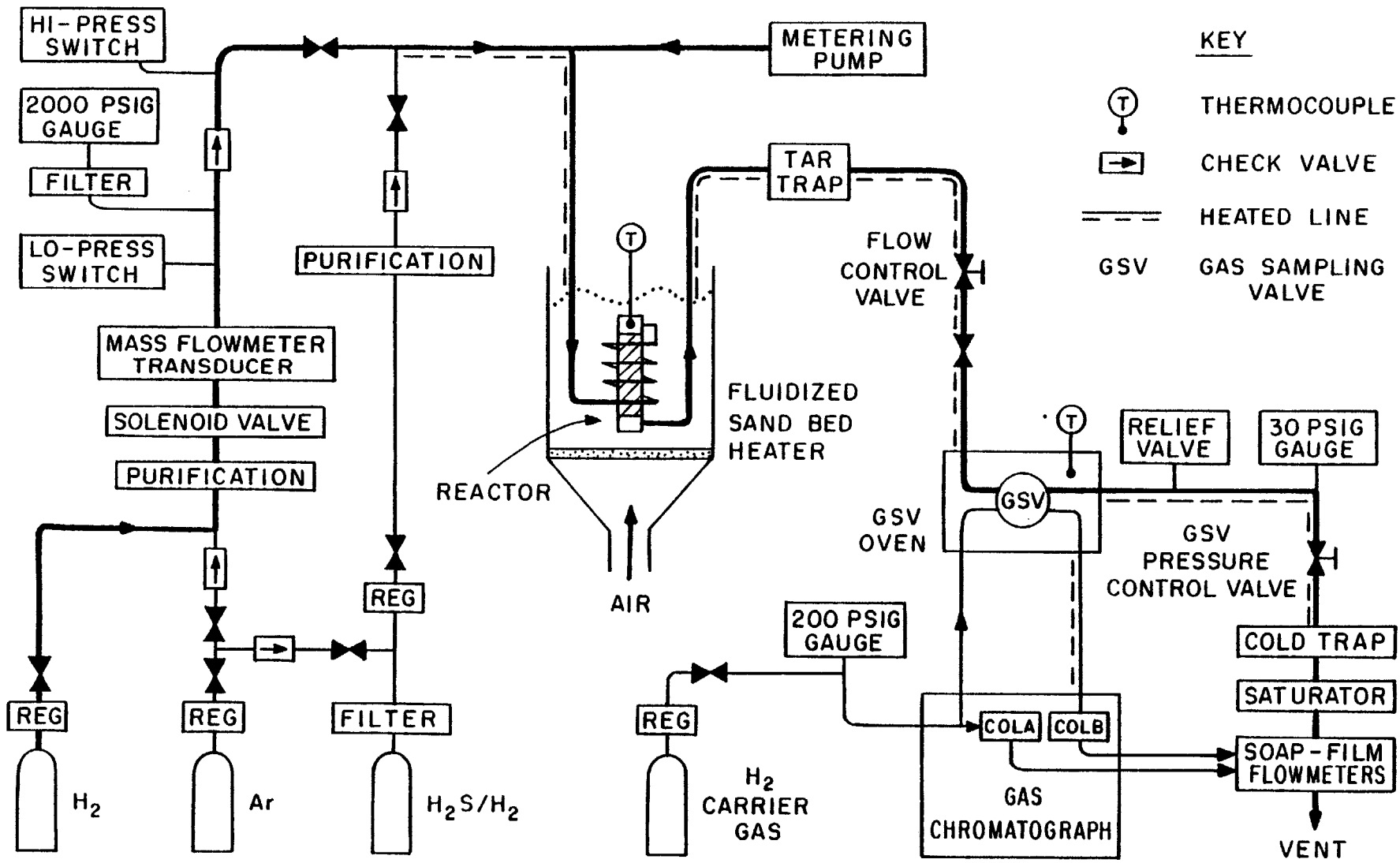


FIGURE 3-1: SCHEMATIC OF EXPERIMENTAL APPARATUS

III. A. 1. Reactant Feed Section

Reactant hydrogen was supplied from a high-pressure (3500 psig) cyclinder equipped with a single-stage regulator (Precision Gas Products model 350-1200-NT01, manufactured by Tescom). This regulator was used to control the reactor pressure to within a few psi of the desired level. The hydrogen was passed over a palladium catalyst (Engelhard Deoxo Purifier D-10-2500) to convert traces of oxygen to water, which was then adsorbed in a drying column packed with type 4A molecular sieves. A seven micron filter removed particulates from the hydrogen stream to protect the small orifices in the solenoid valve (part of the automatic safety system described later) and mass flowmeter transducer (Hastings-Raydist model H-1KMP). The mass flowmeter was used to monitor hydrogen feed rate stability, and was an aid in setting flow rates. The hydrogen then passed through a check valve (installed to prevent back-up of the reaction gas into the hydrogen feed system) and a preheating coil maintained at approximately 225°C.

A high-pressure metering pump (Instrumentation Specialties Company model 314) was used to feed liquid reactant through a short length of capillary tubing (0.419 mm ID) to the mixing tee, where the liquid was flash-

vaporized into the preheated hydrogen stream. The resulting mixture passed through a mixing and preheating coil, maintained at about 225°C, before entering the final preheating coil immersed in the fluidized sand bath. The pump was capable of metering liquid at any rate from a small fraction of a cc/hr to as high as 200 cc/hr. Liquid feed rates in this study varied from about 0.2 to 5 cc/hr, so only the two lowest feed ranges of the pump were calibrated (see Appendix). The pump was equipped with a shear pin in the drive mechanism to prevent damage from over-pressurization. This was important as the liquid feed capillary did plug periodically.

An auxiliary feed system allowed a mixture of 10% H₂S in H₂ to be fed to the reactor to sulfide the catalyst periodically. Leakage of H₂S from the low-pressure regulator (Matheson model 14M-330) had been a problem in an earlier system, but was eliminated by installing a filter and tee-purge assembly between the cylinder and the regulator. Argon was used to purge the H₂S/H₂ feed system as well as the reactant hydrogen feed system. Back-up of hydrogen or H₂S into the argon feed system was prevented by suitably located check valves and shutoff valves.

III. A. 2. Reactor Section

The reactor was a straight length of type 316 stainless steel tubing (3.86 mm ID) packed with 1.50 grams (before sulfiding) of 20/24 mesh catalyst particles (0.774 mm average diameter). The catalyst bed was secured on both ends by small glass wool plugs and stainless steel screens. The radial aspect ratio (ratio of the bed diameter to the catalyst particle diameter) was five, sufficiently large to avoid channeling and wall heat transfer limitations (Doraiswamy and Tajbl, 1974). The axial aspect ratio of approximately 240 was much greater than the minimum value of 30 necessary to insure plug-flow operation, so axial dispersion and conduction were not significant (Doraiswamy and Tajbl, 1974). Consistent with previous work in our laboratory, the use of 20/24 mesh catalyst particles insured that there were no significant heat or mass transfer limitations in the reactor.

The reactor and final preheating coil were both immersed in a fluidized sand bed heater (Tecam model SBS-4), with proportional temperature controller. The sand bed had been modified to increase the original depth (Wilkins, 1977). The heated reactant gas mixture reached reaction temperature in the final preheating coil, before entering the reactor. This reaction mixture then passed downward through the reactor, which was mounted vertically. Reaction temperature

was measured with a 1/16-inch thermocouple inserted through a bored-out reducer into the vapor space just above the catalyst bed. Three additional thermocouples were located in the sand bed a short distance from the outside of the reactor, at heights corresponding to the top, middle, and bottom of the catalyst bed. These three temperatures were all within 1°C of the reaction temperature measured by the process thermocouple, when the sand bed was properly fluidized and at steady state, thus insuring isothermal operation.

Reactor pressure was measured with a 2000 psig Ametek Precision Test Gauge (0.25% accuracy) located just upstream from the check valve in the reactant hydrogen feed system. A filter (Cajon "snubber") was installed at the inlet of the pressure gauge to protect it from potential pressure surges. For the flow rates used in this study there was negligible pressure drop through the high-pressure portion of the apparatus, except across this check valve. The measured pressure drop was about 0.10 MPa (15 psi), essentially independent of hydrogen flow rate, and was taken into account when setting and recording reactor pressures.

The tar trap in the exit line from the reactor was designed to condense very high-boiling compounds that would otherwise have condensed in cooler downstream portions of the experimental apparatus, particularly in the analytical system. The tar trap consisted of two lengths of 9.53 mm ID stainless steel tubing, packed with 3 mm diameter Pyrex

glass beads held in place by stainless steel screens. These lengths of tubing were connected in a U-configuration, with a small dead volume at the bottom for removing any tar accumulation from the flow path. The trap was operated at approximately 240°C - a temperature too high to condense any of the reactants or major reaction products, but sufficiently low to prevent condensation of tar downstream. The short reactor exit line to the tar trap was maintained at a temperature 5 to 10°C higher than the reactor temperature.

Total flow rate through the system was controlled manually with a very fine metering valve (Nupro model SS-2SA), which also served to reduce the reactor effluent from reactor pressure to the low pressure maintained in the gas sampling valve. Since the pressure drop across this valve was much more than half the upstream pressure, there was critical flow through the valve. This was desired to allow the pressure in the gas sampling valve to be controlled independently, without affecting the flow rate through the system. The metering valve was maintained at 250°C (about 10°C hotter than the tar trap, to prevent condensation), so Teflon packing could not be used. Instead, a carefully machined piece of Vespel was used as packing and worked extremely well. A packless bellows valve (Nupro model SS-4TRW) located immediately downstream from the metering valve was used for shutoff service.

III. A. 3. Sampling and Analysis Section

An eight-port gas sampling valve (Carle model 2014) with two matched 4 cc loops was used to inject samples of the reactor effluent into the gas chromatograph. The gas sampling valve was mounted in an isothermal recirculating-air oven maintained at approximately 200°C to prevent condensation of any of the compounds in the reactor effluent. This temperature, monitored by a thermocouple in the oven, was somewhat lower than the tar trap temperature but was more than sufficient to prevent condensation since the pressure in the gas sampling valve was so much lower than the tar trap pressure (essentially the same as the reactor pressure). The reactor effluent passed through a heat transfer coil in the oven before going to the gas sampling valve. This insured that the reactor effluent was at oven temperature when sampled. It was important to maintain constant temperature and pressure in the gas sampling valve in order to inject the same quantity (moles) of gas in each sample, thereby providing a check on sample reproducibility. This pressure was manually controlled, usually at 0.17 MPa (10 psig), with a fine metering valve (Nupro model SS-2MA-TFE) downstream from the gas sampling valve. The pressure control valve and connecting lines were maintained at 190-200°C. A 30 psig Ametek Precision Test Gauge was used to measure the pressure in the gas

sampling valve. The pressure gauge and the gas sampling valve were both protected from potential excessive pressure by a relief valve, set at about 0.27 MPa (25 psig).

Downstream from the gas sample pressure control valve, a 250 ml Erlenmeyer flask maintained at ambient temperature served as a "cold" trap to condense most of the organics in the reactor effluent. The quantity of liquid product collected during an experimental run can be compared with the quantity of liquid reactant fed, as a rough check on the material balance. Some samples of the liquid product were also subjected to GC/MS analysis to identify unknowns and to verify the on-line analyses. Attempts to cool the trap with ice-water to improve condensing efficiency met with limited success due to the tendency of some compounds, mainly PyTHQ, to freeze out in the inlet line causing sporadic flow and pluggage.

The effluent from the cold trap was saturated with water to improve the operation of the soap-film flowmeters used to measure the exhaust gas flow rate. A filter element welded to the bottom of the inlet line to the saturator dispersed the entering gas as very tiny bubbles, and prevented pulsing of the gas through the water even at very low flow rates. Total flow rates through the system varied from about 100 to 4000 standard cc/min, so one of three soap-film flowmeters (50, 250, or 1000 cc) was used to

accurately measure the volumetric flow rate. Thermometers in the flowmeters were used to measure the temperature at which a flow measurement was made; the barometric pressure was obtained from the National Weather Service.

The gas chromatograph (Varian model 2820-30) was equipped with a thermal conductivity detector, dual columns, and temperature programming capability. Hydrogen carrier gas, purified in the same manner as the reactant hydrogen, was used rather than helium to obtain higher sensitivity for all species other than hydrogen in the samples (the reaction gas always contained over 99% hydrogen). A strip-chart recorder (Houston Instruments Omniscribe model A-5113-5) displayed the output from the gas chromatograph, and peak areas were automatically quantified with a digital integrator (Autolab Vidar 6300).

III. A. 4. Gas Chromatographic Analyses

A significant amount of time and effort was spent developing an analytical column capable of separating all of the major quinoline HDN products (including ammonia). The analysis of amines by gas chromatography is often difficult due to the tendency of these basic compounds to adsorb on the diatomite supports commonly employed. This results in asymmetrical "tailing" peaks difficult to quantify, and sometimes even in sample loss due to permanent adsorption. In addition, the HDN samples

contained compounds with widely-varying boiling points, and the analysis time had to be minimized for efficient data collection.

In a preliminary study of quinoline HDN in this laboratory, Declerck (1976) used a 10-foot glass column packed with 3% SP-2250 on Supelcoport. This column, however, did not separate BzTHQ and OPA, and the ammonia analyses were suspect (Satterfield et al., 1978). Wilkens (1977) used 10% SP-2310 on Supelcoport to separate the higher boiling products from pyridine HDN, and this column was evaluated as well. All the major products from quinoline HDN could be separated, but ammonia tailed so badly that it interfered with the hydrocarbons that eluted relatively quickly. As expected, diatomite supports (such as Supelcoport) could not be used here because of the ammonia in the samples. A group at the University of Delaware reported the use of Chromosorb 103 to separate quinoline HDN reaction products (Shih et al., 1977; Eliezer et al., 1977). Chromosorb 103 was evaluated as it is a porous polymer designed specifically for amine separations. A nice ammonia peak was obtained, but with a 6-foot column separation of BzTHQ and OPA was difficult, high-boiler peaks were very broad, and analysis time was too long.

At this point it was decided to try a Teflon support, because of its inertness, with a suitable stationary phase.

As silicones wet Teflon, the SP-2310 (a cyanopropylsilicone) used previously with Supelcoport was tried with Chromosorb T - probably the best Teflon support (Kirkland, 1963). A 10-foot glass column packed with 10% SP-2310 on Chromosorb T was successful in separating ammonia, PCH, PB, DHQ, BzTHQ, OPA, Q, and PyTHQ with essentially no tailing. The column was operated isothermally at 190°C with 80 cc/min hydrogen carrier gas flow (the column was 4 mm ID), and analysis time was only 16 minutes. However, when this column was used for on-line analysis of the quinoline HDN products, several problems arose. Hydrocarbons other than PCH and PB were formed, and were not well-separated. These additional hydrocarbons (later identified as ECH, PCHE, and EB) were separated by temperature programming the analytical column from 110°C to 190°C at 40°C/min and holding at 190°C until the analysis was completed. This added only 2 minutes to the analysis time. A more serious problem was interference in the rapidly-eluted ammonia peak by the gas sampling valve injection upset, and by low-boilers such as H₂S and CH₄. A two-column series/by-pass arrangement with a switching valve would have been required for accurate ammonia analysis. It appeared, however, that there was no deficiency in ammonia relative to hydrocarbons in the quinoline HDN products. For this reason, and because of time and monetary limitations, it was decided that the ammonia analysis was not critical.

10' X 1/4"OD X 2 mm ID glass column packed with 10% SP-2300 on 40/60 mesh Chromosorb T was eventually used for all the quantitative experiments. The SP-2300 gave slightly better separations than the SP-2310 (both are cyanopropyl-silicones with slightly different amounts of cyano groups), and was less expensive. The 2 mm ID column with only 20 cc/min hydrogen carrier gas flow gave the same component retention times as a 4 mm ID column with 80 cc/min carrier gas flow. The advantage of the 2 mm ID column was a four-fold increase in detector sensitivity due to reduced carrier gas dilution of the samples. A much broader ammonia peak also resulted, however, since it took four times as long for the carrier gas to flush each sample from the 4 cc loop in the gas sampling valve.

A chromatogram illustrating the separation of quinoline HDN products is shown in Figure 3-2. The DHQ peak was somewhat asymmetrical, most likely as a result of partial separation of the cis and trans isomers of DHQ. All analyses were performed with a detector filament current of 180 ma and a detector oven temperature of 240°C. Matched reference and analytical columns were temperature programmed from 110°C to 190°C at 40°C/min and held at 190°C until the analysis was completed. Carrier gas flow in each column was 20 cc/min of hydrogen. Injector ports and the transfer line from the gas sampling valve to the analytical column were maintained at about 190°C. The use of Teflon

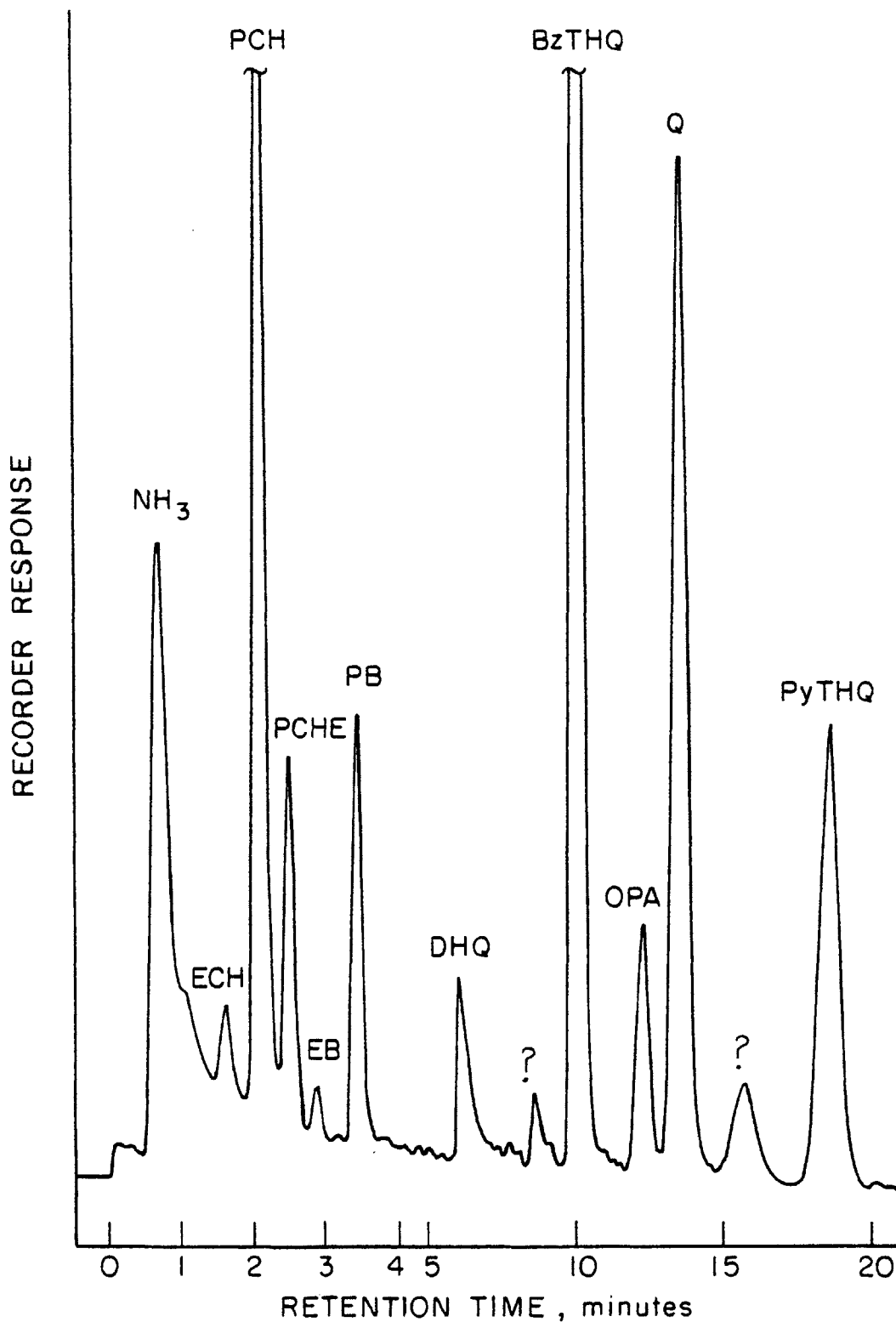


FIGURE 3-2: CHROMATOGRAM ILLUSTRATING SEPARATION OF PRODUCTS FROM QUINOLINE HDN

as a gas chromatographic support is accompanied by the temperature limitations inherent with Teflon.

Absolute detector response factors were determined for each of the major components by injecting (via syringe) known quantities of each compound into the gas chromatograph and measuring the resulting peak areas. These factors were determined at the same conditions used for analysis of the reactor effluent samples. The response factors were non-linear, due most likely to a combination of detector characteristics and digital integrator limitations. Detector response factors are presented in the Appendix.

III. A. 5. Miscellaneous Details

Type 316 stainless steel tubing, fittings, and valves were used in the experimental apparatus. This austenitic stainless steel is recommended for high-temperature, high-pressure hydrogen service, and has good corrosion resistance to H_2S and ammonia. Nonmetallic portions of the apparatus in contact with process streams were constructed primarily of Teflon and Pyrex glass.

Heated lines were wrapped with heating tapes and insulation. The heating tapes were controlled by individual Variacs, and line temperatures were monitored with iron/constantan thermocouples in contact with the exterior tubing surfaces. All thermocouples, including the one in the

reactor process stream, were connected through a selector switch to a digital thermometer with electronic cold junction compensation (Omega model 2160A-J-C).

The high and low pressure switches in the reactant hydrogen feed system were set at approximately 0.34 MPa (50 psi) above and below the reactor operating pressure. These served to activate an automatic safety system designed to shut down the reactant hydrogen (by closing the solenoid valve) and the metering pump, and also sound an alarm in the event of system overpressure or underpressure. Additional details of this safety system are given by Wilkens (1977). As a final precaution, all components of the experimental apparatus except for the gas cylinders and the analytical equipment were located behind a protective barricade.

III. B. Catalyst

The catalyst used in this study was a commercial NiMo/Al₂O₃ hydrotreating catalyst, American Cyanamid AERO HDS-3A, supplied as 1/16-inch extrudates. Typical catalyst properties, provided by the manufacturer, are summarized in Table 3-1.

The catalyst extrudates were crushed and sieved, and a single charge of the 20/24 mesh fraction was used in the experiments. Virgin catalyst must be properly activated before exposure to high-temperature hydrogen, to avoid

Table 3-1

Typical Properties of American Cyanamid
AERO HDS-3A Catalyst

* Composition (wt. %, dry basis):

NiO	3.2
MoO ₃	15.4
Na ₂ O	0.03
Fe	0.03
SO ₄	0.3
SiO ₂	0.1
Loss on ignition	1.2

Physical Properties:

Surface area, m ² /g	200
Pore volume, cc/g	0.60
Poured bulk density, lb/ft ³	41
g/cc	0.66
Compacted bulk density, lb/ft ³	45
g/cc	0.72

* Balance is alumina (Al₂O₃)

permanent loss of catalytic activity. This activation was accomplished by a sulfiding procedure specified by the manufacturer and adapted to the scale of this study.

Sulfiding converts the metal oxides in the virgin catalyst to more active metal sulfides. Details of this formal sulfiding procedure are given in Table 3-2.

In the absence of sulfur compounds, a presulfided catalyst loses sulfur (as H_2S) upon prolonged exposure to high-temperature hydrogen. In this study, sulfur compounds were not present (intentionally) in the reactor feed, so the catalyst was resulfided after each experimental run. As an alternative to the time-consuming formal sulfiding procedure, an easier shutdown sulfiding procedure was used. This procedure was equivalent to the formal sulfiding procedure, for maintaining constant catalyst activity during a pyridine HDN study (Wilkens, 1977). It will be shown that this shutdown sulfiding procedure maintained a constant catalyst activity during this study as well, once the catalyst had "lined-out". Details of this procedure are included in Table 3-2.

Table 3-2

Catalyst Sulfiding Procedures

Formal sulfiding (for activating virgin catalyst):

1. Heat reactor to 175°C under flow of argon.
2. Stop argon flow, and start flow of 10% H₂S in H₂ mixture at 15-20 sccm and approximately 0.20 MPa (15 psig); maintain flow and temperature for 12 hours.
3. Maintaining H₂S/H₂ flow, increase temperature to 315°C at a rate of 1°C per minute.
4. Maintain H₂S/H₂ flow and temperature of 315°C for 1 hour.
5. Cool reactor to 150°C under H₂S/H₂ flow.
6. Cool reactor to room temperature under argon flow.

Shutdown sulfiding (for resulfiding catalyst):

1. After completion of run, heat or cool reactor to 350°C as pressure is vented (H₂ and liquid feeds having been stopped).
2. After ventdown, start H₂S/H₂ flow at approximately 40 sccm and 0.20 MPa (15 psig); maintain flow and temperature of 350°C for 1 hour.
3. Cool reactor to 150°C under H₂S/H₂ flow.
4. Cool reactor to room temperature under argon flow.

III. C. Experimental Procedure

An experimental run consisted of the determination of steady-state HDN product distributions for the model compound under study (quinoline or one of its hydrogenated derivatives), at typically five different feed rates, for a constant reactor temperature, pressure, and feed composition. A few early runs were made in which the feed rate was held constant and the reactor temperature was varied, but the desired data could be obtained more efficiently by conducting experiments in the former mode.

A run was started by heating the reactor to the desired temperature (330°C, 375°C, or 420°C) under an argon purge. As the reactor approached operating temperature the argon was shut off and the shutoff valve just downstream from the metering valve was closed to pressurize the reactor with hydrogen. The reactor was pressurized by adjusting the regulator on the reactant hydrogen cylinder. After the system was pressure tested, hydrogen flow was started by carefully cracking the shutoff valve open. The flow rate was gradually increased to the maximum rate to be studied during the run, by alternately closing the metering valve (initially fully open) and cracking the shutoff valve open. This procedure prevented over-tightening of the delicate metering valve, which was not designed for shutoff service. At this point system temperatures were adjusted to the appropriate levels, to prevent condensation when the liquid

feed was started. These temperatures were held close to the steady-state levels even when the system was not operating. The desired liquid feed rate was set on the pump control unit, and the pump was started. The system was started up at the highest feed rate to minimize the time required for organic products to "break-through" into the cold trap.

The system reached steadystate within about 30 minutes after "break-through", and a set of 3 to 5 samples was taken and analyzed. Before each sample was taken, the reactor temperature and pressure, gas sample valve temperature and pressure, and exhaust gas flow rate were measured and recorded. Any significant trend in three consecutive samples was an indication that a steady state had not been reached, but this was seldom observed.

After a satisfactory set of samples had been taken at the highest feed rate, the hydrogen and liquid feed rates were reduced in the same proportion. A one hour re-equilibration period was usually adequate before another set of steady-state samples could be taken at the new feed rate. This procedure was repeated for each of the remaining feed rates to be studied.

After the last set of samples had been taken, the metering pump was shut off and the system was purged for about 5 minutes with hydrogen. The hydrogen feed was then shut off and the system was slowly vented down. During

ventdown the temperature of the tar trap was reduced from the steady-state level of 240°C to the standby temperature of about 190°C to avoid flash vaporization of any high-boilers that may have condensed in the trap during the run. The reactor temperature was then adjusted to 350°C to prepare the catalyst for shutdown resulfiding. When ventdown was completed, the cold trap sample was removed and the shutdown sulfiding procedure was carried out. The duration of an experimental run was typically 16 to 18 hours.

III. D. Data Reduction

The raw data from each set of steady-state samples were averaged for use in calculations. Absolute detector response factors were used to convert the average component peak areas from the sample analyses to the equivalent number of moles of each component. The product distribution can then be calculated for each set of reactor conditions, along with the average total moles of products in the set of samples. This can be compared with the moles of products theoretically injected (to check the material balance), calculated from the hydrogen and liquid reactant feed rates and the gas sampling valve loop volume, temperature, and pressure. The ideal gas law was used since the low-pressure, high-temperature gas in the sample valve was very nearly

ideal. Reactor feed composition was also calculated from the data. Sample calculations illustrating the data reduction in more detail are included in the Appendix.

It must be pointed out that the reactor feed was always over 99% hydrogen, so even though hydrogen was consumed in the HDN reactions there was a negligible change in the total molar flow rate through the reactor. Also, the measured exhaust gas flow rate (on a mole basis) was very nearly equal to the total molar feed rate to the reactor. The consumption of hydrogen in the reactor, condensation of organics in the cold trap, and absorption of NH_3 in the saturator were compensated by the addition of H_2O to the exhaust gas in the saturator. Thus no correction was made for the presence of water vapor in the exhaust gas.

III. E. Experimental Problems

One of the most difficult problems with the experimental apparatus was achieving a steady liquid feed rate and even vaporization of the liquid into the hydrogen. In an earlier apparatus, used by Wilkens (1977) and Declerck (1976), this problem was less severe as only relatively high feed rates were studied. These investigators attributed the apparent fluctuations in liquid feed rate to the metering pump. My findings, however, indicate that the metering pump was not the major source of the problem. Several different feed

configurations were evaluated. The configuration used by Wilkens and Declerck, and one incorporating a one-liter volume for back-mixing were both unsatisfactory. Standard deviations of component peak areas in sets of steady-state samples were typically 25%.

It was observed during calibration of the metering pump that liquid was fed dropwise from the capillary tubing, since the feed rates were so low (on the order of 1 cc/hr). To prevent this from occurring in the system during actual operation, several modifications to the liquid feed configuration were made. The mixing tee was packed with Pyrex glass wool and the liquid feed capillary was inserted into the glass wool through a bored-out reducer, such that the capillary was perpendicular to the downward hydrogen flow. The glass wool also provided ample surface area for more even vaporization of the liquid feed and increased the linear velocity of the heated hydrogen through the mixing tee. With this configuration preheating of the liquid feed was unnecessary, thereby minimizing thermal decomposition (and pluggage) in the liquid feed capillary. More importantly, standard deviations of component peak areas in sets of steady-state samples were reduced dramatically to an average of 5%.

A second problem, not as satisfactorily resolved, related to the material balance check between the total number of moles of organic products actually detected in

samples and the corresponding amounts calculated from the measured gas sample valve temperature and pressure and reactant feed rates. A chronic excess (up to 60%) in the material balance was observed; that is, more moles of organic products were detected in samples than should have been present in the gas sample valve loop. The excess tended to be greatest at the highest feed rates, while the material balance usually closed (within 10%) at the lowest feed rates. This suggested that there was a pressure drop through the gas sample valve, such that the pressure gauge downstream did not always reflect the true pressure in the sampling valve loop. The gas sample valve loops were connected to the valve body by 0.584 mm ID tubing, and the valve body itself contained tiny grooves through which the gas flowed. Calculations indicate that significant pressure drop is expected through the 0.584 mm ID tubing at higher flow rates. A by-pass of 1.75 mm ID tubing was installed around the gas sampling valve. The by-pass was opened only before sampling, to allow most of the reactor effluent to by-pass the gas sampling valve, thereby minimizing the pressure drop. Experiments indicated that there was indeed a significant pressure drop through the gas sample valve. The by-pass, however, did not eliminate the chronic excess in the material balance.

IV. Results

The effects of reaction variables on quinoline HDN, and on HDN of each of the nitrogen-bearing intermediates (PyTHQ, BzTHQ, DHQ, and OPA) in the reaction network are presented in this chapter. The reaction variables investigated were temperature, total pressure (or hydrogen partial pressure), initial partial pressure of reactant, and reactant feed rate. The reactor time variable selected for presentation of results and for kinetic analysis is W/F_{i_0} , where W was the mass of virgin catalyst (before sulfiding) in the reactor and F_{i_0} was the molar feed rate of the reactant nitrogen compound to the reactor. This time variable is often used for continuous catalytic reactor studies, and its utility in this investigation is discussed in the next chapter. The actual reaction conditions for the HDN experiments are summarized below.

Temperature: 330°C, 375°C, 420°C

Total pressure: 3.55 MPa (500 psig or 35 atm)

7.0 MPa (1000 psig or 69 atm)

Reactant partial pressure: 13.3 kPa (100 torr or 0.13 atm)

26.7 kPa (200 torr or 0.26 atm)

W/F_{i_0} : 41.7 to 667 hr g catalyst/g-mol i

At constant reactor temperature, total pressure, and W/F_{i_0} (constant reactant feed rate), different initial partial pressures of reactant corresponded to different hydrogen feed rates.

For obvious reasons the experimental results are presented primarily in graphical form. Run numbers are indicated on many of the graphs to correlate the graphical results presented in the text with the more detailed numerical results tabulated in the Appendix. The run numbers also identify the order in which experiments were conducted. Most of the graphs show the effects of reaction variables on either nitrogen removal or product distribution. Nitrogen removal, or denitrogenation, is defined here as the mole percentage of the reactant nitrogen compound converted to pure hydrocarbons. The product distributions were calculated on the basis of organic products only (i.e. on an ammonia-free basis). Thus the mole percentage of each organic product (including, of course, unconverted reactant) is equivalent to the mole percentage of the reactant nitrogen compound converted into that product, if minor side reactions such as coking are neglected. Due to limitations on the quantity of data that can be presented clearly in a single graph, however, the graphical product distributions show only the organic nitrogen compounds.

For each nitrogen compound studied, the nitrogen removal results are presented first, to provide a general framework in which the more detailed product distributions can then more meaningfully be presented. A common set of axes is used for all graphical product distributions to facilitate comparison. Finally, extrapolated maxima often appear in the graphical product distributions. These maxima do not signify gross speculation, as they were determined simply by difference (the mole percentages of the organic products must sum to 100%).

IV. A. Catalyst Activity

The activity of the presulfided NiMo/Al₂O₃ catalyst was checked periodically by denitrogenating quinoline at standard reaction conditions. The degree of nitrogen removal was used as a simple measure of catalyst activity. This measure takes into account both the hydrogenation and hydrogenolysis activities of the catalyst, and for this reason is superior to a measure such as quinoline conversion (reactant disappearance), which depends primarily on the hydrogenation activity of the catalyst and on the thermodynamics of ring saturation. Also, observed changes in quinoline HDN product distribution during catalyst deactivation provide clues as to how the individual hydrogenation and hydrogenolysis activities were affected.

Relatively mild standard reaction conditions (375°C, 3.55 MPa total pressure, 13.3 kPa initial quinoline partial pressure, 167 hr g catalyst/g-mol Q) were chosen to follow the initial deactivation of the catalyst. As shown in Figure 4-1, the catalyst activity decreased rapidly with time on stream from 14.5% denitrogenation at 11 hours to only 6% at about 60 hours. After 60 hours of use the catalyst deactivated much more slowly, and appeared to reach a stable level of activity of 3 to 4% denitrogenation at 350 hours. The activity of the catalyst after 100 hours on stream was followed more accurately by employing more severe standard conditions (higher hydrogen partial pressure and lower feed rates), to achieve higher levels of denitrogenation. Thus, complete denitrogenation of quinoline was attained at 375°C, 7.0 MPa, and 667 hr g catalyst/g-mol Q with 116 hour-old catalyst, but only 65% nitrogen removal was observed at the same reaction conditions after 340 hours of catalyst use (see Figure 4-2). The catalyst finally reached a stable level of activity after about 400 hours on stream.

Figure 4-3 provides a more complete picture of catalyst deactivation, by showing that the entire denitrogenation versus W/F_{Q_0} curve shifted downward as the catalyst deactivated. Note, however, that differences in catalyst activity were most easily observed at the lowest quinoline feed rate (highest W/F_{Q_0}). This is why 667 hr g catalyst/g-mol Q was chosen for the more severe standard

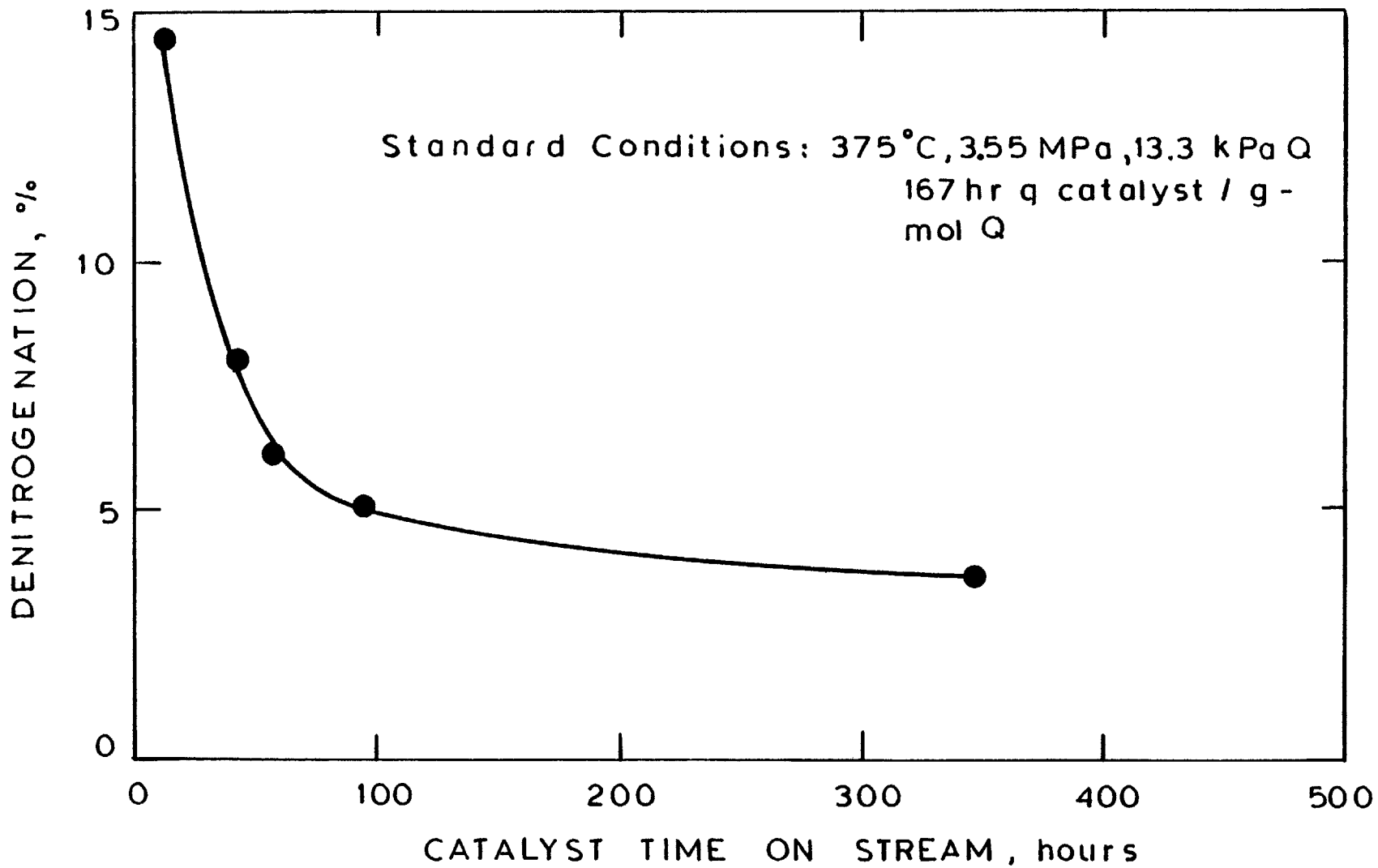


Figure 4-1: Catalyst Deactivation During Quinoline HDN - Mild Standard Conditions

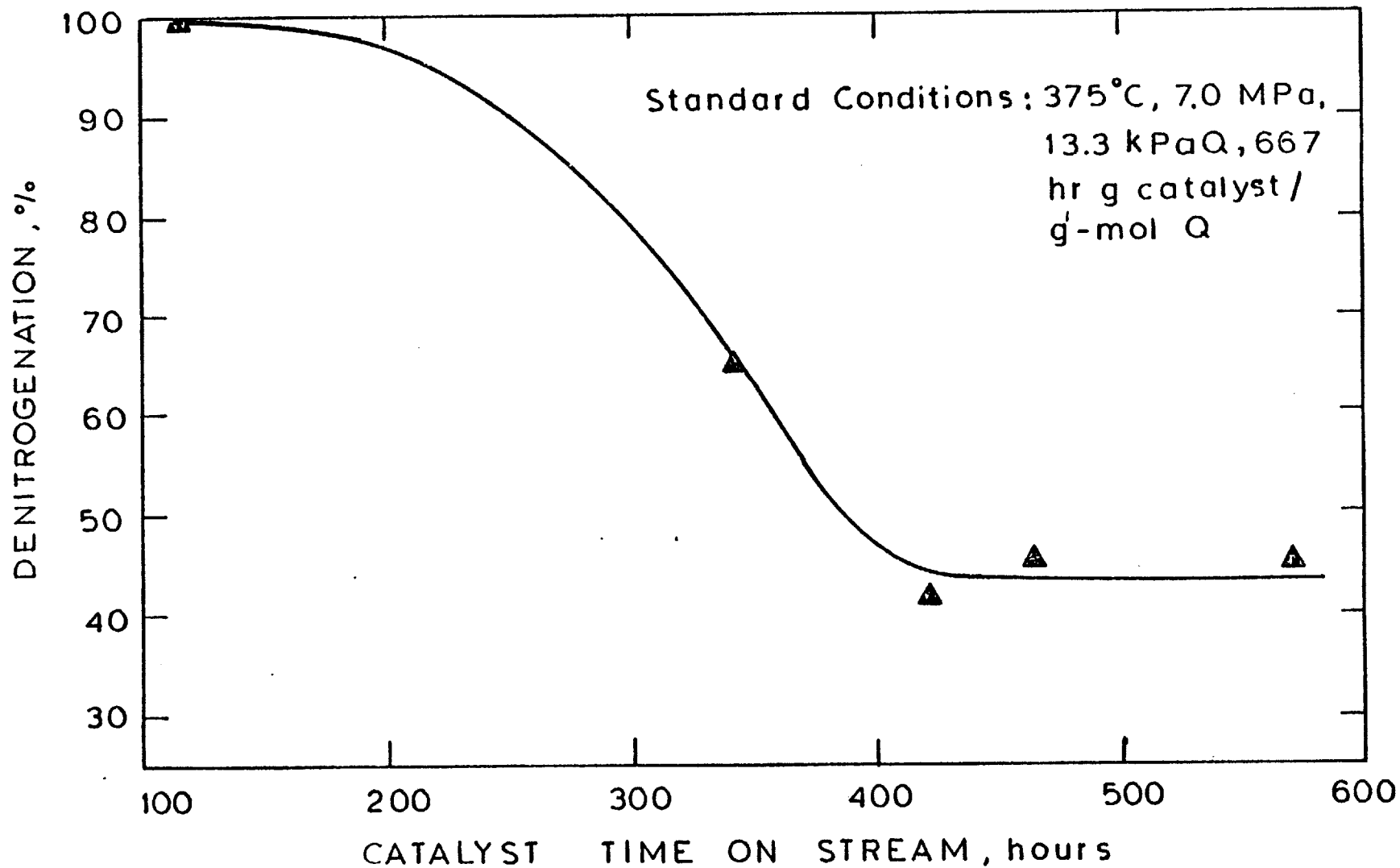


Figure 4-2: Catalyst Deactivation During Quinoline HDN - Severe Standard Conditions

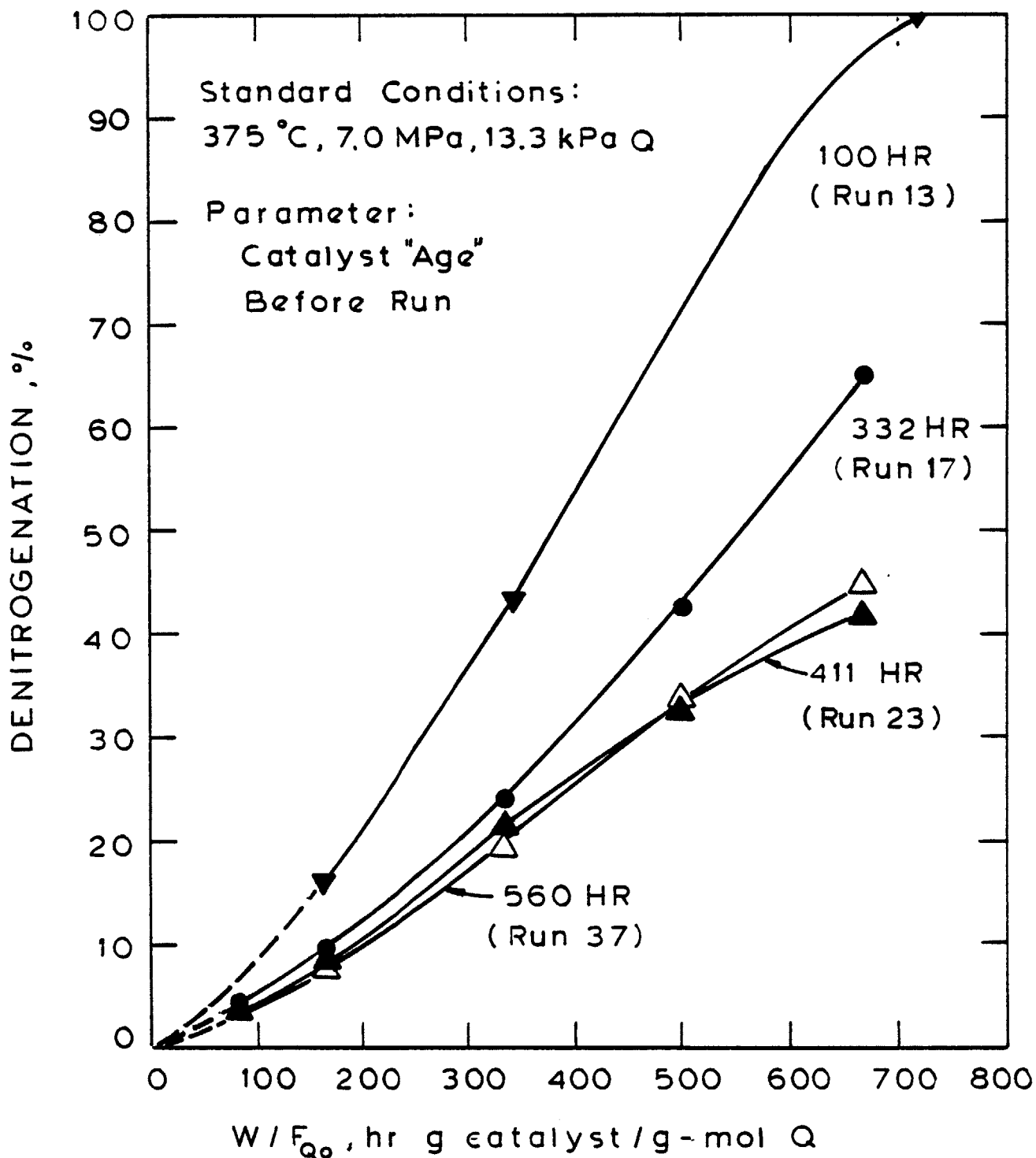


Figure 4-3: Catalyst Deactivation During Quinoline HDN

conditions used to follow catalyst activity. Runs 23 and 37 gave virtually the same denitrogenation versus W/F_{Q_0} curve, reflecting the constant activity of the catalyst after 400 hours of use.

Changes in quinoline HDN product distribution during catalyst deactivation are shown in Figures 4-4 and 4-5 for mild and severe standard reaction conditions, respectively. Over the first 100 hours of catalyst use, the most significant shifts in product distribution under mild reaction conditions were sharp increases in quinoline and PyTHQ (their ratio remained approximately constant, close to the equilibrium ratio) at the expense of hydrocarbon products, BzTHQ, and to a much lesser extent DHQ and OPA. The dominant intermediate with fresh catalyst was BzTHQ, but this was no longer the case after the catalyst had been on stream for 100 hours. At the more severe standard conditions, a relatively stable product distribution in which DHQ was the dominant intermediate was observed after about 400 hours of catalyst use. During catalyst deactivation the dominant intermediate was again BzTHQ, and concentrations of DHQ and PyTHQ were much lower than their "lined-out" levels. It is also interesting to note that the ratio of PyTHQ to quinoline increased dramatically as the catalyst activity stabilized, but the ratio was still well below the equilibrium ratio.

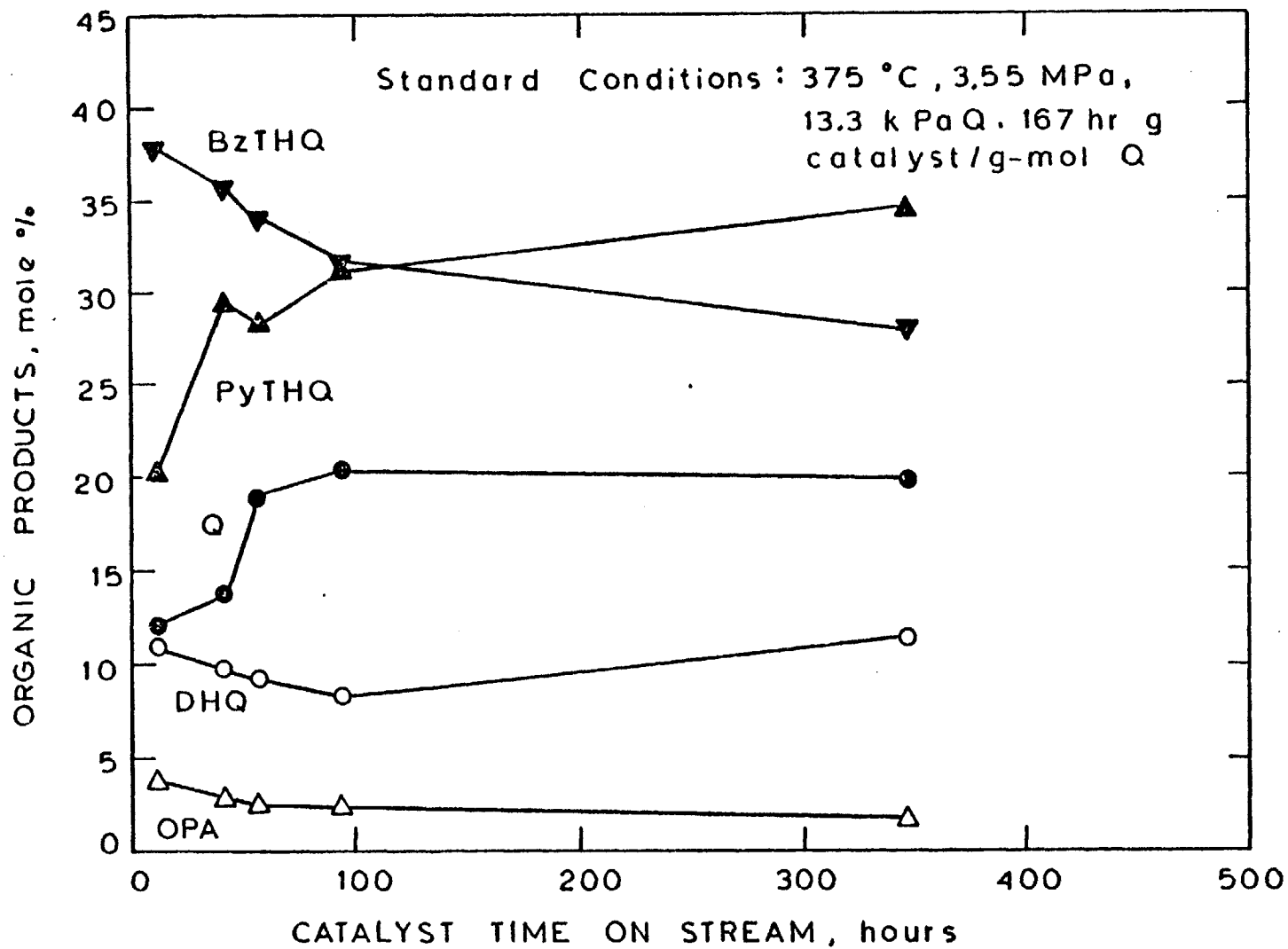


Figure 4-4: Changes in Quinoline HDN Product Distribution During Catalyst Deactivation - Mild Standard Conditions

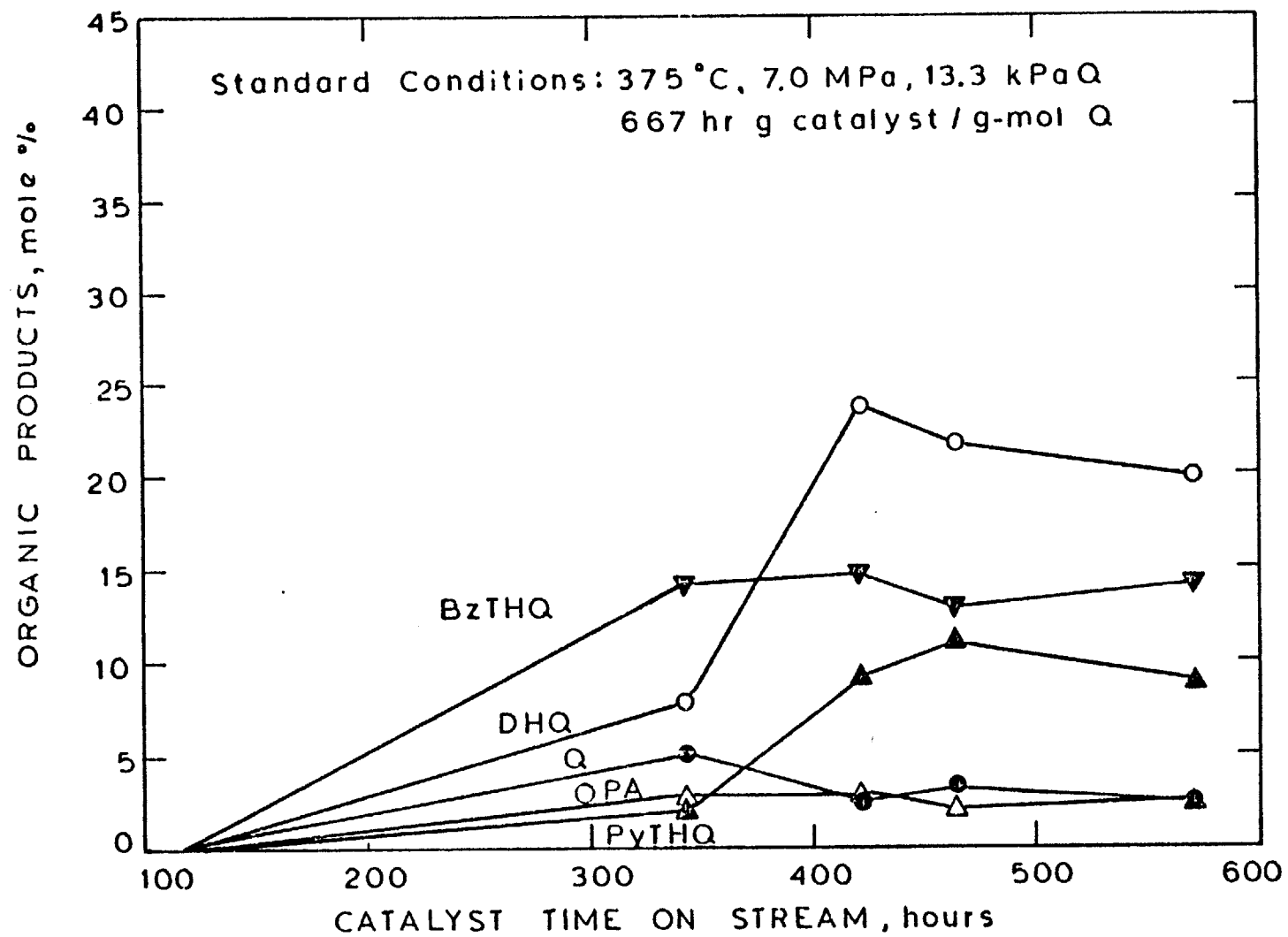


Figure 4-5: Changes in Quinoline HDN Product Distribution During Catalyst Deactivation - Severe Standard Conditions

These results indicate that after the catalyst had been used for about 400 hours, the quinoline HDN product distribution as well as the extent of denitrogenation observed at standard reaction conditions remained essentially constant. Recall that the catalyst was resulfided after each experimental run, but that no sulfur compounds were present in the reactor feed during a run. As a result, some loss of sulfur from the catalyst could have occurred during a run. However, in each of two experimental runs at different reaction conditions, data taken at the beginning of the run were reproduced at the end of the same run (see data for runs 18 and 22 in the Appendix). It appears that no significant catalyst deactivation took place during individual experimental runs, at least not after the catalyst had been used for 340 hours. Thus catalyst activity can safely be eliminated as a variable in the HDN kinetic experiments, essentially all of which were conducted after 400 hours of catalyst use.

IV. B. Hydrodenitrogenation of Quinoline and Py-Tetrahydroquinoline

IV. B. 1. Nitrogen Removal

Figure 4-6 shows the effects of quinoline feed rate (W/F_{Q_0}), hydrogen partial pressure, and initial quinoline partial pressure on nitrogen removal from quinoline

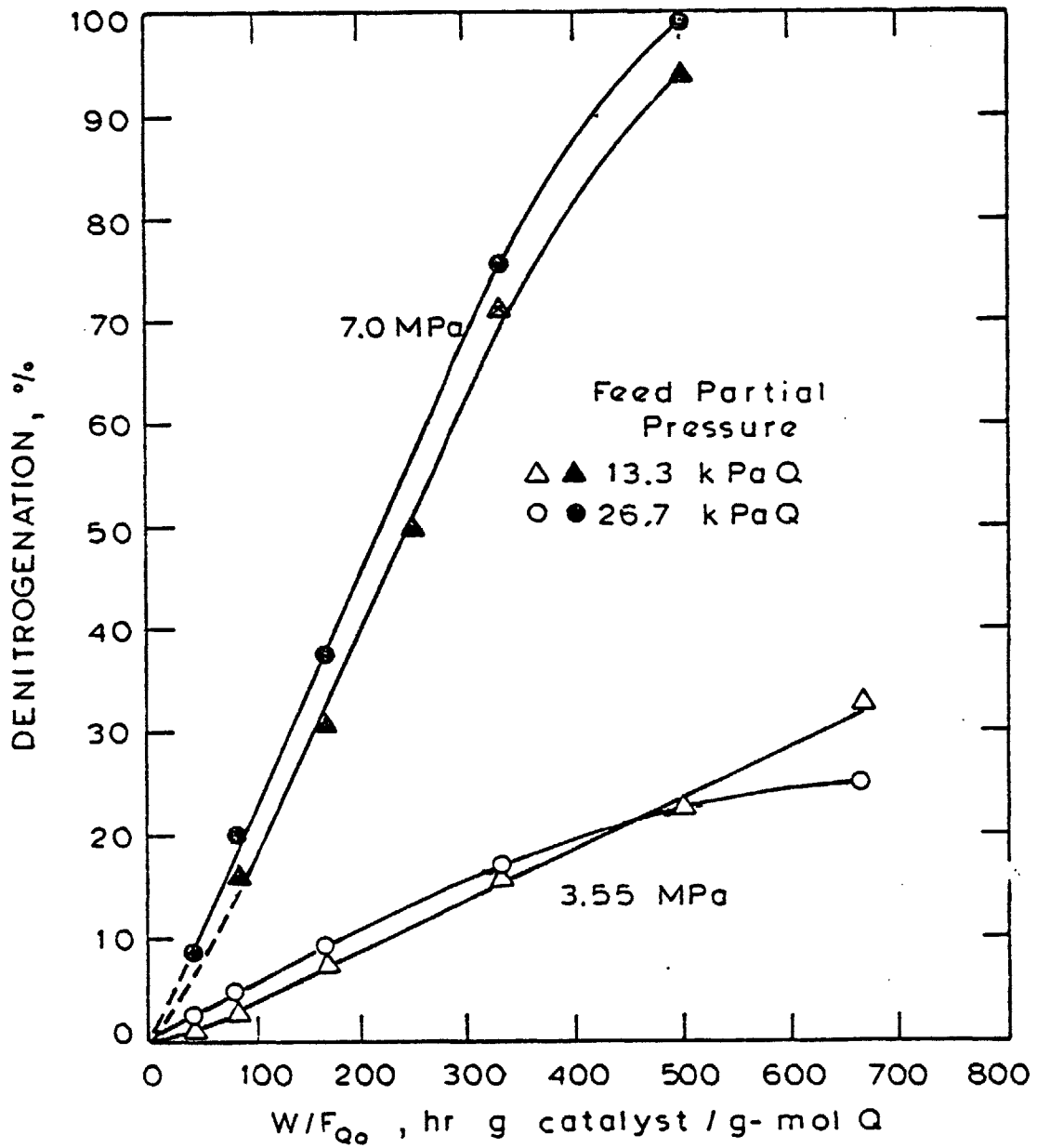


Figure 4-6: Quinoline Denitrogenation at 420°C

at 420°C. The percent denitrogenation increased with W/F_{Q_0} , of course, but was quite insensitive to initial quinoline partial pressure at constant W/F_{Q_0} . This result provides considerable information about the kinetics of quinoline HDN, as discussed in the next chapter. Doubling the hydrogen partial pressure (here, nearly equal to total pressure) increased nitrogen removal by a factor of about four at each quinoline feed rate. Thus for 500 hr g catalyst/g-mol Q essentially complete denitrogenation was achieved at 7.0 MPa, but at 3.55 MPa there was less than 25% nitrogen removal.

Similar results for hydrodenitrogenation of quinoline or PyTHQ at 375°C and 330°C are presented in Figures 4-7 and 4-8, respectively. Note that the same degree of nitrogen removal was achieved from quinoline and from PyTHQ, under the same reaction conditions. Doubling the initial quinoline partial pressure at constant W/F_{Q_0} had essentially no effect on nitrogen removal from quinoline at 375°C and 7.0 MPa. Increased hydrogen pressure significantly increased quinoline denitrogenation at both 375°C and 330°C, but to a lesser extent than it had at 420°C. Comparison of Figures 4-6, 4-7, and 4-8 (note the different scale for the ordinate in Figure 4-8) reveals the strong effect of temperature on nitrogen removal from quinoline. For example, at 7.0 MPa and 667 hr g catalyst/g-mol Q, denitrogenation increased from only 6% at 330°C to 42% at 375°C, and was essentially 100% at 420°C.

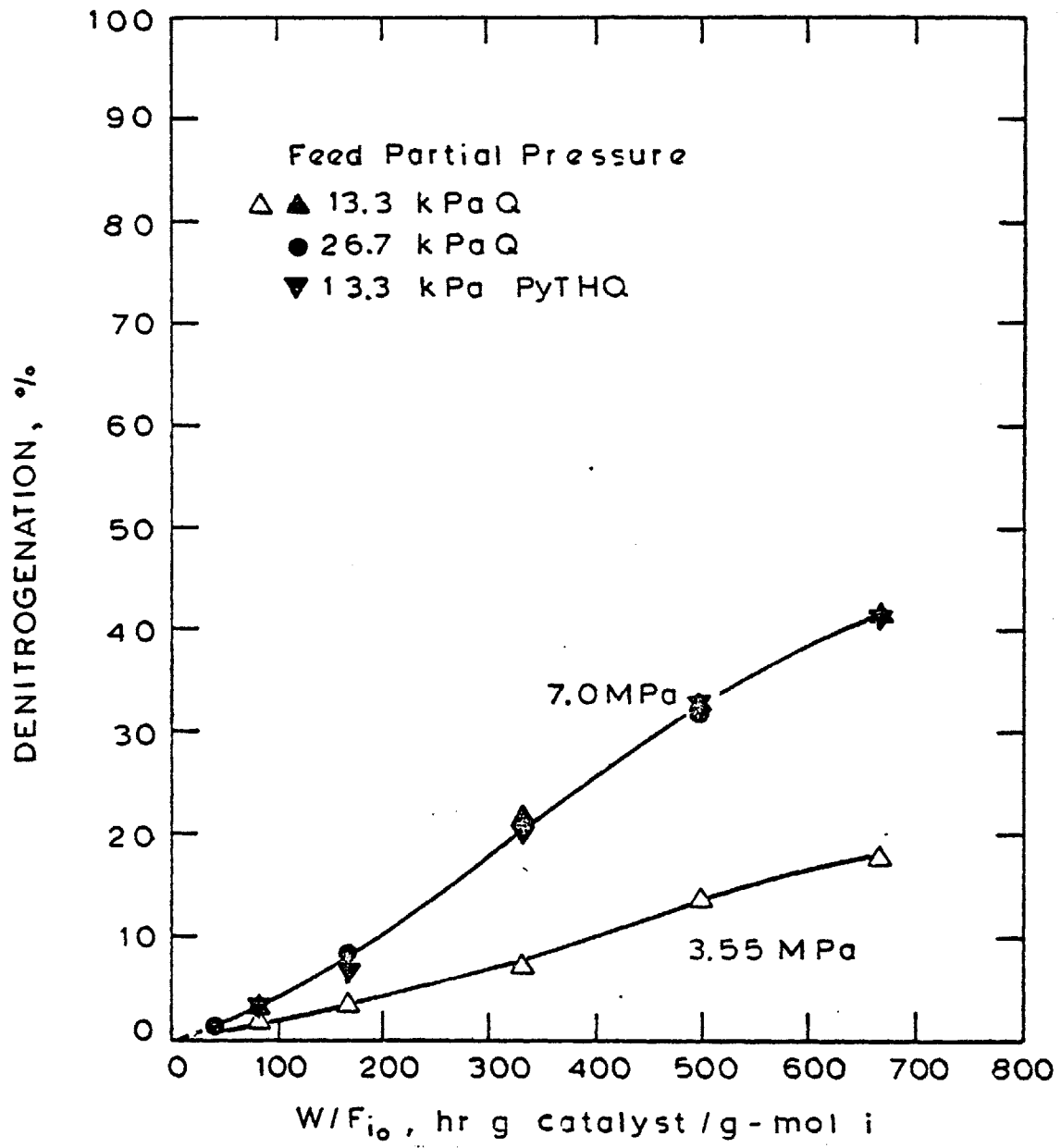


Figure 4-7: Quinoline and Py-Tetrahydroquinoline Denitrogenation at 375 °C

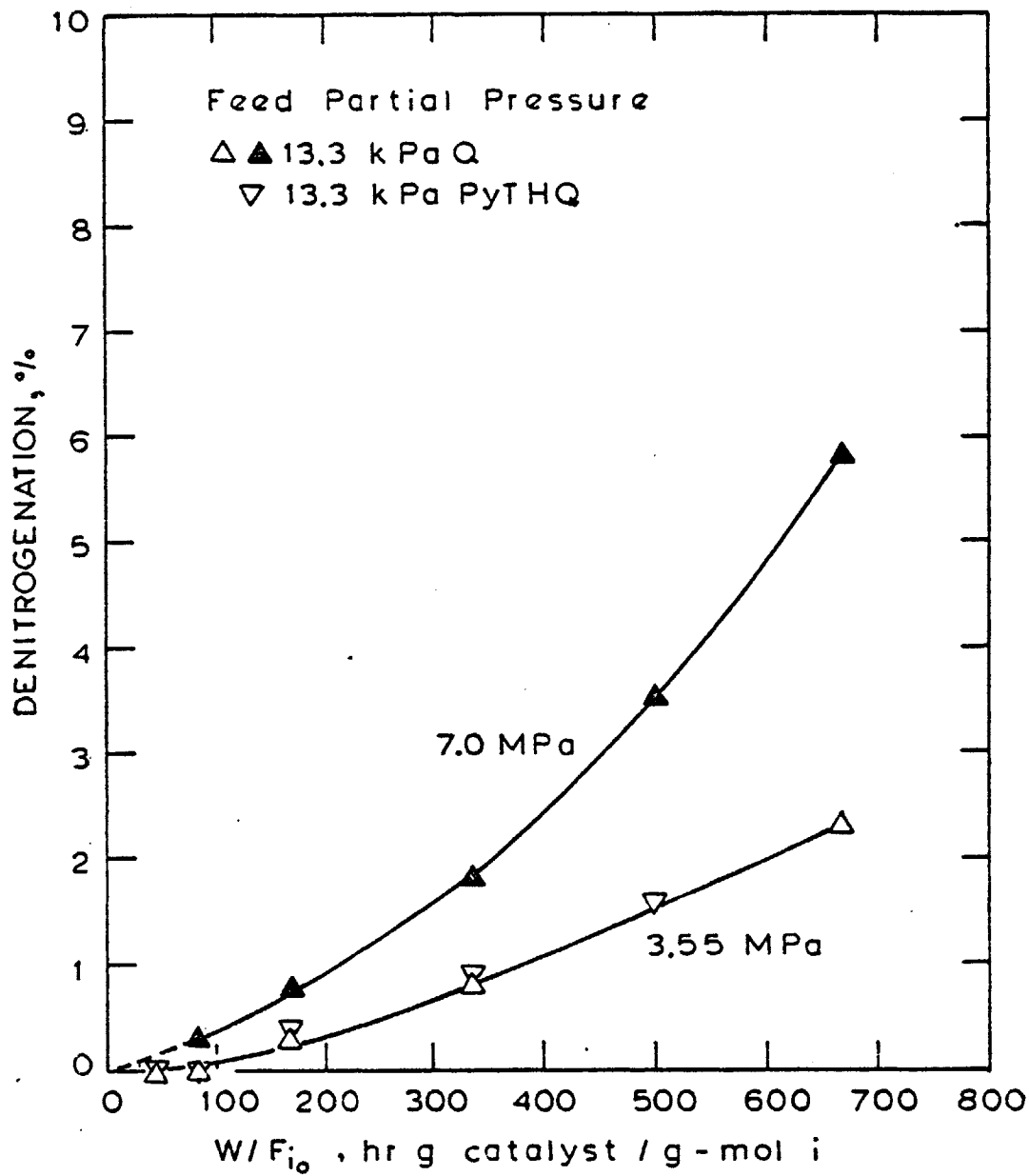


Figure 4-8: Quinoline and Py-Tetrahydroquinoline Denitrogenation at 330°C

IV. B. 2. Product Distributions: Nitrogen-bearing Intermediates

The effect of W/F_{Q_0} on the distribution of nitrogen-bearing products from quinoline HDN at 420°C is illustrated in Figures 4-9 through 4-12. Figures 4-9 and 4-10 correspond to 3.55 MPa total pressure but different initial quinoline partial pressures. Similarly, Figures 4-11 and 4-12 are for 7.0 MPa total pressure. The product distributions in each pair of figures are nearly identical, independent of initial quinoline partial pressure. At both 3.55 MPa and 7.0 MPa, the amount of unconverted quinoline decreased with W/F_{Q_0} , while the concentrations of PyTHQ, BzTHQ, and DHQ intermediates each passed through a maximum. The concentration of OPA, also a reaction intermediate, proceeded through a maximum as W/F_{Q_0} increased at 7.0 MPa total pressure but had not yet peaked at 3.55 MPa over the range of W/F_{Q_0} investigated. The ratio of PyTHQ to quinoline in the reaction products during each run was nearly constant, at essentially the equilibrium ratio (see Figure 2-5 and the data for runs 19 through 22 in the Appendix). This equilibrium, of course, was much more favorable toward PyTHQ at 7.0 MPa than at 3.55 MPa hydrogen pressure. It is noteworthy that BzTHQ was formed in significantly greater quantities than was PyTHQ, at both 3.55 MPa and 7.0 MPa. The DHQ was present in lower concentrations in the reaction products than were the

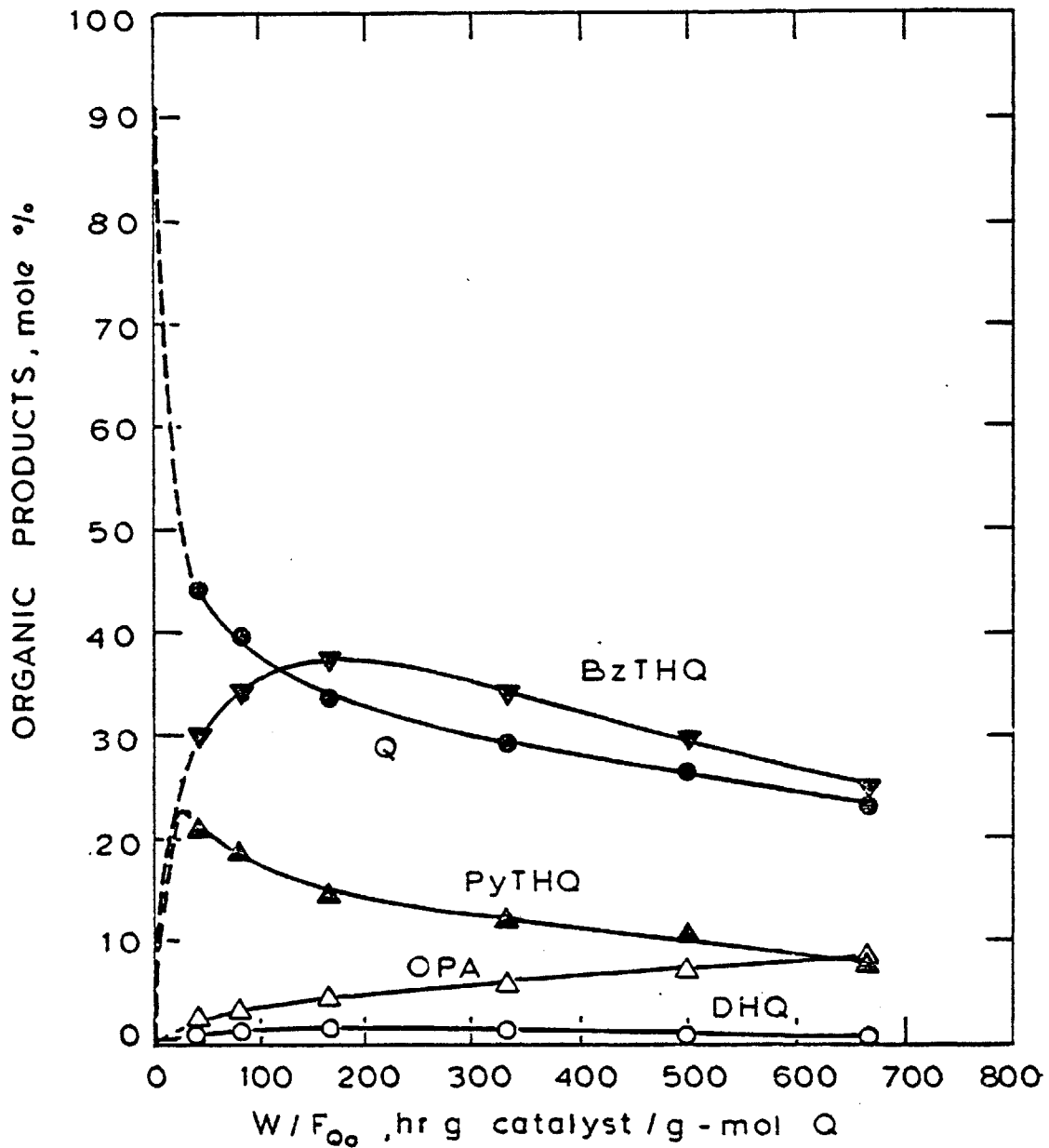


Figure 4-9: Product Distributions for Quinoline HDN
at 420°C, 3.55 MPa, 13.3 k Pa Q (Run 20)

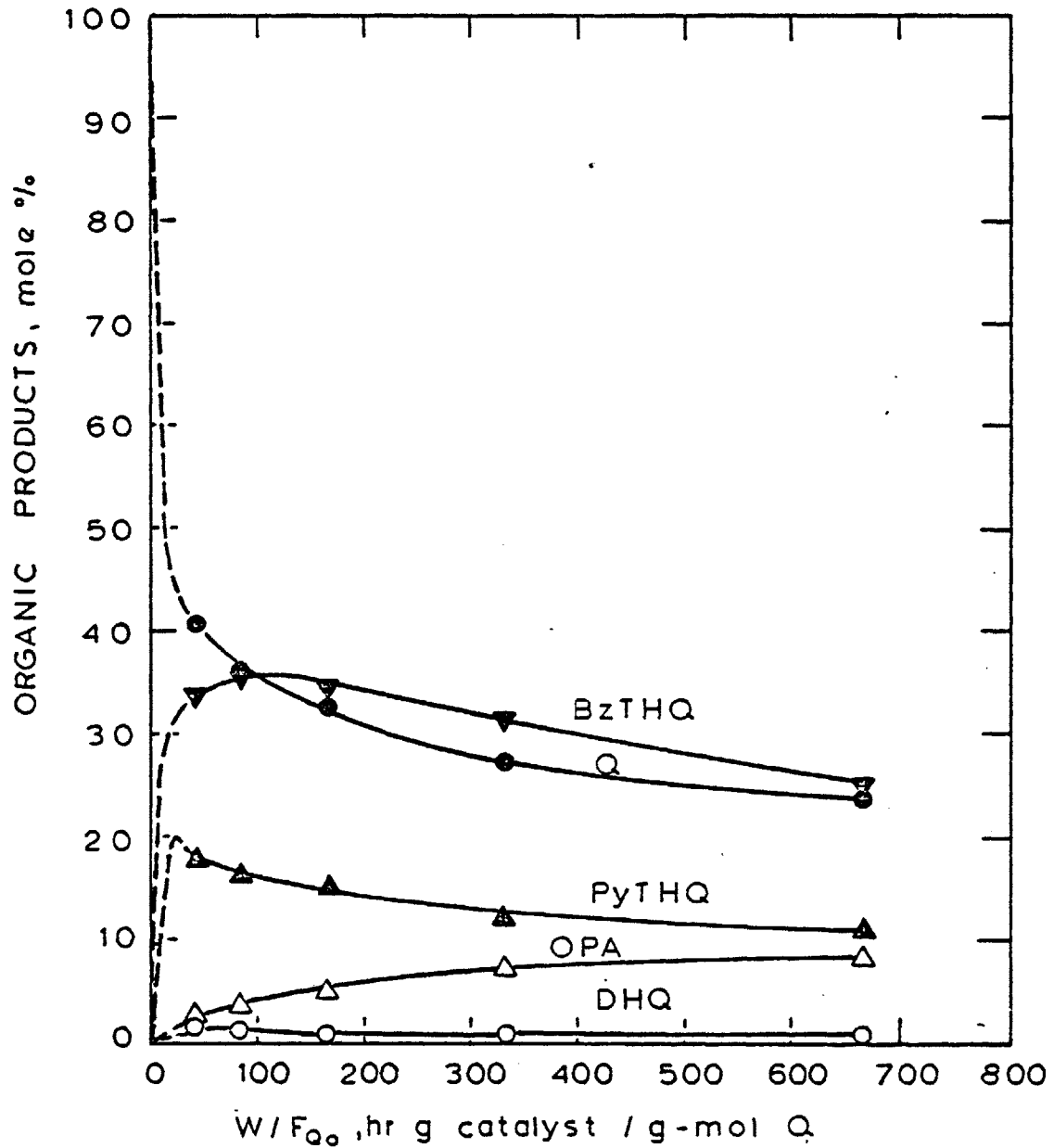


Figure 4-10: Product Distributions for Quinoline HDN at 420°C, 3.55 MPa, 26.7 kPa Q (Run 19)

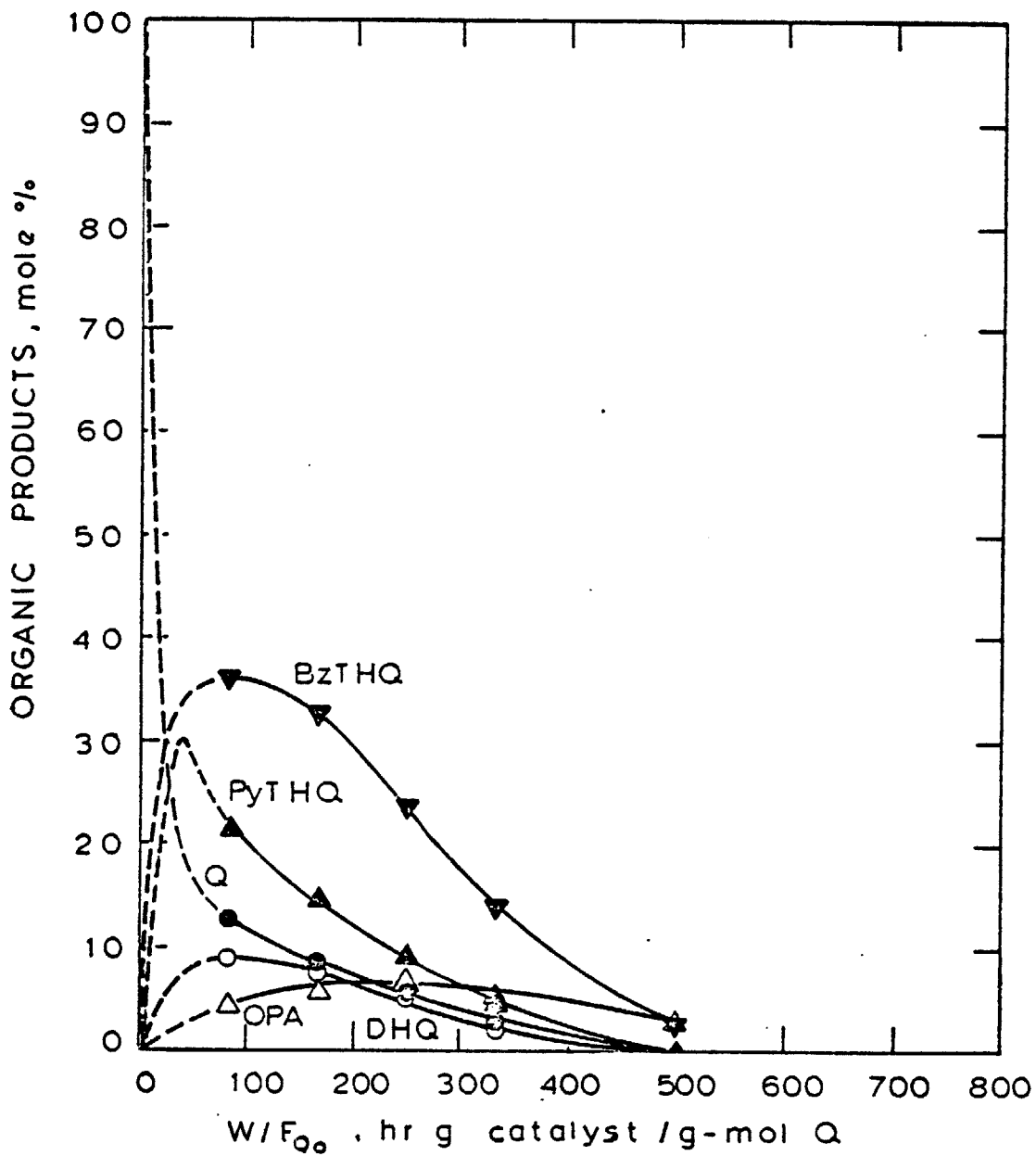


Figure 4-11: Product Distributions for Quinoline HDN at 420 °C, 7.0 MPa, 13.3 kPaQ (Run 22)

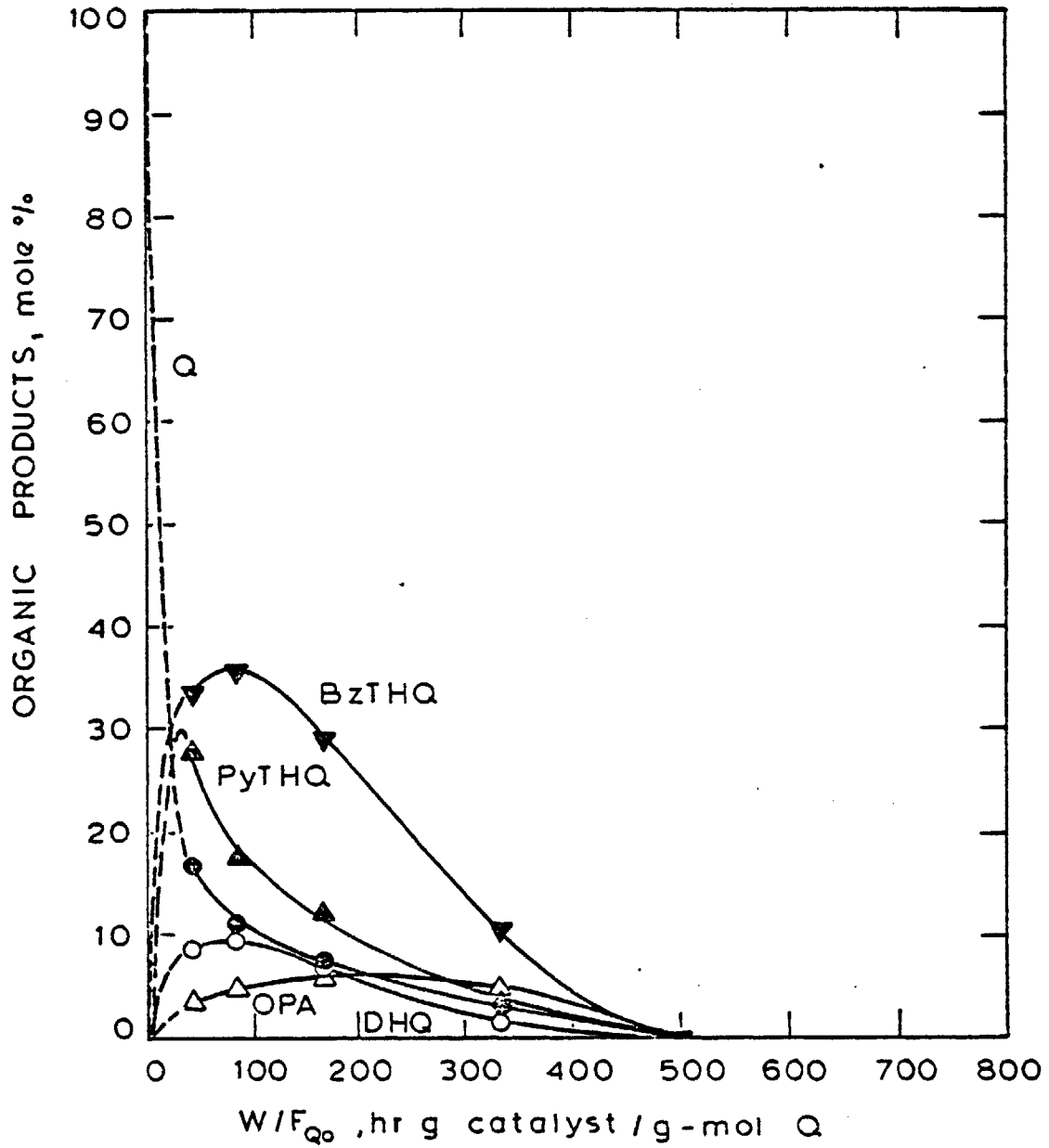


Figure 4-12: Product Distributions for Quinoline HDN at 420°C, 7.0 MPa, 26.7 kPa Q (Run 21)

other heterocyclics. Formation of DHQ from the tetrahydroquinolines was greater at the higher hydrogen partial pressure, consistent with thermodynamic expectations.

Product distributions for quinoline HDN at 375°C are shown in Figures 4-13 through 4-15, where Figure 4-13 corresponds to 3.55 MPa total pressure and Figures 4-14 and 4-15 are for 7.0 MPa and different initial quinoline partial pressures. Again, the effect of initial quinoline partial pressure on product distribution was minimal - somewhat higher yields of DHQ were observed at the lower quinoline partial pressure. At 375°C quinoline was rapidly hydrogenated to an equilibrium amount of PyTHQ. However, as W/F_{Q_0} increased, the amount of unreacted quinoline levelled off while the amount of PyTHQ in the products decreased quite rapidly. In other words, quinoline and PyTHQ were in equilibrium at the shortest reaction times (lowest W/F_{Q_0}), but did not remain in equilibrium at longer reaction times. Increased hydrogen pressure increased the ratios of PyTHQ to quinoline and of DHQ to the tetrahydroquinolines in the products. For example, DHQ was always present in greater quantity than BzTHQ in the products from quinoline HDN at 7.0 MPa, but the opposite result was observed at 3.55 MPa. One would expect lower temperatures to favor the hydrogenated species in each of the initial saturation equilibria, since the saturation reactions are all exothermic. The product distributions from quinoline HDN at 375°C and 420°C are

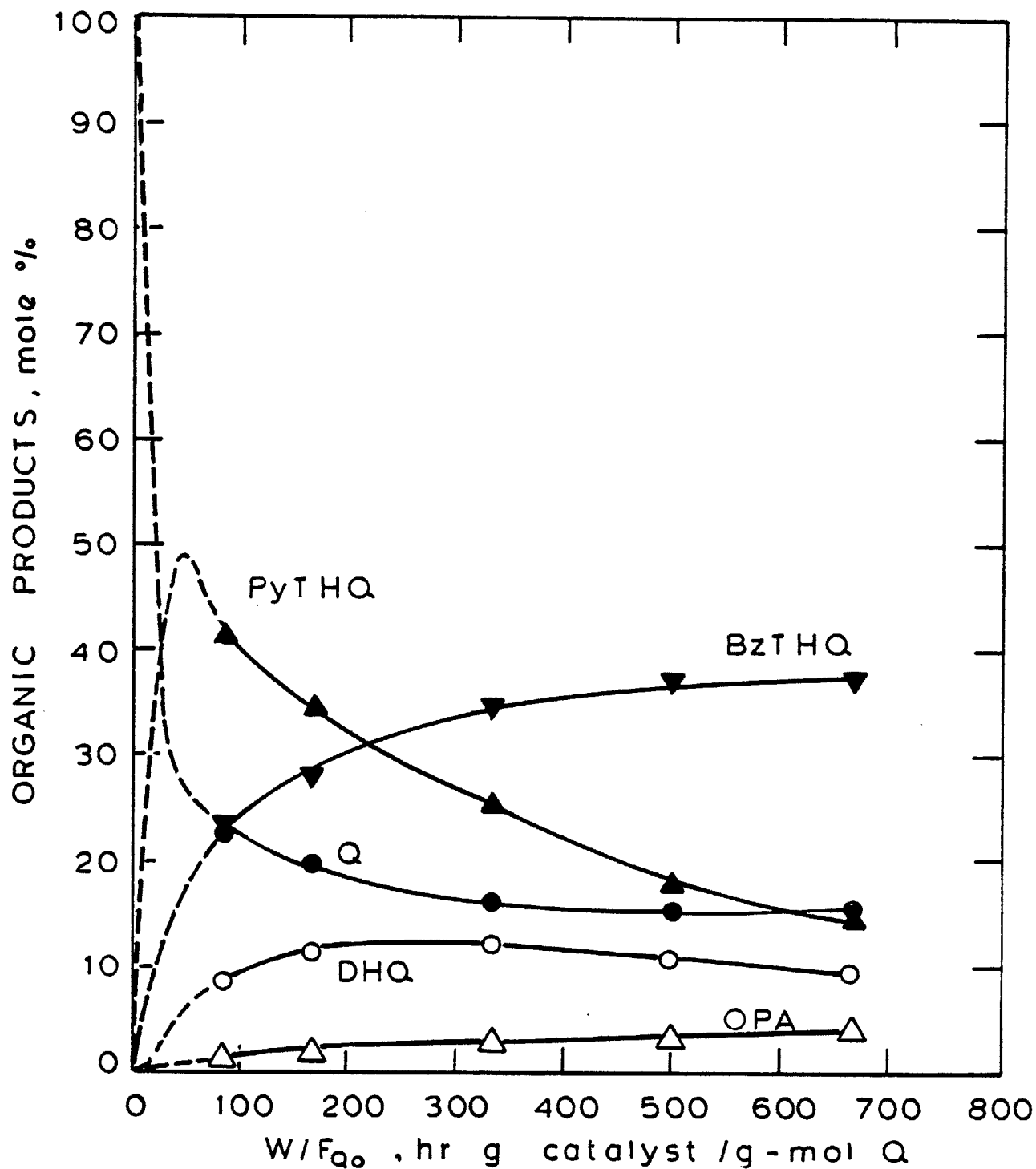


Figure 4-13: Product Distributions for Quinoline HDN at 375 °C , 3.55 MPa, 13.3 k PaQ (Run 18)

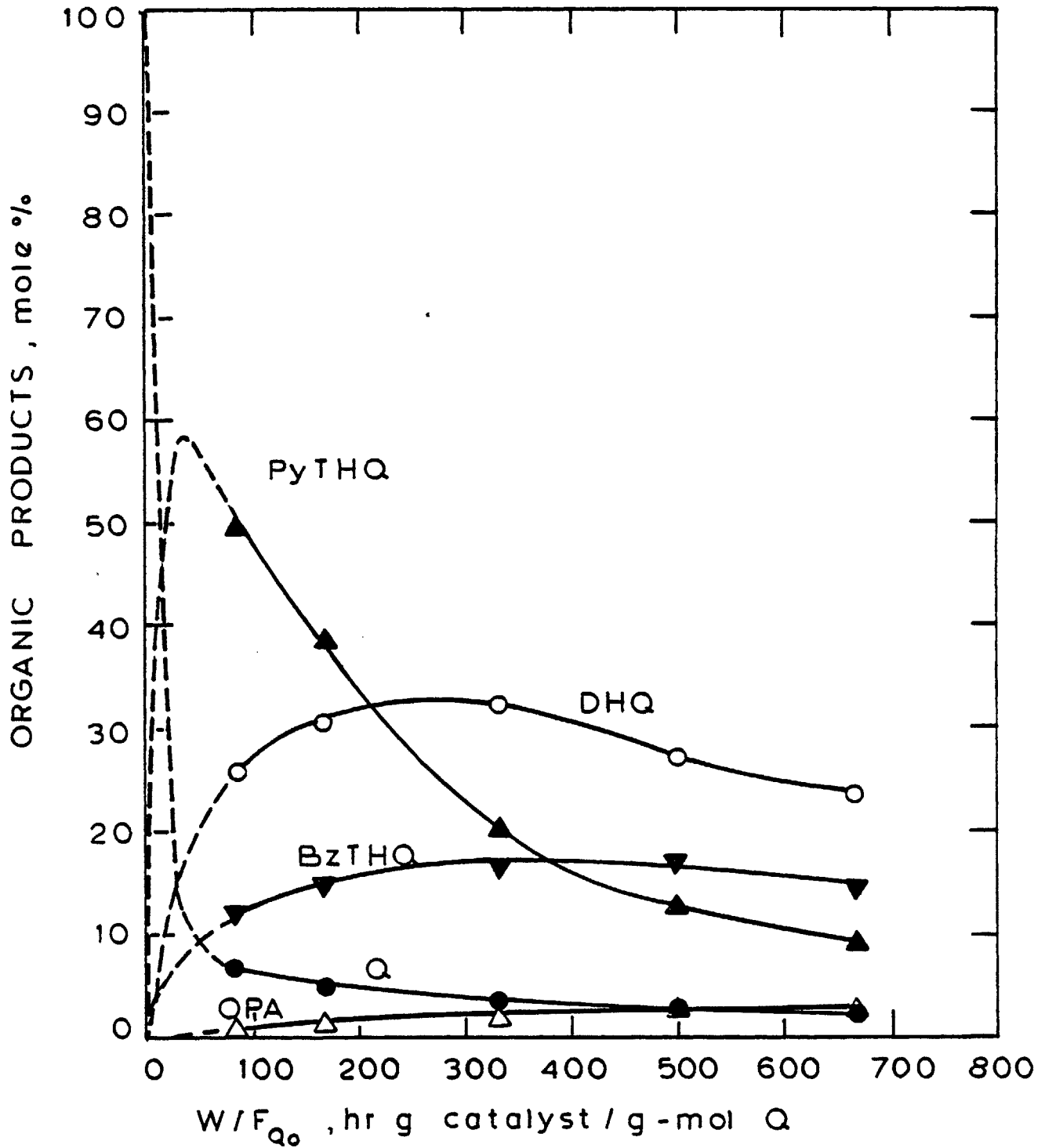


Figure 4-14: Product Distributions for Quinoline HDN at 375 °C, 7.0 MPa, 13,3 kPa Q (Run 23)

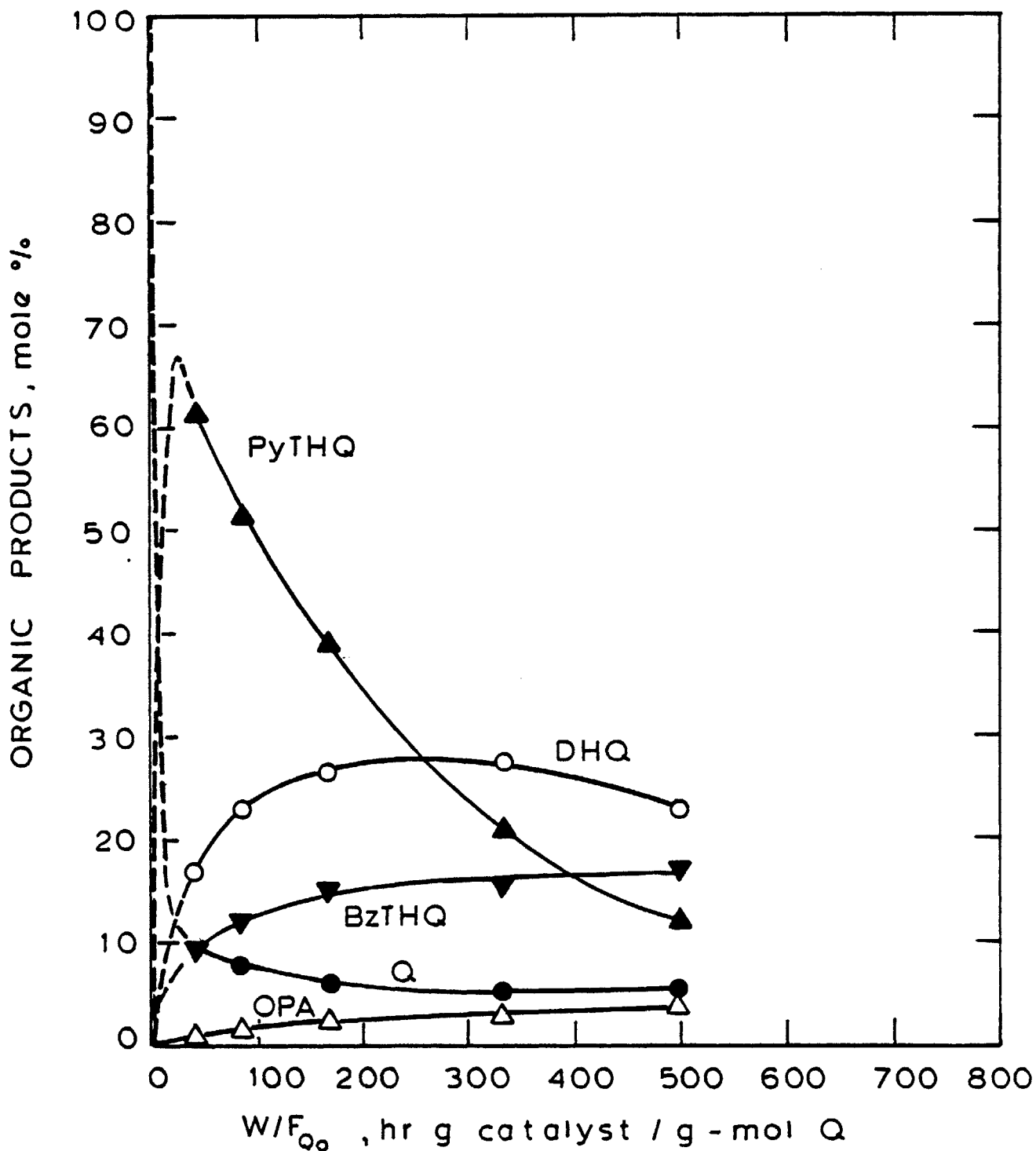


Figure 4-15: Product Distributions for Quinoline HDN at 375 °C, 7.0 MPa, 26.7 kPa Q (Run 24)

consistent with this expectation. Thus at 7.0 MPa, quinoline HDN yielded more BzTHQ than DHQ at 420°C, but more DHQ than BzTHQ at 375°C.

Figure 4-16 shows the distribution of products from PyTHQ HDN at 375°C and 7.0 MPa. This product distribution was essentially the same as that from quinoline HDN at the same reaction conditions (compare Figures 4-14 and 4-16). The peculiar departure of the Q/PyTHQ product ratio from equilibrium at longer reaction times was observed with PyTHQ feed as well as with quinoline feed.

Product distributions for quinoline HDN at 330°C and 3.55 MPa or 7.0 MPa total pressure are shown in Figures 4-17 and 4-18, respectively. The most striking feature in the product distribution observed at 3.55 MPa was the increase in amount of quinoline in the products with increased W/F_{Q_0} . Even at 330°C the hydrogenation of quinoline to PyTHQ proceeded rapidly to equilibrium. However, as W/F_{Q_0} increased there was not only a departure from Q/PyTHQ equilibrium, but it appears that there was a net conversion of PyTHQ to quinoline, though the thermodynamic driving force was seemingly in the opposite direction. This phenomenon was observed at 7.0 MPa as well, but was much less pronounced. The product distributions at 330°C are otherwise reasonable.

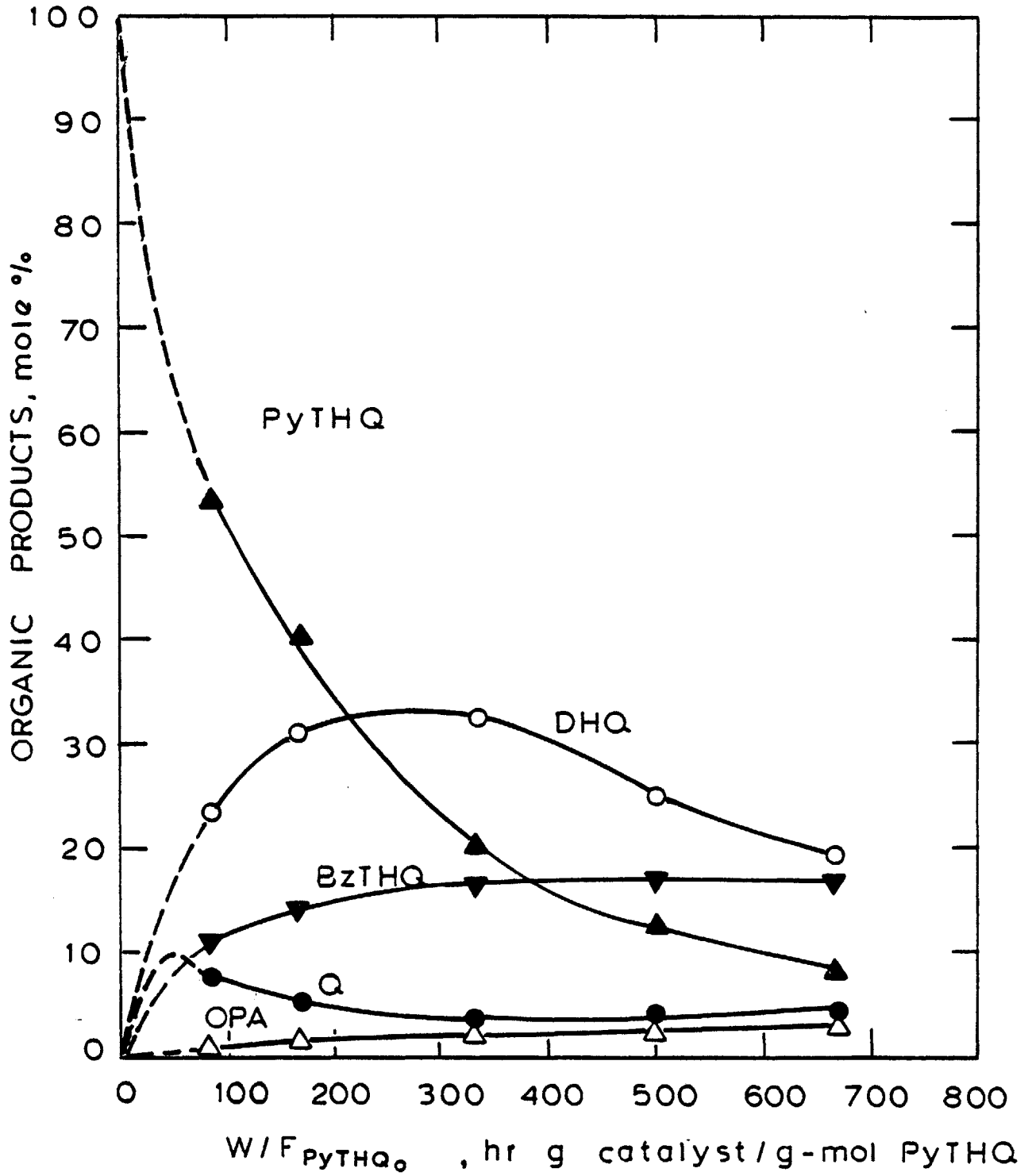


Figure 4-16 : Product Distributions for Py-Tetrahydroquinoline HDN at 375 °C, 7.0 MPa, 13.3 kPa PyTHQ (Run 33)

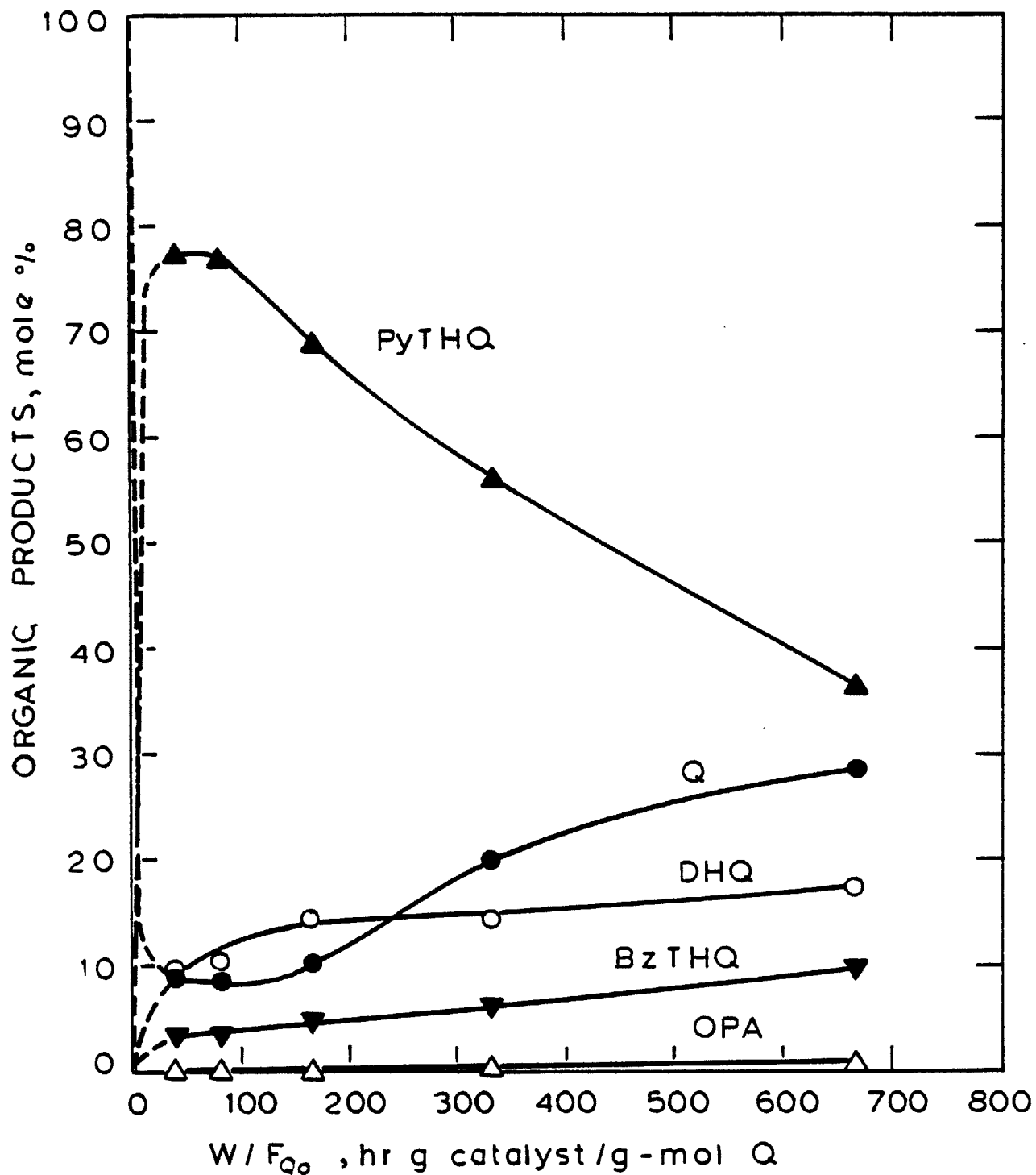


Figure 4-17: Product Distributions for Quinoline HDN at 330 °C, 3.55 MPa, 13.3 kPa Q (Run 25)

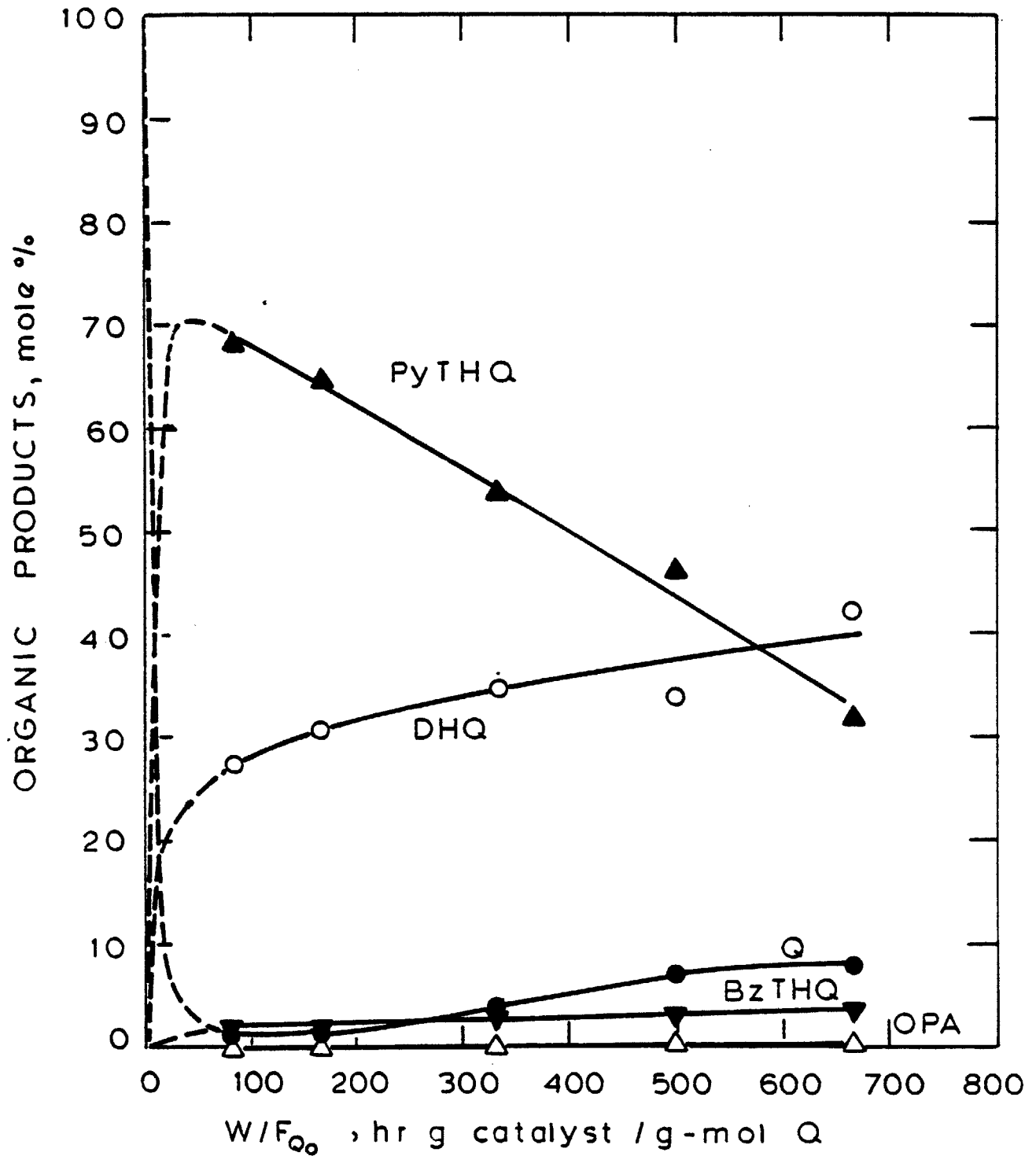


Figure 4-18: Product Distributions for Quinoline HDN at 330°C, 7.0 MPa, 13.3 kPa Q (Run 26)

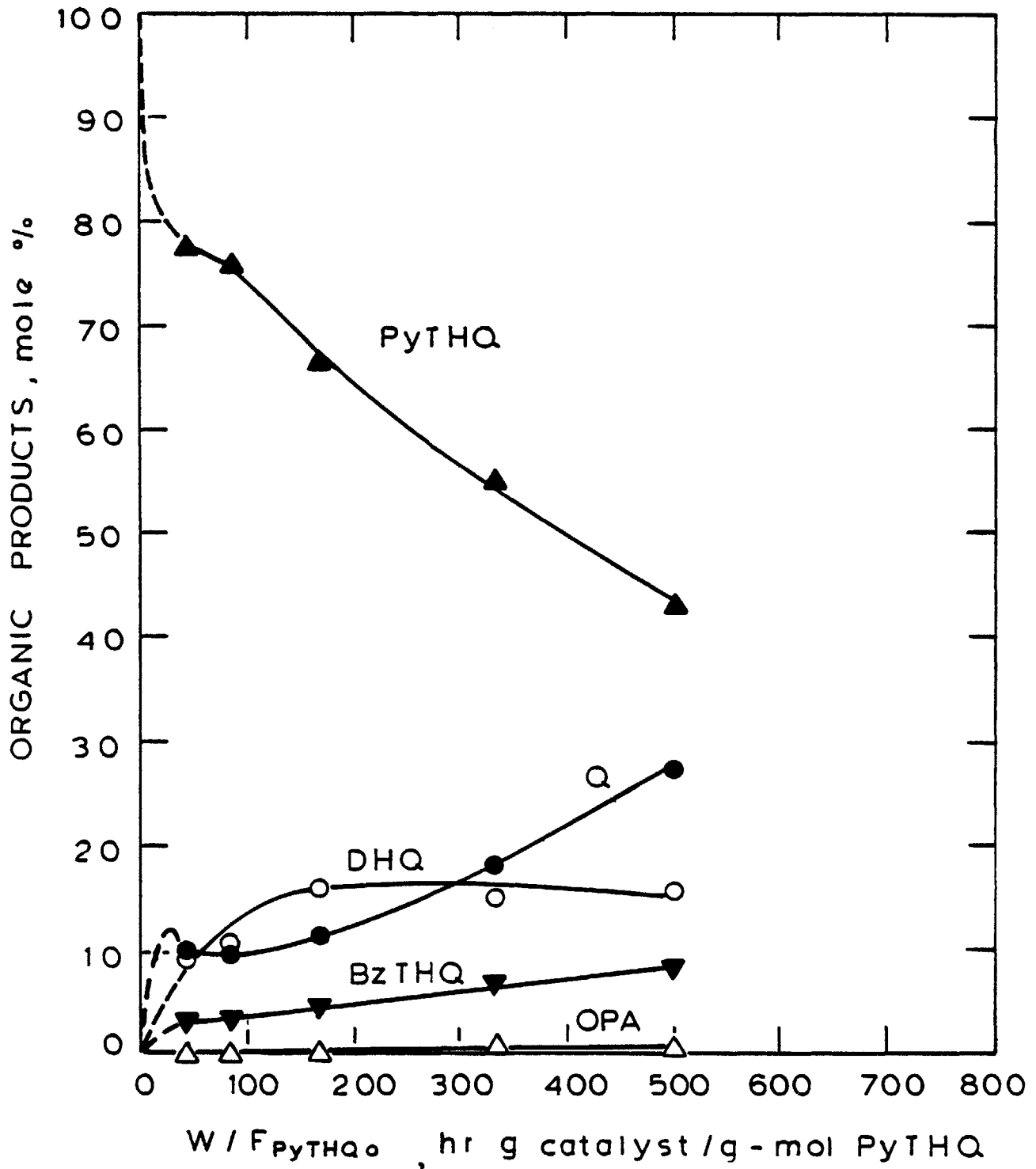


Figure 4-19: Product Distributions for Py-Tetrahydroquinoline HDN at 330°C, 3.55 MPa, 13.3 kPa PyTHQ (Run 34)

This result was so strange and unexpected that another experiment was run at 330°C and 3.55 MPa, but with PyTHQ feed instead of quinoline. As can be seen from Figure 4-19, the same result was obtained for PyTHQ HDN.

IV. B. 3. Product Distributions: Hydrocarbon Products

Thus far only the distributions of nitrogen-bearing reaction intermediates have been presented in addition to the corresponding denitrogenation curves, which represent sum totals of all hydrocarbons formed from the reactant nitrogen compounds. Some comments about the hydrocarbon products are now in order.

The principal hydrocarbons detected in the quinoline or PyTHQ HDN reaction products were propylcyclohexane (PCH), propylbenzene (PB), propylcyclohexene (PCHE), ethylcyclohexane (ECH), and ethylbenzene (EB). The dominant hydrocarbon product was PCH. The same distribution of hydrocarbons was observed for both quinoline and PyTHQ HDN at the same reaction conditions. Increased quantities of PCH, PB, ECH, and EB were formed as W/F_{i_0} ($i = Q$ or PyTHQ) increased, under all conditions, but PCHE formation usually went through a maximum. At 330°C essentially no EB and ECH were formed; their formation was favored at higher reaction temperatures and higher hydrogen pressure. Higher hydrogen pressure, however, increased ECH formation

much more than EB formation, which is not surprising. In quinoline HDN at 420°C, 7.0 MPa, and 500 hr g catalyst/g-mol Q, nitrogen removal was nearly complete and EB and ECH together accounted for about 15% of the hydrocarbon products (PCH and PB accounted for about 65% and 20% of the hydrocarbon products, respectively).

The molar ratios of PCHE to PB and of PCHE to PCH in the reaction products decreased with W/F_{i_0} , but greatly exceeded the corresponding equilibrium ratios under essentially all reaction conditions (equilibrium constants for PCHE dehydrogenation to PB and for PCHE hydrogenation to PCH are shown in Figure 2-4). If these reactions proceeded to equilibrium at the temperatures and hydrogen pressures employed here, only traces of PCHE would be present in the products. The ratio of PCH to PB in the products increased with hydrogen pressure and with W/F_{i_0} (though often remaining constant at higher W/F_{i_0}), but also did not correspond to the equilibrium ratio. Increasing the reaction temperature from 330°C to 375°C, other variables constant, increased the PCH to PB product ratio but further increase in temperature to 420°C then decreased this ratio. At certain reaction conditions the PCH/PB product ratio was less than the equilibrium ratio, but at other conditions the corresponding equilibrium ratio was exceeded. Thus there was no simple correlation between reaction conditions and the PCH/PB product ratio from quinoline or PyTHQ HDN.

Equilibrium PCH/PB ratios as a function of temperature and hydrogen partial pressure are presented in Figure 4-20, and can be compared with the HDN product ratios tabulated in the Appendix.

IV. C. Hydrodenitrogenation of o-Propylaniline

Since o-propylaniline (OPA) was not commercially available, it had to be synthesized for this study. The synthesis selected involved nitration of n-propylbenzene, distillation of the resulting isomer mixture to obtain high purity o-nitropropylbenzene (ONPB), and catalytic reduction of ONPB to OPA. A final distillation gave OPA of 98% purity, the main impurity being the para isomer.

IV. C. 1. Nitrogen Removal

Figure 4-21 illustrates the effects of OPA feed rate (W/F_{OPA}), temperature, and initial OPA partial pressure on the extent of denitrogenation for OPA HDN at 7.0 MPa total pressure. Doubling the partial pressure of OPA from 13.3 kPa to 26.7 kPa in the reactor feed, at constant W/F_{OPA} , had no effect on percent nitrogen removal at 375°C. Increased temperature significantly increased the rate of denitrogenation of OPA. Thus at 420°C complete denitrogenation was achieved at 167 hr g

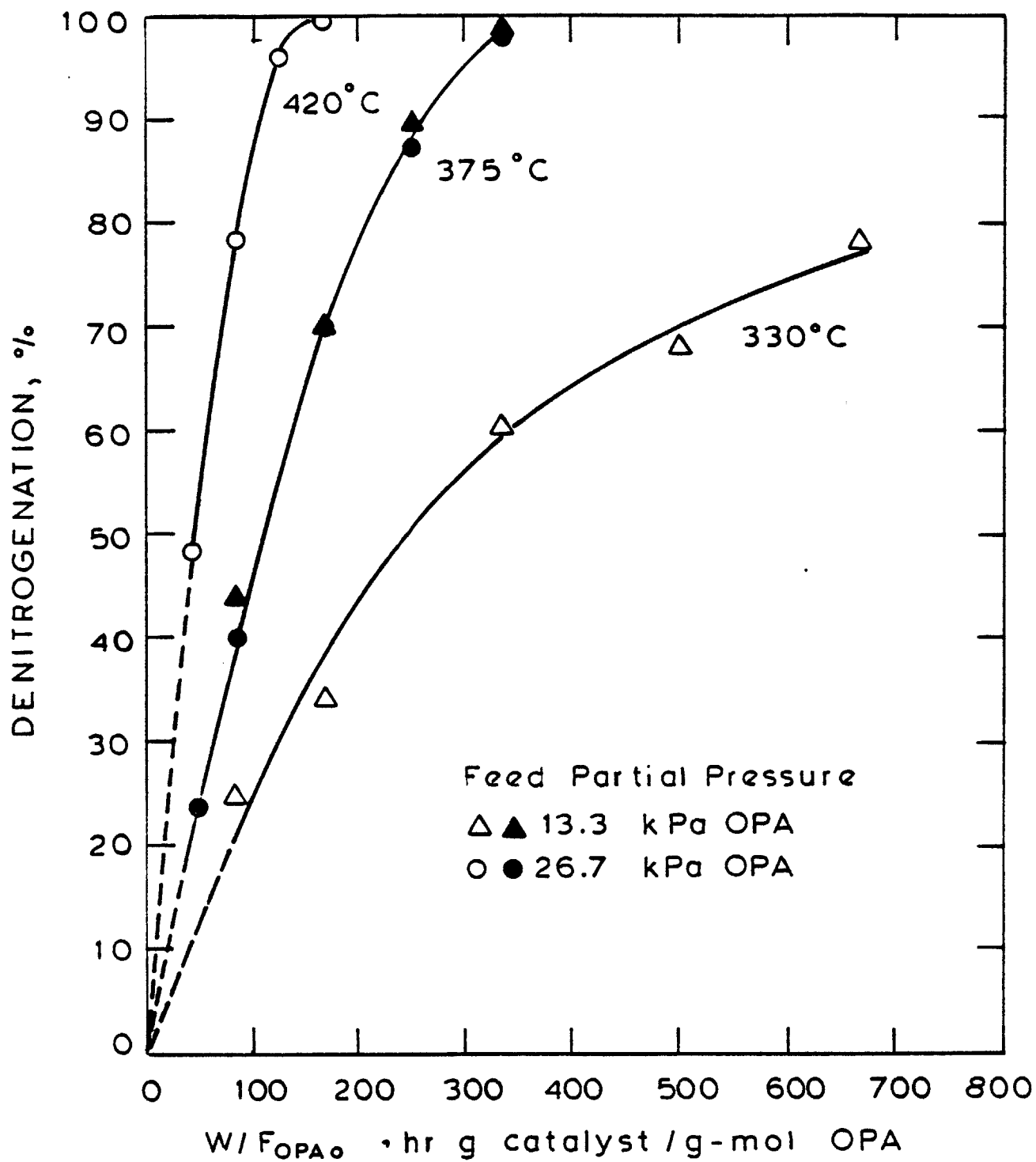


Figure 4-21: o - Propylaniline Denitrogenation at 7.0 MPa

catalyst/g-mol OPA, while at 375°C denitrogenation was complete only at lower feed rates corresponding to W/F_{OPA} greater than 333 hr g catalyst/g-mol OPA. Less than 80% denitrogenation was observed at 330°C even at 667 hr g catalyst/g-mol OPA.

The effect of hydrogen partial pressure on OPA denitrogenation at 375°C is shown in Figure 4-22. Doubling the hydrogen pressure nearly doubled nitrogen removal for W/F_{OPA} less than 333 hr g catalyst/g-mol OPA.

IV. C. 2. Product Distributions

No heterocyclic nitrogen compounds were detected in the products from OPA HDN, but the hydrocarbon products were the same as those from quinoline or PyTHQ HDN. At the reaction conditions investigated, PCH was always formed in greater quantities than PB. Significant amounts of PCHE were formed at the lowest W/F_{OPA} , but then decreased often to trace amounts as W/F_{OPA} increased. Small quantities of ECH, which increased with W/F_{OPA} , and traces of EB were observed in the products from OPA HDN at 420°C. Their formation decreased at 375°C and disappeared completely at 330°C.

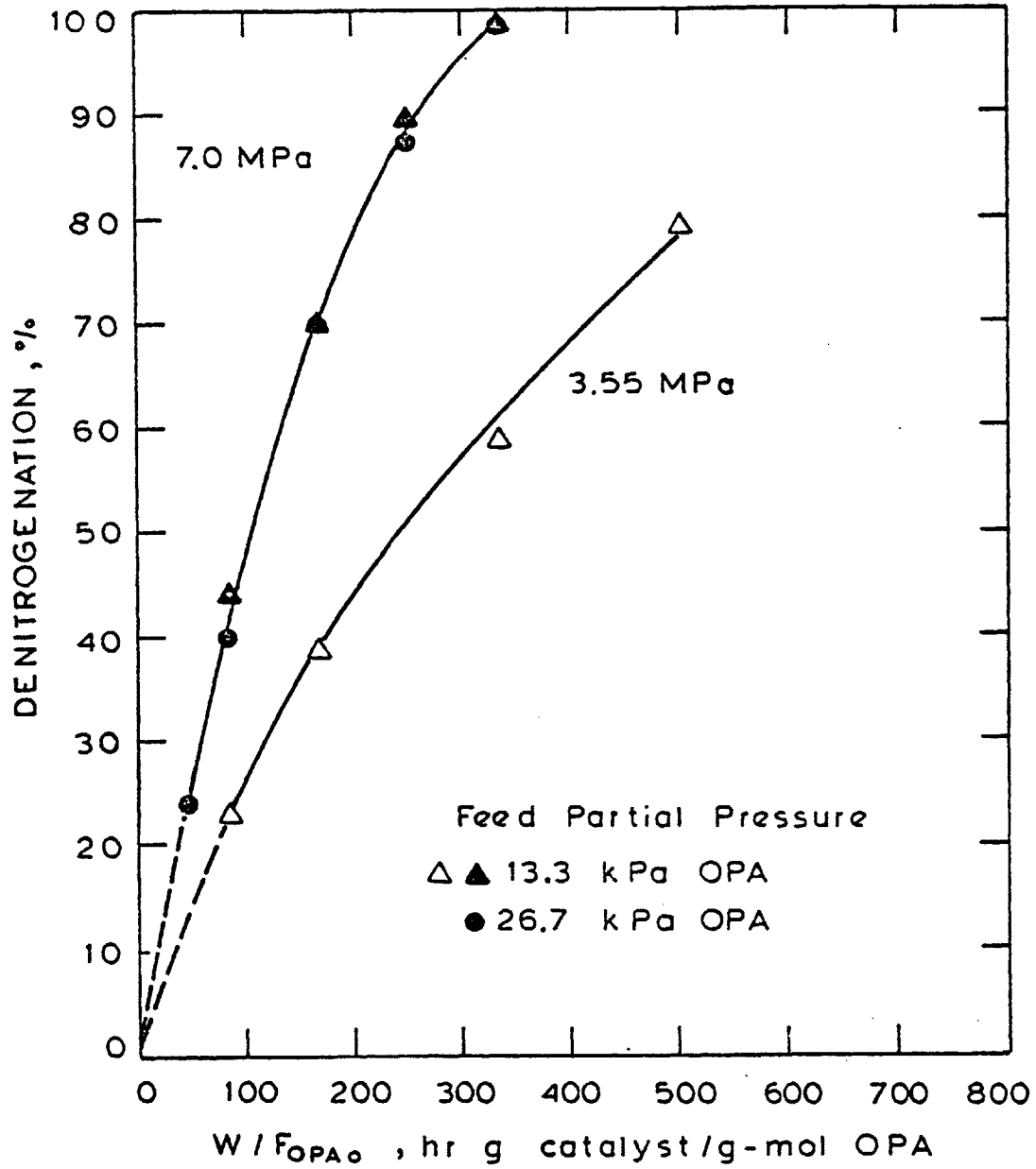


Figure 4-22: o-Propylaniline Denitrogenation at 375°C

As was the case with quinoline or PyTHQ HDN, denitrogenation of OPA did not produce PCH and PB in equilibrium quantities. The PCH/PB product ratio increased only slightly with W/F_{OPA} , and was always less than the corresponding equilibrium ratio.

IV. D. Hydrodenitrogenation of Bz-Tetrahydroquinoline and Decahydroquinoline

Unlike the other model nitrogen compounds studied, DHQ can be either a solid or a liquid at room temperature depending on the relative amounts of the cis and trans isomers. The DHQ used in this study was a solid at room temperature. As a result, a suitable solvent had to be used to prepare a liquid DHQ solution that could be pumped into the high-pressure reactor system. The solvent selected was cyclohexane as it dissolved DHQ quite easily, did not interfere in the gas chromatographic product analyses, was unreactive under HDN conditions, and was not expected to affect the kinetics of DHQ HDN (Doelman and Vlugter, 1963). The DHQ/cyclohexane solution fed to the reactor contained 59.5 weight % or 47.1 mole % DHQ, and was unsaturated with respect to DHQ at room temperature.

IV. D. 1. Nitrogen Removal

Nitrogen removal from BzTHQ and DHQ is shown as a function of W/F_{iO} at 375°C and 7.0 MPa total pressure in Figure 4-23. Similar results previously presented for HDN of quinoline, PyTHQ, or OPA at the same reaction conditions are also shown for comparison. It is apparent that nitrogen removal from DHQ, the completely saturated heterocyclic, was significantly easier than from BzTHQ, while the compounds most resistant to denitrogenation were quinoline and PyTHQ. The most striking and perhaps surprising result was the relative ease with which OPA denitrogenated compared to the heterocyclic nitrogen compounds.

An experiment was also run in which BzTHQ was denitrogenated at 330°C, 3.55 MPa total pressure, and 13.3 kPa initial BzTHQ partial pressure, for a series of feed rates. Again, nitrogen removal from BzTHQ was significantly higher than from either quinoline or PyTHQ at the same reaction conditions (compare data for runs 25, 34, and 36 in Appendix).

IV. D. 2. Product Distributions

The distribution of nitrogen-bearing products from BzTHQ HDN at 375°C and 7.0 MPa is shown in Figure 4-24. The amount of unconverted BzTHQ decreased with

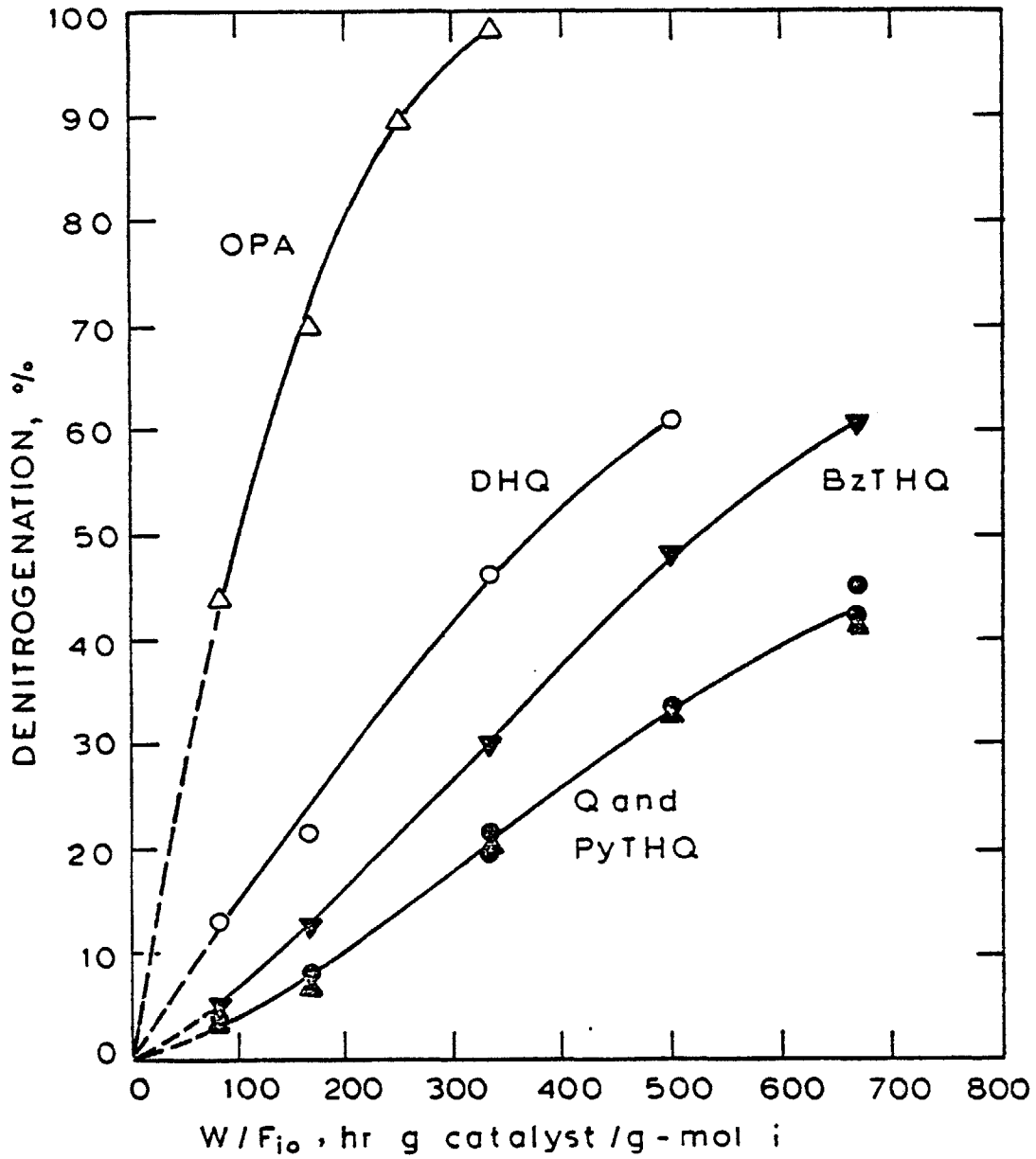


Figure 4-23: Denitrogenation of Individual Nitrogen Compounds at 375 °C, 7.0 MPa, 13.3 kPa Feed Partial Pressure

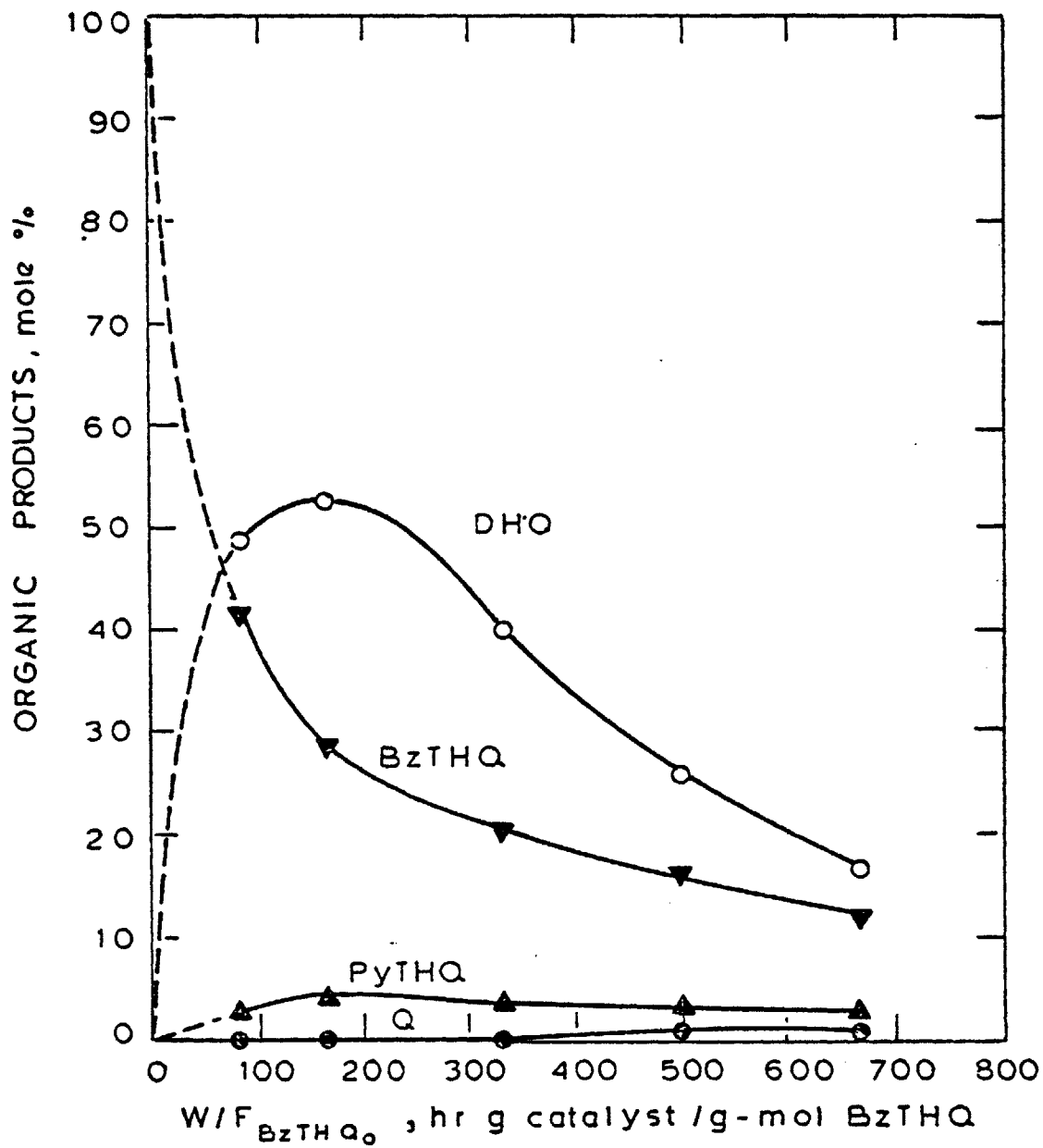


Figure 4-24: Product Distributions for Bz-Tetrahydroquinoline HDN at 375 °C, 7.0 MPa, 13.3 kPa BzTHQ (Run 35).

W/F_{BzTHQ} , as BzTHQ hydrogenated quite rapidly to DHQ. Formation of DHQ went through a maximum as W/F_{BzTHQ} increased, reflecting its role as a reaction intermediate. Some dehydrogenation of BzTHQ or DHQ occurred, as evidenced by the formation of quinoline and PyTHQ.

A similar product distribution resulted from BzTHQ HDN at 330°C and 3.55 MPa, except that the rate of conversion of DHQ to hydrocarbon products was much lower than it was at 375°C and 7.0 MPa (see Figure 4-25). Also, unusually large quantities of "unknowns" were formed at these relatively mild reaction conditions (the maximum quantities observed accounted for 14% of the BzTHQ fed to the reactor at 500 hr g catalyst/g-mol BzTHQ). The unknown peaks appeared in the normal range of the chromatograms, so it is unlikely that these unknowns were high molecular weight "tar" compounds. In both BzTHQ runs only traces of OPA were detected in the reaction products, which is not surprising in view of the low concentrations of PyTHQ in the products.

Figure 4-26 illustrates the product distribution from DHQ HDN at 375°C and 7.0 MPa. The DHQ was simultaneously dehydrogenated to BzTHQ and converted to hydrocarbon products. Some dehydrogenation of DHQ to PyTHQ occurred to a lesser extent, but no OPA was detected in the reaction products. A distinct maximum in BzTHQ formation was

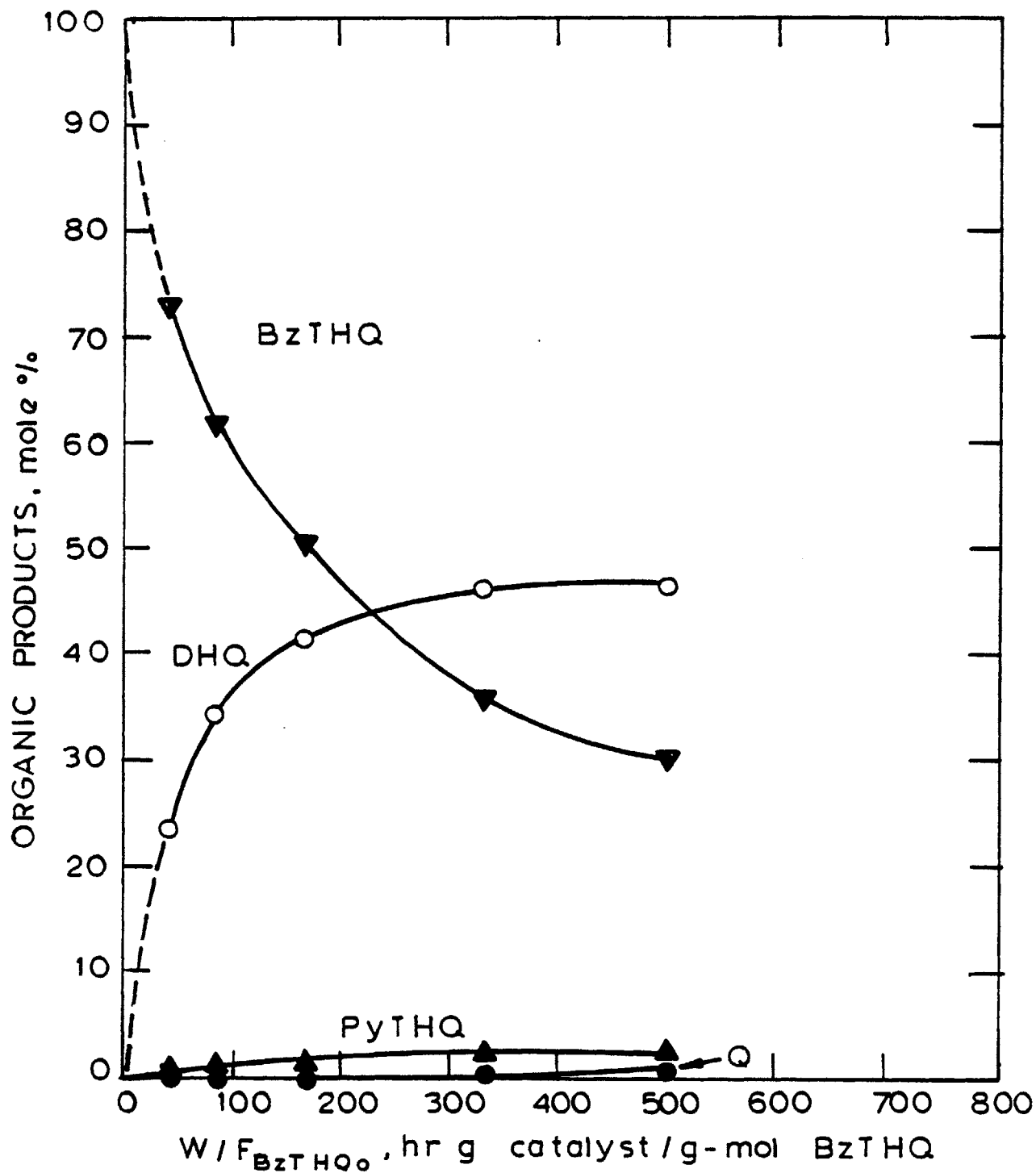


Figure 4-25: Product Distributions for Bz-Tetrahydroquinoline HDN at 330 °C, 3.55 MPa, 13.3 kPa BzTHQ (Run 36)

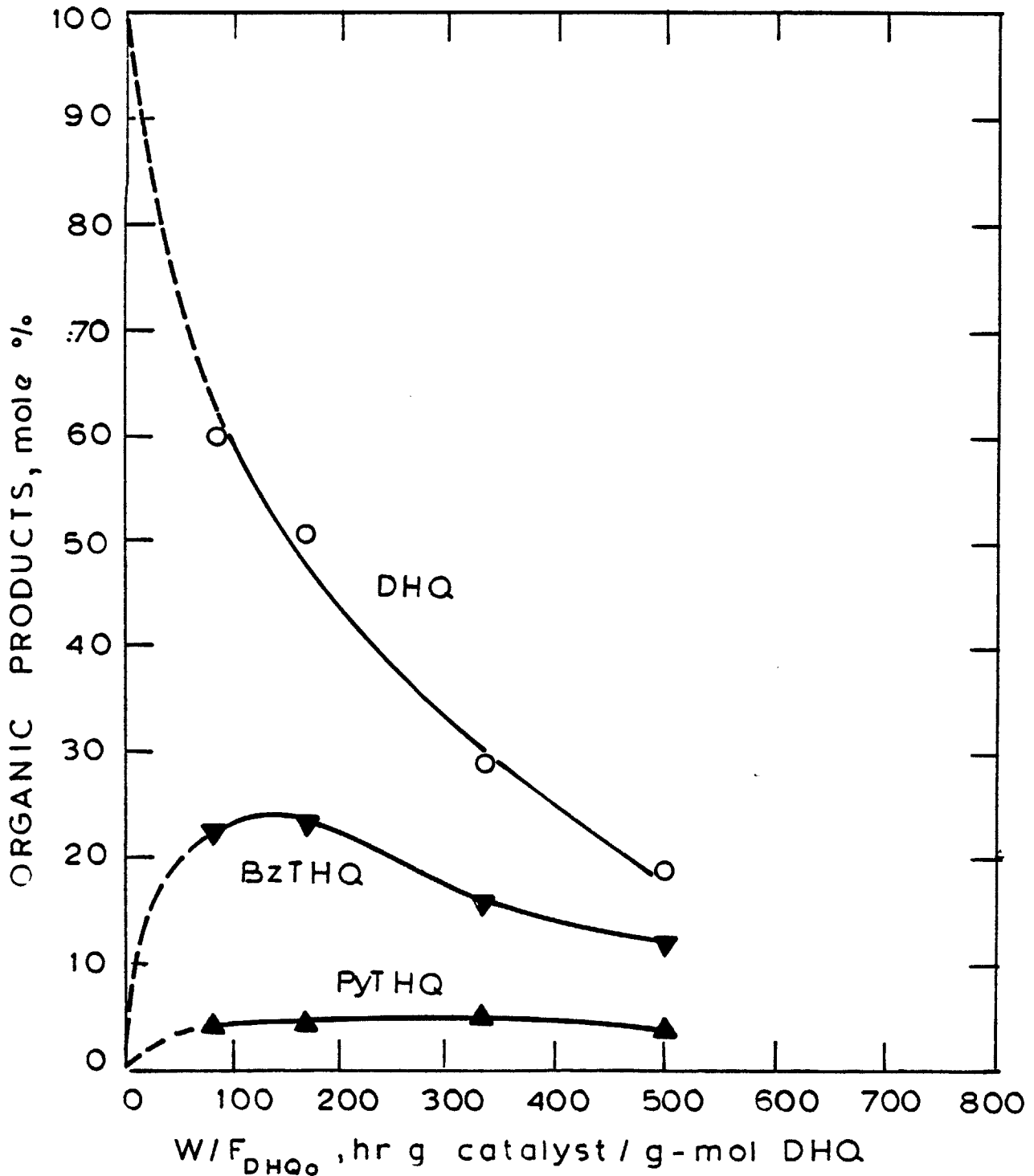


Figure 4-26: Product Distributions for Decahydroquinoline HDN at 375 °C, 7.0 MPa, 13.3 kPa DHQ (Run 38)

observed as W/F_{DHQ_0} increased. This most likely reflects an approach to hydrogenation/dehydrogenation equilibrium between BzTHQ and DHQ, since BzTHQ was not converted to other products (only traces of quinoline were detected in the reaction products, and the concentration of PyTHQ in the products remained fairly constant).

The hydrocarbon products from denitrogenation of BzTHQ or DHQ were again PCH, PB, and PCHE, while ECH and EB were formed only at higher temperatures. Formation of PCHE usually went through a maximum as W/F_{i_0} increased, but formation of the other hydrocarbons increased with W/F_{i_0} . The relative amounts of PCH and PB in the products were essentially the same for BzTHQ or DHQ denitrogenation at the same reaction conditions. Denitrogenation of BzTHQ or DHQ tended to yield a somewhat higher PCH/PB product ratio than quinoline or PyTHQ HDN at the same reaction conditions, particularly at lower W/F_{i_0} and at 330°C . The PCH/PB product ratio was still below the corresponding equilibrium ratio, however.

IV. E. Hydrogenation of Propylbenzene

Figure 4-27 summarizes the results obtained when PB was hydrogenated over the presulfided NiMo/Al₂O₃ catalyst at 375°C and 7.0 MPa total pressure, in the

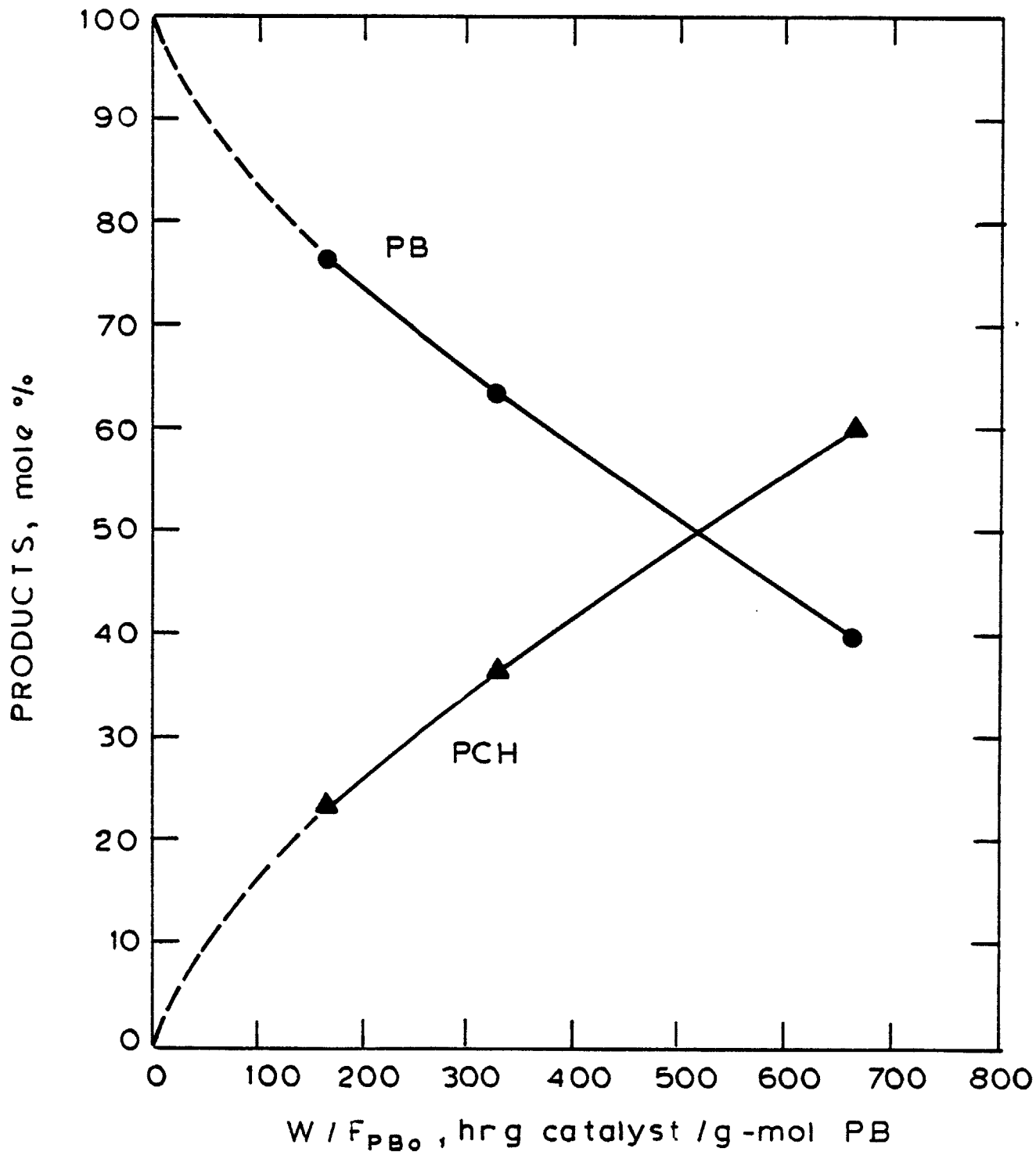


Figure 4-27: Propylbenzene Hydrogenation at 375°C,
7.0 MPa, 13.3 kPa PB (Run 16)

absence of any nitrogen compounds. The PB was increasingly hydrogenated to PCH as W/F_{PB} increased, but no PCHE, ECH, or EB was detected in the reaction products. Recall that all of these hydrocarbons were formed when the various nitrogen compounds were denitrogenated at these same reaction conditions. The quantity of PCH formed from hydrogenation of PB feed was much lower than the equilibrium amount, even at the highest W/F_{PB} studied (equilibrium here corresponds to about 98% conversion of PB to PCH; see Figure 4-20). In fact, the PCH/PB product ratio was much lower for PB hydrogenation than for denitrogenation of the nitrogen compounds. It must be pointed out that the PB hydrogenation experiment was carried out while the catalyst was still deactivating, so the rate of hydrogenation of PB may well have been even lower with "lined-out" catalyst.

IV. F. Homogeneous Reactions

A key experiment was conducted in which quinoline was exposed to a variety of HDN reaction conditions in the absence of the NiMo/Al₂O₃ catalyst. From the results presented in Table 4-1 it is apparent that "homogeneous" reactions did occur. It is not clear, however, whether these reactions were truly homogeneous (occurring in the gas phase) or were catalyzed by the stainless steel surfaces of the preheater and reactor walls.

Table 4-1

Quinoline HDN Without NiMo/Al₂O₃ Catalyst

("Blank" Experiment - Run 39)

Total pressure: 7.0 MPa

Initial quinoline partial pressure: 13.3 kPa

Temperature (°C)	420	420	375	330
*W/F _Q (hr g/g-mol Q)	†83.3	667	667	667
Organic products (mole %):				
PyTHQ	26.5	47.7	55.6	39.8
Q	72.8	45.1	42.2	60.2
OPA	TR	2.4	0.9	-
BzTHQ	0.8	3.4	1.3	-
DHQ	-	0.4	-	-
PB	-	0.1	-	-
PCHE	-	0.9	-	-
PCH	-	0.1	-	-
TOTAL	100.1	100.1	100.0	100.0
PyTHQ/(Q+PyTHQ)	26.7	51.4	56.9	39.8
PyTHQ/(Q+PyTHQ) at equilibrium	65	65	90	98
Q → PyTHQ approach to equilibrium	41%	79%	63%	41%
Denitrogenation	0%	1.1%	0%	0%

* Calculated as if the usual 1.5 g of catalyst was in the reactor (to facilitate comparison with catalytic HDN results)

† For extraneous reasons the initial quinoline partial pressure was 26.7 kPa

Only the hydrogenation of quinoline to PyTHQ occurred at an appreciable rate, but equilibrium was never reached even at the highest temperature (420°C) and lowest quinoline feed rate (corresponding to $W/F_{Q_0} = 667 \text{ hr g "catalyst"/g-mol Q}$ if the usual amount of $\text{NiMo/Al}_2\text{O}_3$ catalyst had been present). This was in sharp contrast to the rapid equilibration of quinoline and PyTHQ at all reaction conditions, in the presence of the $\text{NiMo/Al}_2\text{O}_3$ catalyst. At constant quinoline feed rate and total pressure, the "homogeneous" hydrogenation of quinoline to PyTHQ approached equilibrium more closely as temperature increased from 330°C to 420°C , but the reaction was still far short of equilibrium. Also, a decrease in quinoline feed rate resulted in a closer approach to Q/PyTHQ equilibrium. These results are, of course, expected for a kinetically-controlled reaction.

No hydrocarbons were formed except at the most severe reaction conditions, and then only 1% denitrogenation occurred. Recall that 100% denitrogenation of quinoline was achieved at these conditions in the presence of catalyst (see Figure 4-6). Small quantities of BzTHQ, OPA, and DHQ were formed at the most severe reaction conditions; these decreased as the quinoline feed rate increased and as temperature decreased, disappearing completely at 330°C . Thus all "homogeneous" reaction

rates except for quinoline hydrogenation to PyTHQ were negligible compared to the catalytic rates with NiMo/Al₂O₃.

IV. G. Initial Ring Saturation Equilibria

Each of the heterocyclic nitrogen compounds was studied separately at 375°C and 7.0 MPa, so each of the ring saturation equilibria was approached from both sides at these reaction conditions. For example, with PyTHQ feed the PyTHQ/DHQ equilibrium was approached via hydrogenation of PyTHQ to DHQ; with DHQ feed at the same reaction conditions, the PyTHQ/DHQ equilibrium was approached via dehydrogenation of DHQ to PyTHQ. This is illustrated in the lower portion of Figure 4-28, in which the relative quantities of PyTHQ and DHQ in the reaction products are presented as a function of W/F_{i_0} for reaction of PyTHQ or DHQ. From these data the position of the PyTHQ/DHQ equilibrium at 375°C and 7.0 MPa hydrogen pressure can be estimated, or at least bounded. The upper portion of Figure 4-28 shows analogous results for the Q/BzTHQ equilibrium.

Though the ring saturation equilibria were not approached from both sides at all reaction conditions, careful examination of the ratios of saturated to unsaturated species in the HDN reaction products as a function of feed nitrogen compound, W/F_{i_0} , temperature, and

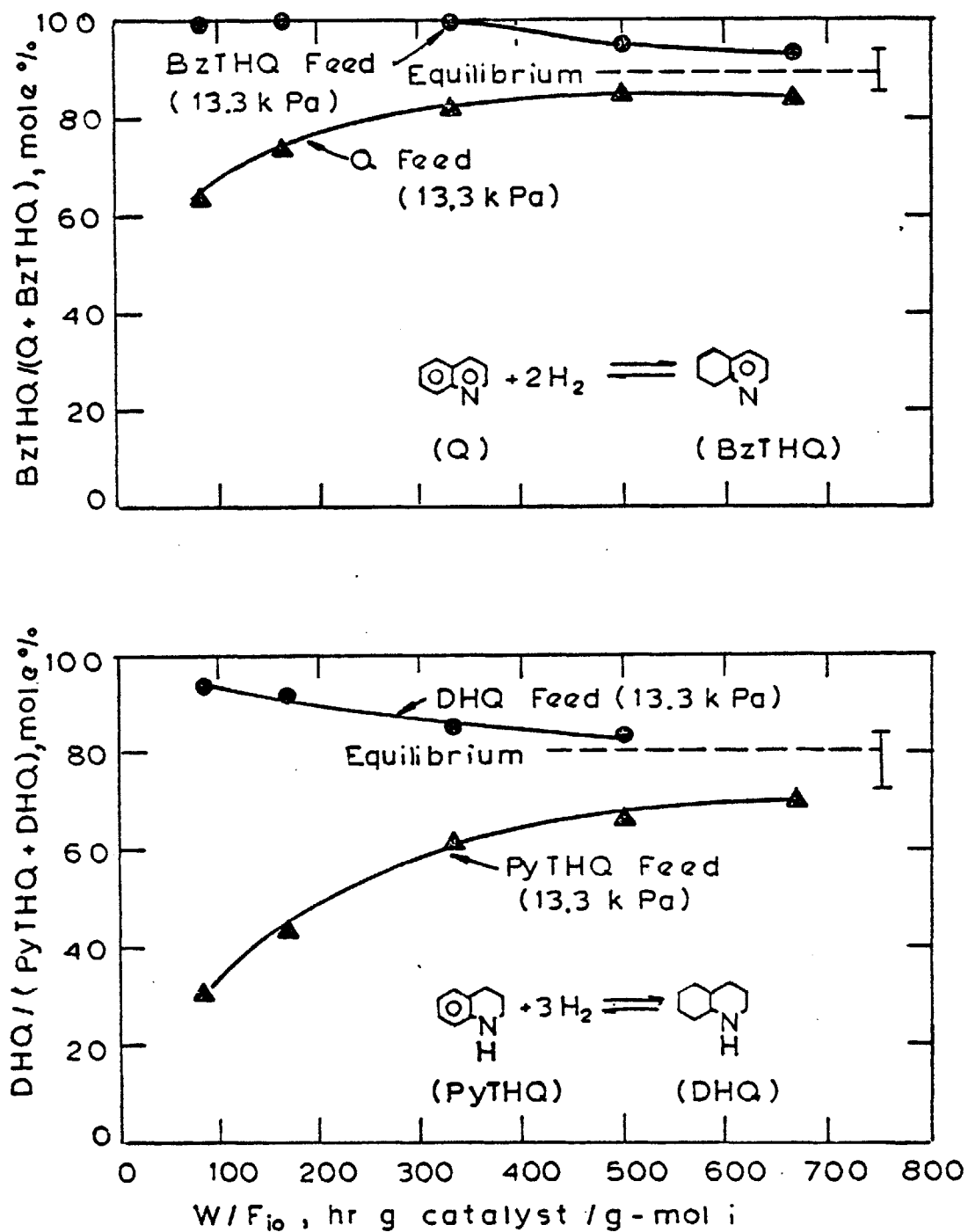


Figure 4-28: Estimation of Equilibrium Q / BzTHQ and PyTHQ / DHQ Ratios at 375°C and 7.0 MPa from Experimental Data

pressure provides estimates of the positions of these equilibria at other reaction conditions. Equilibrium constants for the ring saturation reactions were then calculated from these data, since the equilibrium ratio of each pair of saturated and unsaturated heterocyclic nitrogen compounds is determined by only the corresponding equilibrium constant (a function of temperature) and the hydrogen partial pressure (assuming ideal gas behavior - a reasonable approximation here). These experimentally estimated equilibrium constants are shown in Figures 4-29 and 4-30; also shown, for comparison, are the corresponding equilibrium constants calculated from estimated standard free energies of formation (see Figure 2-2 and the related discussion). The data points signify "best" estimates of the equilibrium constants from experimental data, while the error bars show experimental bounds on these equilibrium constants. Agreement between the equilibrium constants estimated experimentally and theoretically is quite good, considering the latter could be in error by one to two orders of magnitude. The largest discrepancy is observed for the equilibrium constants for hydrogenation of quinoline to PyTHQ, but the experimental estimates are in excellent agreement with those reported by other investigators (Declerck, 1976; Shih et al., 1977; Satterfield et al., 1978). The experimental $\log_{10}K$ versus $1/T$ lines for the other ring saturation reactions are drawn nearly parallel to the theoretical lines in Figures 4-29 and 4-30

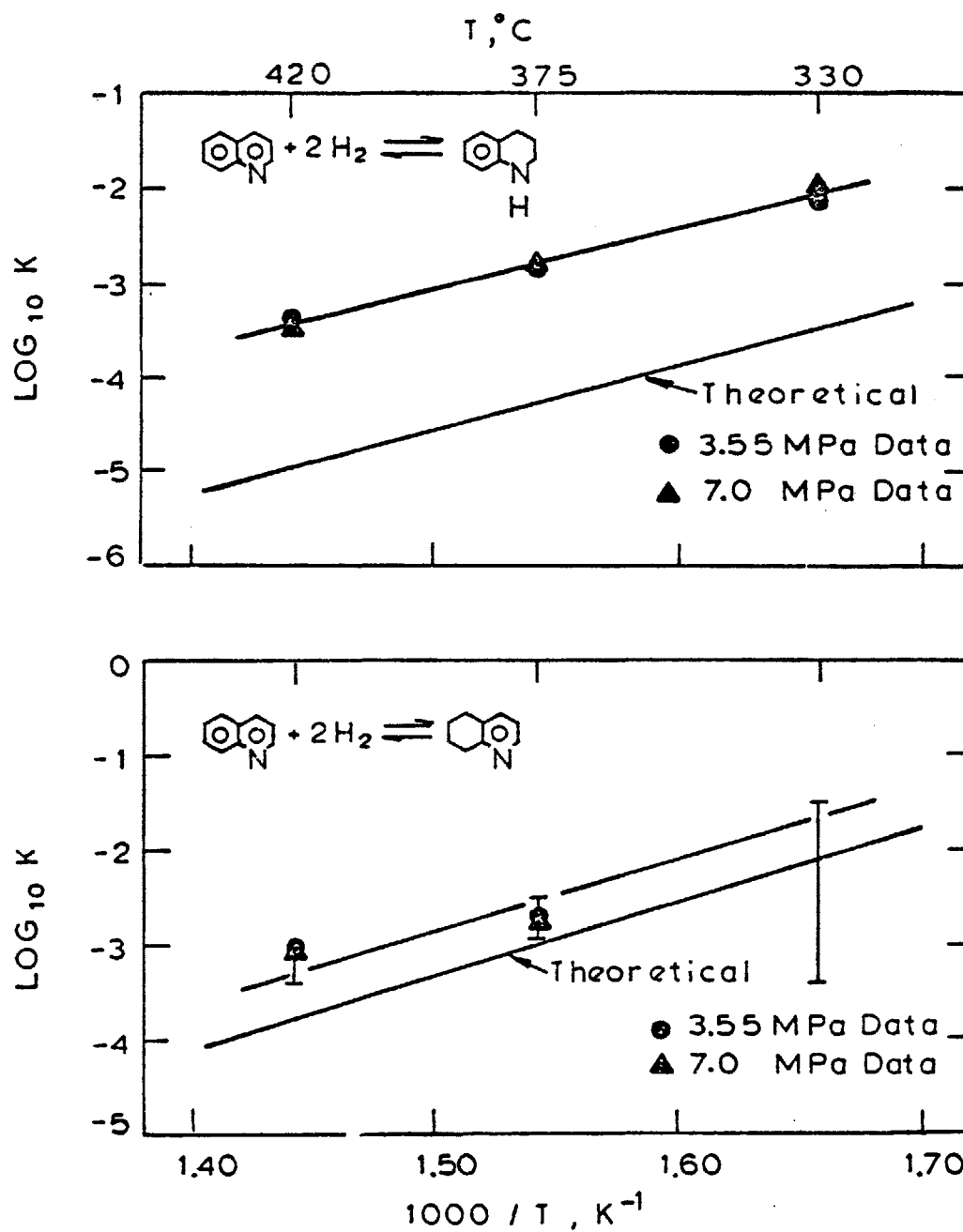


Figure 4-29: Comparison of Experimental and Theoretical Estimates of Equilibrium Constants for Hydrogenation of Quinoline to Tetrahydroquinolines

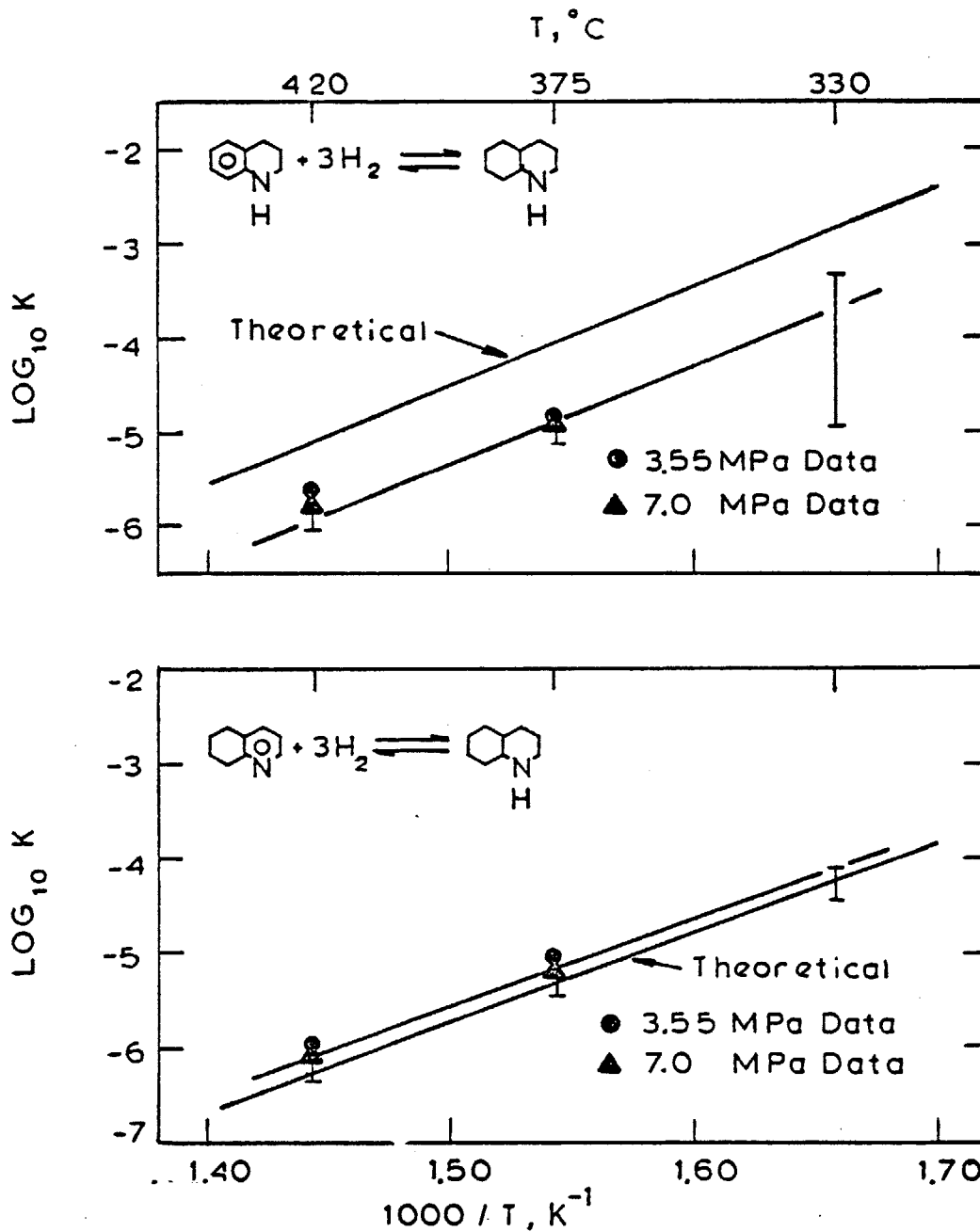


Figure 4-30: Comparison of Experimental and Theoretical Estimates of Equilibrium Constants for Hydrogenation of Tetrahydroquinolines to Decahydroquinoline

because the slopes of the theoretical lines generally provide accurate estimates of the standard heats of reaction (as evidenced by the nearly parallel theoretical and experimental $\log_{10}K$ versus $1/T$ lines in Figure 4-29 for the Q PyTHQ reaction), and equilibrium constants at 330°C for these other reactions could not be estimated accurately from the experimental data due to kinetic limitations at this relatively low temperature. The equilibrium constants estimated from the experimental data must, of course, be self-consistent. The $\log_{10}K$ versus $1/T$ lines through the experimental data in Figures 4-29 and 4-30 have been drawn with this in mind.

These $\log_{10}K$ versus $1/T$ correlations were used to estimate the equilibrium composition of the heterocyclics (Q, PyTHQ, BzTHQ, and DHQ) as a function of temperature, at each of the two hydrogen partial pressures employed in this study. Ideal gas behavior was assumed in the calculations, and the results are shown in Figures 4-31 and 4-32. These figures provide reasonable estimates of the relative quantities of the heterocyclics if each of the initial ring saturation reactions in quinoline HDN is at equilibrium. The thermodynamics favor DHQ at lower temperature and higher hydrogen pressure, while quinoline is favored at higher temperature and lower hydrogen pressure. This is consistent with the fact that the ring

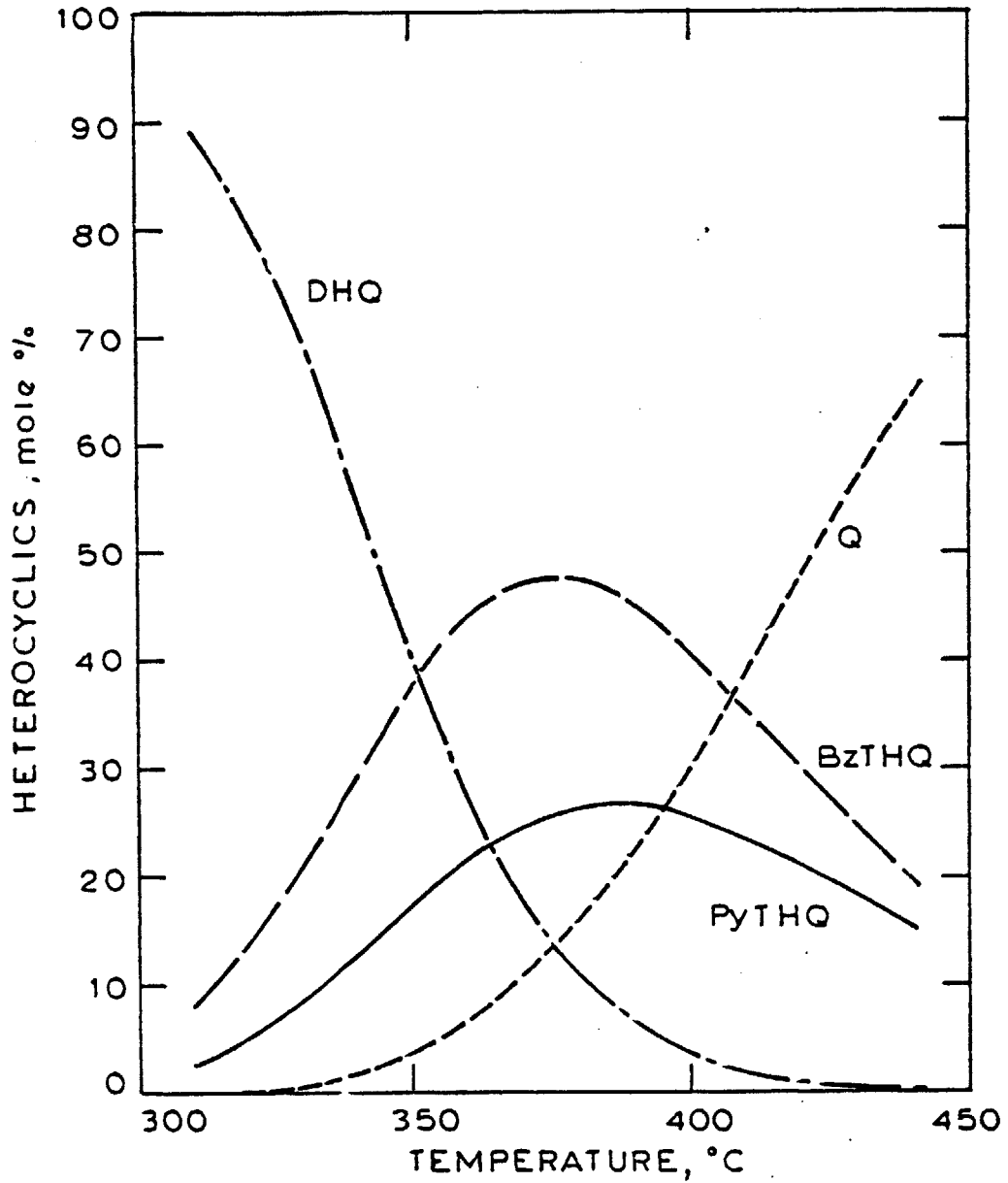


Figure 4-31: Estimated Equilibria Among Quinoline, Tetrahydroquinolines, and Decahydroquinoline at 3.53 MPa Hydrogen Partial Pressure

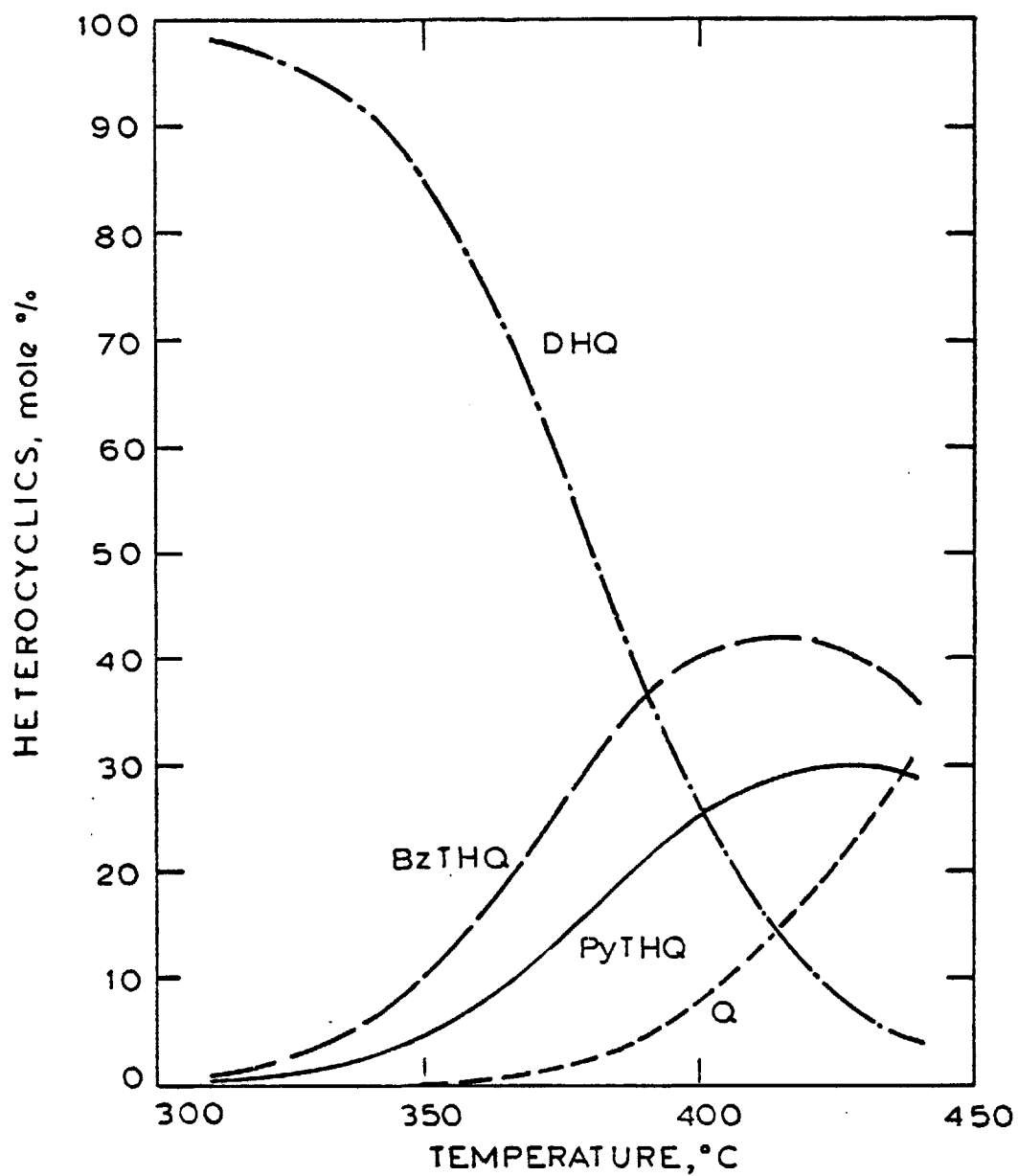


Figure 4-32: Estimated Equilibria Among Quinoline, Tetrahydroquinolines, and Decahydroquinoline at 6.98 MPa Hydrogen Partial Pressure

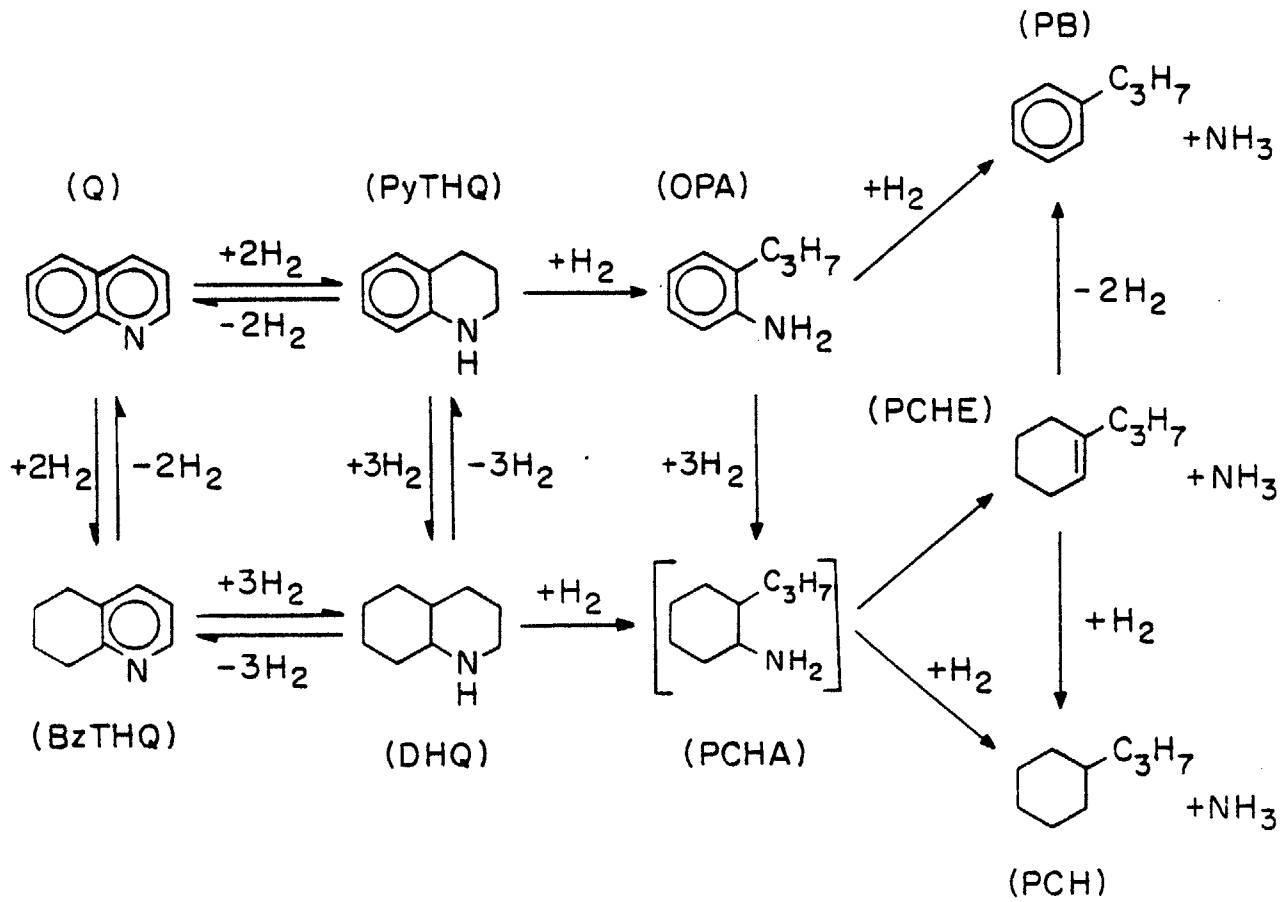
saturation (hydrogenation) reactions are exothermic and consume hydrogen. The behavior of the tetrahydroquinolines is more complex, since they are partially saturated species subject to either hydrogenation or dehydrogenation. Thus at constant hydrogen partial pressure, the equilibrium concentration of PyTHQ or BzTHQ proceeds through a maximum as temperature increases. Also, the effect of hydrogen pressure on the equilibrium concentration of PyTHQ or BzTHQ depends on the temperature. For example, at 420°C an increase in hydrogen pressure from 3.53 MPa to 6.98 MPa increases the equilibrium concentration of PyTHQ or BzTHQ, but the opposite effect occurs at 330°C (compare Figures 4-31 and 4-32). It is noteworthy that under HDN conditions, BzTHQ is thermodynamically more stable than PyTHQ. This is not surprising in light of the fact that under HDN conditions, hydrogenation of benzene to cyclohexane is thermodynamically more favorable than hydrogenation of pyridine to piperidine at the same temperature and hydrogen partial pressure.

V. Discussion of Results

V. A. Quinoline Hydrodenitrogenation Reaction Network and Thermodynamics

The quinoline HDN reaction network proposed in Figure 2-1 can now be justified in light of the results presented in the previous chapter. For convenience, the reaction network is shown again in Figure 5-1. Each of the species included in the reaction network, with the exception of propylcyclohexylamine (PCHA), was found in the quinoline HDN products. PCHA is a plausible reaction intermediate, formed by hydrogenolysis of DHQ or by hydrogenation of OPA. The fact that PCHA was not found in the HDN products reflects its presumed high rate of denitrogenation relative to its rate of formation. Similar compounds, such as cyclohexylamine and ethylcyclohexylamine, and aliphatic amines in general, have been shown to denitrogenate very rapidly under HDN conditions (Stengler et al., 1964; Stern, 1979). Hydrogenation of OPA to PCHA is potentially thermodynamically limited at higher temperatures and lower hydrogen pressures (the equilibrium constant is shown in Figure 2-4), but the reverse reaction can be ignored here since PCHA presumably denitrogenated as rapidly as it was formed.

FIGURE 5-1
QUINOLINE HDN REACTION NETWORK



Q	quinoline
PyTHQ	Py (or 1,2,3,4) - tetrahydroquinoline
BzTHQ	Bz (or 5,6,7,8) - tetrahydroquinoline
DHQ	decahydroquinoline (cis and trans isomers)
OPA	o-propylaniline
PCHA	propylcyclohexylamine
PB	propylbenzene
PCHE	propylcyclohexene
PCH	propylcyclohexane

V. A. 1. Formation of Hydrocarbon Products

Hydrodenitrogenation of OPA or the heterocyclics produced PB, PCHE, and PCH. Greater than equilibrium quantities of PCHE were formed, relative to the amounts of PB and PCH in the HDN products, but no PCHE was observed in the products from hydrogenation of PB in the absence of nitrogen compounds. Thus PCHE was most likely formed by elimination of ammonia from PCHA - a reaction with a very large equilibrium constant, and essentially irreversible, at HDN conditions (see Figure 2-4). This type of reaction is known to occur with aliphatic amines. In a study of indole HDN, Stern (1979) proposed ethylcyclohexylamine (ECHA) as a reaction intermediate, and found that ethylbenzene, ethylcyclohexene, and ethylcyclohexane were all formed from HDN of ECHA. Formation of pentene from pentylamine, the analogous reaction in pyridine HDN, has also been reported, though pentane was the major hydrocarbon product (Sonnemans and Mars, 1974). In the present study, PCHE formation usually went through a maximum as W/F_{i_0} increased, suggesting that PCHE was also a reaction intermediate. Indeed, PCHE was thermodynamically unstable with respect to PB or PCH at the reaction conditions in this study. For example, at 375°C and 7.0 MPa hydrogen partial pressure, the equilibrium PB/PCHE and PCH/PCHE ratios are approximately 60 and 3600,

respectively. In HDN of DHQ at 375°C and 7.0 MPa, no OPA was detected in the reaction products, so it is unlikely that PB was formed by direct hydrogenolysis of OPA. As W/F_{DHQ} increased, formation of PB or PCH increased while PCHE formation went through a maximum (see data for run 38 in Appendix). Thus it appears that the PB was formed here by dehydrogenation of PCHE.

The presence of nitrogen compounds, including ammonia, has been shown to severely inhibit the hydrogenation of unsaturated hydrocarbons. Under HDN conditions, it is unlikely that PB was hydrogenated to PCH. Instead, PB and PCH were formed by parallel reactions, as indicated in Figure 5-1, and their ratio was controlled primarily by kinetics rather than by thermodynamics. This is consistent with the fact that PB and PCH were not present in equilibrium amounts in the HDN products; under some conditions the equilibrium PCH/PB ratio was exceeded (as in quinoline HDN at 420°C and 3.55 MPa), while at other conditions the PCH/PB product ratio was well below the corresponding equilibrium ratio.

Hydrodenitrogenation of OPA yielded PB, PCHE, and PCH (as stated earlier), but PCH was always the dominant product. This result indicates that extensive hydrogenation of OPA (to PCHA) occurred, and that hydrogenation of OPA was much faster than direct hydrogenolysis of OPA to PB. That this latter reaction occurred at all is supported by

the observation that the PCH/PB product ratio from OPA HDN at 375°C and 7.0 MPa was somewhat lower than the PCH/PB product ratio from DHQ HDN at the same reaction conditions (no OPA was formed from the DHQ; compare the data for runs 28 and 38 in the Appendix). These results are not surprising if the chemistry of OPA is considered. The C-N bond in OPA is resonance stabilized, and as a result is much stronger than the C-N bond in aliphatic amines (such as PCHA). Consequently, hydrogenolysis of OPA to PB is much more difficult than nitrogen removal from PCHA. The amine group in OPA activates the aromatic ring, making hydrogenation of OPA much easier than say, hydrogenation of PB (compare Figures 4-21 and 4-27). Doelman and Vlugter (1963) reported that both aromatic and saturated hydrocarbons were formed from HDN of aniline or o-toluidine (o-methylaniline), but that no saturated hydrocarbons were found in the products from HDN of benzylamine (α -phenylmeth-ylamine, an aliphatic amine). They similarly concluded that hydrogenation of the aromatic ring in anilines is closely connected with cleavage of the amine group.

V. A. 2. Initial Ring Saturation Reactions

Theoretical estimates of the equilibrium constants for the initial ring saturation reactions in quinoline HDN (see Figure 2-2) indicate that these reactions are potentially reversible under HDN conditions. The experimental results

show that this is indeed the case, and allow more accurate estimates of these equilibrium constants to be made. At 375°C and 7.0 MPa, HDN of each individual heterocyclic nitrogen compound (Q, PyTHQ, BzTHQ, or DHQ) resulted in the formation of all the other heterocyclics, though only small quantities of quinoline were found in the products from BzTHQ or DHQ HDN at these conditions. However, in an earlier experiment at 375°C and 3.55 MPa, HDN of BzTHQ yielded significant amounts of quinoline as well as PyTHQ and DHQ, since quinoline formation was thermodynamically more favorable at this lower hydrogen pressure (see data for run 15 in the Appendix). This is shown clearly in Figures 4-31 and 4-32, which illustrate the equilibrium behavior of the heterocyclic nitrogen compounds in quinoline HDN.

It must be pointed out that equilibration of the heterocyclics will actually occur under HDN conditions only if the hydrogenation and dehydrogenation reactions are fast relative to the PyTHQ and DHQ hydrogenolysis reactions. In this study, partial equilibration of the heterocyclics was observed under some reaction conditions, but in general the initial ring saturation reactions were subject to complex interactions between kinetics and thermodynamics.

In commercial hydrotreating processes aimed at nitrogen removal, it is desirable to minimize hydrogen consumption

for economic reasons. In quinoline HDN, the Q PyTHQ OPA PB reaction path minimizes hydrogen consumption, but it was not the primary path for nitrogen removal that actually occurred (PCH was always the major product). The equilibrium behavior of the heterocyclics in quinoline HDN has significant implications in this regard. It is apparent from Figures 4-31 and 4-32 that under HDN conditions, particularly at the higher hydrogen pressures often required to achieve satisfactory HDN rates, the thermodynamics favor oversaturation to DHQ. In addition, saturation of the aromatic ring in quinoline is thermodynamically more favorable than saturation of the heterocyclic ring. These results can most likely be extended, at least qualitatively, to other multiring heterocyclic nitrogen compounds such as acridine and carbazole. Thus the burden of selectively hydrogenating only the heterorings is placed solely on the HDN catalyst, which ideally must possess sufficient hydrogenolysis activity to then remove the nitrogen without saturating any aromatic rings. In the case of aniline intermediates, direct hydrogenolysis of the C-N bond is difficult relative to aromatic ring saturation, as shown in this study. The NiMo/Al₂O₃ catalyst, a commercial hydrotreating catalyst, exhibited little selectivity for the reaction path of minimum hydrogen consumption in quinoline HDN. This is discussed in more detail in conjunction with the discussion of quinoline HDN kinetics.

V. B. Catalyst Activity

Significant deactivation of the presulfided NiMo/Al₂O₃ catalyst was observed during its first 400 hours of use for quinoline HDN. During this time, the percent denitrogenation achieved at standard reaction conditions decreased continuously (see Figures 4-1 through 4-3), and the product distribution changed appreciably (see Figures 4-4 and 4-5). These figures clearly indicate that there was a significant loss of hydrogenolysis activity during catalyst deactivation, but the relative changes in hydrogenation and hydrogenolysis activities of the catalyst are not readily apparent.

An attempt was made to quantify the individual changes in hydrogenation and hydrogenolysis activities of the catalyst during deactivation, by looking closely at hydrogen consumption in quinoline HDN. Except for the formation of PCHE from PCHA, all reactions in the quinoline HDN network are either hydrogenolysis reactions (each consuming one mole of hydrogen), hydrogenation reactions, or dehydrogenation reactions (see Figure 5-1). Formation of PCHE from PCHA can be treated as a simultaneous hydrogenolysis/dehydrogenation reaction with no net hydrogen consumption. Thus, regardless of the reaction path, the formation of PB, PCHE, or PCH from quinoline consumes two moles of hydrogen in hydrogenolysis reactions, while the net hydrogen consumption in saturation (hydrogenation) reactions is two,

four, or five moles, respectively. Hydrogen consumptions for the formation of the nitrogen-bearing intermediates from quinoline follow similarly from Figure 5-1. From the quinoline HDN product distribution and knowledge of the reaction network, one can calculate the separate amounts of hydrogen consumed in saturation and in hydrogenolysis reactions. The amount of hydrogen consumed in hydrogenolysis reactions is a direct measure of the hydrogenolysis activity of the catalyst, while the net hydrogen consumption in saturation reactions provides a measure of the catalyst's hydrogenation activity.

Figures 5-2 and 5-3 illustrate the effect of catalyst "age" on hydrogen consumption in quinoline HDN at mild and severe standard conditions. Between 11 and 94 hours of catalyst use, hydrogen consumption in hydrogenolysis reactions declined from 0.335 to 0.128 mole/mole quinoline fed to the reactor, at mild standard conditions (see Figure 5-2). The corresponding decrease in hydrogen consumption in saturation reactions was from 2.41 to 1.94 moles/mole quinoline fed. Thus hydrogenolysis activity decreased by about 62% while the hydrogenation activity decreased by only 19%. At the more severe standard conditions, the hydrogen consumptions were significantly higher, reflecting the higher reaction rates and the more favorable thermodynamics for saturation reactions at the higher hydrogen pressure (see Figure 5-3). The stoichiometric hydrogen consumption in hydrogenolysis reactions is two moles/mole

HYDROGEN CONSUMPTION, moles/mole Q fed

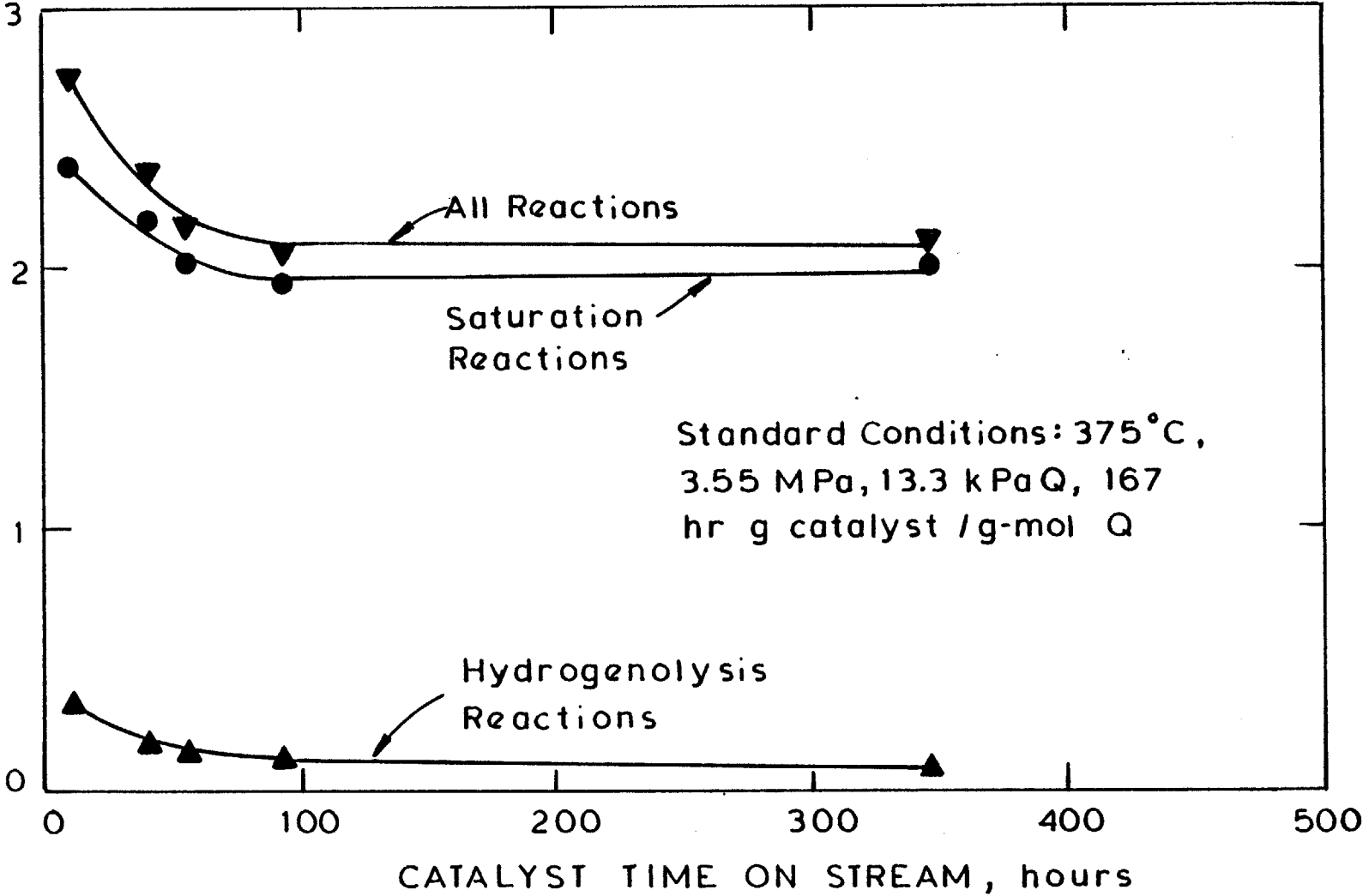


Figure 5-2: Hydrogen Consumption, in Quinoline HDN During Catalyst Deactivation - Mild Standard Conditions

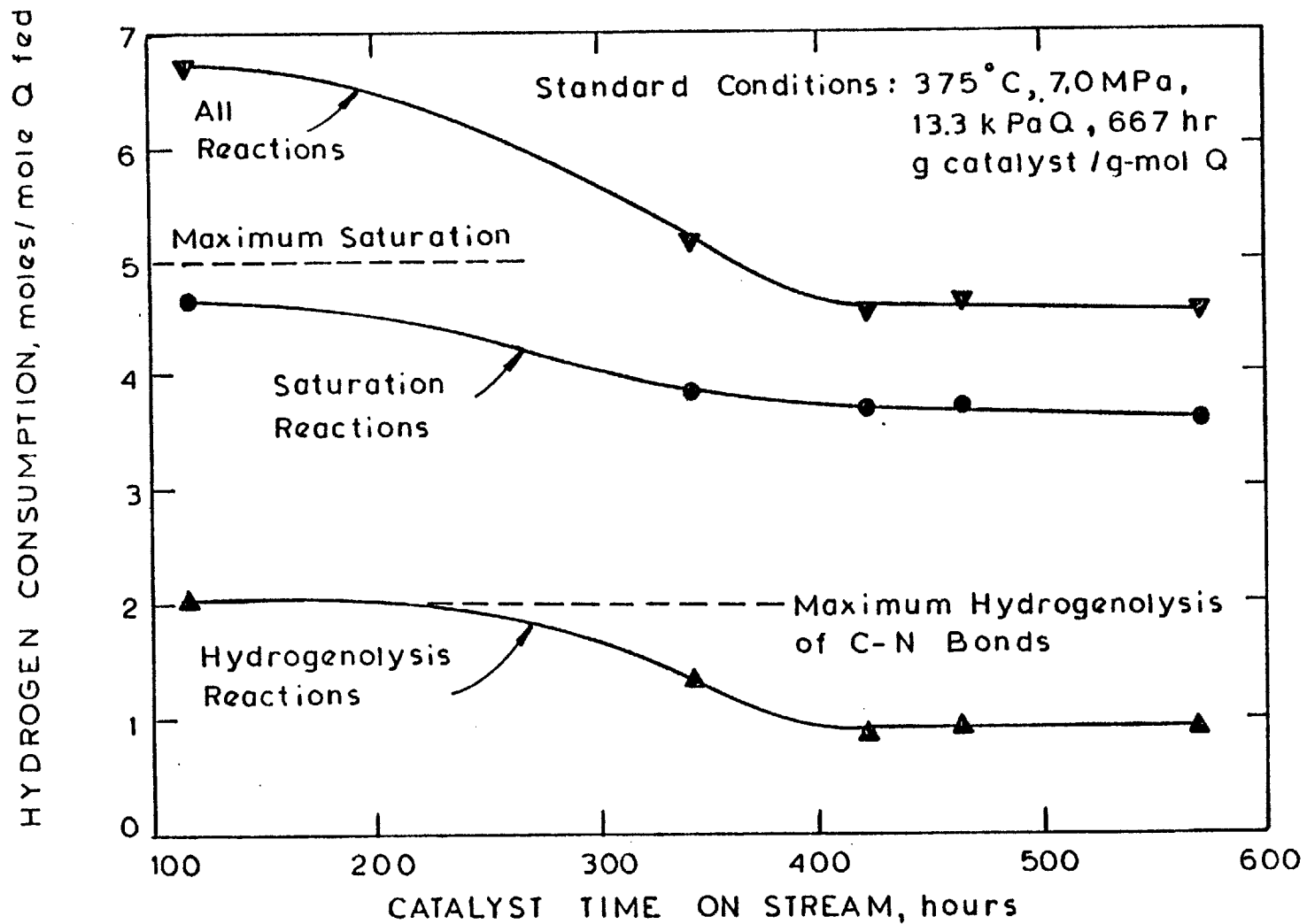


Figure 5-3: Hydrogen Consumption in Quinoline HDN During Catalyst Deactivation- Severe Standard Conditions

quinoline for complete nitrogen removal. The maximum consumption of hydrogen in saturation reactions is five moles/mole quinoline fed, leading to the formation of DHQ or PCHA intermediates or to PCH product. At the severe standard conditions, 100% denitrogenation of quinoline was achieved with 116 hour-old catalyst; in saturation reactions, hydrogen consumption was 4.68 moles/mole quinoline fed while 2.05 moles of hydrogen were consumed in hydrogenolysis reactions per mole of quinoline fed. The slightly greater than stoichiometric hydrogen consumption in hydrogenolysis reactions was due to the formation of some ECH and EB by hydrocracking reactions (hydrogenolysis of C-C bonds). Between 116 and 422 hours of catalyst use, hydrogen consumption in saturation reactions and in hydrogenolysis reactions decreased to 3.68 and 0.881 moles/mole quinoline fed, respectively. During this time, catalyst hydrogenolysis activity decreased by about 57% while the hydrogenation activity appeared to decrease by only 21%. It must be pointed out, however, that as the hydrogenolysis activity of the catalyst decreased, the concentrations of heterocyclic reaction intermediates in the quinoline HDN products increased. As a result, some of the quinoline ring saturation reactions might have become limited by thermodynamics as well as by kinetics, so the actual decrease in hydrogenation activity could have been less than 21%.

This analysis shows quite clearly that during catalyst deactivation, the loss in hydrogenolysis activity was much

greater (by a factor of about three) than the loss in hydrogenation activity. This markedly different behavior of the hydrogenation and hydrogenolysis activities is strong experimental evidence, albeit indirect, that these functionalities are associated with different catalyst sites.

The deactivation of the catalyst was most likely due to the accumulation of carbonaceous deposits (coke) on the surface. After about 580 hours of use, catalyst from the top and bottom halves of the reactor contained 7.1 and 6.1 weight percent carbon, respectively (there is essentially no carbon in the virgin catalyst). The somewhat higher carbon content in the catalyst from the top half (inlet end) of the reactor suggests a slightly higher rate of coke formation, due perhaps to the higher concentration of organic nitrogen compounds in the inlet end of the reactor. These compounds were most likely the coke precursors, since nitrogen was also found in the used catalyst but is not present in virgin catalyst.

A reasonable theory of deactivation can be proposed to account for the behavior of the NiMo/Al₂O₃ catalyst. The essential features of the theory have been postulated by Beuther and Larson (1965) to account for the deactivation of hydrocracking catalysts, which are similar to hydrotreating catalysts in possessing both hydrogenation and hydrogenolysis functionalities. The hydrogenation sites, through their catalytic activity, are much less susceptible to coking and could, in addition, protect

neighboring hydrogenolysis sites. It is postulated that during deactivation, coking eventually occurs on all hydrogenolysis sites not in the vicinity of a hydrogenation site. It is likely, too, that coking occurs preferentially on the more active (more acidic) hydrogenolysis sites. This would account for the observed decrease in the catalyst deactivation rate with time (see Figure 4-1), and for the much greater loss in hydrogenolysis activity than in hydrogenation activity. The catalyst activity attains a steady state after all "unprotected" hydrogenolysis sites have been coked. A steady-state level of activity appeared to have been reached with the NiMo/Al₂O₃ catalyst after about 400 hours of use.

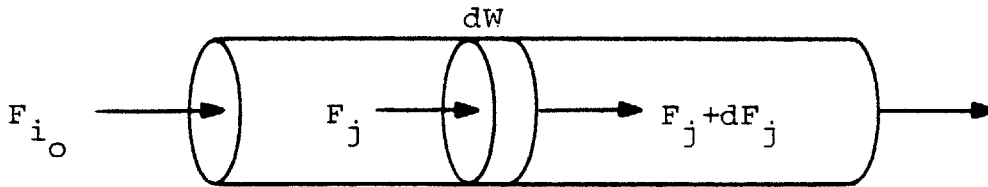
V. C. Quinoline Hydrodenitrogenation Kinetics

The experimental results presented in the previous chapter were all derived from steady-state, plug-flow reactor data. A brief derivation and discussion of the relevant plug-flow reactor equations follows, to aid in kinetic interpretation of these results.

V. C. 1. Relevant Plug-Flow Reactor Equations

The rates of catalytic reactions are most conveniently expressed in terms of catalyst mass, rather than reactor

volume. In an integral plug-flow reactor, concentrations and reaction rates vary significantly in the axial direction, and this must be taken into account. A material balance (for any non-hydrogen species j) over a differential element in the steady-state plug-flow reactor gives the following:



input + generation by reaction = output + accumulation

$$F_j + r_j dW = F_j + dF_j$$

$$r_j = \frac{dF_j}{dW}$$

(eq. 5-1)

where F_j = molar flow rate of j , g-mol j /hr

W = mass of catalyst, g

r_j = net rate of formation of j by chemical
reaction, g-mol j /hr g catalyst

In this study, the reactor was operated at constant temperature and total pressure, with negligible change in total molar flow rate due to the very large excess of hydrogen (the molar ratio of hydrogen to reactant nitrogen compound in the reactor feed varied from 132 to 524). Then for the stoichiometry in the quinoline HDN network:

$$Y_j = \frac{F_j}{F_{i_0}} = \frac{(F_j/F)P}{(F_{i_0}/F)P} = \frac{P_j}{P_{i_0}}$$

$$F_j = F_{i_0} Y_j = F_{i_0} \left(\frac{P_j}{P_{i_0}} \right)$$

$$dF_j = F_{i_0} dY_j = \left(\frac{F_{i_0}}{P_{i_0}} \right) dP_j$$

where F_{i_0} = molar feed rate of reactant nitrogen compound,
g-mol i/hr

F = total molar flow rate through reactor,
g-mol/hr

P_{i_0} = initial partial pressure of reactant nitrogen
compound, Pa (or atm)

P = total pressure, Pa (or atm)

P_j = partial pressure of species j, Pa (or atm)

Y_j = fractional conversion of reactant nitrogen
compound into species j

Substituting into equation 5-1:

$$r_j = \frac{F_{i_o} dY_j}{dW} = \frac{dY_j}{d(W/F_{i_o})} \quad (\text{eq. 5-2})$$

or,

$$r_j = \frac{F_{i_o} dP_j}{P_{i_o} dW} = \frac{dP_j}{d(P_{i_o} W/F_{i_o})} = \frac{dP_j}{d\tau} \quad (\text{eq. 5-3})$$

where

$$\tau = \frac{P_{i_o} W}{F_{i_o}} = \frac{PW}{F}$$

These differential rate expressions can be integrated over the entire plug-flow reactor, to give:

$$\frac{W}{F_{i_o}} = \int_{Y_{j_o}}^{Y_j} \frac{dY_j}{r_j} \quad (\text{eq. 5-4})$$

or,

$$\tau = \frac{P_{i_o} W}{F_{i_o}} = \int_{P_{j_o}}^{P_j} \frac{dP_j}{r_j} \quad (\text{eq. 5-5})$$

Thus the appropriate reaction time variable for kinetic analysis is either W/F_{i_o} or the space time τ . Note that the space time is not a residence (contact) time, and does not vary with reactor temperature for instance.

The integrated form of the plug-flow reactor equation is particularly useful for testing simple kinetic rate expressions against the experimental data. For example, if

hydrocarbon formation (or ammonia formation) in quinoline HDN is assumed to be zero order with respect to the organic nitrogen compounds, then:

$$r_{\text{HC}} = k'$$

and from equation 5-4:

$$\frac{W}{F_{Q_0}} = \int_0^{Y_{\text{HC}}} \frac{dY_{\text{HC}}}{k'} = \frac{Y_{\text{HC}}}{k'} \quad \text{or} \quad Y_{\text{HC}} = k' \left(\frac{W}{F_{Q_0}} \right)$$

If zero order kinetics are followed, a plot of Y_{HC} (or, equivalently, percent denitrogenation) versus W/F_{Q_0} should be linear, with a slope independent of initial quinoline partial pressure, and should pass through the origin. Examination of Figures 4-6 through 4-8 reveals that there are significant deviations from linearity at very low or very high levels of nitrogen removal, but overall, hydrocarbon formation from quinoline can be approximated by zero order kinetics. If, instead of W/F_{Q_0} , the space time is used:

$$Y_{\text{HC}} = \frac{k'}{P_{Q_0}} \left(\frac{P_{Q_0} W}{F_{Q_0}} \right) = \left(\frac{k'}{P_{Q_0}} \right) \tau$$

For zero order kinetics, a plot of percent denitrogenation versus τ should also be linear and pass through the origin, but here the slope is inversely proportional to initial quinoline partial pressure. In this study, product distri-

butions as well as percent denitrogenation were nearly independent of initial partial pressure of the reactant nitrogen compound, at constant temperature, total pressure, and W/F_{i_0} . For this reason, W/F_{i_0} was used for presentation of experimental results.

The HDN product distributions presented in the previous chapter are calculated on the basis of organic products only, i.e. on an ammonia-free basis. Since there was no change in the number of moles of organic species upon reaction, neglecting minor side reactions such as coking, the mole percentage of each organic product corresponds to the mole percentage of the reactant nitrogen compound converted into that product. Thus the product distributions shown as a function of W/F_{i_0} are equivalent to Y_j versus W/F_{i_0} curves, the slopes of which provide the net instantaneous reaction rates of the various species (see equation 5-2).

V. C. 2. Qualitative Discussion

The quinoline HDN network is a complex series/parallel reaction network, including reversible as well as irreversible reactions. Hydrocarbons and ammonia, the desired products, are formed from the DHQ and OPA reaction intermediates (PCHA is a short-lived intermediate, so the rate of formation of hydrocarbons and ammonia from PCHA is determined solely by the rate of formation of PCHA from DHQ or

OPA). As a result, for HDN of quinoline, PyTHQ, or BzTHQ, the rate of denitrogenation (slope of the percent denitrogenation versus W/F_{i_0} curve) was zero initially (at $W/F_{i_0} = 0$), increased with W/F_{i_0} as the concentrations of DHQ and OPA intermediates increased, and eventually decreased at high W/F_{i_0} as the concentrations of intermediates, particularly DHQ, decreased and the ammonia concentration became significant (see, for example, Figure 4-23 and the corresponding product distributions in Figures 4-14, 4-16, and 4-24). Thus the percent denitrogenation versus W/F_{i_0} curves are S-shaped for HDN of quinoline, PyTHQ, or BzTHQ. Very often, the maximum denitrogenation rate of these compounds was observed when the DHQ concentration was a maximum, suggesting that nitrogen removal occurred primarily through the DHQ intermediate. For HDN of DHQ or OPA, the percent denitrogenation versus W/F_{i_0} curve is concave downward; the denitrogenation rate was highest initially, and decreased with W/F_{i_0} as the concentration of DHQ or OPA decreased (see Figures 4-23 and 4-26).

The denitrogenation results presented in Figure 4-23, and the corresponding product distributions, provide considerable insight into the quinoline HDN kinetics, at least at 375°C and 7.0 MPa. Nitrogen removal from DHQ was substantially easier than from the other heterocyclics, since DHQ is already completely saturated and its hydrogenolysis rate was relatively high. However, the initial hydrogenolysis rate was significantly lower than the initial rate of

dehydrogenation to BzTHQ (compare the initial slopes of the percent denitrogenation (Y_{HC}) versus W/F_{DHQ_0} curve in Figure 4-23 and the Y_{BzTHQ} versus W/F_{DHQ_0} curve in Figure 4-26). At these reaction conditions, though, dehydrogenation of DHQ was limited by thermodynamics (see Figure 4-32). Nitrogen removal from BzTHQ was much easier than from PyTHQ. This is seen from Figure 4-23; at any value of W/F_{i_0} , the percent denitrogenation is higher for BzTHQ feed than for PyTHQ feed. The BzTHQ HDN product distributions clearly show that nitrogen removal occurred through hydrogenolysis of DHQ, since the concentration of PyTHQ was always low and only traces of OPA were formed (see Figure 4-24). Even for PyTHQ feed the primary reaction pathway for nitrogen removal was through the DHQ (rather than the OPA) intermediate, since hydrogenation of PyTHQ to DHQ was much faster than hydrogenolysis of PyTHQ to OPA (see Figure 4-16). Comparison of Figures 4-16 and 4-24 reveals that the rate of hydrogenation of BzTHQ to DHQ was higher than the PyTHQ to DHQ hydrogenation rate. In addition, about 20% of the PyTHQ feed was converted to quinoline and BzTHQ (the latter was formed by hydrogenation of quinoline or, more likely, by dehydrogenation of DHQ), while only 5% of the BzTHQ feed was converted to quinoline and PyTHQ (the PyTHQ was most likely formed by dehydrogenation of DHQ, since only traces of quinoline were formed at low W/F_{BzTHQ_0}). The higher rate of dehydrogenation of DHQ to BzTHQ than to PyTHQ was also observed with DHQ feed

(see Figure 4-26), and is consistent with the thermodynamics of the heterocyclics (see Figure 4-32). These factors account for the higher rates of nitrogen removal from BzTHQ than from PyTHQ. For either quinoline or PyTHQ feed, the same product distribution and percent denitrogenation were observed since the Q/PyTHQ equilibrium was established very rapidly (compare Figures 4-14 and 4-16). This does not necessarily imply, however, that the equilibrium between quinoline and PyTHQ was maintained at longer reaction times (higher W/F_{i_0}).

At 375°C and 7.0 MPa, nitrogen removal from OPA was much easier than from any of the heterocyclics, when each of these compounds was studied individually (see Figure 4-23). The primary reaction pathway for nitrogen removal from OPA involved hydrogenation to PCHA (and then rapid nitrogen removal) rather than direct hydrogenolysis to PB and ammonia, as discussed in the first part of this chapter. Thus hydrogenation of OPA was significantly faster than hydrogenolysis of DHQ, at 375°C and 7.0 MPa.

Only low concentrations of OPA were observed in the HDN products from each of the heterocyclics, as a result of the relatively slow hydrogenolysis of PyTHQ to OPA. However, in light of the high reactivity of OPA in the absence of the heterocyclics, the survival of even low concentrations of OPA at long reaction times is somewhat surprising. For example, in quinoline HDN at 375°C and 7.0 MPa, the concentration of OPA in the organic products increased with

W/F_{Q_0} to over 3 mole % at 667 hr g catalyst/g-mol Q (see Figure 4-14); in OPA HDN at 375°C and 7.0 MPa, nitrogen removal was nearly complete in only half the reaction time, corresponding to 333 hr g catalyst/g-mol OPA (see Figure 4-23). These results suggest that in the presence of sufficient concentrations of the heterocyclics, the active catalytic surface was not as accessible to OPA due to competitive adsorption effects.

The product distributions for quinoline HDN at all reaction conditions studied indicate that nitrogen removal occurred primarily through the DHQ intermediate, since the rate of hydrogenolysis of PyTHQ to OPA was slow relative to the rate of hydrogenation of PyTHQ to DHQ and the rate of hydrogenolysis of DHQ to hydrocarbons and ammonia. This will be even more apparent after the quantitative kinetics are presented later in this chapter. At the lower temperatures (330°C and 375°C), quinoline hydrogenated much more rapidly to PyTHQ than to BzTHQ, and DHQ was formed primarily from the PyTHQ (see Figures 4-13, 4-14, 4-15, 4-17, and 4-18). In contrast, the hydrogenation rates of quinoline to PyTHQ and to BzTHQ were comparable at 420°C, and DHQ was formed to a significant extent from both PyTHQ and BzTHQ (see Figures 4-9 through 4-12). The relatively low concentrations of DHQ observed in the products from quinoline HDN at 420°C are due to thermodynamic, rather than kinetic, limitations on the formation of DHQ from the tetrahydroquinolines (see Figures 4-31 and 4-32).

The major hydrocarbon product from quinoline HDN was always PCH, when significant nitrogen removal was achieved. Thus the presulfided NiMo/Al₂O₃ catalyst exhibited little selectivity for the reaction pathway of minimum hydrogen consumption. At lower temperatures the heteroring in quinoline was selectively hydrogenated, at least initially (forming primarily PyTHQ instead of BzTHQ), but the catalyst did not possess sufficient hydrogenolysis activity to readily convert the PyTHQ to OPA and then to PB and ammonia, so significant saturation of the aromatic ring also occurred.

V. D. Behavior of the Quinoline/Py-Tetrahydroquinoline Product Ratio

In Figure 5-4, the relative amounts of quinoline and PyTHQ in the products from quinoline HDN are shown as a function of W/F_{Q_0} , temperature, and hydrogen pressure (the initial quinoline partial pressure was 13.3 kPa), and are compared with the corresponding equilibrium ratios (indicated by the dashed lines). These equilibrium ratios are essentially the same as the equilibrium ratios shown in Figure 2-5; the latter were calculated from experimentally determined equilibrium constants reported in the literature (Declerck, 1976; Shih et al., 1977; Satterfield et al., 1978). At all temperatures and pressures studied, quinoline

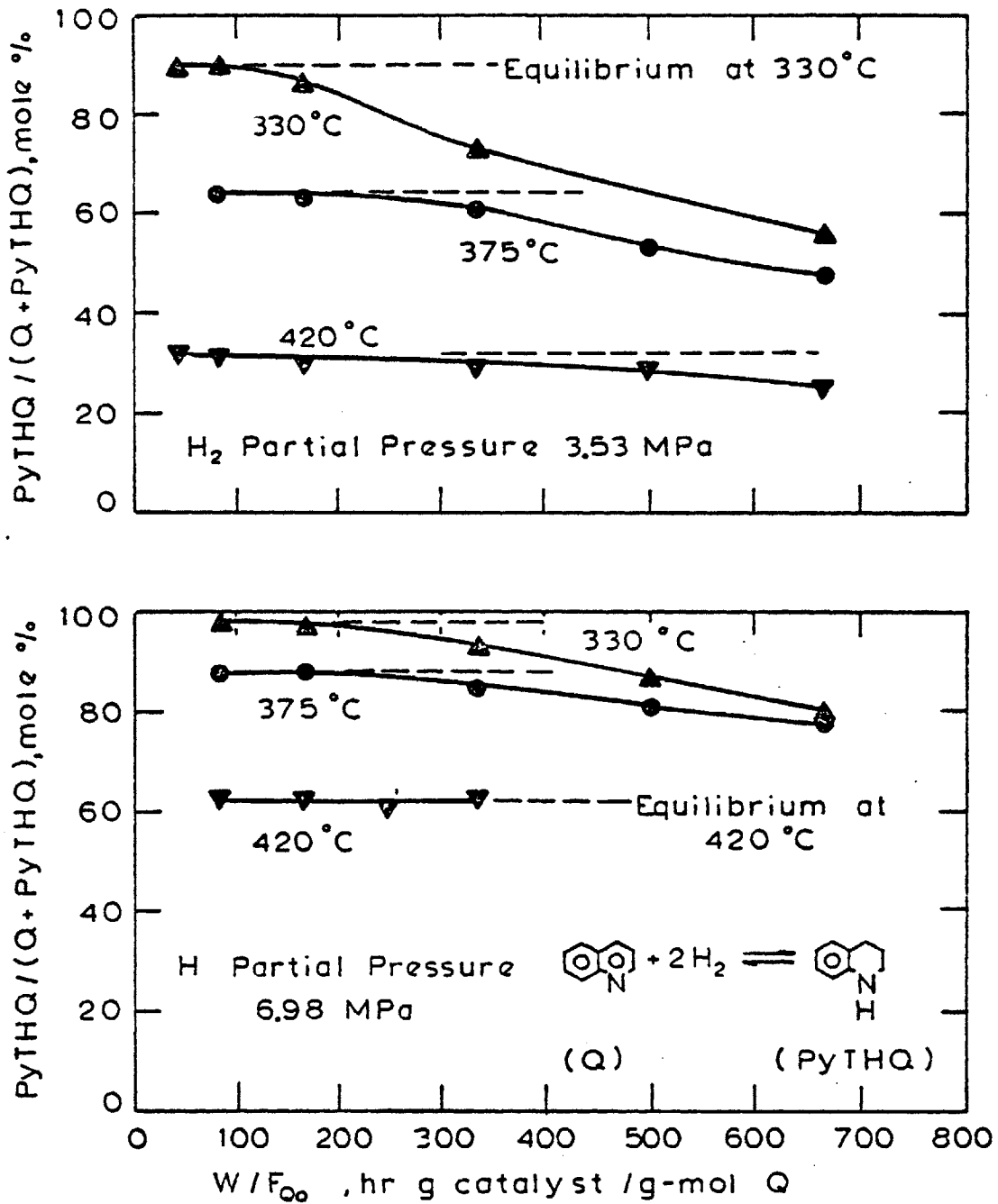


Figure 5-4: Behavior of Q / PyTHQ Product Ratio in Quinoline HDN (13.3 kPa Q)

was rapidly converted to an equilibrium amount of PyTHQ. However, at longer reaction times (higher W/F_{Q_0}) the Q/PyTHQ product ratio departed from equilibrium; i.e. for the amounts of quinoline observed in the products there were less than equilibrium amounts of PyTHQ. This departure from equilibrium was minimal at 420°C, but was more pronounced at 375°C and especially at 330°C (see Figure 5-4).

The product distribution for quinoline HDN at 375°C and 7.0 MPa shows that after the initial rapid equilibration between quinoline and PyTHQ, the concentration of PyTHQ in the products decreased sharply as W/F_{Q_0} increased while the quinoline concentration declined relatively slowly (see Figure 4-14). This behavior can be explained by competitive adsorption effects, if quinoline were more weakly adsorbed than PyTHQ and at least some of its reaction products (such as DHQ or ammonia). Then as the strongly adsorbed PyTHQ was converted to other strongly adsorbed reaction products, quinoline was prevented from adsorbing and reacting on the catalyst until the concentrations of the strongly adsorbed species decreased significantly.

The active sites of the presulfided NiMo/Al₂O₃ catalyst are most likely acidic in nature, and this acidity can be associated with the hydrogenation sites as well as with the hydrogenolysis sites (see the discussion of hydro-treating catalysts in Chapter II). Adsorption of nitrogen compounds is believed to occur through interaction of the

basic nitrogen group with acidic sites on the catalyst, so the more basic nitrogen compounds are likely to be more strongly adsorbed. In quinoline HDN, the PyTHQ and DHQ reaction intermediates are secondary amines, which are much more basic than the aromatic amines (quinoline, BzTHQ, and OPA). Ammonia is more basic than aromatic amines, but is less basic than secondary amines. However, the molecular weight and normal boiling point of ammonia are much lower than those of the organic nitrogen compounds, so basicity alone may not determine the relative adsorptivities of ammonia and the aromatic amines (ammonia is expected to adsorb less strongly than the secondary amines, considering both basicity and molecular weight). Recall the adsorption experiments reported by Sonnemans et al. (1973), in which piperidine (a secondary amine) adsorbed about six times more strongly than pyridine (an aromatic amine) while pyridine adsorbed about four times more strongly than ammonia, on a prerduced Mo/Al₂O₃ catalyst. Thus it is likely that PyTHQ and DHQ are the most strongly adsorbed species in quinoline HDN. This can explain some of the unusual observations related to the departure from equilibrium of the Q/PyTHQ product ratio at longer reaction times (more on this below), and can also account for the apparent low reactivity of OPA in the presence of significant concentrations of PyTHQ and DHQ.

The more dramatic departure from Q/PyTHQ equilibrium at lower temperatures agrees well with the observed "homogeneous" hydrogenation of quinoline to PyTHQ (in the absence of the NiMo/Al₂O₃ catalyst). The catalytic reactions, influenced by competitive adsorption effects, tended to "pull" the Q/PyTHQ product ratio away from equilibrium by converting PyTHQ to other intermediates (primarily DHQ) faster than quinoline could be converted to PyTHQ. "Homogeneous" hydrogenation of quinoline to PyTHQ, on the other hand, tended to restore Q/PyTHQ equilibrium. For a quinoline feed rate corresponding to 667 hr g catalyst/g-mol Q, "homogeneous" reaction resulted in about a 40%, 60%, and 80% approach to Q/PyTHQ equilibrium at 330°C, 375°C, and 420°C, respectively (see Table 4-1). Thus at 420°C, the "homogeneous" reaction rate was high enough to maintain Q/PyTHQ equilibrium at longer reaction times (higher W/F_{Q_0}). At lower temperatures, however, the "homogeneous" reaction was less significant relative to the catalytic reactions, so the Q/PyTHQ equilibrium was not maintained at higher W/F_{Q_0} . Additional support for this hypothesis is the fact that, at the same reaction conditions, the departure from Q/PyTHQ equilibrium was much less severe with "lined-out" catalyst than with the same catalyst before it had fully deactivated (compare the data for runs 17 and 23 in the Appendix).

For quinoline HDN at 330°C and 3.55 MPa, not only was there a departure from Q/PyTHQ equilibrium as W/F_{Q_0} increased, but it also appears that there was significant net conversion of PyTHQ to quinoline, though the thermodynamic driving force was seemingly in the opposite direction (see Figure 4-17). The same results were observed starting with either quinoline or PyTHQ feed at these reaction conditions (compare Figures 4-17 and 4-19). This behavior cannot be accounted for by the factors discussed above, nor can a complete explanation be offered at this time. However, many potential explanations based upon experimental artifacts or disguises can be eliminated. For example, one might postulate that "homogeneous" reaction occurred after the reactor, thus affecting the relative quantities of quinoline and PyTHQ in the products. But temperatures downstream from the reactor were always below the reactor temperature, and lower temperatures shift the Q/PyTHQ equilibrium toward PyTHQ - the wrong direction to account for the experimental results. It might be argued that there were heat or mass transfer limitations in the reactor at the lower feed rates (higher W/F_{i_0}), but this is not consistent with the fact that the same results were obtained starting with either quinoline or PyTHQ feed. Channeling of the reaction gas down the reactor wall at lower feed rates can be proposed, but this too is inconsistent with the fact that either quinoline or PyTHQ

feed gave the same results. One might also suspect that these strange results are a reflection of unsteady-state, rather than steady-state product distributions. However, at each set of reaction conditions the system was allowed to equilibrate for over one hour, and then a set of at least four samples was taken during an additional period of one to two hours. In each set of samples, no trend was ever observed, indicating that a steady state had been reached. Also, it is most unlikely that the identical results observed with either quinoline or PyTHQ feed correspond to identical unsteady states. In several of the earlier experimental runs, the system was started up at the lowest feed rate to be studied, rather than at the highest feed rate, and was allowed to equilibrate overnight before sampling. Samples taken at the lowest feed rate still contained a higher ratio of quinoline to PyTHQ than the corresponding equilibrium ratio. Furthermore, the departure from Q/PyTHQ equilibrium at higher W/F_{Q_0} was observed in these earlier runs, during which feed rates were increased (see data for runs 12 and 14 in the Appendix), as well as in the later runs where data were collected in the opposite sequence, by decreasing the feed rates. Thus the departure from equilibrium was not due to "hysteresis" effects.

The ability of PyTHQ to transfer hydrogen quite readily through dehydrogenation to quinoline is well known, and accounts for the current interest in PyTHQ as a potential donor-solvent for coal liquefaction (Brucker and Kolling, 1965). In the present study, the apparent net conversion of PyTHQ to quinoline at reaction conditions where PyTHQ was thermodynamically favored might be explained by postulating a hydrogen-transfer reaction between PyTHQ and an unsaturated hydrocarbon, forming quinoline and a saturated hydrocarbon. However, for quinoline HDN at 330°C and 3.55 MPa where this behavior was most pronounced, the product distributions indicate that more hydrogen was "transferred" from PyTHQ than can be accounted for in the other products (see Figure 4-17 and the data for run 25 in the Appendix).

Finally, if "homogeneous" reaction occurred in the preheater before the reactor, formation (in the preheater) of PyTHQ from the quinoline feed likely increased as feed rate decreased. This could have resulted in increased competitive adsorption between quinoline and PyTHQ at the reactor inlet, as W/F_{Q_0} increased, accounting for the observed increases in quinoline concentration in the reaction products at higher W/F_{Q_0} . Unfortunately, this proposal also breaks down when tested against the fact that the same results were obtained starting with either quinoline or PyTHQ feed.

The rates of each of the irreversible reactions in the above network can be determined directly from the experimental data, since the reaction network was effectively "segmented" by studying each of the organic nitrogen compounds (particularly OPA) individually. Thus it is not necessary to resort to a computer simulation of the entire network to obtain values of the kinetic parameters which may fit the experimental data mathematically but not necessarily physically.

Consideration of the adsorption phenomena in quinoline HDN suggests that the catalytic reaction rates might best be described by Langmuir-Hinshelwood kinetic expressions, allowing for strong competitive adsorption of the nitrogen compounds on active catalyst sites. There is evidence that hydrogen and the nitrogen compounds adsorb on different, perhaps neighboring, sites, while adsorption of the hydrocarbons can safely be neglected (recall the discussion of adsorption phenomena in Chapter II). Assuming that the Langmuir adsorption isotherm is a reasonable approximation for the actual adsorption behavior, then the fraction of available catalytic sites occupied by each of the nitrogen compounds is given by the following expression:

$$\theta_j = \frac{K_j P_j}{1 + \sum_j K_j P_j} \quad (\text{eq. 5-6})$$

where θ_j = fraction of available sites occupied by j
 K_j = adsorption equilibrium constant of j, Pa⁻¹
 (or atm⁻¹)

Only the nitrogen compounds are included in the summation, since hydrogen is assumed to adsorb on different sites. The rate of each reaction is assumed to be proportional to the fractional surface coverage of the appropriate nitrogen compound, consistent with the stoichiometry in the quinoline HDN network.

If the catalyst surface is completely saturated with nitrogen compounds (all available sites occupied), then $\sum_j \theta_j = 1$ and $\sum_j K_j P_j \gg 1$. Sonnemans et al. (1973) reported studies of the adsorption of pyridine and ammonia on pre-reduced Mo/Al₂O₃ and CoMo/Al₂O₃ catalysts. Maximum surface coverage was observed for nitrogen compound partial pressures of only 1 kPa, even at the high temperatures (e.g. 400°C) relevant to HDN. In the present study, total nitrogen compound partial pressures were 13.3 kPa or 26.7 kPa, so it is likely that the catalyst surface was always saturated with nitrogen compounds. Thus it is reasonable to neglect the "1" in the denominator of equation 5-6.

V. E. 1. Kinetics of o-Propylaniline HDN

Only hydrocarbons and ammonia were formed from reaction of OPA, so the appropriate Langmuir-Hinshelwood rate expression is:

$$-r_{\text{OPA}} = r_{\text{HC}} = r_{\text{NH}_3} = \frac{k_1' K_{\text{OPA}} P_{\text{OPA}}}{1 + K_{\text{OPA}} P_{\text{OPA}} + K_{\text{NH}_3} P_{\text{NH}_3}}$$

where k_1' = pseudo rate constant for nitrogen removal from OPA, g-mol OPA/hr g catalyst

Here, k_1' varies with both the temperature and the hydrogen pressure, so it is termed a pseudo rate constant. Assuming that $K_{\text{OPA}} P_{\text{OPA}} + K_{\text{NH}_3} P_{\text{NH}_3} \gg 1$, the rate expression can be simplified:

$$-r_{\text{OPA}} = \frac{k_1' K_{\text{OPA}} P_{\text{OPA}}}{K_{\text{OPA}} P_{\text{OPA}} + K_{\text{NH}_3} P_{\text{NH}_3}} = \frac{k_1' P_{\text{OPA}}}{P_{\text{OPA}} + (K_{\text{NH}_3}/K_{\text{OPA}}) P_{\text{NH}_3}}$$

Since there was negligible change in total numbers of moles upon reaction, $P_{\text{OPA}} + P_{\text{NH}_3} = P_{\text{OPA}_0}$ and :

$$-r_{\text{OPA}} = \frac{k_1' P_{\text{OPA}}}{P_{\text{OPA}} + (K_{\text{NH}_3}/K_{\text{OPA}}) (P_{\text{OPA}_0} - P_{\text{OPA}})} \quad (\text{eq. 5-7})$$

Note that if $K_{\text{NH}_3}/K_{\text{OPA}} = 1$ (equal adsorption strengths of the nitrogen compounds), a pseudo first order rate expression results:

$$-r_{\text{OPA}} = \frac{k_1' P_{\text{OPA}}}{P_{\text{OPA}_0}}$$

If $K_{\text{NH}_3}/K_{\text{OPA}} = 0$ (negligible adsorption of ammonia), the Langmuir-Hinshelwood expression reduces to a zero order rate:

$$-r_{\text{OPA}} = k_1'$$

The more general rate expression (equation 5-7) can be substituted into the plug-flow reactor material balance equation (see equation 5-5) and integrated:

$$\frac{W}{F_{\text{OPA}_0}} = \frac{1}{P_{\text{OPA}_0}} \int_{P_{\text{OPA}_0}}^{P_{\text{OPA}}} \frac{dP_{\text{OPA}}}{r_{\text{OPA}}} =$$

$$- \frac{1}{P_{\text{OPA}_0}} \int_{P_{\text{OPA}_0}}^{P_{\text{OPA}}} \frac{P_{\text{OPA}} + (K_{\text{NH}_3}/K_{\text{OPA}}) (P_{\text{OPA}_0} - P_{\text{OPA}})}{k_1' P_{\text{OPA}}} dP_{\text{OPA}}$$

$$k_1' \left(\frac{W}{F_{\text{OPA}_0}} \right) = \left(1 - \frac{K_{\text{NH}_3}}{K_{\text{OPA}}} \right) \left(\frac{P_{\text{OPA}_0} - P_{\text{OPA}}}{P_{\text{OPA}_0}} \right) - \left(\frac{K_{\text{NH}_3}}{K_{\text{OPA}}} \right) \ln \left(\frac{P_{\text{OPA}}}{P_{\text{OPA}_0}} \right)$$

or,

$$k_1' \left(\frac{W}{F_{\text{OPA}_0}} \right) = \left(1 - \frac{K_{\text{NH}_3}}{K_{\text{OPA}}} \right) X_{\text{OPA}} - \left(\frac{K_{\text{NH}_3}}{K_{\text{OPA}}} \right) \ln(1 - X_{\text{OPA}}) \quad (\text{eq. 5-8})$$

where X_{OPA} is the fractional conversion (disappearance) of the OPA reactant, and is equal to the fractional (as opposed to percent) denitrogenation of OPA. This equation can be tested against the experimental data by plotting the right hand side as a function of W/F_{OPA_0} , at constant temperature and hydrogen pressure. The "best" value of the adjustable parameter $K_{\text{NH}_3}/K_{\text{OPA}}$ should result in a linear correlation, with the line passing through the origin. The pseudo rate constant can then be determined from the slope of this line.

For $K_{\text{NH}_3}/K_{\text{OPA}} = 0$ (zero order kinetics), a plot of X_{OPA} (or percent denitrogenation) versus W/F_{OPA_0} should be linear (see equation 5-8). However, the actual percent denitrogenation versus W/F_{OPA_0} curves for OPA HDN are all concave downward (see Figures 4-21 and 4-22), so zero order kinetics does not fit the experimental data. Pseudo first order kinetics ($K_{\text{NH}_3}/K_{\text{OPA}} = 1$) fits the data adequately for OPA conversions below about 80%, but not at higher conversions. This is illustrated in the top portion of Figure 5-5 for the OPA HDN data obtained at 375°C and 7.0 MPa. For OPA conversions greater than about 80%, the pseudo first order model predicts lower conversions than were actually observed, suggesting that the product ammonia inhibited the denitrogenation rate less than the OPA reactant did

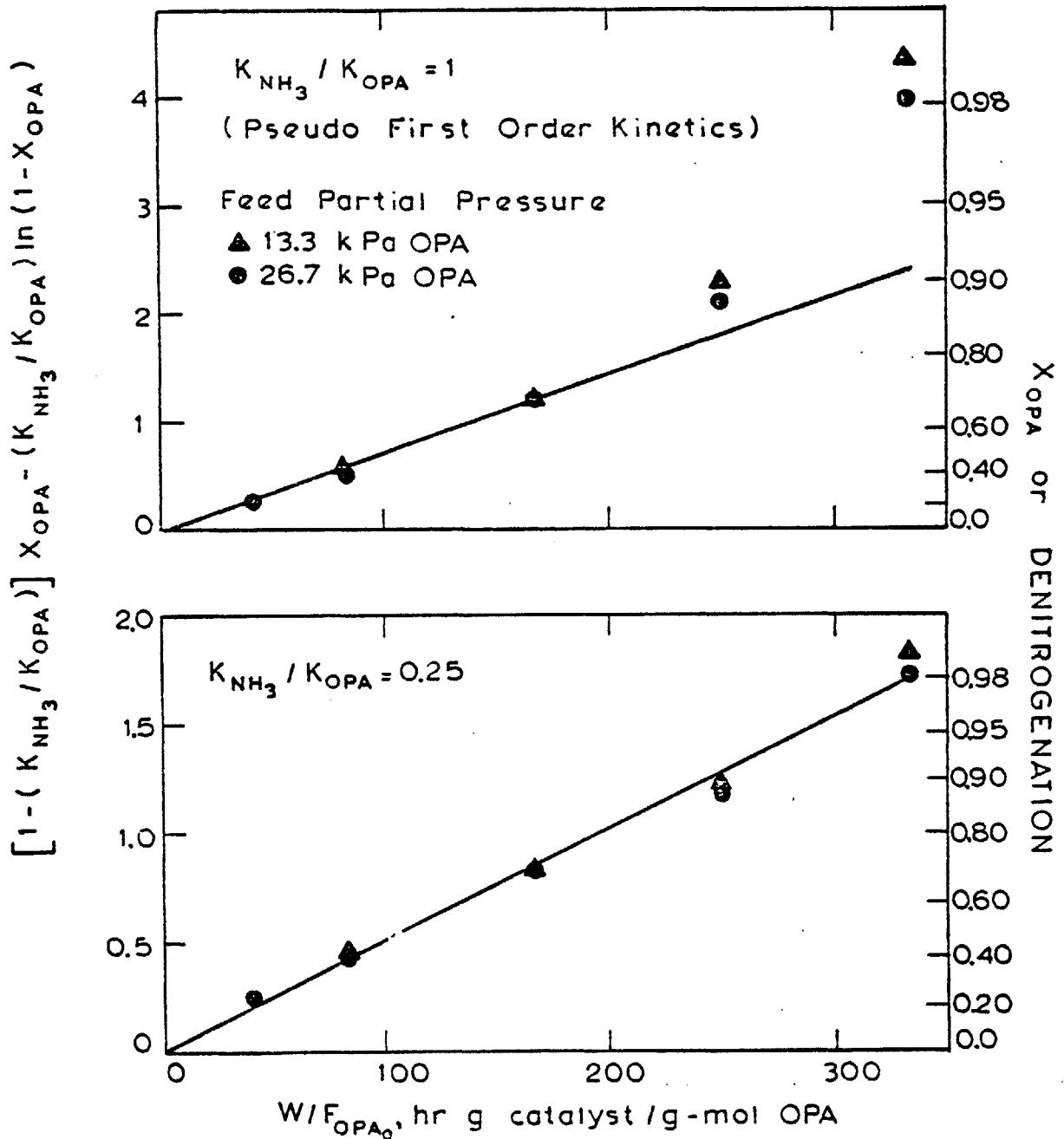


Figure 5-5: Comparison of Langmuir-Hinshelwood Kinetic Models for o-Propylaniline Denitrogenation at 375°C and 7.0 MPa

($K_{\text{NH}_3}/K_{\text{OPA}} < 1$). Various values of $K_{\text{NH}_3}/K_{\text{OPA}}$ were evaluated by a least-squares fitting technique, and the "best" value for correlating all of the OPA HDN data is 0.25, implying that OPA adsorbed about four times as strongly as ammonia on the active sites. The lower portion of Figure 5-5 illustrates the good correlation of the experimental data by Langmuir-Hinshelwood kinetic model, for $K_{\text{NH}_3}/K_{\text{OPA}} = 0.25$. Note that this model correctly predicts that the initial partial pressure of OPA should have no effect on the percent denitrogenation versus W/F_{OPA_0} curve at a given temperature and hydrogen pressure (see equation 5-8 and Figure 4-21).

Figure 5-6 shows the effects of temperature and hydrogen pressure on the pseudo rate constant for conversion of OPA to hydrocarbons and ammonia. The pseudo rate constant increases with both temperature and hydrogen pressure. The Arrhenius plot of the pseudo rate constant values at 7.0 MPa is linear, and the slope gives an activation energy of 79 kJ/g-mol (19 kcal/g-mol) for denitrogenation of OPA. This activation energy is somewhat lower than the value of 100 kJ/g-mol (24 kcal/g-mol) reported by Shih et al. (1977), but the latter was determined from computer simulation of the quinoline HDN kinetics (using a first order kinetic model) rather than from separate study of OPA. If the hydrogen pressure dependence of the OPA denitrogenation rate is approximated by simple power-law kinetics, then

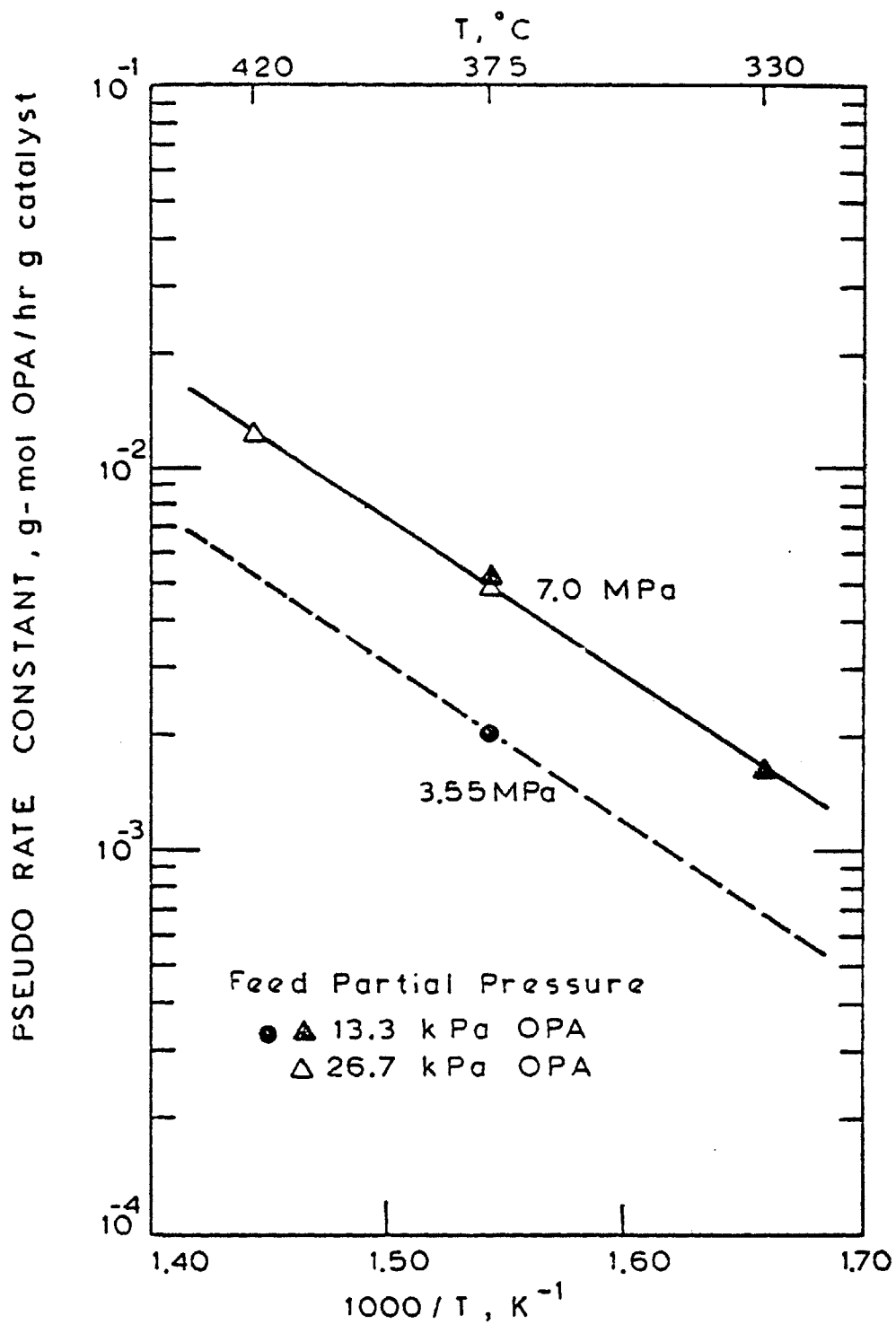


Figure 5-6: Arrhenius Plot of the Pseudo Rate Constant for o-Propylaniline Denitrogenation

$$k_1' = k_1 P_{H_2}^{n_1}$$

where k_1 is the temperature dependent rate constant and n_1 is the reaction order in hydrogen. Comparison of the pseudo rate constants at 375°C but at the different hydrogen pressures gives $n_1 = 1.3$ (see Figure 5-6).

V. E. 2. Kinetics of the Hydrogenolysis Reactions in Quinoline HDN

Knowledge of the OPA denitrogenation kinetics permits relatively easy determination of the kinetics of both PyTHQ hydrogenolysis (to OPA) and DHQ hydrogenolysis (to hydrocarbons and ammonia) from the quinoline HDN data. The previous rate expression for OPA denitrogenation must, of course, be modified to allow for competitive adsorption of the heterocyclics as well as OPA and ammonia. The secondary amines PyTHQ and DHQ are assumed to adsorb equally strongly, with an adsorption equilibrium constant K_{SA} . Equal adsorptivities of the aromatic amines (Q, BzTHQ, and OPA) are likewise assumed, characterized by the adsorption equilibrium constant K_{AA} . This greatly simplifies the kinetic model, but still allows for different adsorptivities of nitrogen compounds with significantly different properties. With these modifications and the previously

justified assumption that $\sum_j K_j P_j \gg 1$, the rate expression for OPA denitrogenation becomes:

$$r_1 = \frac{k_1' K_{AA} P_{OPA}}{K_{AA} P_{AA} + K_{SA} P_{SA} + K_{NH_3} P_{NH_3}} = \frac{k_1' Y_{OPA}}{Y_{AA} + (K_{SA}/K_{AA}) Y_{SA} + (K_{NH_3}/K_{AA}) Y_{NH_3}}$$

where r_1 = rate of reaction of OPA to hydrocarbons and ammonia, g-mol OPA/hr g catalyst

$$P_{AA} = P_Q + P_{BzTHQ} + P_{OPA}$$

$$P_{SA} = P_{PyTHQ} + P_{DHQ}$$

$$Y_{AA} = Y_Q + Y_{BzTHQ} + Y_{OPA}$$

$$Y_{SA} = Y_{PyTHQ} + Y_{DHQ}$$

Similarly, the rate expressions for hydrogenolysis of PyTHQ and for hydrogenolysis of DHQ are:

$$r_2 = \frac{k_2' K_{SA} P_{PyTHQ}}{K_{AA} P_{AA} + K_{SA} P_{SA} + K_{NH_3} P_{NH_3}} = \frac{k_2' (K_{SA}/K_{AA}) Y_{PyTHQ}}{Y_{AA} + (K_{SA}/K_{AA}) Y_{SA} + (K_{NH_3}/K_{AA}) Y_{NH_3}}$$

$$r_3 = \frac{k_3' K_{SA} P_{DHQ}}{K_{AA} P_{AA} + K_{SA} P_{SA} + K_{NH_3} P_{NH_3}} = \frac{k_3' (K_{SA}/K_{AA}) Y_{DHQ}}{Y_{AA} + (K_{SA}/K_{AA}) Y_{SA} + (K_{NH_3}/K_{AA}) Y_{NH_3}}$$

where r_2 = rate of hydrogenolysis of PyTHQ to OPA, g-mol PyTHQ/hr g catalyst

k_2' = pseudo rate constant for hydrogenolysis of PyTHQ to OPA, g-mol PyTHQ/hr g catalyst

r_3 = rate of hydrogenolysis of DHQ to hydrocarbons and ammonia, g-mol DHQ/hr g catalyst

k_3' = pseudo rate constant for hydrogenolysis of DHQ to hydrocarbons and ammonia, g-mol DHQ/hr g catalyst

In quinoline HDN, OPA is formed by hydrogenolysis of PyTHQ but is at the same time converted to hydrocarbons and ammonia, so the net rate of formation of OPA is given by:

$$r_{\text{OPA}} = \frac{dY_{\text{OPA}}}{d(W/F_{Q_0})} = r_2 - r_1 = \frac{k_2'(K_{\text{SA}}/K_{\text{AA}})Y_{\text{PyTHQ}} - k_1'Y_{\text{OPA}}}{D}$$

where $D = Y_{\text{AA}} + (K_{\text{SA}}/K_{\text{AA}})Y_{\text{SA}} + (K_{\text{NH}_3}/K_{\text{AA}})Y_{\text{NH}_3}$

and use has been made of equation 5-2. The above equation can be integrated at constant temperature and hydrogen pressure, and solved for k_2' :

$$k_2' = \frac{Y_{\text{OPA}} + k_1' \int_0^{W/F_{Q_0}} \left(\frac{Y_{\text{OPA}}}{D} \right) d(W/F_{Q_0})}{(K_{\text{SA}}/K_{\text{AA}}) \int_0^{W/F_{Q_0}} \left(\frac{Y_{\text{PyTHQ}}}{D} \right) d(W/F_{Q_0})} \quad (\text{eq. 5-9})$$

An expression for k_3' can be derived in a similar fashion, recognizing that in quinoline HDN, hydrocarbons and ammonia are formed from both OPA and DHQ:

$$r_{HC} = r_{NH_3} = \frac{dY_{HC}}{d(W/F_{Q_0})} = r_1 + r_3 = \frac{k_1' Y_{OPA} + k_3' (K_{SA}/K_{AA}) Y_{DHQ}}{D}$$

$$k_3' = \frac{Y_{HC} - k_1' \int_0^{W/F_{Q_0}} \left(\frac{Y_{OPA}}{D} \right) d(W/F_{Q_0})}{(K_{SA}/K_{AA}) \int_0^{W/F_{Q_0}} \left(\frac{Y_{DHQ}}{D} \right) d(W/F_{Q_0})} \quad (\text{eq. 5-10})$$

A value of 0.25 is used for K_{NH_3}/K_{AA} , since this value gives the best correlation of the OPA HDN data, and OPA and the other aromatic amines are assumed to have equal adsorptivities. Numerical values for k_1' are available from the OPA studies; the k_1' value at 375°C and 3.5 MPa hydrogen pressure can be extrapolated to 330°C and 420°C using the activation energy derived from the 7.0 MPa values (see Figure 5-6). The quinoline HDN product distributions at the various temperatures and pressures studied provide Y_j versus W/F_{Q_0} data (recognize that $Y_{NH_3} = Y_{HC}$), so equations 5-9 and 5-10 can be integrated numerically for assumed values of K_{SA}/K_{AA} . Quality of fit can be assessed from the degree of linearity of the Arrhenius plots, and by checking the calculated k_2' and k_3' values

for constancy as the integrations are carried out to higher W/F_{Q_0} . Additional details of the numerical techniques are given by Marshall (1980). Pseudo first order kinetics, corresponding to equal adsorptivities of all the nitrogen compounds ($K_{NH_3}/K_{AA} = 1$, $K_{SA}/K_{AA} = 1$), result in very poor correlation of the experimental data. This is not surprising in view of the experimental evidence for preferential adsorption of some of the nitrogen compounds. A K_{SA}/K_{AA} value of 6 (with $K_{NH_3}/K_{AA} = 0.25$) gives the "best" correlation of the data. This result implies that the secondary amines (PyTHQ and DHQ) were much more strongly adsorbed than the other nitrogen compounds, at least on those catalyst sites active for hydrogenolysis and for denitrogenation of OPA. Since significant hydrogenation accompanied nitrogen removal from OPA, it is likely that these relative adsorptivities apply to the hydrogenation sites as well. The kinetic modelling results for the relative adsorptivities are thus consistent with the qualitative expectations discussed earlier.

Though derived for quinoline feed, equations 5-9 and 5-10 can also be used to determine the pseudo rate constants for the hydrogenolysis reactions from the HDN data for PyTHQ, BzTHQ, or DHQ feed. Arrhenius plots of the pseudo rate constants for the hydrogenolysis reactions are shown in Figures 5-7 and 5-8. Pseudo rate constants derived from the PyTHQ HDN data are nearly identical to those derived from the quinoline HDN data, so they are not

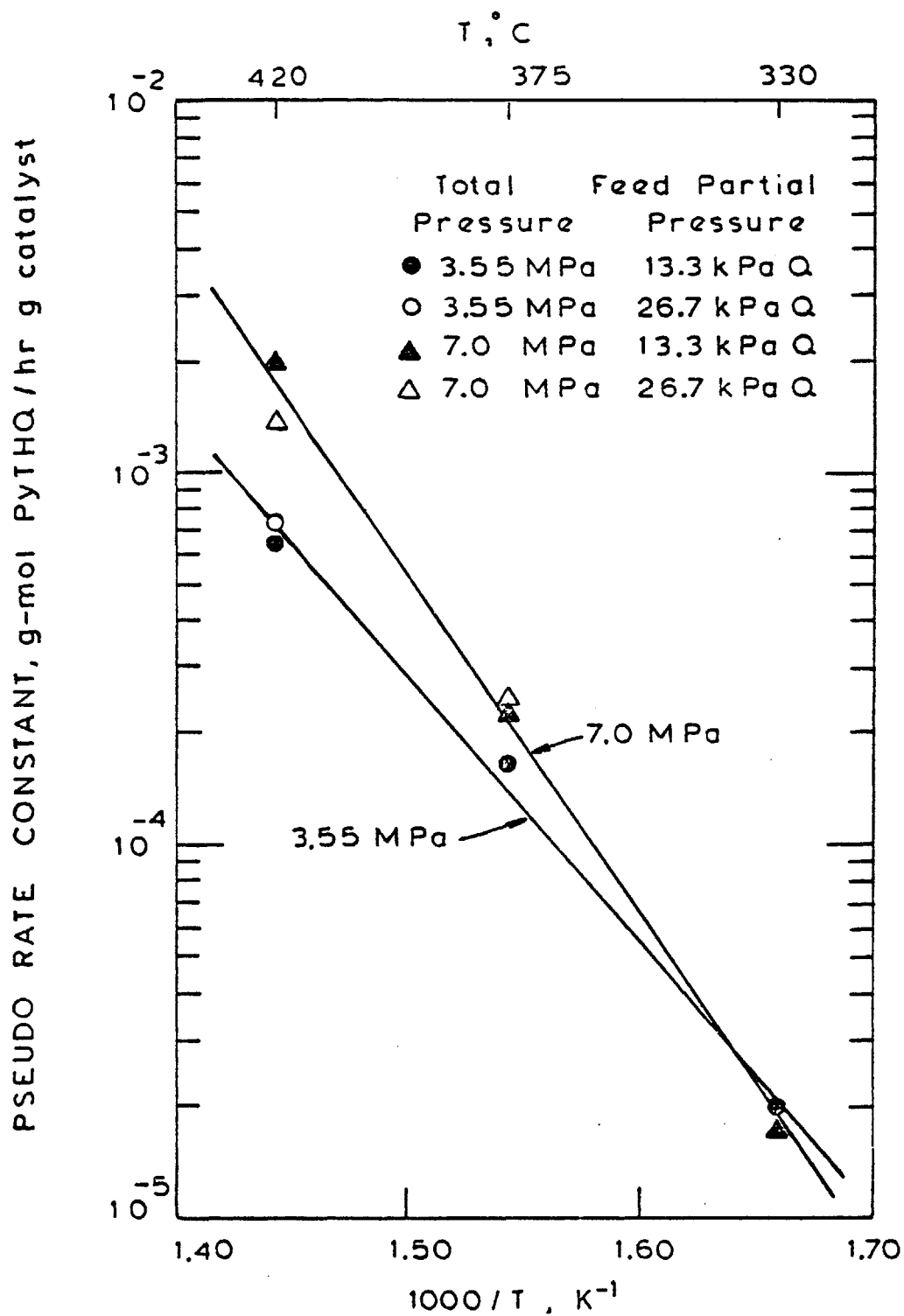


Figure 5-7: Arrhenius Plot of the Pseudo Rate Constant for Hydrogenolysis of Py-Tetrahydroquinoline to o-Propylaniline

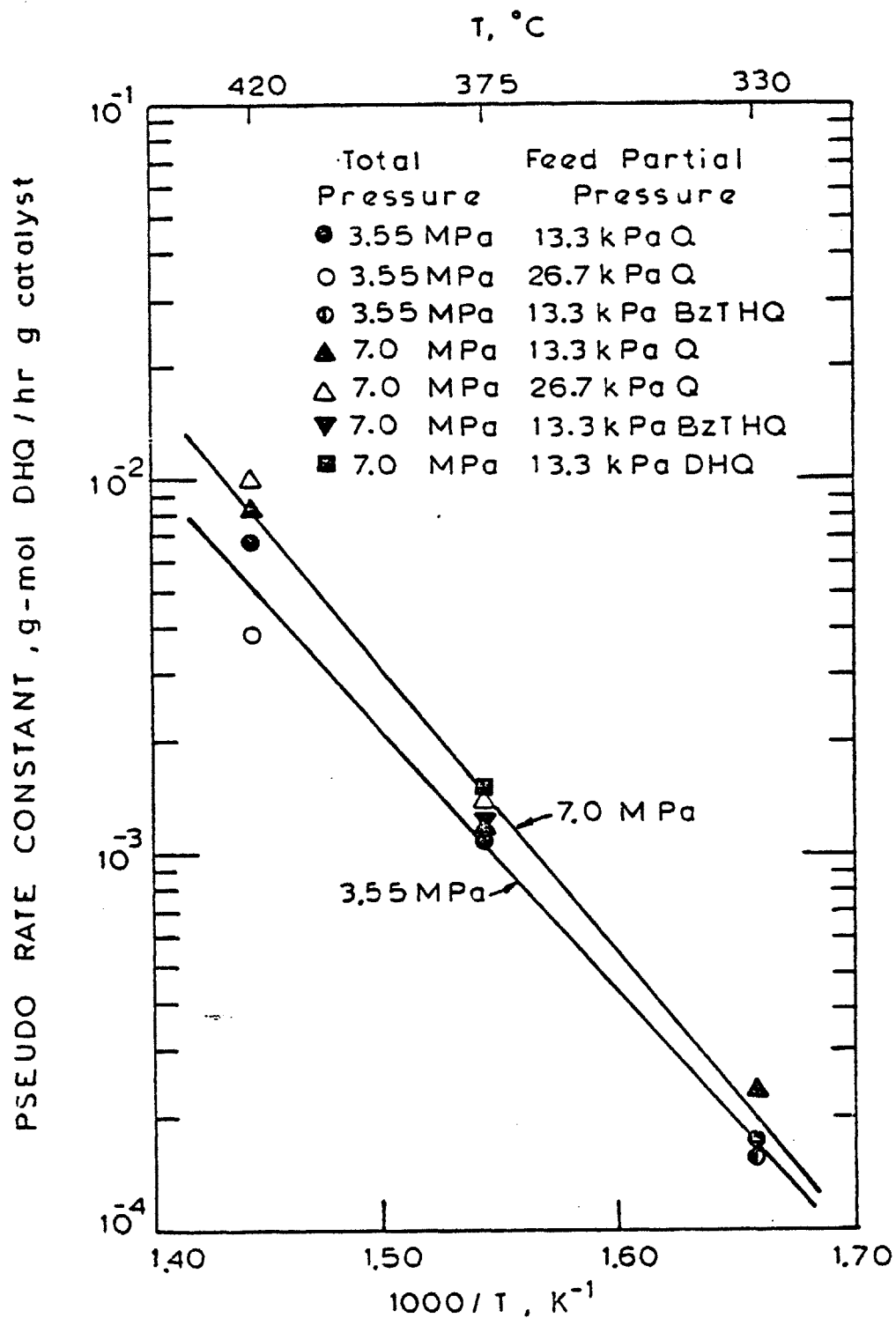


Figure 5-8: Arrhenius Plot of the Pseudo Rate Constant for Hydrogenolysis of Decahydroquinoline to Hydrocarbons and Ammonia

included in these Figures (recall that the same HDN product distributions were obtained starting with either quinoline or PyTHQ, at the same reaction conditions). In the experiments with BzTHQ or DHQ feed, low concentrations of PyTHQ and only traces of OPA were formed, so the pseudo rate constant for hydrogenolysis of PyTHQ to OPA could not be quantified from these data. Note, however, that the same pseudo rate constants for hydrogenolysis of DHQ are derived from the HDN data, independent of the starting heterocyclic nitrogen compound (see Figure 5-8). This result further demonstrates the adequacy of the kinetic model.

Comparison of Figures 5-7 and 5-8 reveals that the pseudo rate constants for hydrogenolysis of DHQ are about an order of magnitude larger than those for hydrogenolysis of PyTHQ. The activation energies of the two reactions are comparable - an average of 155 kJ/g-mol (37 kcal/g-mol) for hydrogenolysis of PyTHQ, and about 138 kJ/g-mol (33 kcal/g-mol) for hydrogenolysis of DHQ. These activation energies agree surprisingly well with the corresponding values of 147 kJ/g-mol (35 kcal/g-mol) and 130 kJ/g-mol (31 kcal/g-mol) reported by Shih et al. (1977), and are in sharp contrast to the 79 kJ/g-mol (19 kcal/g-mol) activation energy for OPA denitrogenation. Shih et al. (1977) reported activation energies of about 84 kJ/g-mol (20 kcal/g-mol) for the hydrogenation reactions in quinoline HDN. Thus the much lower activation energy for OPA denitrogenation than for the

hydrogenolysis reactions is consistent with the conclusion here, that the rate of nitrogen removal from OPA was determined primarily by the rate of hydrogenation of OPA (to PCHA). The pseudo rate constants for OPA denitrogenation are significantly higher than those for hydrogenolysis of DHQ at temperatures below 420°C (compare Figures 5-6 and 5-8). This simply reflects the relatively high intrinsic reactivity of OPA, clearly demonstrated in this study (see Figure 4-23). However, in the presence of significant concentrations of the heterocyclics (particularly PyTHQ and DHQ), the reactivity of OPA was greatly reduced as a result of strong competitive adsorption effects.

Note that the Langmuir-Hinshelwood rate expressions used for kinetic modelling contain only ratios of adsorption equilibrium constants for the various nitrogen compounds. The use of constant relative adsorptivities, independent of temperature, is accompanied by the implicit assumption of equal heats of adsorption for all of the nitrogen compounds. This assumption is not unreasonable, and is supported by adsorption measurements (Sonnemans et al., 1973). Thus the temperature dependencies of the reaction rates are determined solely by the temperature dependencies of the corresponding pseudo rate constants. From Figures 5-7 and 5-8, it is apparent that somewhat different activation energies are obtained at 3.55 MPa and 7.0 MPa, particularly for hydrogenolysis of PyTHQ. Thus

the temperature and hydrogen pressure dependencies of the pseudo rate constants for the hydrogenolysis reactions are to some extent interrelated. Simple power-law kinetics cannot adequately describe the hydrogen pressure dependencies, since the reaction order in hydrogen then varies with temperature. For example, hydrogenolysis of PyTHQ appears to be about zero order in hydrogen at 330°C, but at 420°C the apparent order in hydrogen is greater than one (see Figure 5-7). A less dramatic increase in the apparent order in hydrogen with increased temperature is observed for hydrogenolysis of DHQ (see Figure 5-8). This behavior is not surprising, since adsorbed hydrogen was most likely involved in the catalytic reactions. Assuming that hydrogen and the nitrogen compounds adsorb on different types of catalyst sites, then:

$$\theta_{H_2} = \frac{K_{H_2} P_{H_2}}{1 + K_{H_2} P_{H_2}} \quad (\text{molecular adsorption of } H_2)$$

or,

$$\theta_H = \frac{(K_H P_{H_2})^{1/2}}{1 + (K_H P_{H_2})^{1/2}} \quad (\text{dissociative adsorption of } H_2)$$

For either type of hydrogen adsorption, the apparent reaction order in hydrogen will vary with temperature if both terms in the denominators of the above expressions are significant. In addition, the fraction of sites

occupied by hydrogen decreases less with temperature at higher hydrogen pressures (assuming, of course, exothermic adsorption of hydrogen). This can account for the increase in apparent reaction order in hydrogen with increased temperature.

The above discussion suggests that the activation energies derived from the pseudo rate constants are influenced by the effect of temperature on hydrogen adsorption. However, it is likely that this is a relatively minor effect compared to the effect of temperature on the rate-controlling surface processes, characterized by the so-called "true" activation energies. The apparent activation energies derived in this study should then be close to the true activation energies. Finally, comparison of the pseudo rate constants at 375°C for the two hydrogen pressures reveals a much stronger effect of hydrogen pressure on the rate of nitrogen removal from OPA than on the rates of the hydrogenolysis reactions, which is not surprising (see Figures 5-6, 5-7, and 5-8).

VI. Conclusions

VI. A. Catalyst Activity

The HDN activity of virgin (but sulfided) NiMo/Al₂O₃ catalyst is substantially higher than the "steady-state" level of activity attained after several hundred hours of catalyst use. This deactivation is due primarily to carbon deposition (coking). During deactivation, there is a much greater loss in hydrogenolysis activity than in hydrogenation activity, suggesting that these functionalities are associated with different catalyst sites.

VI. B. Hydrodenitrogenation of o-Propylaniline

Direct hydrogenolysis of OPA to PB and ammonia is slow relative to hydrogenation of the aromatic ring and denitrogenation of the resulting aliphatic amine (PCHA). The rate of conversion of OPA to hydrocarbons and ammonia can be described by a Langmuir-Hinshelwood kinetic model, with an OPA adsorption strength about four times that of ammonia. Denitrogenation of OPA is much easier than denitrogenation of any of the heterocyclics, when the compounds are studied individually. The presence of significant concentrations of the heterocyclics, particularly PyTHQ and DHQ, greatly inhibits the OPA denitrogenation rate, due to competitive adsorption effects.

VI. C. Hydrodenitrogenation of Quinoline

The initial ring saturation reactions of quinoline are all reversible over a wide range of HDN conditions. Saturation of the aromatic ring is thermodynamically (but not necessarily kinetically) more favorable than saturation of the heteroring. In general, these reactions are subject to complex interactions between kinetics and thermodynamics.

Denitrogenation of quinoline occurs primarily through the DHQ intermediate, and PCH is the major hydrocarbon product. The commercial NiMo/Al₂O₃ hydrotreating catalyst (in sulfide form) exhibits little selectivity for the HDN reaction pathway of minimum hydrogen consumption. At lower temperatures the heteroring in quinoline is selectively hydrogenated, initially, but the catalyst does not possess sufficient hydrogenolysis activity to remove the nitrogen without extensive saturation of the aromatic ring.

Quinoline HDN is influenced by strong competitive adsorption of the nitrogen compounds, which vary significantly in adsorptivity. A Langmuir-Hinshelwood kinetic model has been developed for the hydrogenolysis and nitrogen removal reactions, and the HDN data are well-correlated only if the different adsorptivities of the nitrogen compounds are considered. On both the hydrogenation and the hydrogenolysis catalyst sites, the

secondary amines PyTHQ and DHQ appear to adsorb about six times as strongly as the aromatic amines (quinoline, BzTHQ, and OPA), which in turn show an adsorption strength approximately four times greater than that of ammonia.

VII. Appendix

VII. A. Physical Properties of Some Relevant Compounds

<u>Compound</u>	<u>Formula</u>	<u>Molecular Weight</u>	<u>Melting Point (°C)</u>	<u>Boiling Point (°C)</u>	<u>Density (g/cc)</u>
quinoline	C ₉ H ₇ N	129.16	-16	238	1.0929
Py-tetrahydroquinoline	C ₉ H ₁₁ N	133.19	20	251	1.0588
Bz-tetrahydroquinoline	C ₉ H ₁₁ N	133.19	...	222	1.0304
cis-decahydroquinoline	C ₉ H ₁₇ N	139.24	-40	*205	0.8426
trans(dl)- decahydroquinoline	C ₉ H ₁₇ N	139.24	48	*203	0.9610
o-propylaniline	C ₉ H ₁₃ N	135.21
propylbenzene	C ₉ H ₁₂	120.20	-100	159	0.9620
propylcyclohexane	C ₉ H ₁₈	126.24	-95	157	0.7936
cyclohexane	C ₆ H ₁₂	84.16	7	81	0.7785

* Pressure is 735 torr instead of 760 torr (1 atm)

Source: Weast, Handbook of Chemistry and Physics, 51st Edition (1971)

VII. B. Specifications for Chemicals Used

<u>Chemical</u>	<u>Source</u>	<u>Minimum Purity</u>	<u>*Density (g/cc)</u>
quinoline	Baker	99%	1.0929
Py-tetrahydroquinoline	Aldrich	97%	1.061
Bz-tetrahydroquinoline	Aldrich	97%	1.025
decahydroquinoline	Eastern	97%	† 0.842
o-propylaniline	...	98%	‡ 0.983
propylbenzene	Aldrich	98%	0.862
propylcyclohexane	Aldrich	99%	0.793
cyclohexane	Mallinckrodt	99%	0.776
hydrogen (reactant)	Matheson	99.95%	...
hydrogen (carrier gas)	Airco	99.995%	...
10% hydrogen sulfide in hydrogen mixture	Matheson
argon	Airco	99.997%	...

* These densities were used to convert volumetric liquid feed rates to mass feed rates

† Measured density of the decahydroquinoline/cyclohexane feed solution

‡ Measured density of the o-propylaniline synthesized for this study

VII. C. Estimated Standard Free Energies of Formation

Standard free energies of formation of o-propylaniline (OPA), propylcyclohexylamine (PCHA), and propylcyclohexene (PCHE) were estimated by Benson's group contribution technique (Benson et al., 1969); those of the heterocyclic nitrogen compounds (Q, PyTHQ, BzTHQ, and DHQ), for which Benson's method was inapplicable, were estimated by a less accurate modified van Krevelen group contribution technique (van Krevelen and Chermin, 1951; Cocchetto, 1974). Details of the estimation techniques are given by Cocchetto (1974). The estimated standard free energies of formation are listed below.

Estimated Standard Free Energies of Formation of Quinoline
and Some of its Hydrogenated Derivatives

T(K)	ΔG_f° (kcal/g-mol)							
	<u>Q</u>	<u>PyTHQ</u>	<u>BzTHQ</u>	<u>DHQ</u>		<u>OPA</u>	<u>PCHA</u>	<u>PCHE</u>
				<u>cis</u>	<u>trans</u>			
298	68.4	57.6	53.6	39.8	37.6	43.7	25.2	28.4
300	68.5	57.8	53.9	40.3	38.0	-	-	-
400	75.2	71.2	67.3	62.8	60.6	57.7	48.5	45.2
500	81.8	84.6	80.7	85.3	83.1	71.9	72.2	62.3
600	88.5	98.0	94.1	107.9	105.7	86.4	96.4	79.8
700	95.5	111.8	108.0	131.1	128.8	-	-	-
800	102.5	125.6	121.8	154.3	151.8	115.8	145.4	115.5
900	109.5	139.4	135.7	177.5	175.0	-	-	-
1000	116.5	153.2	149.6	200.8	198.0	145.5	194.6	151.6

VII. D. Metering Pump Calibration Curves

The metering pump delivered a constant volumetric feed rate of liquid at each pump setting. Calibration curves were derived for the 2 cc/hr and 8 cc/hr feed ranges. The mass of water collected during a measured time interval was determined at each pump setting calibrated, and the corresponding volumetric feed rate was easily calculated. Precautions were taken to prevent evaporation of water during the calibrations. The metering pump calibration curves are shown in Figures 7-1 and 7-2.

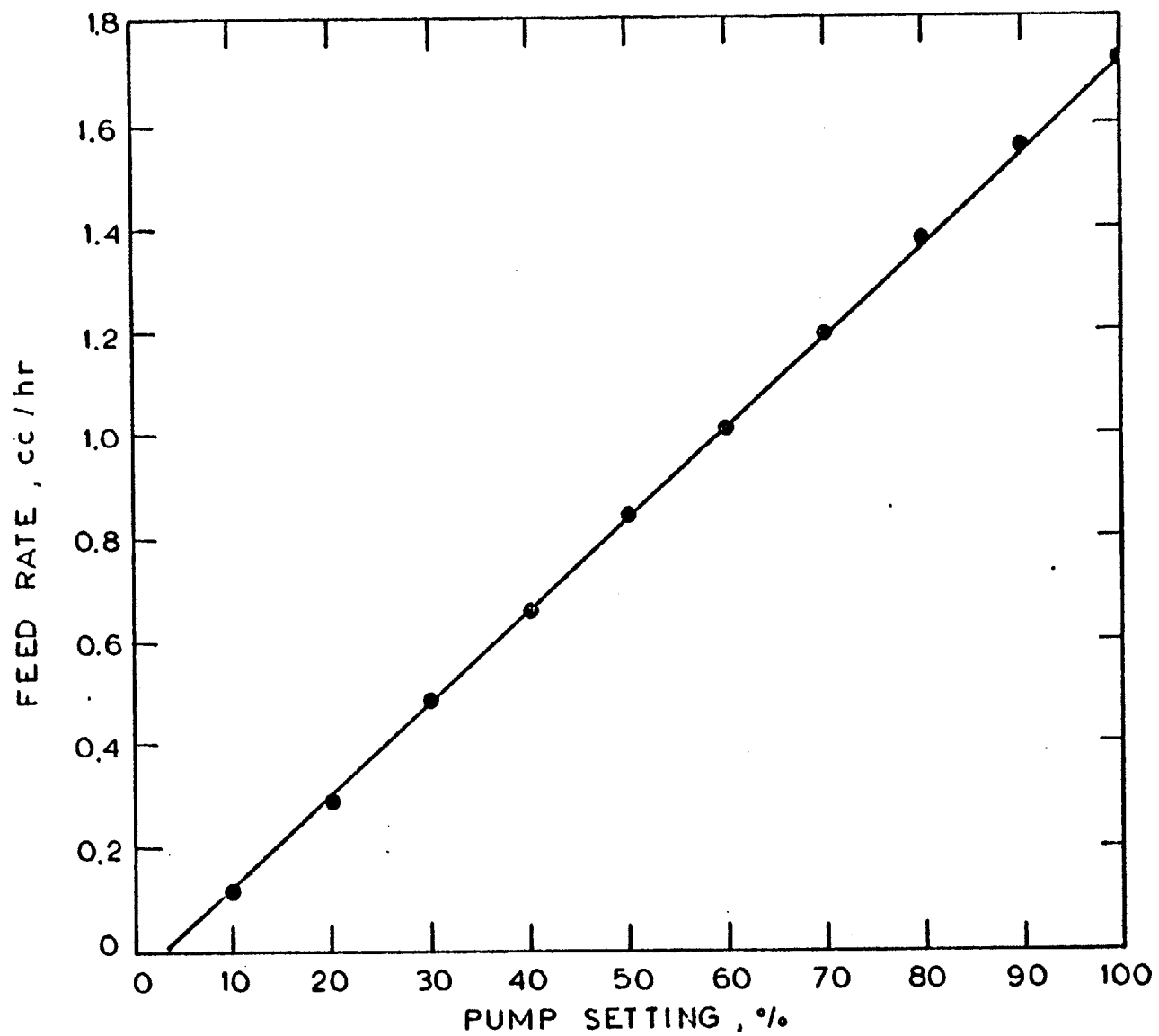


Figure 7-1: Metering Pump Calibration for 2 cc / hr Range

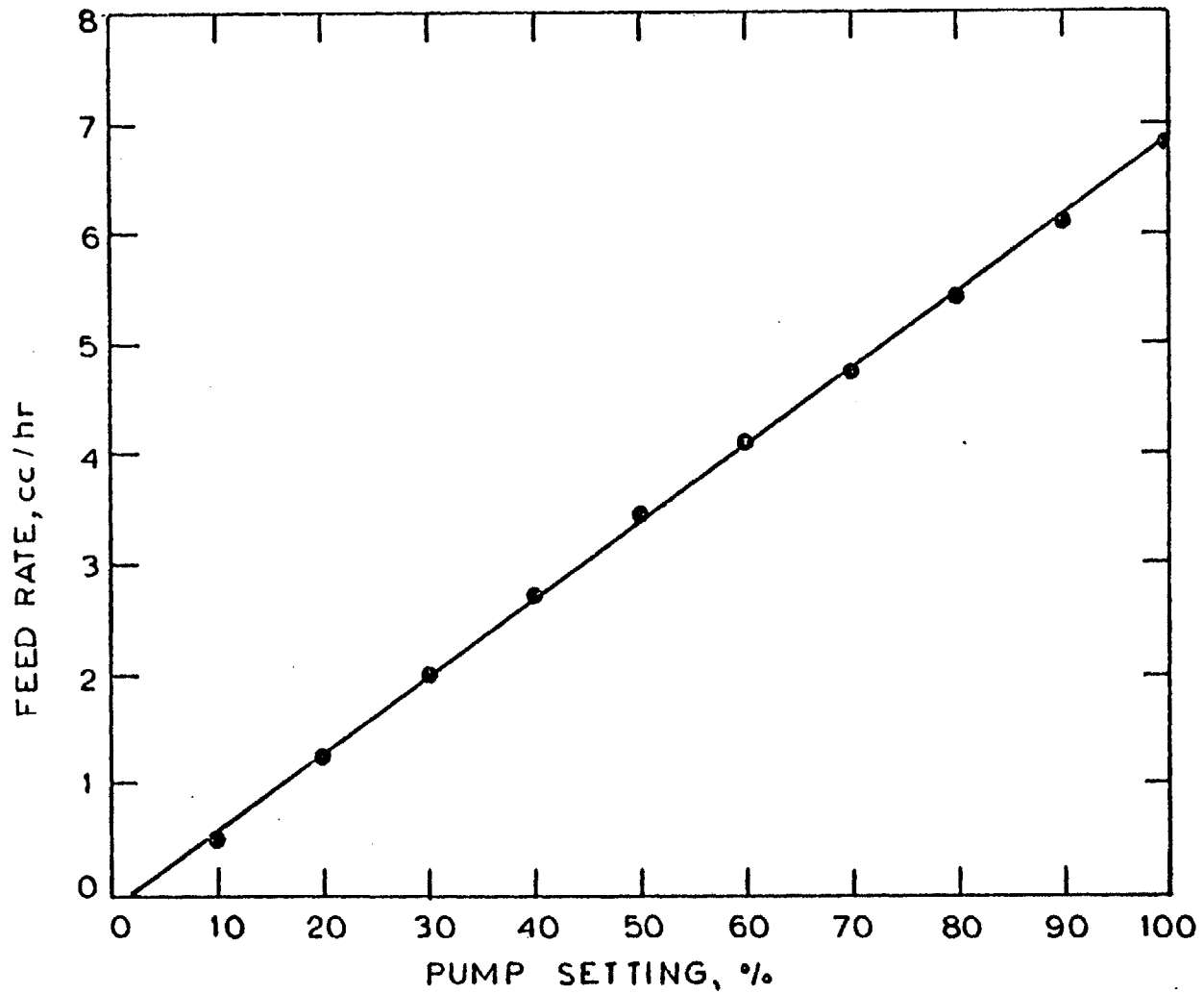


Figure 7-2: Metering Pump Calibration for 8cc/hr Range

VII. E. Gas Chromatographic Detector Response Factors

Absolute detector response factors were determined for quinoline, PyTHQ, BzTHQ, DHQ, OPA, PB, and PCH by injecting (via syringe) known quantities of each compound into the gas chromatograph and measuring the resulting peak areas, at the same conditions used for analysis of the reactor effluent samples. The absolute response factors derived in this study differ significantly from those reported by Declerck (1976), since detector conditions (e.g. filament current, detector temperature, carrier gas flow rate) were quite different. However, the relative response factors are in excellent agreement. The absolute detector response factors are presented in Figure 7-3.

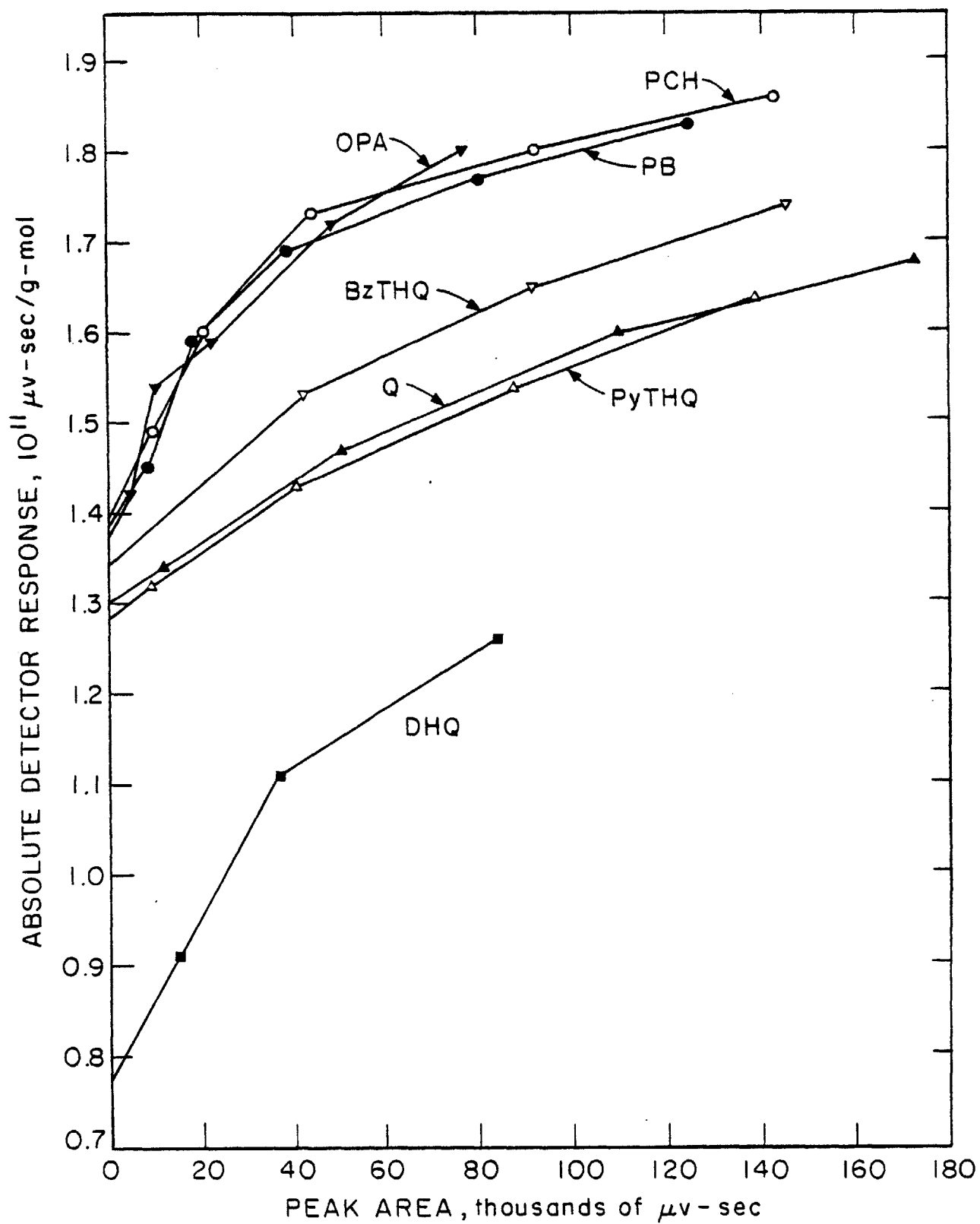


FIGURE 7-3: DETECTOR RESPONSE FACTORS FOR GAS CHROMATOGRAPHIC ANALYSIS OF QUINOLINE HDN PRODUCTS

VII. F. Data Reduction Sample Calculations

Data reduction calculations are illustrated in detail below for a typical set of steady-state samples, obtained from quinoline HDN at 375°C, 7.0 MPa total pressure, 13.3 kPa initial quinoline partial pressure, and 333 hr g catalyst/g-mol Q (run 23). The component peak areas from the sample analyses are first averaged (relative standard deviations are also calculated to provide a measure of sample reproducibility).

	Peak Area ($\mu\text{v-sec}$)				
	<u>Sample 7</u>	<u>Sample 8</u>	<u>Sample 9</u>	<u>Average</u>	<u>σ (%)</u>
PyTHQ	11823	9192	10921	10645	12.6
Q	1966	1800	1749	1838	6.2
OPA	1176	1333	1122	1210	9.1
BzTHQ	9951	8303	9307	9187	9.0
DHQ	11770	10536	11630	11312	6.0
PB	1418	1307	1297	1341	5.0
EB	TR	TR	TR	TR	-
PCHE	1395	1276	1295	1322	4.8
PCH	9927	9428	9775	9710	2.6
ECH	215	167	232	205	16.5
UNKNOWN	1383	1236	1306	1308	5.6

Absolute detector response factors (given in Figure 7-3 in Appendix E) are then used to convert the average component

peak areas to the equivalent number of moles of each component, from which the product distribution is calculated. Absolute detector response factors for EB, PCHE, and ECH were not measured; instead, EB is assumed to have the same response factor as PB, while the PCH response factor is used for PCHE and ECH. This introduces no significant error, since the response factors for these compounds are nearly the same with a thermal conductivity detector (Dietz, 1967). The unknowns are assumed to have an average response factor equivalent to that for BzTHQ.

	<u>Average Peak Area ($\mu\text{v-sec}$)</u>	<u>Response Factor ($\mu\text{v-sec/g-mol}$)</u>	<u>Organic Products (g-mol)</u>	<u>(mole %)</u>
PyTHQ	10645	1.32×10^{11}	0.806×10^{-7}	20.4
Q	1838	1.31×10^{11}	0.140×10^{-7}	3.6
OPA	1210	1.38×10^{11}	0.0877×10^{-7}	2.2
BzTHQ	9187	1.38×10^{11}	0.666×10^{-7}	16.9
DHQ	11312	0.88×10^{11}	1.29×10^{-7}	32.7
PB	1341	1.39×10^{11}	0.0965×10^{-7}	2.4
EB	TR		TR	TR
PCHE	1322	1.41×10^{11}	0.0938×10^{-7}	2.4
PCH	9710	1.49×10^{11}	0.652×10^{-7}	16.5
ECH	205	1.39×10^{11}	0.0147×10^{-7}	0.4
UNKNOWNNS	1308	1.35×10^{11}	0.0969×10^{-7}	2.5
TOTAL			3.944×10^{-7}	100.0

The actual reactor feed composition (initial quinoline partial pressure, P_{Q_0}) can be calculated from the average measured reactor pressure (P) and exhaust gas flow rate (F), and the quinoline feed rate.

$$P = 1001 \text{ psig} = 69.1 \text{ atm} = 7.00 \text{ MPa}$$

$$F = 963 \text{ cc/min at } 25^\circ\text{C, } 30.15 \text{ in Hg}$$

$$F = 2.38 \text{ g-mol/hr}$$

$$W/F_{Q_0} = 333 \text{ hr g catalyst/g-mol Q}$$

$$F_{Q_0} = \frac{1.5 \text{ g catalyst}}{333 \text{ hr g catalyst/g-mol Q}} = 0.00450 \text{ g-mol Q/hr}$$

$$P_{Q_0} = \frac{F_{Q_0}}{F} P = \frac{0.00450 \text{ g-mol Q/hr}}{2.38 \text{ g-mol/hr}} = (7.00 \text{ MPa}) = 13.2 \text{ KPa Q}$$

Finally, the average number of moles of organic products (excluding the methane presumably formed with EB and ECH) theoretically injected in each sample can be calculated from the known gas sampling value loop volume (4cc), and the measured temperature and pressure of the gas in the loop.

$$T_{\text{GSV}} = 197^\circ\text{C} = 470 \text{ K}$$

$$P_{\text{GSV}} = 10.0 \text{ psig} = 1.68 \text{ atm}$$

$$N_{\text{C,GSV}} = \frac{(F_{Q_0}/F) P_{\text{GSV}} V_{\text{GSV}}}{RT_{\text{GSV}}}$$

$$N_{\text{C,GSV}} = \frac{(0.00450/2.38) (1.68 \text{ atm}) (0.004 \text{ l})}{(0.082 \text{ l atm/g-mol K}) (470 \text{ K})} = 3.30 \times 10^{-7} \text{ g-mol}$$

This can be compared with the average number of moles of organic products actually detected in the samples, to check the carbon material balance.

$$\text{Carbon balance} = \frac{(3.944-3.30)10^{-7} \text{ g-mol}}{3.30 \times 10^{-7} \text{ g-mol}} = 0.195$$

$$\text{Carbon balance} = +19.5\%$$

Note the "excess" in the carbon material balance; i.e. more total moles of organic products were detected in the samples than were thought to have been injected via the gas sampling valve. This discrepancy is believed to be due to inaccurate measurement of the pressure in the gas sampling valve loop. However, this problem does not affect the calculated product distributions, which are the basis for all results presented in this study.

VII. G. Summary of Data and Calculated Values

The reduced data are summarized in the following tables. The data for each run are tabulated, from left to right, in the chronological order in which they were obtained. An old charge of catalyst was used for runs 1 through 5, as these runs were made primarily to "de-bug" the experimental apparatus; the corresponding data are not shown. Runs 7, 8, and 27 were terminated shortly after startup due to operating problems, so data for these runs are also not shown.

RUN 6

Feed: quinoline

Catalyst time on stream before run: 0.0 hr (virgin catalyst)

Reaction conditions: 3.55 MPa, 13.3 kPa Q,
167 hr g catalyst/g-mol Q

	Temperature, °C			
	<u>278</u>	<u>328</u>	<u>379</u>	<u>416</u>
Organic products, mole %				
PyTHQ	77.8	50.6	20.5	12.1
Q	0.8	4.6	12.2	22.1
OPA	TR	0.8	3.9	7.2
BzTHQ	0.8	9.5	37.9	28.5
DHQ	20.3	31.0	11.1	1.3
PB	0.1	0.9	2.9	8.9
EB	-	-	0.1	2.8
PCHE	0.1	1.0	2.7	1.9
PCH	0.1	1.5	8.3	13.1
ECH	-	-	0.5	2.0
UNKNOWN	-	-	-	-
TOTAL	100.0	99.9	100.1	99.9
Product ratios, mole %				
PyTHQ/(Q+PyTHQ)	99.0	91.6	62.7	35.3
BzTHQ/(Q+BzTHQ)	50.5	67.4	75.6	56.3
DHQ/(PyTHQ+DHQ)	20.7	38.0	35.1	9.5
DHQ/(BzTHQ+DHQ)	96.1	76.5	22.7	4.3
PCH/(PB+PCH)	42.9	63.6	74.2	59.4
Denitrogenation, %	0.3	3.3	14.5	28.8

RUN 9

Feed: quinoline

Catalyst time on stream before run: 29.4 hr

Reaction conditions: 3.55 MPa, 13.3 kPa Q,
167 hr g catalyst/g-mol Q

	Temperature, °C			
	<u>276</u>	<u>326</u>	<u>378</u>	<u>412</u>
Organic products, mole %				
PyTHQ	72.0	57.1	29.6	21.8
Q	8.9	12.0	13.8	18.6
OPA	TR	0.6	2.9	6.0
BzTHQ	1.4	7.3	35.8	36.1
DHQ	17.7	21.8	9.9	1.6
PB	-	0.4	1.7	5.1
EB	-	-	-	1.2
PCHE	-	0.4	1.7	1.2
PCH	-	0.5	4.5	7.5
ECH	-	-	0.1	1.0
UNKNOWNNS	-	-	-	-
TOTAL	100.0	100.1	100.0	100.1
Product ratios, mole %				
PyTHQ/(Q+PyTHQ)	89.0	82.7	68.2	54.0
BzTHQ/(Q+BzTHQ)	13.7	37.9	72.2	66.0
DHQ/(PyTHQ+DHQ)	19.7	27.6	25.0	6.8
DHQ/(BzTHQ+DHQ)	92.6	74.8	21.6	4.2
PCH/(PB+PCH)	-	55.7	72.5	59.5
Denitrogenation, %	0	1.3	8.1	16.0

RUN 10

Feed: quinoline

Catalyst time on stream before run: 46.4 hr

Reaction conditions: 375°C, 3.55 MPa, 13.3 kPa Q

	W/F _{Q₀} , hr g catalyst/g-mol Q			
	<u>*82.6</u>	<u>82.6</u>	<u>167</u>	<u>344</u>
Organic products, mole %				
PyTHQ	87.0	39.8	28.5	8.0
Q	1.4	22.4	19.1	23.0
OPA	-	1.7	2.7	4.6
BzTHQ	1.0	25.6	34.2	42.3
DHQ	10.5	7.9	9.4	3.7
PB	-	0.6	1.3	3.5
EB	-	TR	TR	0.2
PCHE	-	0.8	1.7	3.4
PCH	-	1.0	3.1	11.0
ECH	-	-	TR	0.5
UNKNOWNNS				
TOTAL	99.9	99.8	100.0	100.2
Product ratios, mole %				
PyTHQ/(Q+PyTHQ)	98.4	64.0	59.8	25.9
BzTHQ/(Q+BzTHQ)	41.5	53.3	64.1	64.8
DHQ/(PyTHQ+DHQ)	10.8	16.6	24.8	31.7
DHQ/(BzTHQ+DHQ)	91.2	23.6	21.5	8.1
PCH/(PB+PCH)	-	63.4	71.6	75.7
Denitrogenation, %	0	2.5	6.1	18.5

*Temperature was 278°C instead of 375°C

RUN 11

Feed: quinoline

Catalyst time on stream before run: 64.8 hr

Reaction conditions: 280°C, 3.55 MPa, 26.7 kPa Q

W/F_{Q_o}, hr g catalyst/g-mol Q

Organic products, mole %	<u>167</u>	<u>82.6</u>	<u>*167</u>
PyTHQ	29.9	76.7	69.7
Q	60.6	15.1	17.7
OPA	0.2	TR	-
BzTHQ	6.0	1.4	2.0
DHQ	3.1	6.8	10.6
PB	0.1	-	-
EB	-	-	-
PCHE	0.1	-	-
PCH	-	-	-
ECH	-	-	-
UNKNOWNNS			
TOTAL	100.0	100.0	100.0

Product ratios, mole %

PyTHQ/(Q+PyTHQ)	33.0	83.6	79.8
BzTHQ/(Q+BzTHQ)	8.9	8.5	10.0
DHQ/(PyTHQ+DHQ)	9.3	8.2	13.2
DHQ/(BzTHQ+DHQ)	34.1	83.1	84.4
PCH/(PB+PCH)	-	-	-

Denitrogenation, %

0.1	0	0
-----	---	---

*Initial quinoline partial pressure was 13.3 kPa instead of 26.7 kPa

RUN 12

Feed: quinoline

Catalyst time on stream before run: 76.2 hr

Reaction conditions: 375°C, 3.55 MPa, 13.3 kPa Q

W/F_{Q₀}, hr g catalyst/g-mol Q

	<u>719</u>	<u>344</u>	<u>167</u>	<u>82.6</u>
Organic products, mole %				
PyTHQ	2.9	12.5	31.4	42.6
Q	18.1	20.8	20.5	24.0
OPA	5.5	4.7	2.6	1.5
BzTHQ	36.3	41.9	31.8	22.7
DHQ	2.2	5.6	8.4	7.4
PB	6.7	2.8	1.1	0.4
EB	0.6	0.2	TR	TR
PCHE	1.7	1.9	1.4	0.7
PCH	24.1	9.2	2.6	0.7
ECH	1.9	0.5	TR	TR
UNKNOWNNS				
TOTAL	100.0	100.1	99.8	100.0
Product ratios, mole %				
PyTHQ/(Q+PyTHQ)	13.6	37.6	60.5	64.0
BzTHQ/(Q+BzTHQ)	66.8	66.8	60.8	48.6
DHQ/(PyTHQ+DHQ)	43.6	30.8	21.2	14.8
DHQ/(BzTHQ+DHQ)	5.7	11.7	20.9	24.6
PCH/(PB+PCH)	78.3	76.8	71.0	60.6
Denitrogenation, %	35	14.6	5.1	1.8

RUN 13

Feed: quinoline

Catalyst time on stream before run: 99.9 hr

Reaction conditions: 375°C, 7.0 MPa, 13.3 kPa Q

W/F_{Q₀}, hr g catalyst/g-mol Q

Organic products, mole %	<u>1585</u>	<u>719</u>	<u>344</u>	<u>167</u>
PyTHQ	-	-	10.8	30.7
Q	-	TR	2.4	3.6
OPA	-	TR	4.1	2.9
BzTHQ	-	TR	15.4	15.4
DHQ	-	-	23.8	31.4
PB	9.3	9.6	4.1	1.7
EB	0.6	0.7	TR	TR
PCHE	-	TR	2.9	2.6
PCH	85.3	84.5	35.2	11.5
ECH	4.9	5.0	1.2	0.3
UNKNOWNNS				
TOTAL	100.1	99.8	99.9	100.1
Product ratios, mole %				
PyTHQ/(Q+PyTHQ)	-	-	81.6	89.5
BzTHQ/(Q+BzTHQ)	-	-	86.4	81.1
DHQ/(PyTHQ+DHQ)	-	-	68.8	50.5
DHQ/(BzTHQ+DHQ)	-	-	60.6	67.1
PCH/(PB+PCH)	90.2	89.8	89.5	87.2
Denitrogenation, %	100	100	43.4	16.1

RUN 14

Feed: quinoline

Catalyst time on stream before run: 125.1 hr

Reaction conditions: 375 °C, 7.0 MPa, 26.7 kPa Q

W/F_{Q₀}, hr g catalyst/g-mol Q

	<u>719</u>	<u>344</u>	<u>167</u>	<u>82.6</u>
Organic products, mole %				
PyTHQ	-	8.8	29.0	43.6
Q	0.9	5.0	4.5	6.7
OPA	2.5	4.6	3.3	2.3
BzTHQ	2.8	17.7	17.2	15.0
DHQ	-	11.4	25.2	25.0
PB	9.0	4.0	1.6	0.9
EB	0.4	TR	TR	-
PCHE	TR	2.8	2.7	2.1
PCH	72.5	31.8	11.2	4.3
ECH	3.8	1.0	0.1	TR
UNKNOWNNS	8.1	12.8	5.0	0.2
TOTAL	100.0	99.9	99.8	100.1
Product ratios, mole %				
PyTHQ/(Q+PyTHQ)	0	63.8	86.5	86.7
BzTHQ/(Q+BzTHQ)	75.3	78.0	79.1	69.1
DHQ/(PyTHQ+DHQ)	-	56.5	46.5	36.5
DHQ/(BzTHQ+DHQ)	0	39.2	59.4	62.6
PCH/(PB+PCH)	88.9	88.7	87.3	82.0
Denitrogenation, %	85.7	39.6	15.6	7.3

RUN 15

Feed: Bz-tetrahydroquinoline

Catalyst time on stream before run: 150.3 hr

Reaction conditions: 375°C, 3.55 MPa, 13.3 kPa BzTHQ

W/F_{BzTHQ₀}, hr g catalyst/g-mol BzTHQ

Organic products, mole %	<u>699</u>	<u>341</u>	<u>166</u>	<u>82.6</u>
PyTHQ	5.1	10.2	11.8	9.1
Q	12.5	11.8	8.5	5.6
OPA	2.4	1.4	0.4	TR
BzTHQ	31.1	42.9	54.0	61.5
DHQ	1.4	6.0	10.9	16.3
PB	8.3	4.4	2.0	0.8
EB	0.6	0.2	TR	TR
PCHE	2.2	3.0	3.0	2.2
PCH	32.0	17.7	7.1	2.6
ECH	1.9	0.8	0.2	TR
UNKNOWNNS	2.4	1.7	2.1	1.8
TOTAL	99.9	100.1	100.0	99.9
Product ratios, mole %				
PyTHQ/(Q+PyTHQ)	29.0	46.2	58.2	61.7
BzTHQ/(Q+BzTHQ)	71.3	78.4	86.4	91.6
DHQ/(PyTHQ+DHQ)	21.3	36.9	47.9	64.1
DHQ/(BzTHQ+DHQ)	4.3	12.2	16.8	20.9
PCH/(PB+PCH)	79.4	80.1	78.5	77.1
Denitrogenation, %	45.0	26.1	12.3	5.6

RUN 16

Feed: propylbenzene.

Catalyst time on stream before run: 332.1 hr*

Reaction conditions: 375°C, 7.0 MPa, 13.3 kPa PB

	W/F _{PB₀} , hr g catalyst/g-mol PB		
	<u>165</u>	<u>662</u>	<u>329</u>
Organic products, mole %			
PyTHQ	-	-	-
Q	-	-	-
OPA	-	-	-
BzTHQ	-	-	-
DHQ	-	-	-
PB	76.5	39.9	63.5
EB	-	-	-
PCHE	-	-	-
PCH	23.5	60.1	36.5
ECH	-	-	-
UNKNOWNNS	-	-	-
TOTAL	100.0	100.0	100.0

Product ratios, mole %

PyTHQ/(Q+PyTHQ)	-	-	-
BzTHQ/(Q+BzTHQ)	-	-	-
DHQ/(PyTHQ+DHQ)	-	-	-
DHQ/(BzTHQ+DHQ)	-	-	-
PCH/(PB+PCH)	23.5	60.1	36.5

*Between runs 15 and 16, the catalyst was used for 154.0 hours in nine runs with quinoline/carbon disulfide feeds, as part of a study on the effect of hydrogen sulfide on quinoline HDN (Gultekin, 1980)

RUN 17

Feed: quinoline

Catalyst time on stream before run: 332.1 hr*

Reaction conditions: 375°C, 7.0 MPa, 13.3 kPa Q

	W/F _{Q₀} , hr g catalyst/g-mol Q				
	<u>83.3</u>	<u>167</u>	<u>333</u>	<u>500</u>	<u>667</u>
Organic products, mole %					
PyTHQ	47.5	34.4	17.5	8.7	2.3
Q	6.3	4.6	3.8	5.2	5.2
OPA	1.3	2.1	2.9	3.1	3.0
BzTHQ	13.1	16.0	17.8	16.8	14.2
DHQ	27.5	33.0	29.8	18.9	7.9
PB	0.7	1.2	2.2	4.1	6.0
EB	-	-	TR	-	TR
PCHE	0.8	1.2	1.4	2.6	1.7
PCH	2.9	6.9	19.6	34.6	54.8
ECH	-	0.2	0.7	1.3	2.6
UNKNOWNNS	-	0.3	4.2	4.8	2.3
TOTAL	100.1	99.9	99.9	100.1	100.0

Product ratios, mole %

PyTHQ/(Q+PyTHQ)	88.3%	88.2%	82.0%	62.7%	31.1%
BzTHQ/(Q+BzTHQ)	67.6%	77.6%	82.3%	76.5%	73.2%
DHQ/(PyTHQ+DHQ)	36.7%	48.9%	63.0%	68.5%	77.1%
DHQ/(BzTHQ+DHQ)	67.8%	67.3%	62.6%	52.9%	35.7%
PCH/(PB+PCH)	79.7%	85.0%	90.0%	89.4%	90.2%

Denitrogenation, % 4.4% 9.6% 23.9% 42.6% 65.1%

*The catalyst time on stream during run 16 is not included, since organic nitrogen compounds were not present.

RUN 18

Feed: quinoline

Catalyst time on stream before run: 343.2 hr

Reaction conditions: 375°C, 3.55 MPa, 13.3 kPa Q

W/F_{Q₀}, hr g catalyst/g-mol Q

	<u>83.3</u>	<u>167</u>	<u>333</u>	<u>500</u>	<u>667</u>	<u>167</u>
Organic products, mole %						
PyTHQ	41.7	34.6	25.5	17.8	14.5	34.4
Q	22.9	19.9	16.2	15.4	15.8	19.8
OPA	1.5	1.9	3.1	3.7	4.1	1.9
BzTHQ	23.3	28.1	34.5	37.0	37.3	28.0
DHQ	8.5	11.5	12.3	10.8	9.7	11.9
PB	0.5	0.8	1.5	2.7	3.3	0.9
EB	-	TR	TR	TR	0.2	TR
PCHE	0.6	1.0	1.3	1.6	1.3	1.2
PCH	0.8	1.8	4.5	9.1	12.4	1.8
ECH	-	TR	0.1	0.4	0.8	TR
UNKNOWNNS	0.2	0.4	1.1	1.5	0.6	0.2
TOTAL	100.0	100.0	100.1	100.0	100.0	100.1

Product ratios, mole %

PyTHQ/(Q+PyTHQ)	64.5	63.5	61.2	53.5	47.9	63.5
BzTHQ/(Q+BzTHQ)	50.5	58.5	68.1	70.6	70.2	58.6
DHQ/(PyTHQ+DHQ)	17.0	24.9	32.5	37.9	40.0	25.7
DHQ/(BzTHQ+DHQ)	26.8	29.0	26.2	22.6	20.7	29.9
PCH/(PB+PCH)	63.6	67.8	75.7	76.9	79.0	65.8

Denitrogenation, % 1.9% 3.7% 7.4% 13.8% 18.0% 3.9%

activity/reproducibility check

RUN 19

Feed: quinoline

Catalyst time on stream before run: 357.4 hr

Reaction conditions: 420°C, 3.55 MPa, 26.7 kPa Q

	W/F _{Q₀} , hr g catalyst/g-mol Q				
	<u>41.7</u>	<u>83.3</u>	<u>167</u>	<u>333</u>	<u>667</u>
Organic products, mole %					
PyTHQ	17.9	16.4	15.4	12.1	10.9
Q	40.5	36.3	32.6	27.3	23.7
OPA	3.0	4.0	5.4	7.7	8.4
BzTHQ	33.8	36.0	34.7	31.3	25.0
DHQ	1.6	1.5	0.9	0.9	0.9
PB	1.0	1.8	3.3	6.1	8.3
EB	0.1	0.4	0.7	1.5	2.6
PCHE	0.5	0.6	0.7	0.5	0.4
PCH	1.0	1.9	4.0	7.8	11.4
ECH	0.1	0.2	0.6	1.3	2.4
UNKNOWN	0.5	0.9	1.8	3.4	5.9
TOTAL	100.0	100.0	100.1	99.9	99.9
Product ratios, mole %					
PyTHQ/(Q+PyTHQ)	30.7	31.1	32.0	30.8	31.6
BzTHQ/(Q+BzTHQ)	45.5	49.8	51.6	53.3	51.4
DHQ/(PyTHQ+DHQ)	8.1	8.5	5.3	7.2	7.7
DHQ/(BzTHQ+DHQ)	4.5	4.1	2.4	2.9	3.5
PCH/(PB+PCH)	48.6	51.4	55.2	55.9	57.8
Denitrogenation, %	2.7	4.9	9.3	17.2	25.1

RUN 20

Feed: quinoline

Catalyst time on stream before run: 369.6 hr

Reaction conditions: 420°C, 3.55 MPa, 13.3 kPa Q

W/F_{Q₀}, hr g catalyst/g-mol Q

	<u>41.7</u>	<u>83.3</u>	<u>167</u>	<u>333</u>	<u>500</u>	<u>667</u>
Organic products, mole %						
PyTHQ	20.9	18.5	14.3	12.2	10.8	7.9
Q	44.0	39.5	33.7	29.0	26.4	23.2
OPA	2.5	3.3	4.8	5.9	7.3	8.3
BzTHQ	29.8	34.2	37.4	34.0	29.6	25.0
DHQ	1.0	1.2	1.4	1.3	0.8	0.5
PB	0.7	1.1	2.8	5.7	7.9	11.0
EB	0.1	0.1	0.6	1.4	2.0	3.0
PCHE	0.3	0.4	0.7	0.7	0.8	0.7
PCH	0.5	1.0	3.1	7.2	10.2	15.0
ECH	TR	0.1	0.5	1.2	1.8	2.9
UNKNOWN	0.4	0.5	0.8	1.6	2.3	2.4
TOTAL	100.2	99.9	100.1	100.2	99.9	99.9
Product ratios, mole %						
PyTHQ/(Q+PyTHQ)	32.2%	31.9%	29.9%	29.5%	29.0%	25.4%
BzTHQ/(Q+BzTHQ)	40.4%	46.4%	52.6%	54.0%	52.8%	51.9%
DHQ/(PyTHQ+DHQ)	4.5%	6.2%	9.0%	9.6%	7.1%	6.3%
DHQ/(BzTHQ+DHQ)	3.2%	3.4%	3.7%	3.7%	2.7%	2.1%
PCH/(PB+PCH)	42.7%	48.5%	52.0%	55.7%	56.3%	57.7%
Denitrogenation, %	1.5%	2.8	7.7%	16.1%	22.8%	32.7%

RUN 21

Feed: quinoline

Catalyst time on stream before run: 385.3 hr

Reaction conditions: 420°C, 7.0 MPa, 26.7 kPa Q

	W/F _{Q₀} , hr g catalyst/g-mol Q				
	<u>41.7</u>	<u>83.3</u>	<u>167</u>	<u>333</u>	<u>500</u>
Organic products, mole %					
PyTHQ	28.1	17.8	12.4	3.8	TR
Q	16.9	11.2	7.5	3.0	TR
OPA	3.8	5.0	5.9	5.1	TR
BzTHQ	33.8	35.8	29.3	10.5	TR
DHQ	8.6	9.6	6.7	1.5	-
PB	1.9	4.2	7.8	15.6	20.7
EB	0.1	0.4	1.0	2.7	3.6
PCHE	1.6	2.3	1.9	0.8	TR
PCH	4.6	12.1	24.2	49.0	64.1
ECH	0.4	1.2	2.9	7.7	10.8
UNKNOWNNS	0.2	0.3	0.5	0.3	0.8
TOTAL	100.0	99.9	100.1	100.0	100.0
Product ratios, mole %					
PyTHQ/(Q+PyTHQ)	62.4	61.3	62.4	56.1	-
BzTHQ/(Q+BzTHQ)	66.7	76.1	79.6	78.0	-
DHQ/(PyTHQ+DHQ)	23.4	35.1	35.2	28.3	-
DHQ/(BzTHQ+DHQ)	20.2	21.2	18.7	12.5	-
PCH/(PB+PCH)	70.9	74.3	75.6	75.9	75.6
Denitrogenation, %	8.6	20.3	37.7	75.8	99.2

RUN 22

Feed: quinoline

Catalyst time on stream before run: 397.4 hr

Reaction conditions: 420°C, 7.0 MPa, 13.3 kPa Q

W/F_{Q₀}, hr g catalyst/g-mol Q


	<u>83.3</u>	<u>167</u>	<u>250</u>	<u>333</u>	<u>500</u>	<u>167</u>
Organic products, mole %						
PyTHQ	21.6	14.6	9.1	4.7	TR	15.4
Q	12.8	8.7	5.9	2.8	TR	9.2
OPA	4.4	5.9	6.3	5.0	2.8	6.2
BzTHQ	36.0	32.7	23.7	13.9	2.7	32.9
DHQ	9.1	7.3	5.1	2.1	-	7.5
PB	3.3	6.4	10.1	14.6	19.8	5.8
EB	0.4	0.9	1.6	2.6	3.8	0.9
PCHE	2.0	1.8	1.7	1.2	TR	2.0
PCH	9.3	19.2	31.7	45.1	59.5	17.6
ECH	1.1	2.6	4.7	7.7	11.1	2.5
UNKNOWNNS	TR	TR	TR	0.3	0.4	TR
TOTAL	100.0	100.1	99.9	100.0	100.1	100.0

Product ratios, mole %

PyTHQ/(Q+PyTHQ)	62.8%	62.5%	60.9%	63.1%	-	62.6%
BzTHQ/(Q+BzTHQ)	73.7%	78.9%	80.2%	83.4%	-	78.2%
DHQ/(PyTHQ+DHQ)	29.6%	33.2%	35.9%	30.5%	-	32.7%
DHQ/(BzTHQ+DHQ)	20.2%	18.2%	17.7%	12.9%	-	18.5%
PCH/(PB+PCH)	73.8%	74.8%	75.8%	75.6%	75.0%	75.1%

Denitrogenation, %

16.0% 30.9% 49.8% 71.3% 94.1% 28.8%



activity/reproducibility check

RUN 23

Feed: quinoline

Catalyst time on stream before run: 411.1 hr

Reaction conditions: 375°C, 7.0 MPa, 13.3 kPa Q

	W/F _{Q₀} , hr g catalyst/g-mol Q				
	<u>83.3</u>	<u>167</u>	<u>333</u>	<u>500</u>	<u>667</u>
Organic products, mole %					
PyTHQ	49.8	38.8	20.4	13.0	9.3
Q	6.9	5.2	3.6	2.9	2.7
OPA	1.2	1.7	2.2	3.0	3.1
BzTHQ	12.5	15.0	16.9	17.2	14.8
DHQ	26.1	31.0	32.7	27.4	23.8
PB	0.6	1.1	2.4	3.5	4.1
EB	-	-	TR	TR	TR
PCHE	0.9	1.6	2.4	2.0	2.1
PCH	2.1	5.5	16.5	26.6	34.5
ECH	-	0.1	0.4	0.8	1.2
UNKNOWN	TR	TR	2.5	3.6	4.5
TOTAL	100.1	100.0	100.0	100.0	100.0
Product ratios, mole %					
PyTHQ/(Q+PyTHQ)	87.9	88.2	85.2	81.5	77.5
BzTHQ/(Q+BzTHQ)	64.5	74.3	82.6	85.4	84.6
DHQ/(PyTHQ+DHQ)	34.3	44.4	61.5	67.9	72.0
DHQ/(BzTHQ+DHQ)	67.6	67.4	66.0	61.4	61.7
PCH/(PB+PCH)	78.1	84.0	87.1	88.4	89.3
Denitrogenation, %	3.5	8.3	21.7	32.9	41.8

RUN 24

Feed: quinoline

Catalyst time on stream before run: 423.8 hr

Reaction conditions: 375°C, 7.0 MPa, 26.7 kPa Q

	W/F _{Q₀} , hr g catalyst/g-mol Q				
	<u>41.7</u>	<u>83.3</u>	<u>167</u>	<u>333</u>	<u>500</u>
Organic products, mole %					
PyTHQ	61.5	51.4	39.0	20.8	12.4
Q	9.4	8.0	6.3	5.3	5.7
OPA	1.0	1.7	2.5	3.0	3.8
BzTHQ	9.4	12.2	15.2	15.5	17.0
DHQ	17.1	22.9	26.7	27.6	22.9
PB	0.3	0.6	1.1	2.4	3.3
EB	-	-	TR	TR	TR
PCHE	0.5	1.1	1.9	2.8	2.3
PCH	0.6	1.8	5.4	16.2	25.2
ECH	-	-	0.0	0.3	0.7
UNKNOWN	0.2	0.3	1.8	6.2	6.7
TOTAL	100.0	100.0	99.9	100.1	100.0
Product ratios, mole %					
PyTHQ/(Q+PyTHQ)	86.7	86.6	86.1	79.7	68.5
BzTHQ/(Q+BzTHQ)	49.8	60.6	70.7	74.6	74.8
DHQ/(PyTHQ+DHQ)	21.7	30.9	40.7	57.0	64.8
DHQ/(BzTHQ+DHQ)	64.6	65.2	63.7	64.0	57.4
PCH/(PB+PCH)	68.1	76.1	83.6	87.1	88.4
Denitrogenation, %	1.4	3.5	8.5	21.6	31.5

RUN 25

Feed: quinoline

Catalyst time on stream before run: 435.7 hr

Reaction conditions: 330°C, 3.55 MPa, 13.3 kPa Q

W/F_{Q₀}, hr g catalyst/g-mol Q

	<u>41.7</u>	<u>83.3</u>	<u>167</u>	<u>333</u>	<u>667</u>	<u>*500</u>
Organic products, mole %						
PyTHQ	77.6	77.2	69.0	56.0	36.6	18.5
Q	8.9	8.6	10.4	20.1	28.6	16.4
OPA	TR	TR	TR	0.4	0.9	3.7
BzTHQ	3.5	3.6	4.9	6.3	9.9	36.9
DHQ	9.8	10.4	14.4	14.5	17.7	10.1
PB	TR	TR	0.1	0.2	0.5	2.7
EB	-	-	-	-	-	TR
PCHE	TR	TR	0.1	0.3	0.7	2.2
PCH	-	-	0.1	0.3	1.1	7.7
ECH	-	-	-	-	-	0.4
UNKNOWNNS	0.2	0.1	1.0	2.0	3.9	1.5
TOTAL	100.0	99.9	100.0	100.1	99.9	100.1

Product ratios, mole %

PyTHQ/(Q+PyTHQ)	89.7%	90.0%	86.8%	73.6%	56.1%	53.0%
BzTHQ/(Q+BzTHQ)	28.1%	29.7%	31.8%	23.7%	25.8%	69.2%
DHQ/(PyTHQ+DHQ)	11.2%	11.9%	17.2%	20.6%	32.6%	35.3%
DHQ/(BzTHQ+DHQ)	73.7%	74.1%	74.7%	69.9%	64.0%	21.5%
PCH/(PB+PCH)	-	-	40.6%	53.8%	69.0%	74.2%
Denitrogenation, %	0%	0%	0.3%	0.8%	2.3%	13.0%

*Temperature was 375°C instead of 330°C

RUN 26

Feed: quinoline

Catalyst time on stream before run: 451.0 hr

Reaction conditions: 330°C, 7.0 MPa, 13.3 kPa Q

W/F_{Q₀}, hr g catalyst/g-mol Q

	<u>83.3</u>	<u>167</u>	<u>333</u>	<u>500</u>	<u>667</u>	<u>*667</u>
Organic products, mole %						
PyTHQ	68.5	64.9	53.8	46.3	31.9	11.1
Q	1.3	1.6	4.0	7.1	7.9	3.4
OPA	TR	TR	TR	0.4	0.6	2.3
BzTHQ	2.2	2.0	2.7	3.0	3.6	13.0
DHQ	27.6	30.8	34.8	33.9	42.3	21.8
PB	0.1	0.2	0.5	0.6	0.8	5.0
EB	-	-	-	-	-	TR
PCHE	0.1	0.1	0.3	0.5	0.7	1.8
PCH	0.1	0.4	1.0	2.3	4.3	37.1
ECH	-	-	-	-	-	1.5
UNKNOWNNS	TR	TR	3.0	5.9	7.8	3.1
TOTAL	99.9	100.0	100.1	100.0	99.9	100.1

Product ratios, mole %

PyTHQ/(Q+PyTHQ)	98.1%	97.6%	93.1%	86.8%	80.2%	76.4%
BzTHQ/(Q+BzTHQ)	62.9%	56.3%	39.9%	29.7%	31.6%	79.2%
DHQ/(PyTHQ+DHQ)	28.7%	32.2%	39.3%	42.3%	57.0%	66.3%
DHQ/(BzTHQ+DHQ)	92.5%	93.8%	92.9%	91.9%	92.1%	62.6%
PCH/(PB+PCH)	57.9%	63.0%	69.8%	79.2%	83.6%	88.2%
Denitrogenation, %	0.3%	0.8%	1.8%	3.5%	5.8%	45.3%

*Temperature was 375°C instead of 330°C

RUN 28

Feed: o-propylaniline

Catalyst time on stream before run: 469.8 hr

Reaction conditions: 375°C, 7.0 MPa, 13.3 kPa OPA

W/F_{OPA}, hr g catalyst/g-mol OPA

	<u>83.3</u>	<u>167</u>	<u>250</u>	<u>333</u>
Organic products, mole %				
PyTHQ	-	-	-	-
Q	-	-	-	-
OPA	55.8	29.8	10.2	1.2
BzTHQ	-	-	-	-
DHQ	-	-	-	-
PB	8.1	12.4	16.1	17.2
EB	-	-	-	TR
PCHE	4.0	1.8	TR	TR
PCH	32.2	55.9	73.7	81.5
ECH	-	TR	TR	TR
UNKNOWNNS	TR	-	-	-
TOTAL	100.1	99.9	100.0	99.9
Product ratios, mole %				
PyTHQ/(Q+PyTHQ)	-	-	-	-
BzTHQ/(Q+BzTHQ)	-	-	-	-
DHQ/(PyTHQ+DHQ)	-	-	-	-
DHQ/(BzTHQ+DHQ)	-	-	-	-
PCH/(PB+PCH)	80.0	81.8	82.1	82.6
Denitrogenation, %	44.2	70.2	89.8	98.7

RUN 29

Feed: o-propylaniline

Catalyst time on stream before run: 476.7 hr

Reaction conditions: 375°C, 7.0 MPa, 26.7 kPa OPA

W/F_{OPA₀}, hr g catalyst/g-mol OPA

	<u>41.7</u>	<u>83.3</u>	<u>167</u>	<u>250</u>	<u>333</u>
Organic products, mole %					
PyTHQ	-	-	-	-	-
Q	-	-	-	-	-
OPA	75.9	59.6	29.7	12.4	1.9
BzTHQ	-	-	-	-	-
DHQ	-	-	-	-	-
PB	4.7	7.8	12.4	15.1	16.4
EB	-	-	-	-	TR
PCHE	4.8	3.8	1.8	TR	TR
PCH	14.5	28.5	55.8	72.2	81.6
ECH	TR	TR	TR	0.1	0.2
UNKNOWNNS	0.1	0.3	0.2	0.1	TR
TOTAL	100.0	100.0	99.9	99.9	100.1
Product ratios, mole %					
PyTHQ/(Q+PyTHQ)	-	-	-	-	-
BzTHQ/(Q+BzTHQ)	-	-	-	-	-
DHQ/(PyTHQ+DHQ)	-	-	-	-	-
DHQ/(BzTHQ+DHQ)	-	-	-	-	-
PCH/(PB+PCH)	75.6	78.6	81.8	82.7	83.3
Denitrogenation, %	24.0	40.1	70.1	87.5	98.1

RUN 30

Feed: o-propylaniline

Catalyst time on stream before run: 486.9 hr

Reaction conditions: 375°C, 3.55 MPa, 13.3 kPa OPA

W/F_{OPA}, hr g catalyst/g-mol OPA

	<u>83.3</u>	<u>167</u>	<u>333</u>	<u>500</u>
Organic products, mole %				
PyTHQ	-	-	-	-
Q	-	-	-	-
OPA	76.7	60.4	40.3	19.9
BzTHQ	-	-	-	-
DHQ	-	-	-	-
PB	6.5	10.7	15.8	21.3
EB	-	-	TR	TR
PCHE	5.3	4.7	2.1	0.6
PCH	11.3	23.7	41.0	57.3
ECH	-	TR	0.1	0.2
UNKNOWNNS	0.2	0.5	0.7	0.7
TOTAL	100.0	100.0	100.0	100.0

Product ratios, mole %

PyTHQ/(Q+PyTHQ)	-	-	-	-
BzTHQ/(Q+BzTHQ)	-	-	-	-
DHQ/(PyTHQ+DHQ)	-	-	-	-
DHQ/(BzTHQ+DHQ)	-	-	-	-
PCH/(PB+PCH)	63.6	68.9	72.1	72.9

Denitrogenation, %

	23.1	39.1	58.9	79.4
--	------	------	------	------

RUN 31

Feed: o-propylaniline

Catalyst time on stream before run: 496.7 hr

Reaction conditions: 330°C, 7.0 MPa, 13.3 kPa OPA

W/F_{OPA₀}, hr g catalyst/g-mol OPA

	<u>83.3</u>	<u>167</u>	<u>333</u>	<u>500</u>	<u>667</u>
Organic products, mole %					
PyTHQ	-	-	-	-	-
Q	-	-	-	-	-
OPA	73.8	64.9	39.5	31.6	21.4
BzTHQ	-	-	-	-	-
DHQ	-	-	-	-	-
PB	2.3	3.4	6.1	6.9	8.1
EB	-	-	-	-	-
PCHE	6.2	4.4	2.8	1.2	0.5
PCH	16.3	26.5	51.6	60.3	70.0
ECH	-	-	-	-	-
UNKNOWNNS	1.4	0.8	TR	-	-
TOTAL	100.0	100.0	100.0	100.0	100.0
Product ratios, mole %					
PyTHQ/(Q+PyTHQ)	-	-	-	-	-
BzTHQ/(Q+BzTHQ)	-	-	-	-	-
DHQ/(PyTHQ+DHQ)	-	-	-	-	-
DHQ/(BzTHQ+DHQ)	-	-	-	-	-
PCH/(PB+PCH)	87.7	88.6	89.4	89.7	89.6
Denitrogenation, %	24.8	34.4	60.5	68.4	78.6

RUN 32

Feed: o-propylaniline

Catalyst time on stream before run: 507.0 hr

Reaction conditions: 420°C, 7.0 MPa, 26.7 kPa OPA

W/F_{OPA₀}, hr g catalyst/g-mol OPA

	<u>41.7</u>	<u>83.3</u>	<u>167</u>	<u>125</u>	<u>*250</u>
Organic products, mole %					
PyTHQ	-	-	-	-	-
Q	-	-	-	-	-
OPA	50.4	20.4	TR	3.4	7.2
BzTHQ	-	-	-	-	-
DHQ	-	-	-	-	-
PB	14.1	22.7	27.9	27.6	15.3
EB	TR	TR	TR	TR	TR
PCHE	4.7	1.2	TR	TR	TR
PCH	29.7	54.2	71.1	67.9	77.5
ECH	0.2	0.4	0.9	0.7	TR
UNKNOWN	1.0	1.1	0.1	0.4	TR
TOTAL	100.1	100.0	100.0	100.0	100.0

Product ratios, mole %

PyTHQ/(Q+PyTHQ)	-	-	-	-	-
BzTHQ/(Q+BzTHQ)	-	-	-	-	-
DHQ/(PyTHQ+DHQ)	-	-	-	-	-
DHQ/(BzTHQ+DHQ)	-	-	-	-	-
PCH/(PB+PCH)	67.8	70.5	71.9	71.1	83.5

Denitrogenation, % 48.6 78.6 99.9 96.2 92.8

*Temperature was 375°C instead of 420°C

RUN 33

Feed: Py-tetrahydroquinoline

Catalyst time on stream before run: 516.8 hr

Reaction conditions: 375°C, 7.0 MPa, 13.3 kPa PyTHQ

	W/F _{PyTHQ₀} , hr g catalyst/g-mol PyTHQ				
	<u>83.3</u>	<u>167</u>	<u>333</u>	<u>500</u>	<u>667</u>
Organic products, mole %					
PyTHQ	53.5	40.5	20.2	12.6	8.3
Q	7.7	5.4	3.7	4.1	4.4
OPA	1.0	1.8	2.3	2.3	3.1
BzTHQ	11.1	14.1	16.7	16.8	16.6
DHQ	23.4	31.3	32.4	24.9	19.3
PB	0.5	1.0	2.4	3.5	4.4
EB	-	-	TR	TR	TR
PCHE	0.9	1.4	2.5	2.4	1.9
PCH	1.8	4.5	15.1	26.3	33.9
ECH	-	TR	0.3	0.7	1.3
UNKNOWNNS	0.1	0.1	4.4	6.3	6.9
TOTAL	100.0	100.1	100.0	99.9	100.1
Product ratios, mole %					
PyTHQ/(Q+PyTHQ)	87.4	88.2	84.3	75.3	65.5
BzTHQ/(Q+BzTHQ)	58.9	72.3	81.7	80.2	79.2
DHQ/(PyTHQ+DHQ)	30.4	43.6	61.6	66.3	70.0
DHQ/(BzTHQ+DHQ)	67.9	69.0	65.9	59.6	53.8
PCH/(PB+PCH)	77.4	81.7	86.5	88.1	88.4
Denitrogenation, %	3.2	6.9	20.2	33.0	41.5

RUN 34

Feed: Py-tetrahydroquinoline

Catalyst time on stream before run: 529.2 hr

Reaction conditions: 330°C, 3.55 MPa, 13.3 kPa PyTHQ

	W/F _{PyTHQ_o} , hr g catalyst/g-mol Q				
	<u>41.7</u>	<u>83.3</u>	<u>167</u>	<u>333</u>	<u>500</u>
Organic products, mole %					
PyTHQ	77.8	76.0	66.6	55.2	43.0
Q	10.1	9.5	11.4	18.2	27.4
OPA	TR	TR	TR	0.6	0.7
BzTHQ	3.2	3.5	4.7	7.0	8.3
DHQ	9.0	10.9	16.0	15.2	15.7
PB	TR	0.0	0.2	0.3	0.4
EB	-	-	-	-	-
PCHE	TR	TR	0.2	0.3	0.5
PCH	-	TR	0.1	0.3	0.7
ECH	-	-	-	-	-
UNKNOWNNS	TR	TR	0.8	2.8	3.3
TOTAL	100.1	99.9	100.0	99.9	100.0
Product ratios, mole %					
PyTHQ/(Q+PyTHQ)	88.5	88.9	85.4	75.2	61.1
BzTHQ/(Q+BzTHQ)	23.8	27.1	29.2	27.9	23.4
DHQ/(PyTHQ+DHQ)	10.3	12.6	19.3	21.6	26.8
DHQ/(BzTHQ+DHQ)	73.9	75.5	77.2	68.4	65.4
PCH/(PB+PCH)	-	-	33.5	55.1	64.5
Denitrogenation, %	0%	0%	0.4%	0.9%	1.6%

RUN 35

Feed: Bz-tetrahydroquinoline

Catalyst time on stream before run: 540.4 hr

Reaction conditions: 375°C, 7.0 MPa, 13.3 kPa BzTHQ

	W/F _{BzTHQ₀} , hr g catalyst/g-mol BzTHQ				
	<u>83.3</u>	<u>167</u>	<u>333</u>	<u>500</u>	<u>667</u>
Organic products, mole %					
PyTHQ	3.0	4.5	3.7	3.4	3.0
Q	TR	TR	TR	0.9	0.8
OPA	-	TR	TR	TR	TR
BzTHQ	41.6	28.8	20.4	16.2	12.2
DHQ	49.1	52.8	40.1	26.0	16.6
PB	0.4	1.1	2.6	4.3	5.5
EB	-	TR	TR	TR	TR
PCHE	1.7	2.6	2.8	2.3	1.6
PCH	2.9	8.7	24.0	40.3	52.1
ECH	TR	0.2	0.7	1.1	1.6
UNKNOWN	1.2	1.3	5.6	5.6	6.5
TOTAL	99.9	100.0	99.9	100.1	99.9
Product ratios, mole %					
PyTHQ/(Q+PyTHQ)	-	-	-	78.9	78.7
BzTHQ/(Q+BzTHQ)	100	100	100	94.8	93.7
DHQ/(PyTHQ+DHQ)	94.2	92.1	91.5	88.6	84.6
DHQ/(BzTHQ+DHQ)	54.1	64.7	66.3	61.6	57.6
PCH/(PB+PCH)	87.5	89.2	90.2	90.5	90.4
Denitrogenation, %	5.0%	12.7%	30.2%	48.0%	60.8

RUN 36

Feed: Bz-tetrahydroquinoline

Catalyst time on stream before run: 550.8 hr

Reaction conditions: 330°C, 3.55 MPa, 13.3 kPa BzTHQ

	W/F _{BzTHQ₀} , hr g catalyst/g-mol BzTHQ				
	<u>41.7</u>	<u>83.3</u>	<u>167</u>	<u>333</u>	<u>500</u>
Organic products, mole %					
PyTHQ	0.9	1.4	1.4	2.3	2.3
Q	TR	TR	TR	0.6	0.8
OPA	-	-	-	TR	TR
BzTHQ	73.1	61.9	50.5	35.7	30.0
DHQ	23.7	34.5	41.5	46.4	46.7
PB	TR	TR	0.1	0.3	0.4
EB	-	-	-	-	-
PCHE	0.1	0.3	0.7	1.5	2.1
PCH	TR	0.2	0.6	2.0	3.6
ECH	-	-	-	-	-
UNKNOWNNS	2.1	1.9	5.3	11.2	14.1
TOTAL	99.9	100.2	100.1	100.0	100.0
Product ratios, mole %					
PyTHQ/(Q+PyTHQ)	-	-	-	78.2	74.0
BzTHQ/(Q+BzTHQ)	100	100	100	98.2	97.4
DHQ/(PyTHQ+DHQ)	96.2	96.2	96.8	95.3	95.3
DHQ/(BzTHQ+DHQ)	24.5	35.8	45.1	56.6	60.8
PCH/(PB+PCH)	-	-	84.8	85.2	89.9
Denitrogenation, %	0.1%	0.4%	1.4%	3.9%	6.1%

RUN 37

Feed: quinoline

Catalyst time on stream before run: 560.4 hr

Reaction conditions: 375°C, 7.0 MPa, 13.3 kPa Q

W/F_{Q₀}, hr g catalyst/g-mol Q

	<u>83.3</u>	<u>167</u>	<u>333</u>	<u>500</u>	<u>667</u>
Organic products, mole %					
PyTHQ	49.9	38.7	21.1	12.6	9.0
Q	7.2	5.2	3.5	2.7	2.7
OPA	1.1	1.7	2.6	2.8	2.7
BzTHQ	12.7	15.1	16.8	16.2	14.2
DHQ	25.3	31.2	33.4	27.9	20.0
PB	0.7	1.2	2.2	3.7	4.9
EB	-	TR	TR	TR	TR
PCHE	1.0	1.5	2.4	2.0	1.9
PCH	2.1	5.2	14.5	27.1	37.1
ECH	-	0.1	0.4	0.8	1.3
UNKNOWNNS	TR	0.1	3.1	4.2	6.2
TOTAL	100.0	100.0	100.1	100.0	100.0
Product ratios, mole %					
PyTHQ/(Q+PyTHQ)	87.3	88.1	85.8	82.2	76.7
BzTHQ/(Q+BzTHQ)	63.7	74.2	82.7	85.6	83.8
DHQ/(PyTHQ+DHQ)	33.6	44.6	61.3	68.8	68.9
DHQ/(BzTHQ+DHQ)	66.6	67.3	66.6	63.2	58.5
PCH/(PB+PCH)	75.6	81.2	86.7	88.1	88.3
Denitrogenation, %	3.8%	8.0%	19.5%	33.6	45.2

RUN 38

Feed: decahydroquinoline*

Catalyst time on stream before run: 571.9 hr

Reaction conditions: 375°C, 7.0 MPa, 13.3 kPa DHQ

	W/F _{DHQ_o} , hr g catalyst/g-mol DHQ			
	<u>83.3</u>	<u>167</u>	<u>333</u>	<u>500</u>
Organic products, mole %				
PyTHQ	4.1	4.5	5.0	3.9
Q	TR	TR	TR	TR
OPA	-	-	-	-
BzTHQ	22.4	23.3	15.6	11.9
DHQ	60.1	50.7	29.0	19.1
PB	1.1	1.7	4.6	5.9
EB	-	-	TR	TR
PCHE	4.0	4.5	2.6	2.3
PCH	8.3	15.4	38.7	51.9
ECH	TR	TR	0.5	0.9
UNKNOWNNS	TR	TR	3.9	4.2
TOTAL	100.0	100.1	99.9	100.1

Product ratios, mole %

PyTHQ/(Q+PyTHQ)	-	-	-	-
BzTHQ/(Q+BzTHQ)	-	-	-	-
DHQ/(PyTHQ+DHQ)	93.6	91.9	85.2	83.2
DHQ/(BzTHQ+DHQ)	72.9	68.5	65.0	61.7
PCH/(PB+PCH)	88.5	90.0	89.4	89.8

Denitrogenation, % 13.4 21.6 46.5 61.0

*Cyclohexane was used as solvent; the feed solution was
59.5 weight % or 47.1 mole % DHQ

VII. H. Location of Original Data

The original data are in the possession of the author at Cornell University, Ithaca, New York.

Bibliography

- Aboul-Gheit, A. K., and I. K. Abdou, "The Hydrodenitrogenation of Petroleum-Model-Nitrogen Compounds", Journal of the Institute of Petroleum, 59(568), 188 (1973)
- Benson, S. W., F. R. Cruickshank, D. M. Golden, G. R. Haugen, H. E. O'Neal, A. S. Rodgers, R. Shaw, and R. Walsh, "Additivity Rules for the Estimation of Thermochemical Properties", Chem. Rev., 69, 279 (1969)
- Beuther, H., and O. A. Larson, "Role of Catalytic Metals in Hydrocracking", Ind. Eng. Chem. Process Des. Dev., 4(2), 177 (1965)
- Brucker, R., and G. Kolling, "Dissolution of Coal in Tetrahydroquinoline", Brennstoff Chemie, 46(2), 41-43 (1965)
- Cocchetto, J. F., "Thermodynamic Equilibria of Heterocyclic Nitrogen Compounds with Their Hydrogenated Derivatives", S. M. Thesis, M.I.T., Cambridge, Mass. (1974)
- Cocchetto, J. F., and C. N. Satterfield, "Thermodynamic Equilibria of Selected Heterocyclic Nitrogen Compounds with Their Hydrogenated Derivatives", Ind. Eng. Chem. Process Des. Dev., 15(2), 272 (1976)
- Considine, D. M., Ed., Energy Technology Handbook, McGraw-Hill, New York (1977)
- Declerck, C. J., "Catalytic Hydrodenitrogenation of Quinoline", S. M. Thesis, M.I.T., Cambridge, Mass. (1976)
- Dietz, W. A., "Response Factors for Gas Chromatographic Analyses", J. of Gas Chromatography, 5, 68 (1967)
- Dinneen, G. U., "Sulfur and Nitrogen Compounds in Shale Oil", Proc. Am. Petrol. Inst., 42(8), 41 (1962)
- Doelman, J., and J. C. Vlugter, "Model Studies on the Catalytic Hydrogenation of Nitrogen-Containing Oils", Proc. Sixth World Petrol. Congr., III, 247, Frankfurt (1963)
- Doraiswamy, L. K., and D. G. Tajbl, "Laboratory Catalytic Reactors", Cat. Rev.-Sci. Eng., 10(2), 177 (1974)

- Eliezer, K. F., M. Bhide, M. Houalla, D. Broderick, B. C. Gates, J. R. Katzer, and J. H. Olson, "A Flow Microreactor for Study of High-Pressure Catalytic Hydroprocessing Reactions", Ind. Eng. Chem. Fundam., 16(3), 380 (1977)
- Flinn, R. A., O. A. Larson, and H. Beuther, "How Easy Is Hydrodenitrogenation?", Hydrocarbon Proc. and Petrol. Ref., 42(9), 129 (1963)
- Frost, C. M., and H. B. Jensen, "Hydrodenitrification of Crude Shale Oil", Am. Chem. Soc. Div. Petrol. Chem. Preprints, 18(1), 119 (1973)
- Gates, B. C., J. R. Katzer, and G. C. A. Schuit, Chemistry of Catalytic Processes, McGraw-Hill, New York (1979)
- Goudriaan, F., "Hydrodenitrogenation of Pyridine" Thesis, Twente University of Technology, Enschede, The Netherlands (1974)
- Katzer, J. R., and R. Sivasubramanian, "Process and Catalyst Needs for Hydrodenitrogenation", Cat. Rev., 20(2), (1979)
- Kirkland, J. J., "Fluorine-Containing Polymers as Solid Supports in Gas Chromatography", Anal. Chem., 35(13), 2003 (1963)
- Koros, R. M., et al., Am. Chem. Soc. Div. Petrol. Chem. Prepr., 12(4), B-165 (1967)
- Madkour, M. M., B. H. Mahmoud, I. K. Abdou, and J. C. Vlughter, "The Effect of Chlorides on the Hydrogenation of Nitrogen Containing Model Substances", J. Indian Chem. Soc., 46(8), 720 (1969)
- Marshall, M. E., S. B. Thesis, M.I.T., Cambridge, Mass. (1980)
- McIlvried, H. G., "Kinetics of the Hydrodenitrification of Pyridine", Ind. Eng. Chem. Process Des. Dev., 10(1), 125 (1971)
- Qader, S. A., W. H. Wiser, and G. R. Hill, "Kinetics of the Hydroremoval of Sulfur, Oxygen, and Nitrogen from a Low Temperature Coal Tar", Ind. Eng. Chem. Process Des. Dev., 7(3), 390 (1968)
- Samoilov, S. M., and A. M. Rubinshtein, Izv. AN SSSR, Otd. Khim. Nauk, 427 (1960)

- Satterfield, C. N., and J. F. Cocchetto, "Pyridine Hydrodenitrogenation: An Equilibrium Limitation on the Formation of Piperidine Intermediate", AICHE J., 21(6), 1107 (1975)
- Satterfield, C. N., M. Modell, R. A. Hites, and C. J. Declerck, "Intermediate Reactions in the Catalytic Hydrodenitrogenation of Quinoline", Ind. Eng. Chem. Process Des. Dev., 17(2), 141 (1978)
- Shih, S. S., J. R. Katzer, H. Kwart, and A. B. Stiles, "Quinoline Hydrodenitrogenation: Reaction Network and Kinetics", Am. Chem. Soc. Div. Petrol. Chem. Preprints, 22(3), 919 (1977)
- Shih, S., E. Reiff, R. Zawadzki, and J. R. Katzer, Am. Chem. Soc. Preprints of the Fuels Div., p. 99 (1978)
- Sonnemans, J., and P. Mars, "The Mechanism of Pyridine Hydrogenolysis on Molybdenum-Containing Catalysts: III. Cracking, Hydrocracking, Dehydrogenation, and Disproportionation of Pentylamine", J. Catal., 34, 215 (1974)
- Sonnemans, J., G. H. van den Berg, and P. Mars, "The Mechanism of Pyridine Hydrogenolysis on Molybdenum-Containing Catalysts: II. Hydrogenation of Pyridine to Piperidine", J. Catal., 31, 220 (1973)
- Stengler, W., J. Welker, and E. Leibnitz, "Behavior of Organic Nitrogen Compounds under Gas-Phase, Medium-Pressure Hydrogenation Refining Conditions", Freiberger Forschungshefte, A 329, 51 (1964)
- Stern, E. W., "Reaction Networks in Catalytic Hydrodenitrogenation", J. Catal., 57, 390 (1979)
- Stull, D. R., E. F. Westrum, Jr., and G. C. Sinke, The Chemical Thermodynamics of Organic Compounds, John Wiley & Sons, New York (1969)
- van Krevelen, D. W., and H. A. G. Chermin, "Estimation of the Free Enthalpy (Gibbs Free Energy) of Formation of Organic Compounds from Group Contributions", Chem. Eng. Sci., 1(2), 66 (1951)
- Weast, R. C., Ed., Handbook of Chemistry and Physics, 51st Edition, The Chemical Rubber Co., Cleveland (1971)
- Weisser, O., and S. Landa, Sulphide Catalysts, Their Properties and Applications, Pergamon Press, New York (1973)

Wilkins, J. A., "Kinetics and Interactions of the Simultaneous Catalytic Hydrodenitrogenation of Pyridine and Hydrodesulfurization of Thiophene", Ph.D. Thesis, M.I.T., Cambridge, Mass. (1977)